Models for Persistence and Spread of Structured Populations in Patchy Landscapes

Yousef Alqawasmeh

Thesis submitted to the Faculty of Graduate and Postdoctoral Studies in partial fulfillment of the requirements for the degree of
Doctor of Philosophy in Mathematics[1]

Department of Mathematics and Statistics
Faculty of Science
University of Ottawa

[1]The Ph.D. program is a joint program with Carleton University, administered by the Ottawa-Carleton Institute of Mathematics and Statistics.

Abstract

In this dissertation, we are interested in the dynamics of spatially distributed populations. In particular, we focus on persistence conditions and minimal traveling periodic wave speeds for stage-structured populations in heterogeneous landscapes. The model includes structured populations of two age groups, juveniles and adults, in patchy landscapes.

First, we present a stage-structured population model, where we divide the population into pre-reproductive and reproductive stages. We assume that all parameters of the two age groups are piecewise constant functions in space. We derive explicit formulas for population persistence in a single-patch landscape and in heterogeneous habitats. We find the critical size of a single patch surrounded by a non-lethal matrix habitat. We derive the dispersion relation for the juveniles-adults model in homogeneous and heterogeneous landscapes. We illustrate our results by comparing the structured population model with an appropriately scaled unstructured model. We find that a long pre-reproductive state typically increases habitat requirements for persistence and decreases spatial spread rates, but we also identify scenarios in which a population with intermediate maturation rate spreads fastest. We apply sensitivity and elasticity formulas to the critical size of a single-patch landscape and to the minimal traveling wave speed in a homogeneous landscape.

Secondly, we use asymptotic techniques to find an explicit formula for the traveling periodic wave speed and to calculate the spread rates for structured populations in heterogeneous landscapes. We illustrate the power of the homogenization method

by comparing the dispersion relation and the resulting minimal wave speeds for the approximation and the exact expression. We find an excellent agreement between the fully heterogeneous speed and the homogenized speed, even though the landscape period is on the same order as the diffusion coefficients and not as small as the formal derivation requires. We also generalize this work to the case of structured populations of n age groups.

Lastly, we use a finite difference method to explore the numerical solutions for the juveniles-adults model. We compare numerical solutions to analytic solutions and explore population dynamics in non-linear models, where the numerical solution for the time-dependent problem converges to a steady state. We apply our theory to study various aspects of marine protected areas (MPAs). We develop a model of two age groups, juveniles and adults, in which only adults can be harvested and only outside MPAs, and recruitment is density dependent and local inside MPAs and fishing grounds. We include diffusion coefficients in density matching conditions at interfaces between MPAs and fishing grounds, and examine the effect of fish mobility and bias movement on yield and fish abundance. We find that when the bias towards MPAs is strong or the difference in diffusion coefficients is large enough, the relative density of adults inside versus outside MPAs increases with adult mobility. This observation agrees with findings from empirical studies.

Acknowledgments

First and foremost, I would like to express my deepest gratitude and sincerest appreciation to my supervisor Prof. Frithjof Lutscher who supervised the subject of this thesis continuously; he helped me in every step of this thesis through his valuable advice and any possible help I needed till the last moment of this work. I am also grateful for his financial support through research grants and conferences fund.

I would like to thank my thesis committee, Prof. David Amundsen and Prof. Yves Bourgault for insightful discussions and valuable feedback. I am also grateful to them, along with Prof. Michael Neubert and Prof. Victor LeBlanc for their careful reading of my thesis. I would also like to thank Dr. Robert Roy for the valuable time he has provided to review the manuscript's language.

I want to thank the Faculty of Graduate and Postdoctoral Studies and the Department of Mathematics and Statistics at the University of Ottawa for their scholarships and financial support during my Ph.D. study. I also wish to acknowledge the financial support of Ontario Student Assistant Program and Swartzen Memorial Scholarship.

I would like to express my gratitude to my M.Sc. thesis supervisor, Prof. Fuad Kittaneh, who continuously encourages and supports me. I would also like to thank all professors who taught me at the University of Jordan, Carleton University and University of Ottawa.

Last but not least, I would like to thank all my family members for their unlimited support, warmth and encouragement. Without your sacrifices, this work would not be possible.

Dedication

"I sustain myself with the love of family."

-Maya Angelou

I proudly dedicate this work to my lovely wife Raeda, my sons Ahmad, Abdalrahman and Abdallah, my sweet daughter Dua'a and my beloved family in Jordan.

Contents

List of Figures

List of Tables

1. Introduction

This thesis investigates several aspects of the dynamics of biological populations via mathematical models. More specifically, the biological questions motivating this work arise in conservation ecology and invasion biology. In conservation ecology, one asks for conditions under which a population can persist locally in a given area. Invasion biology aims to quantify the rate at which a species spreads spatially in a given landscape. In this thesis, we choose reaction-diffusion equations as the mathematical modeling framework to investigate these questions theoretically.

1.1. Modeling Background

Whether a biological population can persist and spread in a given landscape depends on the interplay of population dynamics (growth, reproduction and death), individual movement through the landscape, and landscape characteristics (favorable and unfavorable conditions). Hence, mathematical models need to take these processes into account.

If individuals in a population are identical, we speak of an unstructured population. Typically, individuals differ in various respects (e.g. size, age, sex, ...), which we call stages. If these stages are taken into account, we speak of a structured population. Similarly, if the landscape is identical everywhere, we speak of a homogeneous landscape. If landscape conditions change in space, we say that the landscape is heterogeneous.

One fundamental insight in spatial ecology is that a population needs a certain amount of space to persist. This is most easily understood with the example of a plant population with wind-dispersal seed on an island. If the island is small, then most of seeds will fall into the surrounding water and will be lost from the population. Consequently, the population will die out. If the island is large, then sufficiently many seeds will land and germinate on the island so that the population can grow and persist. The minimal patch size is the threshold between these two cases.

The problem of assigning the minimal patch size of a bounded domain surrounded by a hostile landscape that allows a diffusing population to persist was originally studied by Skellam [82] and Kierstead and Slobodkin [42]. This critical patch size has many ecological applications, for example, designing marine reserves [50, 59] and assigning harvesting rates.

Populations that can persist are expected to spread through time in the spatial environment. This spread occurs according to different biological scenarios. One of these scenarios is the point release scenario, in which the population is introduced locally and spreads in all directions. An example of this scenario is the spread of emerald ash borer (*Agrilus planipennis*), an invasive forest insect, which was identified in 2002 as the cause of extensive ash decline and mortality in Detroit, Michigan, and has since killed millions of ash trees in the United States and Canada (Siegert et al. [80]). Another spread scenario is the traveling front scenario, in which the population is already settled over a large region and moves forward into a new area. For example, *Aedes aegypti* and *Aedes albopictus* mosquitoes move northward rapidly with global warming (Shope [79]). Much of the research on traveling waves focused on minimal wave speeds for unstructured populations. For example, Fisher [23] derived the minimal traveling wave speed for unstructured populations in homogeneous landscapes, while Aronson and Weinberger [3] and Novick-Cohen and Segel [67] studied the traveling wave speed in unbounded homogeneous landscapes, and Shigesada et al. [77] and Maciel and Lutscher [55] considered traveling wave speeds in unbounded

heterogeneous landscapes.

Ecologically, individuals differ in their vital rates and dispersal abilities. These differences are related to age, size, or developmental stages (Neubert and Caswell [65]). In addition, empirical studies show that adults in some species do not move (for example, reef fish have sedentary adults; White [89]), while juveniles in other species stay with their parents (details about juveniles movement of urban peregrines can be found in the book of Drewitt [20]). From this perspective, there was a necessity to study persistence conditions and traveling wave speeds for structured populations.

From this point of view, Gurtin and MacCamey [32] considered continuous age-structured populations. They derived the critical patch size of a limited environment according to three different scenarios of age dependence. For discrete-time structured population models, Lui [52] was the first one who studied the wave speed for these populations. Later, Neubert and Caswell [65] used integrodifference equations to study how the wave speed depends on population parameters.

In this dissertation, we are interested in the dynamics of spatially distributed populations. In particular, we focus on persistence conditions and minimal traveling wave speeds for age-structured populations in heterogeneous landscapes. The model includes structured populations of juveniles and adults in patchy landscapes, and our work builds mainly on the work of Maciel and Lutscher [55] and the work of Shigesada et al. [77]. In the next section, we present the mathematical background of persistence conditions and traveling waves for both structured and unstructured population models.

1.2. Mathematical Background

In this section, we present some of the mathematical models mentioned in the previous section and explain some of the techniques used to study them. We also present some of the classical results that will serve as comparison for the results obtained in this

thesis. This section is divided into two parts, one for unstructured populations and one for structured populations.

1.2.1. Unstructured Populations in Homogeneous Landscapes

For an unstructured population, the basic reaction diffusion equation is

$$\frac{\partial u(t,x)}{\partial t} = D\frac{\partial^2 u(t,x)}{\partial x^2} + F\left(u\right), \tag{1.2.1}$$

where $u(t,x)$ is the density function at time $t \geq 0$ and location $x \in \Omega \subset \mathbb{R}$, $D > 0$ is the diffusion coefficient that measures the movement of individuals, and $F(u)$ is the population growth function. For example, the logistic growth function is $F(u) = ru\left(1 - \frac{u}{K}\right)$.

Skellam [82] and Kierstead and Slobodkin [42] considered equation (1.2.1) with logistic growth function in a single 'good patch', $\Omega = \left(\frac{-L}{2}, \frac{L}{2}\right)$, with hostile boundary conditions

$$u\left(t, \frac{L}{2}\right) = u\left(t, \frac{-L}{2}\right) = 0. \tag{1.2.2}$$

After linearizing equation (1.2.1) about $u = 0$ and assuming an exponential solution $u\left(t,x\right) = e^{\lambda t}U\left(x\right)$, the corresponding eigenvalue problem of equation (1.2.1) can be written as follows

$$\lambda U\left(x\right) = D\frac{d^2U\left(x\right)}{dx^2} + rU\left(x\right). \tag{1.2.3}$$

Note that equation (1.2.3) with boundary conditions (1.2.2) has infinitely many eigenvalues [51], $\lambda_1 > \lambda_2 > \cdots > -\infty$. The largest of these eigenvalues has an eigenfunction that is of one sign. This eigenvalue is known as the dominant eigenvalue. Since we will be only interested in this dominant eigenvalue, we will simply call it $\lambda = \lambda_1$. The reason why we are interested in it is that it determines the stability of the zero solution. If $\lambda > 0$, then $u = 0$ is unstable and the population will persist, while if $\lambda < 0$, then $u = 0$ is stable and the population will go extinct. Hence, $\lambda = 0$ assigns

the persistence boundary. Substituting $\lambda = 0$ into (1.2.3) and solving the characteristic equation $Dp^2 + r = 0$ with hostile boundary conditions gives the critical patch size formula

$$L^* = \pi\sqrt{\frac{D}{r}}. \tag{1.2.4}$$

Fisher [23] used equation (1.2.1) with logistic growth function to find the traveling wave speed. A traveling wave is a solution of the form $u(t,x) = U(z)$, where $z = x - Ct$, and C is the speed of the traveling wave front. Since $\frac{\partial}{\partial t}u = -CU'$, and $\frac{\partial}{\partial x}u = U'$, Fisher could write equation (1.2.1) as an ordinary differential equation

$$D\frac{d^2U}{dz^2} + C\frac{dU}{dz} + F(U) = 0.$$

After linearizing the last equation about $U = 0$, the characteristic equation will be of the form $Dp^2 + Cp + r = 0$. For a monotone wave front one needs real solutions for this equation. We have real roots only if $C^2 \geq 4rD$. Since Fisher searched for the speed of a traveling wave, he wrote the formula of the minimum traveling wave speed as

$$C^* = 2\sqrt{rD}. \tag{1.2.5}$$

Traveling waves are studied in many contexts, for example to explain the spread of epidemic diseases, pest species, and dispersal of seeds, see Kolmogorov et al. [44], Aronson and Weinberger [3], and Novick-Cohen and Segel [67].

1.2.2. Unstructured Populations in Heterogeneous Landscapes

An early landmark paper in the investigation of population dynamics in heterogeneous landscapes is the work of Shigesada et al. [77]. They considered a logistic growth function in a periodically varying, piecewise constant landscape of two patch types: a 'favorable patch' and an 'unfavorable patch' (see Figure 1.1). Their model has the

following differential equations

$$\frac{\partial u_1(t,x)}{\partial t} = D_1 \frac{\partial^2 u_1(t,x)}{\partial x^2} + (r_1 - \mu_1 u_1(t,x))\, u_1(t,x), \quad x \in (0, L_1) + L\mathbb{Z}, \tag{1.2.6}$$

and

$$\frac{\partial u_2(t,x)}{\partial t} = D_2 \frac{\partial^2 u_2(t,x)}{\partial x^2} + (r_2 - \mu_2 u_2(t,x))\, u_2(t,x), \quad x \in (-L_2, 0) + L\mathbb{Z}, \tag{1.2.7}$$

where $L = L_1 + L_2$ is the period, $D_i > 0$ are the diffusion coefficients, r_i are the growth rates, μ_i are the coefficients of intraspecific competition, and $u_i(t,x)$ are the population density functions at time t and location x in patch i.

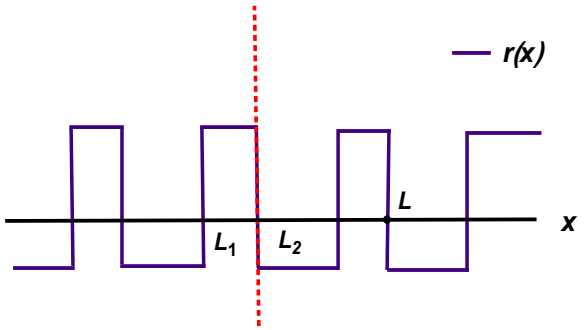

Figure 1.1.: Spatial pattern of a patchy landscape (periodically varying) with favorable patch size, L_1, and unfavorable patch size, L_2. The dashed line represents the interface between the two patches.

A favorable patch is characterized by $r_1 > 0$ whereas an unfavorable patch has $r_2 < 0$. At $x = x_n = nL$, Shigesada et al. [77] used the interface conditions

$$u_1(t, x_n^+) = u_2(t, x_n^-), \tag{1.2.8}$$

$$D_1 \frac{\partial u_1}{\partial x}(t, x_n^+) = D_2 \frac{\partial u_2}{\partial x}(t, x_n^-), \tag{1.2.9}$$

while at $x = x_n = L_1 + nL$, the matching conditions are changed to

$$u_1(t, x_n^-) = u_2(t, x_n^+), \tag{1.2.10}$$

$$D_1 \frac{\partial u_1}{\partial x}(t, x_n^-) = D_2 \frac{\partial u_2}{\partial x}(t, x_n^+). \tag{1.2.11}$$

They nondimensionalized the equations as follows: $T = r_1 t$, $X = \sqrt{\frac{r_1}{D_1}} x$, $U_i = \frac{\mu_i}{r_1} u_i$, $D = \frac{D_2}{D_1}$, $r = \frac{r_2}{r_1}$, $S_1 = \sqrt{\frac{r_1}{D_1}} L_1$, and $S_2 = \sqrt{\frac{r_1}{D_1}} L_2$. Consequently, (1.2.6) and (1.2.7) are changed to

$$\frac{\partial U_1(T,X)}{\partial T} = \frac{\partial^2 U_1(T,X)}{\partial X^2} + U_1(T,X)\left(1 - U_1(T,X)\right), \; X \in (0, S_1), \tag{1.2.12}$$

$$\frac{\partial U_2(T,X)}{\partial T} = D\frac{\partial^2 U_2(T,X)}{\partial X^2} + U_2(T,X)\left(r - U_2(T,X)\right), \; X \in (-S_2, 0). \tag{1.2.13}$$

We begin by determining conditions for population persistence. Linearizing equations (1.2.12) and (1.2.13) about $U = 0$ gives

$$\frac{\partial U_1}{\partial T} = \frac{\partial^2 U_1}{\partial X^2} + U_1 \quad \text{(in favorable patches)}, \tag{1.2.14}$$

$$\frac{\partial U_2}{\partial T} = D\frac{\partial^2 U_2}{\partial X^2} + rU_2 \quad \text{(in unfavorable patches)}. \tag{1.2.15}$$

Assuming exponential solutions $U_i(T,X) = e^{\lambda T} V_i(X)$ $(i = 1, 2)$, we get the ordinary differential equations

$$\frac{d^2 V_1(X)}{dX^2} + (1 - \lambda) V_1(X) = 0 \quad \text{(in favorable patches)}, \tag{1.2.16}$$

$$\frac{d^2 V_2(X)}{dX^2} + \frac{(r - \lambda)}{D} V_2(X) = 0 \quad \text{(in unfavorable patches)}, \tag{1.2.17}$$

with corresponding solutions

$$V_1(X) = A\cos\left(\sqrt{1-\lambda}X\right) + B\sin\left(\sqrt{1-\lambda}X\right),$$

$$V_2(X) = A' \cosh\left(\sqrt{\frac{-r+\lambda}{D}}X\right) + B' \sinh\left(\sqrt{\frac{-r+\lambda}{D}}X\right).$$

We need to find conditions on $A,\ A',\ B,\ B'$ for these solutions to satisfy the matching conditions. By applying the conditions (1.2.8) and (1.2.9) at $X = \frac{S_1}{2}$, we get

$$V_1\left(\frac{S_1}{2}^-\right) = V_2\left(\frac{-S_2}{2}^+\right), \tag{1.2.18}$$

$$\frac{dV_1}{dX}\left(\frac{S_1}{2}^-\right) = D\frac{dV_2}{dX}\left(\frac{-S_2}{2}^+\right). \tag{1.2.19}$$

Since the solutions of (1.2.16) and (1.2.17) are symmetric, we conclude $B = B' = 0$ and the matching conditions (1.2.18), (1.2.19) give a linear system of two equations for A and A'. A non-trivial solution for this linear system exists if the determinant of the coefficient matrix equals zero. This condition leads to

$$\sqrt{1-\lambda}\tan\left(\sqrt{1-\lambda}\frac{S_1}{2}\right) = \sqrt{(-r+\lambda)D}\tanh\left(\sqrt{\frac{(-r+\lambda)}{D}}\frac{S_2}{2}\right). \tag{1.2.20}$$

The persistence boundary is given by setting $\lambda = 0$ in (1.2.20).

If $S_2 \to \infty$, where we have a favorable patch surrounded by a non-lethal matrix habitat, then the critical length of the favorable patch will be $S_1^* = 2\arctan\left(\sqrt{-rD}\right)$.

1.2.3. Spread in Heterogeneous Landscapes

Shigesada et al. [77] also studied traveling periodic waves in heterogeneous landscapes. They defined the function $U(T, X)$ as U_1 on good patches and as U_2 on bad patches. Then they described the condition for a traveling periodic wave front as follows: for a certain time T^*, the value of U at $T + T^*$ and at $X + L$ is the same as the value of U at time T and location X. This property is described by the equations: $U(T, X) = U(T + T^*, X + L)$ for $X > 0$ and $U(T, X) \to 0$ as $X \to \infty$. To satisfy these conditions, they proposed that $U_i(T, X)$ is given by a product of two functions,

f_i and g_i as

$$U_i(T,X) = f_i(Z)\, g_i(X), \quad Z = X - CT, \ (C = L/T^*), \tag{1.2.21}$$

where $f_i(Z)$ and $g_i(X)$ satisfy $f_i(Z) \to 0$ as $Z \to \infty$ and $g_i(X) = g_i(X+L)$. C is called the speed of the traveling periodic wave.

By substituting the ansatz in (1.2.21) into (1.2.14) and (1.2.15), they concluded that $f_i(z) = e^{-sz}$, $s > 0$, and wrote the differential equations for g_1 and g_2 as

$$g_1'' - 2sg_1' + \left(s^2 - Cs + 1\right) g_1 = 0,$$

$$g_2'' - 2sg_2' + \left(s^2 + \frac{r - Cs}{D}\right) g_2 = 0.$$

By solving the last two equations, we get

$$g_1(X) = e^{sX}\left[A\cosh(q_1 X) + B\sinh(q_1 X)\right],$$

$$g_2(X) = e^{sX}\left[A'\cosh(q_2 X) + B'\sinh(q_2 X)\right],$$

where $q_1 = \sqrt{Cs-1}$ and $q_2 = \sqrt{\frac{Cs-r}{D}}$. They applied the interface conditions at $X = 0$ and $X = S_1$

$$g_1\left(0^+\right) = g_2\left(0^-\right), \quad g_1\left(S_1^-\right) = g_2\left(-S_2^+\right), \tag{1.2.22}$$

$$g_1'\left(0^+\right) - sg_1\left(0^+\right) = D\left(g_2'\left(0^-\right) - sg_2\left(0^-\right)\right), \tag{1.2.23}$$

and

$$g_1'\left(S_1^-\right) - sg_1\left(S_1^-\right) = D\left(g_2'\left(-S_2^+\right) - sg_2\left(-S_2^+\right)\right). \tag{1.2.24}$$

The interface conditions (1.2.22)-(1.2.24) produce a system of four linear equations for the constants A, A', B, B' above. By equating the determinant of the coefficient

matrix for this linear system to zero, they got the dispersion relation

$$\cosh s(S_1+S_2)=\cosh q_1S_1\cosh q_2S_2+\frac{q_1^2+(Dq_2)^2}{2Dq_1q_2}\sinh q_1S_1\sinh q_2S_2, \quad (1.2.25)$$

in which the traveling wave speed C is defined implicitly in terms of the wave shape parameter s and the coefficients $q_1,\ q_2$.

1.2.4. Deriving Interface Conditions from Random Walks

Maciel and Lutscher [55] re-visited the work of Shigesada et al. [77] but with different matching conditions at the interfaces. They chose a logistic growth function for the reaction diffusion equation. Hence, the density function u_i on patch type i satisfies

$$\frac{\partial u_i}{\partial t}=D_i\frac{\partial^2 u_i}{\partial x^2}+u_i\left(r_i-\mu_i u_i\right).$$

Similarly, as in [77] they assumed that the landscape contains infinitely many patches and is periodically alternating. To derive interface conditions, they took the position $x=0$ as the interface between two different patch types, patch type I $(x>0)$ and patch type II $(x<0)$. Inside patch type i individuals may jump a distance Δx_i to the right or to the left with equal probability $\frac{p_i}{2}$ in a time step Δt. At the interface, individuals may move to the patch type I with probability α_1 and to patch type II with probability α_2. An individual can stay at the interface with probability $1-\alpha_1-\alpha_2$. They wrote three master equations for the probability density functions $u\left(t,-\Delta x_2\right),\ u\left(t,0\right),$ and $u\left(t,\Delta x_1\right)$

$$\Delta x_2u\left(t+\Delta t,-\Delta x_2\right)=\frac{p_2}{2}\Delta x_2u\left(t,-2\Delta x_2\right)+\left(1-p_2\right)\Delta x_2u\left(t,-\Delta x_2\right)+\alpha_2\Delta x_0u\left(t,0\right),$$

$$\Delta x_0u\left(t+\Delta t,0\right)=\frac{p_2}{2}\Delta x_2u\left(t,-\Delta x_2\right)+\frac{p_1}{2}\Delta x_1u\left(t,\Delta x_1\right)+\left(1-\alpha_1-\alpha_2\right)\Delta x_0u\left(t,0\right),$$

$$\Delta x_1u\left(t+\Delta t,\Delta x_1\right)=\frac{p_1}{2}\Delta x_1u\left(t,2\Delta x_1\right)+\left(1-p_1\right)\Delta x_2u\left(t,\Delta x_1\right)+\alpha_1\Delta x_0u\left(t,0\right),$$

where Δx_1 and Δx_2 are the step sizes in patch type I and patch type II, respectively. By expanding the terms on the left-hand sides of the master equations in Taylor series of Δt and terms containing $2\Delta x_1$ and $2\Delta x_2$ in series of Δx_1 and Δx_2, and by doing some algebra with taking the limits as Δx_1, Δx_2, and Δt tend to 0, they reached the interface condition

$$\alpha_1 p_2 \lim_{\Delta x_i \to 0} \left(\frac{\Delta x_2}{\Delta x_1} \right) u\left(t, 0^-\right) = \alpha_2 p_1 u\left(t, 0^+\right). \tag{1.2.26}$$

(1.2.26) generates different interface conditions according to the following scenarios

1. If the probability of moving from the interface to patch i equals the probability of moving inside the patch i, and the step sizes are equal in the two patches, then

$$u_1\left(t, 0^+\right) = u_2\left(t, 0^-\right). \tag{1.2.27}$$

2. If the probability of moving from the interface to patch i is independent of the movement probability inside the patch i, step sizes are different in the two patches, and movement rates in the two patches are equal, then

$$u_1\left(t, 0^+\right) = \frac{\alpha}{1-\alpha}\sqrt{\frac{D_2}{D_1}} u_2\left(t, 0^-\right), \tag{1.2.28}$$

where α is the probability of moving from the interface to patch type I.

3. If the probability of moving from the interface to patch i is independent of the movement probability inside the patch i, step sizes are equal in the two patches and movement rates in the two patches are different, they reached the interface condition

$$u_1\left(t, 0^+\right) = \frac{\alpha}{1-\alpha}\frac{D_2}{D_1} u_2\left(t, 0^-\right), \tag{1.2.29}$$

where

$$D_i = p_i \lim_{\Delta x_i,\, \Delta t \to 0} \frac{(\Delta x_i)^2}{\Delta t}.$$

They also derived continuity of flux interface condition at $x = 0$

$$D_1 \frac{\partial u_1}{\partial x}\left(t, 0^+\right) = D_2 \frac{\partial u_2}{\partial x}\left(t, 0^-\right). \tag{1.2.30}$$

To derive population persistence conditions, they assumed a positive growth rate in a 'favorable patch' and a negative growth rate in an 'unfavorable patch'. Then they nondimensionalized the quantities as in [77].

Redoing the same analysis as Shigesada et al. [77], but with the modified interface conditions, Maciel and Lutscher found the persistence boundary as

$$k \tan\left(\frac{S_1}{2}\right) = \sqrt{-rD}\tanh\left(\sqrt{\frac{-r}{D}}\frac{S_2}{2}\right), \tag{1.2.31}$$

where k is the parameter that measures the discontinuity in density at the interface as it appears in equations (1.2.27)-(1.2.29). If we let $S_2 \to \infty$ in equation (1.2.31), then we get the critical patch size formula $S_1^* = 2\arctan\left(\sqrt{\frac{-rD}{k}}\right)$.

They also studied the minimal speed of traveling periodic waves by following the same procedure in [77]. The new interface matching conditions result in

$$g_1\left(0^+\right) = k g_2\left(0^-\right), \quad g_1\left(S_1^-\right) = k g_2\left(-S_2^+\right).$$

They got the dispersion relation

$$\cosh\left(s\left(S_1 + S_2\right)\right) = \cosh\left(q_1 S_1\right)\cosh\left(q_2 S_2\right) + \frac{q_1^2 k^2 + q_2^2 D^2}{2 D q_1 q_2 k}\sinh\left(q_1 S_1\right)\sinh\left(q_2 S_2\right). \tag{1.2.32}$$

1.2.5. Structured Populations in Homogeneous Landscapes

So far, we presented the mathematical background for unstructured populations but populations can be classified as structured populations according to age, size, stage, etc.

Gurtin and MacCamey [32], considered continuous, age-structured populations. They described age stage by a, and wrote $\rho(a,t,x)$ to represent the population density of age a at time t and location x, $p(t,x)=\int_0^\infty \rho(a,t,x)\,da$ to represent the spatial density, $\mu(p)$ and $\beta(p)$ to represent death and birth rates, respectively, and D for the diffusion term. They derived reaction diffusion equations which appear in their model by using the balance law

$$\frac{\partial \rho(a,t,x)}{\partial a}+\frac{\partial \rho(a,t,x)}{\partial t}+d(a,t,x)=-\frac{\partial q(a,t,x)}{\partial x}, \tag{1.2.33}$$

and the birth law

$$\rho(0,t,x)=B(t,x)=\int_0^\infty \beta(a,p(t,x))\,\rho(a,t,x)\,da, \tag{1.2.34}$$

where

$$d(a,t,x)=\mu(a,p(t,x))\,\rho(a,t,x) \quad \text{and} \quad q(a,t,x)=-D\frac{\partial \rho(a,t,x)}{\partial x} \tag{1.2.35}$$

represent loss due to death and flux of population by spatial diffusion, respectively. They assumed $\rho(a,t,x)\to 0$ as $a\to\infty$.

They assumed constant birth and death rates, with hostile boundary conditions $p(t,0)=p(t,L)=0$. They found the critical patch size according to three different forms of age dependence

1. If $\beta(a,p)=\beta$ and $\mu(a,p)=\mu$, the equation above can be reduced to the

reaction diffusion equation

$$p_t + (\mu - \beta)\, p = D p_{xx}, \tag{1.2.36}$$

which yields the critical patch size $L^* = \pi\sqrt{\frac{D}{\beta-\mu}}$.

2. If $\beta(a,p) = \beta e^{-\alpha a}$, $\alpha > 0$ and $\mu(a,p) = \mu$, the equations can be reduced to the reaction diffusion equations

$$p_t + \mu p - \beta C = D p_{xx}, \tag{1.2.37}$$

$$C_t + [\mu + \alpha - \beta]\, C = D C_{xx}, \tag{1.2.38}$$

where $C(t,x) = \int_0^\infty e^{-\alpha a}\rho(a,t,x)\, da$. Then the critical patch size formula is $L^* = \pi\sqrt{\frac{D}{\beta-\mu-\alpha}}$.

3. If $\beta(a,p) = \beta(ae^{-\alpha a})$, $\alpha > 0$ and $\mu(a,p) = \mu$, the equations can be reduced to the reaction diffusion equations

$$p_t + \mu p - \beta G = D p_{xx}, \tag{1.2.39}$$

$$C_t + [\mu + \alpha]\, C - \beta G = D C_{xx}, \tag{1.2.40}$$

$$G_t + [\mu + \alpha]\, G - C = D G_{xx}, \tag{1.2.41}$$

where $G(t,x) = \int_0^\infty a e^{-\alpha a}\rho(a,t,x)\, da$. Then the critical patch size will be $L^* = \pi\sqrt{\frac{D}{\sqrt{\beta}-\mu-\alpha}}$.

To get the reaction diffusion equation (1.2.36), we integrate (1.2.33) with respect to a

$$\int_0^\infty \frac{\partial\rho(a,t,x)}{\partial a} da + \int_0^\infty \frac{\partial\rho(a,t,x)}{\partial t} da + \int_0^\infty d(a,t,x)\, da = -\int_0^\infty \frac{\partial q(a,t,x)}{\partial x} da.$$

Since $\rho(a,t,x) \to 0$ as $a \to \infty$ and by using (1.2.34, 1.2.35), we get

$$-\beta p + p_t + \mu p = D p_{xx},$$

which is the reaction diffusion equation in (1.2.36). One can derive equations (1.2.37) and (1.2.38) by integrating both (1.2.33) and its multiplication by $e^{-\alpha a}$ with respect to a. In mathematical notation, we have

$$\int_0^\infty \frac{\partial \rho(a,t,x)}{\partial a} da + \int_0^\infty \frac{\partial \rho(a,t,x)}{\partial t} da + \int_0^\infty d(a,t,x)\, da = -\int_0^\infty \frac{\partial q(a,t,x)}{\partial x} da,$$

which is equivalent to

$$p_t + \mu p - \beta C = D p_{xx}.$$

Likewise,

$$\int_0^\infty e^{-\alpha a}\left(\frac{\partial \rho(a,t,x)}{\partial a} + \frac{\partial \rho(a,t,x)}{\partial t} + d(a,t,x)\right) da = -\int_0^\infty e^{-\alpha a} \frac{\partial q(a,t,x)}{\partial x} da,$$

implies

$$C_t + [\mu + \alpha - \beta] C = D C_{xx}.$$

Similarly, we get (1.2.39), (1.2.40) and (1.2.41) by integrating (1.2.33) and its multiplications by $e^{-\alpha a}$ and by $a e^{-\alpha a}$ with respect to a.

Continuous age-structured population models were also used by Bocharov and Hadeler [5]. They derived delay equations for the model of structured populations and discussed how the system can be affected by the initial data, and how the parameters of delay equations can be defined in terms of mortality and fertility rates. Fang et al. [22] also used continuous age-structured population models to calculate the spreading speed for Asian Clams. They showed that the invasion speed for Asian Clams coincides with the minimal speed of traveling wave front.

For discrete-time structured populations, Caswell and Werner [9] considered the popu-

lation of teasel (*Dipsacus sylvestris*). They defined seven stages for this plant: Seeds, Dormant seeds (year 1), Dormant seeds (year 2), Small rosettes, Medium rosettes, Large rosettes, and Flowering plants. According to Caswell [8], the non-spatial model for discrete-time, structured populations of m stages can be written as follows

$$\vec{\boldsymbol{u}}\,(t+1) = B\,(\vec{\boldsymbol{u}}\,(t))\,\vec{\boldsymbol{u}}\,(t)\,,$$

where $\vec{\boldsymbol{u}} = [u_1, u_2, \ldots, u_m]^T$, and b_{ij} is the production rate of stage i individuals by stage j individuals.

One can introduce movement in space into the matrix model via dispersal kernels and obtains the integrodifference equation for a structured population of m stages

$$\boldsymbol{n}(x, t+1) = \int_{-\infty}^{\infty} [\boldsymbol{k}(x,y) \circ \boldsymbol{B_n}(y)]\boldsymbol{n}(y,t)dy, \tag{1.2.42}$$

where n_i is the population density in the ith stage, $k_{ij}(x,y)$ is the probability density function for an individual to move from location y to location x given that it makes the transition from stage j at time t to stage i at time $t+1$. $\boldsymbol{B_n}(y)$ is the population projection matrix at location y; b_{ij} is the per capita production of stage i individuals at time $t+1$ by stage j individuals at time t, and the symbol '$\circ$' refers to the Hadamard product of pointwise matrix multiplication (Horn and Johnson [39]). Lui [52, 53] used (1.2.42) to prove the existence of an asymptotic spreading speed and of traveling waves. He showed that the minimal traveling wave speed and the asymptotic spreading speed are identical in homogeneous landscapes. Later, Neubert and Caswell [65] used integrodifference equations to study how the wave speed depends on population parameters. They considered the wave speed formula for discrete-time structured populations as appears in [52]

$$C\,(s) = \frac{1}{s} \ln\,(\rho_1\,(s))\,,$$

where $\rho_1(s)$ is the dominant eigenvalue of the matrix $H(s) = B \circ M(s)$, B is the matrix of vital rates at low population densities ($\boldsymbol{B_n}$ evaluated at $\boldsymbol{n} = 0$), $M(s)$ is the matrix of moment generating functions of dispersal kernels; $m_{ij}(s) = \int_{-\infty}^{\infty} k_{ij}(z) e^{sz} dz$, and s is the wave shape parameter. Then they used the minimal traveling wave speed formula, $C^* = \min_{s>0} \left[\frac{1}{s} \ln(\rho_1(s))\right]$, to study sensitivity and elasticity of the invasion speed for teasel (*Dispacus sylvestris*) and *Calathea ovandensis* to demographic parameters.

1.3. Glossary of the Most Important Terms

In this section, we summarize the most important concepts that will show up later in more detail in this dissertation.

Persistence **[38]**

The population is said to persist in an environment if it has a positive per capita growth rate at low density.

Critical Patch Size **[82]**

The habitat size, below which the population will go extinct and above which the population will persist.

Traveling Wave **[77]**

For the reaction-diffusion equation (1.2.1), a solution of the form $u(t,x) = U(x - Ct)$ is called a traveling wave solution, and C is called the traveling wave speed.

Minimal Traveling Wave Speed **[64]**

A value $\hat{C}$ is called the minimum traveling wave speed if there exists a positive traveling wave solution for all $C \geq \hat{C}$ and none for $C < \hat{C}$.

Traveling Periodic Wave Solution **[77]**

If L denotes the periodicity of the environmental variation, then a solution $u(t,x)$ is called a traveling periodic wave solution if there exists a time T^* such that, for all $x \in \mathbb{R}$ and $t > 0$, $u(t,x) = u(t + T^*, x + L)$ and $u(t,x) \to 0$ as $x \to \infty$.

Asymptotic Spreading Speed **[3]**

The population is said to spread with asymptotic speed C^* if an observer who travels at some speed $C > C^*$ will eventually be ahead of the population whereas an observer who travels at speed $C < C^*$ will eventually be surrounded by the population.

Dispersion Relation **[77]**

The implicit relation between the traveling wave speed C and the wave shape parameter s.

1.4. Model Formulation

We develop our theory here using a two-stage model where individuals are classified as either non-reproductive juveniles or as reproductive adults. This distinction is the simplest meaningful extension of the common unstructured modeling approach. We model spatial movement by using the ecological diffusion formulation for random movement in heterogeneous habitats (Turchin [87]), and restrict population dynamics to three linear processes, reproduction, maturation and mortality. Hence, our model has the differential equations

$$\frac{\partial u(t,x)}{\partial t} = \frac{\partial^2 \left(D_u(x)u(t,x)\right)}{\partial x^2} + r(x)v(t,x) - \left(m(x) + \mu_u(x)\right)u(t,x), \tag{1.4.1}$$

and

$$\frac{\partial v(t,x)}{\partial t} = \frac{\partial^2 \left(D_v(x)v(t,x)\right)}{\partial x^2} + m(x)u(t,x) - \mu_v(x)v(t,x), \tag{1.4.2}$$

where $u(t,x)$ and $v(t,x)$ are the density functions at time t and location x for juveniles and adults, respectively, $D_u(x)$ and $D_v(x)$ are the diffusion coefficients, $r(x)$ is the reproduction rate, $m(x)$ is the maturation rate, and $\mu_{u,v}(x)$ are the respective death rates.

This model requires a large amount of empirical data to estimate population parameters at different spatial locations. Instead, we follow the view of previous authors

[77, 55, 64, 17, 56]. In this view, the landscape consists of different patches; within each patch all population parameters are constant, between patches, they differ. For simplicity, we assume that there are only two types of patches: 'good' where the population can grow locally and 'bad' where the population goes extinct locally. With only two types of patches, we denote the values of the density and parameter functions by indices, i.e. we write $u_i(t,x)$ for the density of juveniles on patch type i (with $i = 1, 2$) and r_i for the value of $r(x)$ of a patch of type i, and similarly for all other densities and parameters. At the interfaces between two patch types where the parameter functions are discontinuous, we impose matching conditions of the form (1.2.29) and (1.2.30) for both densities.

1.5. Outline of the Thesis

In this thesis, we study in detail persistence conditions and traveling periodic waves of the model (1.4.1) and (1.4.2).

In Chapter 2, we use the Routh-Hurwitz criterion for stability to find the persistence condition for the non-spatial model. We also derive persistence conditions in homogeneous and heterogeneous landscapes. We then use analytic techniques to find the critical size of a single good patch surrounded by an infinite bad patch. We use the explicit expression for the critical size of a single patch to obtain formulas for the sensitivity and elasticity of L^* to population parameters.

In Chapter 3, we derive the dispersion relation for the juveniles-adults model in patchy landscapes. We then generalize the work of Fisher [23] to the spread speed of structured populations in homogeneous landscapes. We also apply sensitivity and elasticity formulas to the spread speed in a homogeneous landscape. We illustrate how the biased movement of one age group affects population persistence and spread. Finally, we discuss the importance of maturation rate in our model.

In Chapter 4, we consider structured populations with a sessile, i.e. immobile, age-

group. We derive persistence conditions in a single patch and in a heterogeneous habitat. We also derive the dispersion relation in patchy landscapes and find an explicit formula for the traveling wave speed in homogeneous landscapes.

In Chapter 5, we use asymptotic techniques to find the wave speed and the spread speed for structured populations in heterogeneous habitats. We write the density functions of juveniles and adults in a series expansion in some small parameter ϵ, and we solve the resulting differential equations of order ϵ^0, ϵ^1 and ϵ^2. We find an explicit formula for the traveling periodic wave speed for structured populations in heterogeneous landscapes. We illustrate the power of the homogenization method by comparing the dispersion relation and the resulting minimal wave speeds for the approximation and the exact expression. We also generalize this work to structured populations of n age groups.

In Chapter 6, we explore numerical solutions for the juveniles-adults model. In a single-patch landscape, we compare the numerical solution to the analytic solution for the linear model and explore how the numerical solution behaves in non-linear models. We also use numerical techniques to track the front location for different age groups and compare it with the location of theoretical speed for the juveniles-adults model.

In Chapter 7, we apply our model to study some aspects of population dynamics and harvesting in a marine setting. A good patch will correspond to a marine protected area whereas fishing will be allowed in a bad patch. We will study numerically how the movement behavior of individuals will affect population abundance and harvesting yield.

2. Persistence Conditions for the Juveniles-Adults Model

In this chapter, we study various aspects of persistence conditions of the model (1.4.1) and (1.4.2). We begin with the non-spatial model, then we study the model on a single suitable patch with various boundary conditions, and finally we consider the model on a periodic landscape consisting of alternating suitable and unsuitable patches.

2.1. Persistence Condition for the Non-Spatial Model

We begin with the persistence conditions for the non-spatial population dynamics of the model (1.4.1) and (1.4.2). Setting diffusion terms in equations (1.4.1) and (1.4.2) equal to zero, we have the following ordinary differential equations

$$\frac{d}{dt}u = rv - (m + \mu_u)\, u, \tag{2.1.1}$$

$$\frac{d}{dt}v = mu - \mu_v v. \tag{2.1.2}$$

For the purpose of this thesis, we say that the population can persist if the zero state of the linear system is unstable. We discuss population persistence in nonlinear models in Chapter 8. Since the system (2.1.1, 2.1.2) is linear, we obtain the stability conditions from analyzing the eigenvalues of the Jacobian matrix

$$J = \begin{bmatrix} -(m+\mu_u) & r \\ m & -\mu_v \end{bmatrix}.$$

The eigenvalues of J are given by the characteristic equation $\lambda^2 - \mathrm{tr}(J)\lambda + \det(J) = 0$, which is equivalent to $\lambda^2 + (m+\mu_v+\mu_u)\lambda + (m\mu_v + \mu_v\mu_u - rm) = 0$.
According to Routh-Hurwitz [45], the zero state is unstable if $\mathrm{tr}(J) > 0$ or $\det(J) < 0$. In terms of population parameters, these conditions are

$$-(m+\mu_v+\mu_u) > 0 \quad \text{or} \quad (m\mu_v + \mu_v\mu_u - rm) < 0.$$

Since $(m+\mu_v+\mu_u) > 0$, we get the persistence condition for non-spatial juveniles-adults model as $m\mu_v + \mu_v\mu_u - rm < 0$, which is equivalent to

$$r > \mu_v\left(1 + \frac{\mu_u}{m}\right). \tag{2.1.3}$$

We summarize these calculations in the following proposition.

Proposition 2.1.1. *If* $r > \mu_v\left(1+\frac{\mu_u}{m}\right)$, *then the equilibrium at the origin of* (*2.1.1*) *and* (*2.1.2*) *is unstable.*

The proposition states that the growth rate r must not only exceed the death rate of the adults μ_v but also account for juvenile mortality. As $1/m$ is the mean time to maturation, the term μ_u/m measures the mortality of juveniles before becoming adults. From now on, we define a patch to be 'good' if (2.1.3) holds and 'bad' when the reverse inequality holds.

2.2. Persistence Conditions in a Single-Patch Landscape

In this section we derive the persistence condition for the juveniles-adults model in a single-patch landscape. We consider equations (1.4.1) and (1.4.2) on a patch of length L. Without loss of generality, we choose the patch to be the interval $[0, L]$. In the simplest and classical case, we impose hostile boundary conditions

$$u(t,0) = u(t,L) = 0, \quad \text{and} \quad v(t,0) = v(t,L) = 0. \tag{2.2.1}$$

Ecologically, the boundary conditions in (2.2.1) mean that individuals who leave this patch will not return.

Like in the previous section, we determine persistence conditions by studying the stability of the zero state of our model. Since equations (1.4.1) and (1.4.2) are linear, we look for exponential solutions of the form

$$\begin{bmatrix} u(t,x) \\ v(t,x) \end{bmatrix} = e^{\lambda t} \begin{bmatrix} U(x) \\ V(x) \end{bmatrix}.$$

The corresponding eigenvalue problem of equations (1.4.1) and (1.4.2) can be written as the following system of ordinary differential equations

$$\lambda U(x) = D_u U_{xx}(x) - (m + \mu_u) U(x) + rV(x), \tag{2.2.2}$$

$$\lambda V(x) = D_v V_{xx}(x) + m\, U(x) - \mu_v V(x). \tag{2.2.3}$$

From equation (2.2.2) we get

$$V(x) = \frac{D_u U_{xx}(x) - (m + \mu_u + \lambda) U(x)}{-r}. \tag{2.2.4}$$

Substituting $V(x)$ and $\mathrm{V}_{xx}(x)$ into (2.2.3), we get

$$\frac{D_v}{r}\left[D_u\frac{d^4U(x)}{\mathrm{d}x^4} - B\,U_{xx}(x)\right] - m\,U(x) - \frac{(\mu_v+\lambda)}{r}\left[D_u U_{xx}(x) - B\,U(x)\right] = 0, \quad (2.2.5)$$

where $B = m + \mu_u + \lambda$.

Sorting by derivatives of U, we get the following ordinary differential equation for the function $U(x)$

$$\frac{\mathrm{d}^4U(x)}{\mathrm{d}x^4} - \frac{[D_v B + (\mu_v+\lambda)D_u]}{D_v D_u}U_{xx}(x) - \frac{[r\,m - (\mu_v+\lambda)B]}{D_v D_u}U(x) = 0, \quad (2.2.6)$$

with boundary conditions

$$U(0) = U(L) = 0, \quad \text{and} \quad U_{xx}(0) = U_{xx}(L) = 0.$$

The linear differential equation (2.2.6) has a bi-quadratic characteristic equation

$$z^4 - az^2 - b = 0, \quad (2.2.7)$$

with coefficients

$$a = \frac{D_v B + (\mu_v+\lambda)D_u}{D_v D_u},\ b = \frac{r\,m - (\mu_v+\lambda)B}{D_v D_u}.$$

Equation (2.2.7) has the four roots

$$z = \pm\sqrt{\frac{a \pm (a^2+4b)^{\frac{1}{2}}}{2}}. \quad (2.2.8)$$

We are interested in the case where $\lambda = 0$ because it assigns the boundary between extinction and persistence regions. If $\lambda = 0$, then $a > 0$, while the sign of the parameter b still has two possibilities. We consider the case $b > 0$ here; at the end of this section we discuss the other case.

If $b > 0$, then $a + (a^2 + 4b)^{\frac{1}{2}} > 0$ and $a - (a^2 + 4b)^{\frac{1}{2}} < 0$. Therefore (2.2.8) has two real roots and two pure imaginary roots. The two real roots have the same magnitude with different signs, the same property holds for the imaginary roots.
Therefore,

$$U(x) = C\cosh(z_1 x) + G\sinh(z_1 x) + H\cos(z_2 x) + F\sin(z_2 x), \tag{2.2.9}$$

where

$$z_1 = \sqrt{\frac{a + (a^2 + 4b)^{\frac{1}{2}}}{2}}, \quad \text{and} \quad z_2 = \sqrt{\frac{(a^2 + 4b)^{\frac{1}{2}} - a}{2}}. \tag{2.2.10}$$

Applying the boundary condition $U(0) = 0$ to equation (2.2.9), we get $C + H = 0$. Also, the boundary condition $U_{xx}(0) = 0$ gives $Cz_1^2 - Hz_2^2 = 0$. As a consequence, we get $C = H = 0$. From the boundary condition $U(L) = 0$, we have

$$G\sinh(z_1 L) + F\sin(z_2 L) = 0. \tag{2.2.11}$$

Finally, the boundary condition $U_{xx}(L) = 0$ implies

$$Gz_1^2\sinh(z_1 L) - Fz_2^2\sin(z_2 L) = 0. \tag{2.2.12}$$

We conclude that $G = 0$ and reach the persistence condition for a single-patch landscape as $\sin(z_2 L) = 0$. We summarize the calculations as follows.

Proposition 2.2.1. *The persistence boundary for the juveniles-adults model in a single-patch landscape is*

$$\sin(z_2 L) = 0. \tag{2.2.13}$$

Accordingly, the minimal patch-size is given by

$$L^* = \frac{\pi}{z_2}, \tag{2.2.14}$$

with z_2 as in (2.2.10).

We illustrate how the critical patch size depends on model parameters. We notice that the critical patch size decreases with the reproduction rate (Figure 2.1(a)) and with maturation rate (Figure 2.1(b)). We investigated the relationship with all other parameters (D_u, D_v, μ_u and μ_v) and found that the critical patch size increases with each of them (plots not shown).

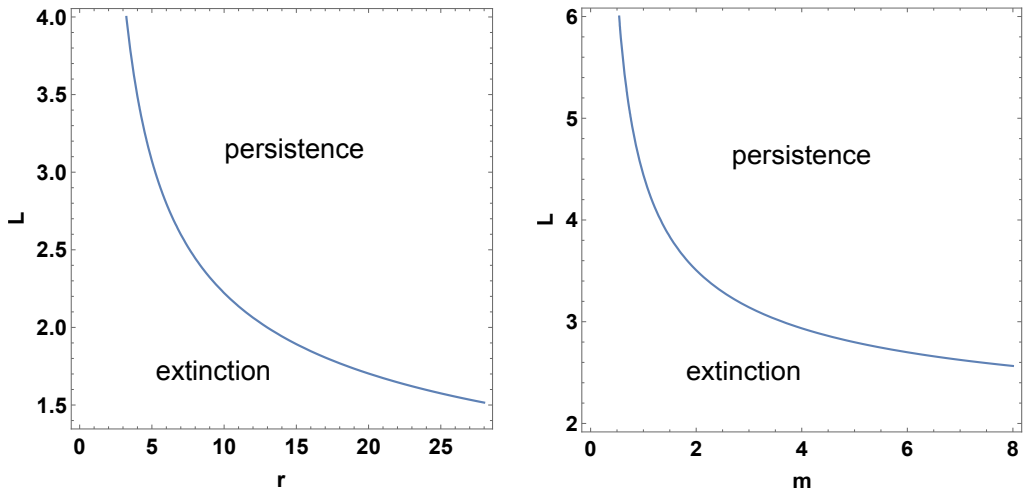

Figure 2.1.: Critical patch size for the juveniles-adults model in a single-patch landscape (2.2.13): (a) as a function of reproduction rate r; (b) as a function of maturation rate m. Parameters are as follows unless otherwise noted: $r = 6$, $m = 5$, $\mu_{\mathrm{u}} = \mu_v = 1$, and $D_v = D_{\mathrm{u}} = 2$.

Remark 2.2.2. *If b in equation (2.2.7) is a negative number, and $a > 0$, then by following the same steps that we presented in this section one can derive the persistence condition for a single-patch landscape as*

$$\sinh(Lz_1)\sinh(Lz_2) = 0. \tag{2.2.15}$$

The last equation cannot hold unless $L = 0$. So, there is no need to consider this case. We can understand this result by the following ecological explanation. Since

$b < 0$, then by Proposition 2.1.1, this single-patch will be a 'bad patch', which means that the population will go extinct in this single-patch landscape. And so, there is no persistence condition in a single-patch landscape under the assumption $b < 0$.

2.3. Persistence Conditions in a Periodically Varying Landscape

We assume that the landscape has infinitely many patches of two types, periodically alternating (see Figure 1.1): 'good patches' and 'bad patches'. We use L_1 and L_2 to represent the good patch size and the bad patch size, respectively. And so, $L = L_1 + L_2$ represents the spatial period. Hence we study model (1.4.1), (1.4.2) with piecewise constant, periodic coefficients. We need to characterize the behavior of individuals at the interface between two patch types. We assume that no individuals are created or lost as they cross from one patch type into another. This assumption translates into the population fluxes being continuous at the interface. On the other hand, we allow individuals to have a preference for one or the other patch type. The derivation in Section 1.2.1 and in [55, 69] then shows that the population density across an interface need not be continuous.

For the sake of the argument, let us assume that $x = 0$ is an interface between a good patch to the right (i.e. $x > 0$) and a bad patch to the left (i.e. $x < 0$). Later, we shall use the same formulation for any interface location. Let us further denote by $\alpha \in (0, 1)$ the probability that an individual at the interface will move into the good patch. Then the density matching conditions for juveniles at $x = 0$ (according to (1.2.29)) are given by

$$u_1\left(t, 0^+\right) = \frac{\alpha_u}{1 - \alpha_u} \frac{D_{u2}}{D_{u_1}} u_2\left(t, 0^-\right), \tag{2.3.1}$$

and

$$\frac{\partial u_1}{\partial x}\left(t,0^+\right)=\frac{D_{u_2}}{D_{u_1}}\frac{\partial u_2}{\partial x}\left(t,0^-\right), \tag{2.3.2}$$

and similarly for adults (see also (2.3.12) and (2.3.15)). A value of $\alpha=0.5$ indicates no preference whereas a value of $\alpha=1$ indicates the strongest preference for the good patch type. We will abbreviate the dimensionless parameter combination in (2.3.1) and write

$$k_u=\frac{\alpha_u}{1-\alpha_u}\frac{D_{u_2}}{D_{u_1}}, \tag{2.3.3}$$

and similarly for k_v.

We now derive a persistence condition for the juveniles-adults model in the periodic landscape for the general case in which diffusion coefficients in (1.4.1) and (1.4.2) are positive. To make use of the symmetric in the model, it turns out to be helpful to choose the good patches as $\left(\frac{-L_1}{2},\frac{L_1}{2}\right)+L\mathbb{Z}$ and the bad patches as $\left(\frac{-L_1}{2},\frac{L_1}{2}\right)+L\mathbb{Z}$. Hence, the interfaces will be at $\frac{L_1}{2}+L\mathbb{Z}$ and $\frac{L_1}{2}+L\mathbb{Z}$. We follow the same procedure in Section 2.2 to reach the following periodic system of ordinary differential equations for the eigenvalue problem

$$\begin{aligned}0=&\frac{d^4U_1}{dx^4}-\frac{\left(D_{v1}\left(m_1+\mu_{u_1}+\lambda\right)+\left(\mu_{v_1}+\lambda\right)D_{u_1}\right)}{D_{u_1}D_{v_1}}\frac{d^2U_1}{dx^2}\\&-\frac{\left(r_1m_1-\left(m_1+\mu_{u_1}+\lambda\right)\left(\mu_{v_1}+\lambda\right)\right)}{D_{u_1}D_{v_1}}U_1,\quad x\in\left(\frac{-L_1}{2},\frac{L_1}{2}\right)+L\mathbb{Z},\end{aligned} \tag{2.3.4}$$

and

$$\begin{aligned}0=&\frac{d^4U_2}{dx^4}-\frac{\left(D_{v_2}\left(m_2+\mu_{u_2}+\lambda\right)+\left(\mu_{v_2}+\lambda\right)D_{u_2}\right)}{D_{u_2}D_{v_2}}\frac{d^2U_2}{dx^2}\\&-\frac{\left(r_2m_2-\left(m_2+\mu_{u_2}+\lambda\right)\left(\mu_{v_2}+\lambda\right)\right)}{D_{u_2}D_{v_2}}U_2,\quad x\in\left(\frac{L_1}{2},L-\frac{L_1}{2}\right)+L\mathbb{Z}.\end{aligned} \tag{2.3.5}$$

Since the landscape is periodically varying and we are looking for periodic solutions of the same period, we can restrict the analysis to one good patch and one bad patch.

Solutions are symmetric in the intervals $\left(\frac{-L_1}{2}, \frac{L_1}{2}\right)$ and $\left(\frac{L_1}{2}, L - \frac{L_1}{2}\right)$ (see Figure 2.2). Therefore, we can equivalently study the solutions on the intervals $\left(0, \frac{L_1}{2}\right)$ and $\left(\frac{L_1}{2}, \frac{L}{2}\right)$ with no-flux boundary conditions in the original variables, see (2.3.10) and (2.3.11) below.

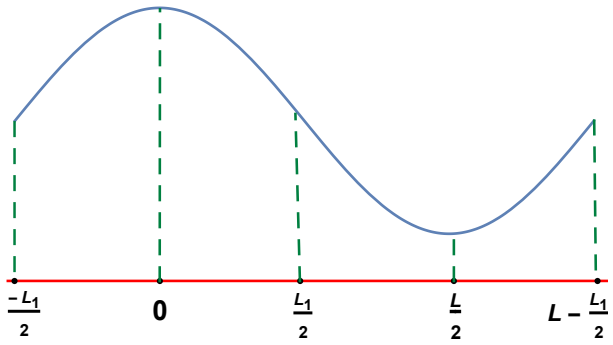

Figure 2.2.: Illustration of the solution of (2.3.4) and (2.3.5) in a good patch located at $\left(\frac{-L_1}{2}, \frac{L_1}{2}\right)$ and in a bad patch situated at $\left(\frac{L_1}{2}, L - \frac{L_1}{2}\right)$.

The linear differential equation (2.3.4) has a bi-quadratic characteristic equation

$$z^4 - az^2 - b = 0, \tag{2.3.6}$$

where

$$a = \frac{D_{v1}\left(m_1 + \mu_{u_1} + \lambda\right) + \left(\mu_{v_1} + \lambda\right) D_{u1}}{D_{u_1} D_{v_1}}, \quad b = \frac{r_1 m_1 - \left(m_1 + \mu_{u_1} + \lambda\right)\left(\mu_{v_1} + \lambda\right)}{D_{u_1} D_{v_1}}.$$

The roots of (2.3.6) are

$$z = \pm\sqrt{\frac{a \pm \left(a^2 + 4b\right)^{\frac{1}{2}}}{2}}.$$

We are interested in the case in which $\lambda = 0$ because it assigns the boundary between extinction and persistence regions. When $\lambda = 0$, we have $a > 0$. The sign of the parameter b changes according to the patch type: in good patches we have $b > 0$ while in bad patches we have $b < 0$ (see Proposition 2.1.1).

If $b > 0$, then $a + (a^2 + 4b)^{\frac{1}{2}} > 0$ and $a - (a^2 + 4b)^{\frac{1}{2}} < 0$. Thus, the roots of (2.3.6) are two real roots and two pure imaginary roots. The two real roots have the same magnitude with different signs, the same property holds for the imaginary roots. The eigenfunction U_1 is given by

$$U_1(x) = B_1 \cosh(z_1 x) + C_1 \sinh(z_1 x) + G_1 \cos(z_2 x) + H_1 \sin(z_2 x), \tag{2.3.7}$$

$$\text{where } z_1 = \sqrt{\frac{a + (a^2 + 4b)^{\frac{1}{2}}}{2}}, \quad z_2 = \sqrt{\frac{-a + (a^2 + 4b)^{\frac{1}{2}}}{2}}.$$

Similarly, the linear differential equation (2.3.5) has the following bi-quadratic characteristic equation

$$(z')^4 - a' (z')^2 - b' = 0, \tag{2.3.8}$$

where

$$a' = \frac{D_{v_2} (m_2 + \mu_{u_2} + \lambda) + (\mu_{v_2} + \lambda) D_{u2}}{D_{u_2} D_{v_2}}, \quad b' = \frac{r_2 m_2 - (m_2 + \mu_{u_2} + \lambda)(\mu_{v_2} + \lambda)}{D_{u_2} D_{v_2}}.$$

The roots then of (2.3.8) are

$$z' = \pm \sqrt{\frac{a' \pm \left((a')^2 + 4b'\right)^{\frac{1}{2}}}{2}}.$$

If $b' < 0$, then $a' + \left((a')^2 + 4b'\right)^{\frac{1}{2}} > 0$ and $a' - \left((a')^2 + 4b'\right)^{\frac{1}{2}} > 0$.
We can use the invariance of the equations under the reflection at $x = L/2$ to write the eigenfunction U_2 as

$$\begin{aligned} U_2(x) = \Bigg(& B_2 \cosh\left(z_3 \left(\frac{L}{2} - x\right)\right) + C_2 \sinh\left(z_3 \left(\frac{L}{2} - x\right)\right) \\ & + G_2 \cosh\left(z_4 \left(\frac{L}{2} - x\right)\right) + H_2 \sinh\left(z_4 \left(\frac{L}{2} - x\right)\right) \Bigg), \end{aligned} \tag{2.3.9}$$

where

$$z_3 = \sqrt{\frac{a' + \left((a')^2 + 4b'\right)^{\frac{1}{2}}}{2}}, \quad z_4 = \sqrt{\frac{a' - \left((a')^2 + 4b'\right)^{\frac{1}{2}}}{2}}.$$

Since solutions are symmetric in $\left(\frac{-L_1}{2}, \frac{L_1}{2}\right)$ and $\left(\frac{L_1}{2}, L - \frac{L_1}{2}\right)$, we have the following boundary conditions

$$U_1'(0) = V_1'(0) = 0, \tag{2.3.10}$$

and

$$U_2'\left(\frac{L}{2}\right) = V_2'\left(\frac{L}{2}\right) = 0. \tag{2.3.11}$$

We use the following relations when we apply the boundary and interface conditions

$$V_i(x) = \frac{D_{u_i} U_i''(x) - (m_i + \mu_{u_i} + \lambda) U_i(x)}{-r_i}, \quad i = 1, 2.$$

From (2.3.10), we have $z_1 C_1 + z_2 H_1 = 0$ and $(z_1)^3 C_1 - (z_2)^3 H_1 = 0$. As a consequence, we get $C_1 = 0 = H_1$. Similarly, the boundary conditions in (2.3.11) produce $-z_3 C_2 - z_4 H_2 = 0$ and $-(z_3)^3 C_2 - (z_4)^3 H_2 = 0$, which implies $C_2 = 0 = H_2$. Hence, the eigenfunctions $U_1(x)$, $U_2(x)$ become as follows

$$U_1(x) = B_1 \cosh(z_1 x) + G_1 \cos(z_2 x), \; x \in \left(0, \frac{L_1}{2}\right),$$

$$U_2(x) = B_2 \cosh\left(z_3\left(\frac{L}{2} - x\right)\right) + G_2 \cosh\left(z_4\left(\frac{L}{2} - x\right)\right), \; x \in \left(\frac{L_1}{2}, \frac{L}{2}\right).$$

The next step is to apply the interface conditions

$$u_1\left(t, \frac{L_1^-}{2}\right) = k_u u_2\left(t, \frac{L_1^+}{2}\right), \tag{2.3.12}$$

$$D_{u_1} \frac{\partial u_1}{\partial x}\left(t, \frac{L_1^-}{2}\right) = D_{u_2} \frac{\partial u_2}{\partial x}\left(t, \frac{L_1^+}{2}\right), \tag{2.3.13}$$

$$v_1\left(t, \frac{L_1^-}{2}\right) = k_v v_2\left(t, \frac{L_1^+}{2}\right), \tag{2.3.14}$$

and

$$D_{v_1}\frac{\partial v_1}{\partial x}\left(t, \frac{L_1^-}{2}\right) = D_{v_2}\frac{\partial v_2}{\partial x}\left(t, \frac{L_1^+}{2}\right). \tag{2.3.15}$$

Here, k_u, k_v denote the parameters that measure the discontinuity in density at the interface for juveniles and adults, respectively, as they appear in equations $(1.2.27) - (1.2.29)$.

Applying the interface conditions (2.3.12)-(2.3.15), we get

$$0 = B_1\cosh\left(\frac{z_1L_1}{2}\right) + G_1\cos\left(\frac{z_2L_1}{2}\right) - k_uB_2\cosh\left(\frac{z_3L_2}{2}\right) - k_uG_2\cosh\left(\frac{z_4L_2}{2}\right), \tag{2.3.16}$$

$$\begin{aligned} 0 = {} & B_1\cosh\left(\frac{z_1L_1}{2}\right)\left(rD_{u_1}(z_1)^2 - rA\right) + B_2\cosh\left(\frac{z_3L_2}{2}\right)\left(k_vB - k_vD_{u_2}(z_3)^2\right) \\ & - G_1\cos\left(\frac{z_2L_1}{2}\right)\left(rD_{u_1}(z_2)^2 + rA\right) + G_2\cosh\left(\frac{z_4L_2}{2}\right)\left(k_vB - k_vD_{u_2}(z_4)^2\right), \end{aligned} \tag{2.3.17}$$

$$0 = z_1B_1\sinh\left(\frac{z_1L_1}{2}\right) - z_2G_1\sin\left(\frac{z_2L_1}{2}\right) + D_uz_3B_2\sinh\left(\frac{z_3L_2}{2}\right) + D_uz_4G_2\sinh\left(\frac{z_4L_2}{2}\right), \tag{2.3.18}$$

$$\begin{aligned} 0 = {} & B_1\sinh\left(\frac{z_1L_1}{2}\right)\left(rD_{u_1}(z_1)^3 - rAz_1\right) + B_2D_v\sinh\left(\frac{z_3L_2}{2}\right)\left(D_{u_2}(z_3)^3 + Bz_3\right) \\ & + G_1\sin\left(\frac{z_2L_1}{2}\right)\left(rD_{u_1}(z_2)^3 + rAz_2\right) + G_2D_v\sinh\left(\frac{z_4L_2}{2}\right)\left(D_{u_2}(z_4)^3 + Bz_4\right), \end{aligned} \tag{2.3.19}$$

where $A = (m_1 + \mu_{u_1})$ and $B = (m_2 + \mu_{u_2})$. This is a linear system of equations for $B_{1,2}$, $G_{1,2}$. We write the coefficient matrix of (2.3.16)-(2.3.19) as follows

$$
W = \begin{bmatrix}
\cosh\left(\frac{z_1 L_1}{2}\right) & \cos\left(\frac{z_2 L_1}{2}\right) & -k_u \cosh\left(\frac{z_3 L_2}{2}\right) & -k_u \cosh\left(\frac{z_4 L_2}{2}\right) \\
z_1 \sinh\left(\frac{z_1 L_1}{2}\right) & -z_2 \sin\left(\frac{z_2 L_1}{2}\right) & D_u z_3 \sinh\left(\frac{z_3 L_2}{2}\right) & D_u z_4 \sinh\left(\frac{z_4 L_2}{2}\right) \\
r\left(D_{u_1}\left(z_1\right)^2 - A\right)\cosh\left(\frac{z_1 L_1}{2}\right) & r\left(-D_{u_1}\left(z_2\right)^2 - A\right)\cos\left(\frac{z_2 L_1}{2}\right) & -k_v\left(D_{u_2}\left(z_3\right)^2 - B\right)\cosh\left(\frac{z_3 L_2}{2}\right) & k_v\left(-D_{u_2}\left(z_4\right)^2 + B\right)\cosh\left(\frac{z_4 L_2}{2}\right) \\
r\left(D_{u_1}\left(z_1\right)^3 - z_1 A\right)\sinh\left(\frac{z_1 L_1}{2}\right) & r\left(D_{u_1}\left(z_2\right)^3 + z_2 A\right)\sin\left(\frac{z_2 L_1}{2}\right) & D_v\left(D_{u_2}\left(z_3\right)^3 - z_3 B\right)\sinh\left(\frac{z_3 L_2}{2}\right) & D_v\left(D_{u_2}\left(z_4\right)^3 - z_4 B\right)\sinh\left(\frac{z_4 L_2}{2}\right)
\end{bmatrix}
$$

The determinant is given by

$$
\begin{aligned}
\det W = {} & D_v z_3 z_2 \left(D_{u_2}(z_3)^2 - B\right)\left(Bk_v - Ak_u r + D_{u_1}k_u r(z_1)^2 + D_{u_2}k_v(z_4)^2\right) \\
& \times \sin\left(\frac{z_2 L_1}{2}\right)\cosh\left(\frac{z_4 L_2}{2}\right)\cosh\left(\frac{z_1 L_1}{2}\right)\sinh\left(\frac{z_3 L_2}{2}\right) \\
& - D_v z_3 z_4 \left(-B + D_{u_2}(z_3)^2\right) D_{u_2} r \left(z_1^2 + z_2^2\right) \\
& \times \cosh\left(\frac{z_1 L_1}{2}\right)\cos\left(\frac{z_2 L_1}{2}\right)\sinh\left(\frac{z_4 L_2}{2}\right)\sinh\left(\frac{z_3 L_2}{2}\right) \\
& + D_u r z_3 z_2 \left(A + D_{u_1}(z_2)^2\right)\left(Bk_v - Ak_u r + D_{u_1}k_u r z_1^2 - D_{u_2}k_v z_4^2\right) \\
& \times \cosh\left(\frac{z_1 L_1}{2}\right)\cosh\left(\frac{z_4 L_2}{2}\right)\sin\left(\frac{z_2 L_1}{2}\right)\sinh\left(\frac{z_3 L_2}{2}\right) \\
& + r z_1 z_2 \left(A + D_{u_1} z_2^2\right)\left(D_{u_2} k_v k_u\right)\left(z_3^2 - z_4^2\right) \\
& \times \sinh\left(\frac{z_1 L_1}{2}\right)\cosh\left(\frac{z_3 L_2}{2}\right)\cosh\left(\frac{z_4 L_2}{2}\right)\sin\left(\frac{z_2 L_1}{2}\right) \\
& + r z_2 z_4 \left(A + D_{u_1} z_2^2\right) D_u \left(-Bk_v + Ak_u r - D_{u_1}k_u r z_1^2 + D_{u_2}k_v z_3^2\right) \\
& \times \sin\left(\frac{z_2 L_1}{2}\right)\cosh\left(\frac{z_3 L_2}{2}\right)\cosh\left(\frac{z_1 L_1}{2}\right)\sinh\left(\frac{z_4 L_2}{2}\right) \\
& - z_1 z_3 \left(-B + D_{u_2} z_3^2\right) D_v \left(-Bk_v + Ak_u r + D_{u_1}k_u r z_2^2 + D_{u_2}k_v z_4^2\right) \\
& \times \cos\left(\frac{z_2 L_1}{2}\right)\sinh\left(\frac{z_1 L_1}{2}\right)\cosh\left(\frac{z_4 L_2}{2}\right)\sinh\left(\frac{z_3 L_2}{2}\right) \\
& + D_v z_4 z_1 \left(-B + D_{u_2} z_4^2\right)\left(-Bk_v + Ak_u r + D_{u_1}k_u r z_2^2 + D_{u_2}k_v z_3^2\right) \\
& \times \sinh\left(\frac{z_4 L_2}{2}\right)\cos\left(\frac{z_2 L_1}{2}\right)\cosh\left(\frac{z_3 L_2}{2}\right)\sinh\left(\frac{z_1 L_1}{2}\right) \\
& - D_v z_4 z_2 \left(-B + D_{u_2} z_4^2\right)\left(Bk_v - Ak_u r + D_{u_1}k_u r z_1^2 - D_{u_2}k_v z_3^2\right) \\
& \times \sinh\left(\frac{z_4 L_2}{2}\right)\cosh\left(\frac{z_1 L_1}{2}\right)\cosh\left(\frac{z_3 L_2}{2}\right)\sin\left(\frac{z_2 L_1}{2}\right) \\
& + D_v z_4 z_3 \left(-B + D_{u_2} z_4^2\right) D_{u_2} r \left(z_1^2 + z_2^2\right) \\
& \times \sinh\left(\frac{z_4 L_2}{2}\right)\cos\left(\frac{z_2 L_1}{2}\right)\cosh\left(\frac{z_1 L_1}{2}\right)\sinh\left(\frac{z_3 L_2}{2}\right) \\
& - r z_2 z_1 D_{u_2} k_v k_u \left(-A + D_{u_1} z_1^2\right)\left(-z_3^2 + z_4^2\right) \\
& \times \sinh\left(\frac{z_1 L_1}{2}\right)\cosh\left(\frac{z_4 L_2}{2}\right)\cosh\left(\frac{z_3 L_2}{2}\right)\sin\left(\frac{z_2 L_1}{2}\right)
\end{aligned}
$$

$$
\begin{aligned}
&- rz_1z_4\left(-A+D_{u_1}z_1^2\right)D_u\left(-Bk_v+Ak_ur+D_{u_1}k_ur z_2^2+D_{u_2}k_vz_3^2\right)\\
&\times\sinh\left(\frac{z_1L_1}{2}\right)\cos\left(\frac{z_2L_1}{2}\right)\cosh\left(\frac{z_3L_2}{2}\right)\sinh\left(\frac{z_4L_2}{2}\right)\\
&- rz_1z_3\left(-A+D_{u_1}z_1^2\right)D_u\left(Bk_v-Ak_ur-D_{u_1}k_ur z_2^2-D_{u_2}k_vz_4^2\right)\\
&\times\sinh\left(\frac{z_1L_1}{2}\right)\cos\left(\frac{z_2L_1}{2}\right)\cosh\left(\frac{z_4L_2}{2}\right)\sinh\left(\frac{z_3L_2}{2}\right),
\end{aligned}
$$

where $D_u=\frac{D_{u_2}}{D_{u_1}}$, $D_v=\frac{D_{v_2}}{D_{v_1}}$, $r=\frac{r_2}{r1}$, $A=(m_1+\mu_{u_1})$ and $B=(m_2+\mu_{u_2})$.
A linear system has a nontrivial solution if the determinant of the coefficient matrix equals zero. By equating the previous determinant to zero and dividing the whole equation by

$$\cosh\left(\frac{z_1L_1}{2}\right)\cos\left(\frac{z_2L_1}{2}\right)\cosh\left(\frac{z_3L_2}{2}\right)\cosh\left(\frac{z_4L_2}{2}\right),$$

we reach the persistence condition for the juveniles-adults model

$$
\begin{aligned}
0 &= z_3z_2\left(-BD_v+AD_ur+D_{u_2}z_2^2r+D_vD_{u_2}z_3^2\right)\\
&\times\left(Bk_v-Ak_ur+D_{u_1}k_ur z_1^2-D_{u_2}k_vz_4^2\right)\tan\left(\frac{z_2L_1}{2}\right)\tanh\left(\frac{z_3L_2}{2}\right)\\
&+ z_4z_3\left(D_{u_2}\right)^2D_vr\left(z_1^2+z_2^2\right)\left(z_4^2-z_3^2\right)\tanh\left(\frac{z_4L_2}{2}\right)\tanh\left(\frac{z_3L_2}{2}\right)\\
&+ z_1z_2rD_{u_1}D_{u_2}k_vk_u\left(z_2^2+z_1^2\right)\left(z_3^2-z_4^2\right)\tanh\left(\frac{z_1L_1}{2}\right)\tan\left(\frac{z_2L_1}{2}\right)\\
&+ z_1z_4\left(-rD_{u_2}z_1^2+rAD_u-D_vB+D_vD_{u_2}z_4^2\right)\\
&\times\left(Ak_ur-Bk_v+D_{u_1}k_ur z_2^2+D_{u_2}k_vz_3^2\right)\tanh\left(\frac{z_1L_1}{2}\right)\tanh\left(\frac{z_4L_2}{2}\right)\\
&+ z_1z_3\left(rD_{u_2}z_1^2-AD_ur+D_vB-D_vD_{u_2}z_3^2\right)\\
&\times\left(-Bk_v+Ak_ur+D_{u_1}k_ur z_2^2+D_{u_2}k_vz_4^2\right)\tanh\left(\frac{z_1L_1}{2}\right)\tanh\left(\frac{z_3L_2}{2}\right)\\
&- z_2z_4\left(-BD_v+D_vD_{u_2}z_4^2+rAD_u+rD_{u_2}z_2^2\right)\\
&\times\left(Bk_v-Ak_ur+D_{u_1}k_ur z_1^2-D_{u_2}k_vz_3^2\right)\tan\left(\frac{z_2L_1}{2}\right)\tanh\left(\frac{z_4L_2}{2}\right). \qquad (2.3.20)
\end{aligned}
$$

Proposition 2.3.1. *The persistence boundary for the juveniles-adults model on a*

periodic landscape is given by the relation in (2.3.20).

We illustrate how population persistence depends on model parameters. In Figure 2.3, we notice that the critical good patch size increases with the bad patch size. Figure 2.4 shows that the critical good patch size decreases with both reproduction and maturation rates in good patches.

Remark 2.3.2. *In deriving persistence conditions we assumed that* a^2+4b *is a positive real number. To prove this assumption, assume first* $a^2+4b=0$. *Hence,*

$$\frac{\left[D_{v_1}\left(m_1+\mu_{u_1}+\lambda\right)+\left(\mu_{v_1}+\lambda\right)D_{u_1}\right]^2}{\left(D_{v_1}D_{u_1}\right)^2}=\frac{4\left[\left(m_1+\mu_{u_1}+\lambda\right)\left(\mu_{v_1}+\lambda\right)-r_1m_1\right]}{D_{v_1}D_{u_1}}.$$

Simplifying the last equation, we get

$$\begin{aligned}&\left(D_{v_1}\right)^2\left(m_1+\mu_{u_1}+\lambda\right)^2+\left(D_{u_1}\right)^2\left(\mu_{v_1}+\lambda\right)^2-4D_{v_1}D_{u_1}r_1m_1\\ =\;&4D_{v_1}D_{u_1}\left(m_1+\mu_{u_1}+\lambda\right)\left(\mu_{v_1}+\lambda\right)+2D_{u_1}D_{v_1}\left(\mu_{v_1}+\lambda\right)\left(m_1+\mu_{u_1}+\lambda\right),\end{aligned}$$

which is equivalent to

$$\begin{aligned}&\left(D_{v_1}\right)^2\left(m_1+\mu_{u_1}+\lambda\right)^2+\left(D_{u_1}\right)^2\left(\mu_{v_1}+\lambda\right)^2-2D_{u_1}D_{v_1}\left(\mu_{v_1}+\lambda\right)\left(m_1+\mu_{u_1}+\lambda\right)\\ &=-4D_{v_1}D_{u_1}r_1m_1.\end{aligned}$$

Therefore

$$\left(D_{v_1}\left(m_1+\mu_{u_1}+\lambda\right)-D_{u_1}\left(\mu_{v_1}+\lambda\right)\right)^2=-4D_{v_1}D_{u_1}r_1m_1.$$

The left hand side and the right hand side of the last equation have opposite signs, which is a contradiction. Thus, $a^2+4b\neq 0$. *By following the same argument it can be shown that* $a^2+4b\not<0$. *This proves that* a^2+4b *is always a positive number.*

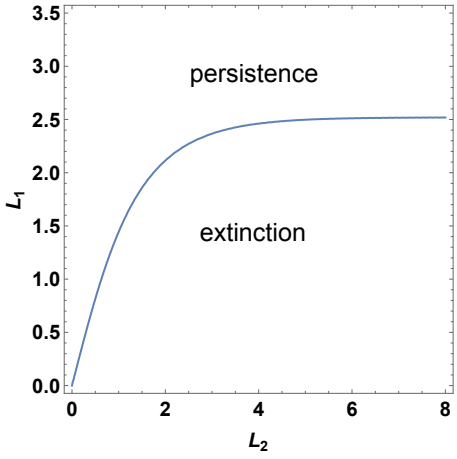

Figure 2.3.: Persistence boundary according to (2.3.20) for the juveniles-adults model in a patchy landscape as a function of 'bad patch' size L_2 and 'good patch' size L_1. Parameters are as follows unless otherwise noted: $r_1 = 2$, $r_2 = 0.2$, $\mu_{u_2} = 2 = \mu_{v_2}$, $D_{u_1} = 1 = D_{v_1}$, $D_{v_2} = 2 = D_{u_2}$, $\mu_{u_1} = \mu_{v_1} = 1$, $m_1 = 5$, $m_2 = 1$, and $\alpha_u = \alpha_v = 0.5$.

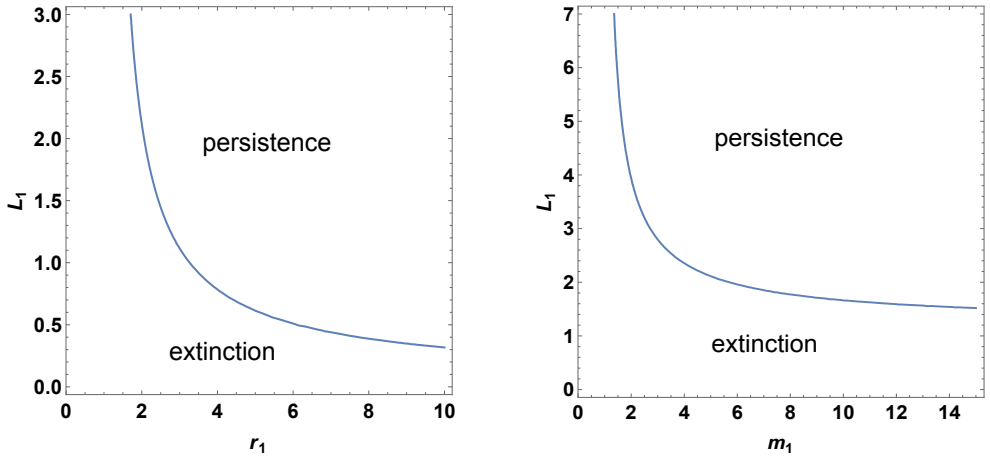

(a) **(b)**

Figure 2.4.: Persistence boundary according to (2.3.20) for the juveniles-adults model in a patchy landscape: (a) as a function of reproduction rate in 'good patches' r_1 and 'good patch' size L_1; (b) as a function of maturation rate in 'good patches' m_1 and 'good patch' size L_1. Parameters are as follows unless otherwise noted: $L_2 = 2$, $r_1 = 2$, $r_2 = 0.2$, $\mu_{u_2} = 2 = \mu_{v_2}$, $D_{u_1} = 1 = D_{v_1}$, $D_{v_2} = 2 = D_{u_2}$, $\mu_{u_1} = \mu_{v_1} = 1$, $m_1 = 5$, $m_2 = 1$, and $\alpha_u = \alpha_v = 0.5$.

2.4. Single-Patch Landscapes Via Patchy Landscapes

In Sections 2.2 and 2.3, we derived persistence conditions for both single-patch landscapes and patchy landscapes. Here, we derive the former as a limit of the latter. We use the behavior of juveniles and adults at the interface. If $\alpha_u = \alpha_v \ll 1$, we expect juveniles and adults to move to the bad patch when they reach an interface and not return to the good patch. This is equivalent to a single-patch landscape with hostile boundary conditions. Analytically, taking the limit for (2.3.20) as α_u, $\alpha_v \to 0$, gives the condition

$$\cos\left(\frac{L_1}{2}z_2\right)\cosh\left(\frac{L_1}{2}z_1\right)\sinh\left(\frac{L_2}{2}z_3\right)\sinh\left(\frac{L_2}{2}z_4\right) = 0, \tag{2.4.1}$$

which holds only if $\cos\left(\frac{L_1}{2}z_2\right) = 0$. This implies the critical patch size for a single-patch landscape

$$L_1^* = \frac{\pi}{z_2}, \tag{2.4.2}$$

which is the same as (2.2.14). The other case that produces a single-patch landscape is the case with very large mortality parameters in the bad patches. Ecologically, when mortality becomes very large in bad patches, all individuals who leave the good patches will not be able to survive. Hence, the environment will be consisting of one good patch surrounded by a completely hostile bad patch. Mathematically, we get the same formulas in (2.4.1) and (2.4.2) when we take the limit of (2.3.20) as μ_{u_2}, $\mu_{v_2} \to \infty$.

Illustrations also confirm the above conclusions: Figure 2.5(a) and (b) explain how L^* behaves when we have very small habitat preference and very large mortality in bad patches.

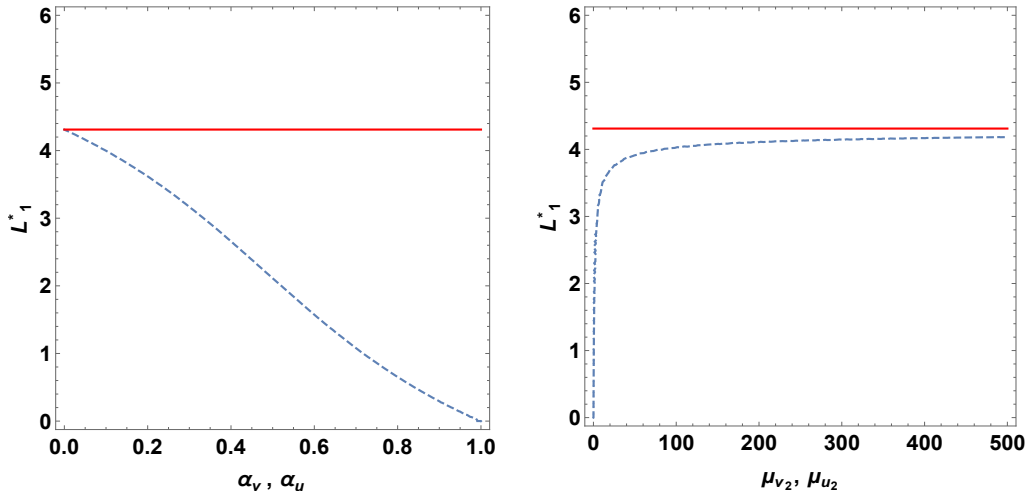

Figure 2.5.: The critical good patch size L_1^*: (a) as a function of preference to the good patch; (b) as a function of mortality coefficients in the bad patch. Dashed curves correspond to the persistence condition in (2.3.20), while the solid curves refer to persistence condition in a single-patch landscape (2.2.13). Parameters are as follows unless otherwise noted: $D_{u_1} = D_{v_1} = 1$, $D_{u_2} = D_{v_2} = 2$, $r_1 = 2$, $r_1 = 0.2$, $\mu_{u_1} = \mu_{v_1} = 1$, $\mu_{u_2} = \mu_{v_2} = 2$, $m_1 = 5$, $m_2 = 1$, $L_2 = 2$, and $\alpha_u = \alpha_v = 0.5$.

2.5. The Critical Size of a Single Patch Surrounded by a Non-Lethal Matrix Habitat

In Section 2.2, we derived the minimal patch size, L^*, that allows a structured population to persist in a single patch with hostile boundary. In this section, we derive an implicit formula for the critical size of a single good patch surrounded by an unbounded bad patch on either side, this situation can be visualized by Figure 1.1 with $L_2 = \infty$. In this case, the critical size depends on discontinuity parameters k_u and k_v. As in Section 2.3, we set $\lambda = 0$ and find the eigenfunctions to be of the form

$$U_1(x) = B_1 \cosh(z_1 x) + C_1 \sinh(z_1 x) + G_1 \cos(z_2 x) + H_1 \sin(z_2 x),$$
$$x \in \left(\tfrac{-L}{2}, \tfrac{L}{2}\right).$$

$$U_2(x) = B_2 \cosh(z_3 x) + C_2 \sinh(z_3 x) + G_2 \cosh(z_4 x) + H_2 \sinh(z_4 x),$$
$$\frac{L}{2} < x \quad \text{or} \quad x < \frac{-L}{2}.$$

Since solutions are bounded in patch type II, $U_2(x)$ will be of the form

$$U_2(x) = Be^{-z_3|x|} + He^{-z_4|x|}, \ \frac{L}{2} < x \quad \text{or} \quad x < \frac{-L}{2}. \tag{2.5.1}$$

But $U_1(x)$ is symmetric around $x = 0$, which implies that $C_1 = H_1 = 0$. Hence, we write $U_1(x)$ as follows

$$U_1(x) = B_1 \cosh(z_1 x) + G_1 \cos(z_2 x), \ x \in \left(0, \frac{L}{2}\right). \tag{2.5.2}$$

We need to apply the following conditions at the interface $x = \frac{L}{2}$

$$U_1\left(\frac{L}{2}^-\right) = k_u U_2\left(\frac{L}{2}^+\right), \quad V_1\left(\frac{L}{2}^-\right) = k_v V_2\left(\frac{L}{2}^+\right), \tag{2.5.3}$$

$$U_1'\left(\frac{L}{2}^-\right) = D_u U_2'\left(\frac{L}{2}^+\right), \quad V_1'\left(\frac{L}{2}^-\right) = D_v V_2'\left(\frac{L}{2}^+\right). \tag{2.5.4}$$

The eigenfunctions V_i are defined as follows

$$V_i(x) = \frac{D_{u_i} U_i''(x) - (m_i + \mu_{u_i}) U_i(x)}{-r_i}, \quad i = 1, 2. \tag{2.5.5}$$

Applying interface conditions $(2.5.3) - (2.5.4)$ gives the following linear equations

$$B_1 \cosh\left(z_1 \frac{L}{2}\right) + G_1 \cos\left(z_2 \frac{L}{2}\right) = k_u \left(Be^{-z_3 \frac{L}{2}} + He^{-z_4 \frac{L}{2}}\right), \tag{2.5.6}$$

$$B_1 z_1 \sinh\left(z_1 \frac{L}{2}\right) - G_1 z_2 \sin\left(z_2 \frac{L}{2}\right) = D_u \left(-Bz_3 e^{-z_3 \frac{L}{2}} - Hz_4 e^{-z_4 \frac{L}{2}}\right), \tag{2.5.7}$$

$$0 = B_1\left(rD_{u_1}z_1^2\cosh\left(z_1\frac{L}{2}\right) - r\alpha\cosh\left(z_1\frac{L}{2}\right)\right) - B\left(-\beta k_v e^{-z_3\frac{L}{2}} + k_v D_{u_2}z_3^2 e^{-z_3\frac{L}{2}}\right)$$
$$+ G_1\left(-rD_{u_1}z_2^2\cos\left(z_2\frac{L}{2}\right) - r\alpha\cos\left(z_2\frac{L}{2}\right)\right) - H\left(-\beta k_v e^{-z_4\frac{L}{2}} + k_v D_{u_2}z_4^2 e^{-z_4\frac{L}{2}}\right), \tag{2.5.8}$$

and

$$0 = B_1\left(rD_{u_1}z_1^3\sinh\left(z_1\frac{L}{2}\right) - r\alpha z_1\sinh\left(z_1\frac{L}{2}\right)\right) - B\left(\beta D_v z_3 e^{-z_3\frac{L}{2}} - D_v D_{u_2}z_3^3 e^{-z_3\frac{L}{2}}\right)$$
$$+ G_1\left(rD_{u_1}z_2^3\sin\left(z_2\frac{L}{2}\right) + r\alpha z_2\sin\left(z_2\frac{L}{2}\right)\right) - H\left(\beta D_v z_4 e^{-z_4\frac{L}{2}} - D_v D_{u_2}z_4^3 e^{-z_4\frac{L}{2}}\right), \tag{2.5.9}$$

where $\alpha = m_1 + \mu_{u_1}$, $\beta = m_2 + \mu_{u_2}$, $r = \frac{r_2}{r_1}$, and $D_v = \frac{D_{v_2}}{D_{v_1}}$. We then write the coefficient matrix for the linear system (2.5.6)-(2.5.9) and equate the determinant to zero to get the persistence condition for the juveniles-adults model in a single good patch surrounded by a non-lethal matrix habitat

$$\begin{aligned}
0 &= z_3 z_2\left(-\beta D_v + \alpha D_u r + D_{u_2}z_2^2 r + D_v D_{u_2}z_3^2\right)\\
&\times\left(\beta k_v - \alpha k_u r + D_{u_1}k_u r z_1^2 - D_{u_2}k_v z_4^2\right)\tan\left(\frac{z_2 L}{2}\right)\\
&+ z_4 z_3\left(D_{u_2}\right)^2 D_v r\left(z_1^2 + z_2^2\right)\left(z_4^2 - z_3^2\right)\\
&+ z_1 z_4\left(-rD_{u_2}z_1^2 + r\alpha D_u - D_v\beta + D_v D_{u_2}z_4^2\right)\\
&\times\left(\alpha k_u r - \beta k_v + D_{u_1}k_u r z_2^2 + D_{u_2}k_v z_3^2\right)\tanh\left(\frac{z_1 L}{2}\right)\\
&+ z_1 z_2 r D_{u_1}D_{u_2}k_v k_u\left(z_2^2 + z_1^2\right)\left(z_3^2 - z_4^2\right)\tan\left(\frac{z_2 L}{2}\right)\tanh\left(\frac{z_1 L}{2}\right)\\
&+ z_1 z_3\left(rD_{u_2}z_1^2 - \alpha D_u r + D_v\beta - D_v D_{u_2}z_3^2\right)\\
&\times\left(-\beta k_v + \alpha k_u r + D_{u_1}k_u r z_2^2 + D_{u_2}k_v z_4^2\right)\tanh\left(\frac{z_1 L}{2}\right)\\
&- z_2 z_4\left(-\beta D_v + D_v D_{u_2}z_4^2 + r\alpha D_u + rD_{u_2}z_2^2\right)\\
&\times\left(\beta k_v - \alpha k_u r + D_{u_1}k_u r z_1^2 - D_{u_2}k_v z_3^2\right)\tan\left(\frac{z_2 L}{2}\right).
\end{aligned} \tag{2.5.10}$$

Proposition 2.5.1. *The critical size of a single good patch surrounded by a non-lethal matrix habitat is given implicitly by the relation in* (2.5.10).

Remark 2.5.2. *One can derive the relation* (*2.5.10*) *from the persistence condition for the juveniles-adults model* (*2.3.20*), *which we have seen in Section 2.3, by taking the limit for* (*2.3.20*) *as the bad patch size* L_2 *tends to infinity. The numerical comparison in Figure 2.6 shows that the critical size for a good patch according to* (*2.3.20*) *increases to the critical size of a single good patch surrounded by a non-lethal matrix habitat* (*2.5.10*).

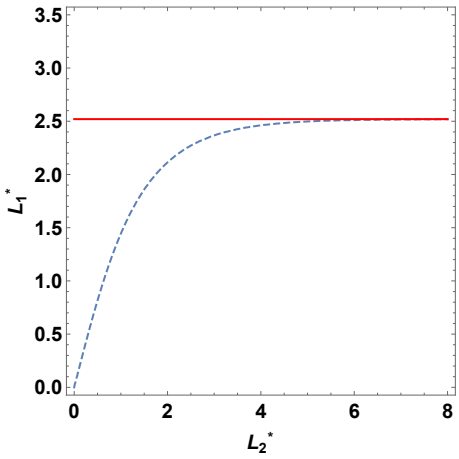

Figure 2.6.: Minimal good patch size in a patchy periodic landscape as a function of minimal bad patch size. The dashed curve corresponds to the structured populations persistence condition (2.3.20), while the solid curve represents the critical size of a single good patch surrounded by a non-lethal matrix habitat (2.5.10). Parameters are as follows: $r_1 = 2$, $r_2 = 0.2$, $\mu_{u_2} = 2 = \mu_{v_2}$, $D_{u_1} = 1 = D_{v_1}$, $D_{v_2} = 2 = D_{u_2}$, $\mu_{u_1} = \mu_{v_1} = 1$, $m_1 = 5$, $m_2 = 1$, and $\alpha_u = \alpha_v = 0.5$.

2.6. Sensitivity and Elasticity for the Critical Patch Size in a Single-Patch Landscape

Elasticity and sensitivity are used to measure how the change in one variable affects a result of interest, for example the critical patch size, L^*. We use the following formulas

of sensitivity and elasticity as mentioned in [65]

$$\text{Sensitivity of } L^* \text{ to the variable } b = \frac{\partial L^*}{\partial b}, \tag{2.6.1}$$

$$\text{Elasticity of } L^* \text{ to the variable } b = \frac{b}{L^*}\frac{\partial L^*}{\partial b}. \tag{2.6.2}$$

While sensitivity measures the absolute change in L^* that can be attributed to the variable b [21], elasticity measures the proportional change [19].

In this section, we study sensitivity and elasticity of the critical patch size in a single-patch landscape to population parameters. In Section 2.2, we have found the following critical patch size formula for structured populations of juveniles and adults living in a single-patch landscape

$$L^* = \frac{\pi}{z_2},$$

where

$$z_2 = \sqrt{\frac{(a^2+4b)^{\frac{1}{2}} - a}{2}},$$

$$a = \frac{D_v\,(m+\mu_u) + D_u\mu_{\mathrm{v}}}{D_vD_u}, \quad \text{and} \quad b = \frac{r\,m - \mu_v\,(m+\mu_u)}{D_vD_u}.$$

The sensitivities are given as follows

$$\frac{\partial L^*}{\partial r} = -\frac{m\pi}{2D_uD_v\,(z_2)^3\sqrt{a^2+4b}}, \tag{2.6.3}$$

$$\frac{\partial L^*}{\partial m} = -\frac{\pi}{4\,(z_2)^3}\left(\frac{-1}{D_u} + \frac{\frac{4(r-\mu_v)}{D_uD_v} + \frac{2a}{D_u}}{2\sqrt{a^2+4b}}\right), \tag{2.6.4}$$

$$\frac{\partial L^*}{\partial D_u} = -\frac{\pi}{4\,(z_2)^3}\left(\frac{-\mu_v}{D_uD_v} + \frac{a}{D_u} + \frac{\frac{a\mu_v}{D_uD_v} - \frac{a^2}{D_u} - \frac{2b}{D_u}}{\sqrt{a^2+4b}}\right), \tag{2.6.5}$$

$$\frac{\partial L^*}{\partial D_v} = -\frac{\pi}{4\,(z_2)^3}\left(-\frac{m+\mu_u}{D_uD_v} + \frac{a}{D_v} + \frac{\frac{a(\mu_u+m)}{D_uD_v} - \frac{a^2}{D_v} - \frac{2b}{D_v}}{\sqrt{a^2+4b}}\right), \tag{2.6.6}$$

$$\frac{\partial L^*}{\partial \mu_u} = -\frac{\pi}{4\left(z_2\right)^3}\left(\frac{-1}{D_u} + \frac{\frac{-2\mu_v}{D_u D_v} + \frac{a}{D_u}}{\sqrt{a^2+4b}}\right), \tag{2.6.7}$$

and

$$\frac{\partial L^*}{\partial \mu_v} = -\frac{\pi}{4\left(z_2\right)^3}\left(\frac{-1}{D_v} + \frac{\frac{-2(m+\mu_u)}{D_u D_v} + \frac{a}{D_v}}{\sqrt{a^2+4b}}\right). \tag{2.6.8}$$

Table 2.1.: Sensitivity and Elasticity of the minimal patch size L^* to population parameters

Population Parameter	Sensitivity Value	Elasticity Value
reproduction rate (r)	-0.23047	-0.494162
maturation rate (m)	-0.114276	-0.204187
juveniles diffusion term (D_u)	0.204547	0.146193
adults diffusion term (D_v)	0.495031	0.353807
juveniles mortality term (μ_u)	0.162287	0.057995
adults mortality term (μ_v)	0.392757	0.140355

We present the sensitivities and elasticities for our chosen default parameter values in Table 2.1. In Figure 2.1, we saw that L^* decreases with r and m and increases with all other parameters. Accordingly, the sensitivity of L^* with respect to m, r is negative but it is positive with respect to all other parameters. The sensitivity of L^* with respect to D_v is higher than with respect to D_u. While the actual numbers in the table change with parameter values, we expect the sign pattern to persist independently of parameter values.

3. Traveling Periodic Waves for the Juveniles-Adults Model

In the previous chapter, we studied conditions for a population to persist in a given landscape. If a population is introduced locally and if it can persist, then we expect it to spread spatially. The question of spatial spread in ecological models is related to questions of alien species invasion. It is typically studied through the analysis of traveling wave patterns. In this chapter, we derive and study the dispersion relation that gives us the minimal speed of a traveling periodic wave (TPW) for the linear system [77]. In many cases, this minimal speed is also the so-called spreading speed, i.e., the speed at which a locally introduced population spreads in the non-linear equation [88, 92]. For brevity, we will use the term 'spread speed' interchangeably with minimal speed of a TPW.

3.1. Minimal Speed of Traveling Periodic Waves

In this section, we derive the dispersion relation for the juveniles-adults model in a heterogeneous environment. We assume that the landscape consists of infinitely many patches of two types, periodically alternating 'good patches' and 'bad patches'. We use L_1, L_2 to represent the size of the good patch and the bad patch, respectively. Hence, $L = L_1 + L_2$ represents the spatial period.

To find the minimal traveling wave speed, we seek traveling periodic waves of the

form

$$u(t,x) = f(z)g(x), \quad v(t,x) = \widetilde{f}(z)\widetilde{g}(x); \quad z = x - Ct, \tag{3.1.1}$$

where the velocity C can be written as $C = L/t^*$ and t^* is the time required for traveling one spatial period [77]. We are looking for rightward traveling waves and therefore require $f(z),\ \widetilde{f}(z) \to 0$ as $z \to \infty$. Since we seek periodic solutions, we require $g(x) = g\,(x + L)$ and $\widetilde{g}(x) = \widetilde{g}\,(x + L)$.
By substituting (3.1.1) into (1.4.1) and (1.4.2), we conclude that $f'/f,\ f''/f,\ \widetilde{f}'/\widetilde{f}$ and $\widetilde{f}''/\widetilde{f}$ should be constants. Hence, we write $f(z) = Ae^{-sz},\ \widetilde{f}(z) = Be^{-sz}$,

$$u\,(t,x) = e^{-sz}g\,(x) \quad \text{and} \quad v\,(t,x) = e^{-sz}\widetilde{g}\,(x) \quad (s > 0)\,. \tag{3.1.2}$$

We write $g = g_{1,2}$ and $\widetilde{g} = \widetilde{g}_{1,2}$ on good and bad patches, respectively.
With the ansatz in (3.1.2), the equation in (1.4.1) becomes

$$\begin{aligned} sCe^{-s(x-Ct)}g_1(x) = D_{u_1}\left(f_1''(z)g_1(x) + f_1(z)g_1''(x) + 2f_1'(z)g_1'(x)\right) \\ + r_1\widetilde{f}_1(z)\widetilde{g}_1(x) - (m_1 + \mu_{u_1})\,f_1(z)g_1(x), \end{aligned} \tag{3.1.3}$$

which is equivalent to

$$sCg_1(x) = D_{u_1}\left(s^2g_1(x) + g_1''(x) - 2sg_1'(x)\right) + r_1\widetilde{g}_1(x) - (m_1 + \mu_{u_1})\,g_1(x). \tag{3.1.4}$$

Similarly, (1.4.2) becomes

$$sC\widetilde{g}_1(x) = D_{v_1}\left(s^2\widetilde{g}_1(x) + \widetilde{g}_1''\,(x) - 2s\widetilde{g}_1'(x)\right) + m_1g_1(x) - \mu_{v_1}\widetilde{g}_1(x). \tag{3.1.5}$$

From (3.1.4), we write $\widetilde{g}_1(x)$ explicitly as follows

$$\widetilde{g}_1(x) = \frac{-D_{u_1}g_1''(x) + 2sD_{u_1}g_1'(x) + (sC + m_1 + \mu_{u_1} - s^2D_{u_1})\,g_1(x)}{r_1}. \tag{3.1.6}$$

We then substitute $\widetilde{g}_1(x)$, $\widetilde{g}_1'(x)$ and $\widetilde{g}_1''(x)$ into (3.1.5) to get

$$0 = -D_{v_1}D_{u_1}g_1^{(4)}(x) + 4sD_{v_1}D_{u_1}g_1^{(3)}(x) + \left(D_{u_1}\alpha + D_{v_1}\beta - 4s^2D_{u_1}D_{v_1}\right)g_1''(x) + g_1'(x)\left(-2sD_{u_1}\alpha - 2sD_{v_1}\beta\right) + g_1(x)\left(r_1m_1 - \alpha\beta\right), \tag{3.1.7}$$

where $\alpha = (sC + \mu_{v_1} - s^2D_{v_1})$ and $\beta = (sC + m_1 + \mu_{u_1} - s^2D_{u_1})$.
We then divide (3.1.7) by $(-D_{v_1}D_{u_1})$ to get

$$0 = g_1^{(4)}(x) - 4sg_1^{(3)}(x) - \left(\frac{\alpha}{D_{v_1}} + \frac{\beta}{D_{u_1}} - 4s^2\right)g_1''(x) + \left(\frac{2s\alpha}{D_{v_1}} + \frac{2s\beta}{D_{u_1}}\right)g_1'(x) - \frac{(r_1m_1 - \alpha\beta)}{D_{v_1}D_{u_1}}g_1(x). \tag{3.1.8}$$

We need to find conditions for this equation to have non-trivial solutions. First, we write the characteristic equation for (3.1.8) as

$$z^4 - 4sz^3 - \left(\frac{\alpha}{D_{v_1}} + \frac{\beta}{D_{u_1}} - 4s^2\right)z^2 + \left(\frac{2s\alpha}{D_{v_1}} + \frac{2s\beta}{D_{u_1}}\right)z - \frac{(r_1m_1 - \alpha\beta)}{D_{v_1}D_{u_1}} = 0.$$

This has the following roots

$$z = s \pm \frac{1}{\sqrt{2D_{u_1}D_{v_1}}}\sqrt{D_{v_1}(m_1 + sC + \mu_{u_1}) + D_{u_1}(sC + \mu_{v_1}) \pm \Delta_1}, \tag{3.1.9}$$

where $\Delta_1 = \sqrt{[D_{v_1}(m_1 + sC + \mu_{u_1}) - D_{u_1}(sC + \mu_{v_1})]^2 + 4D_{u_1}D_{v_1}r_1m_1}$.
The form of the solution of the differential equation (3.1.8) depends on the sign of the quantity

$$D_{v_1}(m_1 + sC + \mu_{u_1}) + D_{u_1}(sC + \mu_{v_1}) - \Delta_1. \tag{3.1.10}$$

If the sign of (3.1.10) is negative, then

$$D_{v_1}(m_1 + sC + \mu_{u_1}) + D_{u_1}(sC + \mu_{v_1}) < \Delta_1. \tag{3.1.11}$$

The left hand side of (3.1.11) is positive, therefore squaring the last inequality gives

$$\begin{aligned} &D_{v_1}^2(m_1+sC+\mu_{u_1})^2+D_{u_1}^2(sC+\mu_{v_1})^2+2D_{u_1}D_{v_1}(m_1+sC+\mu_{u_1})(sC+\mu_{v_1}) \\ &< D_{v_1}^2(m_1+sC+\mu_{u_1})^2-2D_{u_1}D_{v_1}(m_1+sC+\mu_{u_1})(sC+\mu_{v_1}) \\ &\qquad + D_{u_1}^2(sC+\mu_{v_1})^2+4D_{u_1}D_{v_1}r_1m_1, \end{aligned}$$

which is equivalent to the inequality

$$(sC)^2+sC(m_1+\mu_{u_1}+\mu_{v_1})+\mu_{u_1}\mu_{v_1}+m_1\mu_{v_1}-r_1m_1<0.$$

We made the ansatz assuming s, $C>0$ and therefore we get

$$0<sC<\frac{-(m_1+\mu_{u_1}+\mu_{v_1})+\sqrt{(m_1+\mu_{u_1}+\mu_{v_1})^2-4(\mu_{u_1}\mu_{v_1}+m_1\mu_{v_1}-r_1m_1)}}{2}.$$

Therefore, the sign of (3.1.10) is negative if and only if

$$C<\frac{-(m_1+\mu_{u_1}+\mu_{v_1})+\sqrt{(m_1+\mu_{u_1}+\mu_{v_1})^2-4(\mu_{u_1}\mu_{v_1}+m_1\mu_{v_1}-r_1m_1)}}{2s}. \tag{3.1.12}$$

Similarly, the sign of (3.1.10) is positive if and only if

$$C>\frac{-(m_1+\mu_{u_1}+\mu_{v_1})+\sqrt{(m_1+\mu_{u_1}+\mu_{v_1})^2-4(\mu_{u_1}\mu_{v_1}+m_1\mu_{v_1}-r_1m_1)}}{2s}. \tag{3.1.13}$$

Before we continue, we note that the exact same procedure applied to the equation in bad patches leads to the differential equation for $g_2(x)$ as

$$\begin{aligned} g_2^{(4)}(x)-4sg_2^{(3)}(x)-\left(\frac{\gamma}{D_{v_2}}+\frac{\delta}{D_{u_2}}-4s^2\right)g_2''(x)+\left(\frac{2s\gamma}{D_{v_2}}+\frac{2s\delta}{D_{u_2}}\right)g_2'(x) \\ -\frac{(r_2m_2-\gamma\delta)}{D_{v_2}D_{u_2}}g_2(x)=0, \end{aligned} \tag{3.1.14}$$

where $\gamma = (sC + \mu_{v_2} - s^2 D_{v_2})$ and $\delta = (sC + m_2 + \mu_{u_2} - s^2 D_{u_2})$.
The condition in (3.1.12) can be written in terms of the reproduction rate r_1 as follows: the sign of (3.1.10) is negative if and only if

$$r_1 > \frac{(m_1 + sC + \mu_{u_1})\,(sC + \mu_{v_1})}{m_1}. \tag{3.1.15}$$

In bad patches, and according to Proposition 2.1.1, we have

$$r_2 < \frac{\mu_{v_2}\,(m_2 + \mu_{u_2})}{m_2} < \frac{(m_2 + sC + \mu_{u_2})\,(sC + \mu_{v_2})}{m_2}.$$

Therefore, solutions of the differential equation (3.1.14) will be of the form

$$g_2(x) = e^{sx}\left[A' \cosh(z_3 x) + B' \sinh(z_3 x) + G' \cosh(z_4 x) + H' \sinh(z_4 x)\right],$$

where

$$z_3 = \frac{1}{\sqrt{2D_{u_2}D_{v_2}}}\sqrt{D_{v_2}(m_2 + sC + \mu_{u_2}) + D_{u_2}(sC + \mu_{v_2}) - \Delta_2},$$

$$z_4 = \frac{1}{\sqrt{2D_{u_2}D_{v_2}}}\sqrt{D_{v_2}(m_2 + sC + \mu_{u_2}) + D_{u2}(sC + \mu_{v_2}) + \Delta_2},$$

and

$$\Delta_2 = \sqrt{[D_{v_2}(m_2 + sC + \mu_{u_2}) - D_{u_2}(sC + \mu_{v_2})]^2 + 4D_{u_2}D_{v_2}r_2 m_2}.$$

In good patches, we have the two different cases

- **Case A:** $r_1 > \frac{(m_1 + sC + \mu_{u_1})(sC + \mu_{v_1})}{m_1}$.
- **Case B:** $r_1 < \frac{(m_1 + sC + \mu_{u_1})(sC + \mu_{v_1})}{m_1}$.

To study the minimal speed of traveling periodic waves for the juveniles-adults model in a heterogeneous landscape, we present the calculations for **Case A** here and supply the corresponding calculations for **Case B** in Appendix B.

Since the function g is assumed to be periodic, it is sufficient to consider only one good patch and one bad patch.

If condition (3.1.15) holds, we can write the solution of the differential equation (3.1.8) as

$$g_1(x) = e^{sx}\left[A\cos(z_1 x) + B\sin(z_1 x) + G\cosh(z_2 x) + H\sinh(z_2 x)\right],$$

where

$$z_1 = \frac{1}{\sqrt{2D_{u_1}D_{v_1}}}\sqrt{-D_{v_1}(m_1 + sC + \mu_{u_1}) - D_{u_1}(sC + \mu_{v_1}) + \Delta_1},$$

$$z_2 = \frac{1}{\sqrt{2D_{u_1}D_{v_1}}}\sqrt{D_{v_1}(m_1 + sC + \mu_{u_1}) + D_{u_1}(sC + \mu_{v_1}) + \Delta_1},$$

and

$$\Delta_1 = \sqrt{[D_{v_1}(m_1 + sC + \mu_{u_1}) - D_{u_1}(sC + \mu_{v_1})]^2 + 4D_{u_1}D_{v_1}r_1 m_1}.$$

To find a nontrivial solution for the functions g_1 and g_2, we need to obtain relations to determine the coefficients A, B, G, H, A', B', G' and H'. We apply the following interface conditions at $x = 0$ and $x = L_1$

$$g_1\left(0^+\right) = k_u g_2\left(0^-\right), \quad g_1\left(L_1^-\right) = k_u g_2\left(-L_2^+\right), \tag{3.1.16}$$

$$g_1'\left(0^+\right) - s g_1\left(0^+\right) = D_u\left[g_2'\left(0^-\right) - s g_2\left(0^-\right)\right], \tag{3.1.17}$$

$$g_1'\left(L_1^-\right) - s g_1\left(L_1^-\right) = D_u\left[g_2'\left(-L_2^+\right) - s g_2\left(-L_2^+\right)\right], \tag{3.1.18}$$

$$\widetilde{g}_1\left(0^+\right) = k_v \widetilde{g}_2\left(0^-\right), \quad \widetilde{g}_1\left(L_1^-\right) = k_v \widetilde{g}_2\left(-L_2^+\right), \tag{3.1.19}$$

$$\widetilde{g}_1'\left(0^+\right) - s\widetilde{g}_1\left(0^+\right) = D_v\left[\widetilde{g}_2'\left(0^-\right) - s\widetilde{g}_2\left(0^-\right)\right], \tag{3.1.20}$$

and

$$\widetilde{g}_1'\left(L_1^-\right) - s\widetilde{g}_1\left(L_1^-\right) = D_v\left[\widetilde{g}_2'\left(-L_2^+\right) - s\widetilde{g}_2\left(-L_2^+\right)\right]. \tag{3.1.21}$$

The interface conditions (3.1.16)-(3.1.21) produce the following system of linear equa-

tions for our coefficients:

$$A + G = k_u \left(A' + G'\right), \quad z_1 B + z_2 H = D_u \left(z_3 B' + z_4 H'\right), \tag{3.1.22}$$

$$\begin{aligned} &e^{s(L_1+L_2)} \left[A \cos\left(z_1 L_1\right) + B \sin\left(z_1 L_1\right) + G \cosh\left(z_2 L_1\right) + H \sinh\left(z_2 L_1\right)\right] = \\ &k_u \left[A' \cosh\left(z_3 L_2\right) - B' \sinh\left(z_3 L_2\right) + G' \cosh\left(z_4 L_2\right) - H' \sinh\left(z_4 L_2\right)\right], \end{aligned} \tag{3.1.23}$$

$$\begin{aligned} 0 = {} & A \left[D_{u_1} z_1^2 \cos\left(z_1 L_1\right) + D_{u_1} s^2 \cos\left(z_1 L_1\right) + \beta \cos\left(z_1 L_1\right)\right] r e^{s(L_1+L_2)} \\ & + B \left[D_{u_1} z_1^2 \sin\left(z_1 L_1\right) + D_{u_1} s^2 \sin\left(z_1 L_1\right) + \beta \sin\left(z_1 L_1\right)\right] r e^{s(L_1+L_2)} \\ & + G \left[-D_{u_1} z_2^2 \cosh\left(z_2 L_1\right) + D_{u_1} s^2 \cosh\left(z_2 L_1\right) + \beta \cosh\left(z_2 L_1\right)\right] r e^{s(L_1+L_2)} \\ & + H \left[-D_{u_1} z_2^2 \sinh\left(z_2 L_1\right) + D_{u_1} s^2 \sinh\left(z_2 L_1\right) + \beta \sinh\left(z_2 L_1\right)\right] r e^{s(L_1+L_2)} \\ & + A' \left[D_{u_2} z_3^2 \cosh\left(z_3 L_2\right) - D_{u_2} s^2 \cosh\left(z_3 L_2\right) - \delta \cosh\left(z_3 L_2\right)\right] k_v \\ & + B' \left[-D_{u_2} z_3^2 \sinh\left(z_3 L_2\right) + D_{u_2} s^2 \sinh\left(z_3 L_2\right) + \delta \sinh\left(z_3 L_2\right)\right] k_v \\ & + G' \left[D_{u_2} z_4^2 \cosh\left(z_4 L_2\right) - D_{u_2} s^2 \cosh\left(z_4 L_2\right) - \delta \cosh\left(z_4 L_2\right)\right] k_v \\ & + H' \left[-D_{u_2} z_4^2 \sinh\left(z_4 L_2\right) + D_{u_2} s^2 \sinh\left(z_4 L_2\right) + \delta \sinh\left(z_4 L_2\right)\right], \end{aligned} \tag{3.1.24}$$

$$\begin{aligned} &e^{s(L_1+L_2)} \left[-z_1 A \sin\left(z_1 L_1\right) + z_1 B \cos\left(z_1 L_1\right) + z_2 G \sinh\left(z_2 L_1\right) + z_2 H \cosh\left(z_2 L_1\right)\right] = \\ &D_u \left[-z_3 A' \sinh\left(z_3 L_2\right) + z_3 B' \cosh\left(z_3 L_2\right) - z_4 G' \sinh\left(z_4 L_2\right) + z_4 H' \cosh\left(z_4 L_2\right)\right], \end{aligned} \tag{3.1.25}$$

$$\begin{aligned} 0 = {} & A \left[D_{u_1} s^2 + D_{u_1} z_1^2 + \beta\right] r + G \left[D_{u_1} s^2 - D_{u_1} z_2^2 + \beta\right] r \\ & + A' \left[-D_{u_2} s^2 + D_{u_2} z_3^2 - \delta\right] k_v + G' \left[-D_{u_2} s^2 + D_{u_2} z_4^2 - \delta\right] k_v, \end{aligned} \tag{3.1.26}$$

$$0 = B\left[D_{u_1}z_1^3 + D_{u_1}s^2z_1 + \beta z_1\right]r + H\left[-D_{u_1}z_2^3 + D_{u_1}s^2z_2 + \beta z_2\right]r + B'\left[D_{u_2}z_3^3 - D_{u_2}s^2z_3 - \delta z_3\right]D_v + H'\left[D_{u_2}z_4^3 - D_{u_2}s^2z_4 - \delta z_4\right]D_v, \quad (3.1.27)$$

and

$$\begin{aligned}0 = {} & A\left[-D_{u_1}s^2z_1\sin(z_1L_1) - D_{u_1}z_1^3\sin(z_1L_1) - \beta z_1\sin(z_1L_1)\right]re^{s(L_1+L_2)} \\ & + B\left[D_{u_1}s^2z_1\cos(z_1L_1) + D_{u_1}z_1^3\cos(z_1L_1) + \beta z_1\cos(z_1L_1)\right]re^{s(L_1+L_2)} \\ & + G\left[D_{u_1}s^2z_2\sinh(z_2L_1) - D_{u_1}z_2^3\sinh(z_2L_1) + \beta z_2\sinh(z_2L_1)\right]re^{s(L_1+L_2)} \\ & + H\left[D_{u_1}s^2z_2\cosh(z_2L_1) - D_{u_1}z_2^3\cosh(z_2L_1) + \beta z_2\cosh(z_2L_1)\right]re^{s(L_1+L_2)} \\ & + A'\left[D_{u_2}s^2z_3\sinh(z_3L_2) - D_{u_2}z_3^3\sinh(z_3L_2) + \delta z_3\sinh(z_3L_2)\right]D_v \\ & + B'\left[-D_{u_2}s^2z_3\cosh(z_3L_2) + D_{u_2}z_3^3\cosh(z_3L_2) - \delta z_3\cosh(z_3L_2)\right]D_v \\ & + G'\left[D_{u_2}s^2z_4\sinh(z_4L_2) - D_{u_2}z_4^3\sinh(z_4L_2) + \delta z_4\sinh(z_4L_2)\right]D_v \\ & + H'\left[-D_{u_2}s^2z_4\cosh(z_4L_2) + D_{u_2}z_4^3\cosh(z_4L_2) - \delta z_4\cosh(z_4L_2)\right]D_v. \quad (3.1.28)\end{aligned}$$

We write the coefficient matrix of the linear system (3.1.22)-(3.1.28) as

$$V = \begin{bmatrix} V_1 & V_2 \\ V_3 & V_4 \end{bmatrix},$$

where

$$V_1 = \begin{bmatrix} 1 & 0 & 1 & 0 \\ 0 & z_1 & 0 & z_2 \\ -z_1e^{sL}\sin(z_1L_1) & z_1e^{sL}\cos(z_1L_1) & z_2e^{sL}\sinh(z_2L_1) & z_2e^{sL}\cosh(z_2L_1) \\ e^{sL}\cos(z_1L_1) & e^{sL}\sin(z_1L_1) & e^{sL}\cosh(z_2L_1) & e^{sL}\sinh(z_2L_1) \end{bmatrix},$$

$$V_2 = \begin{bmatrix} -k_u & 0 & -k_u & 0 \\ 0 & -D_u z_3 & 0 & -D_u z_4 \\ D_u z_3 \sinh(z_3 L_2) & -D_u z_3 \cosh(z_3 L_2) & D_u z_4 \sinh(z_4 L_2) & -D_u z_4 \cosh(z_4 L_2) \\ -k_u \cosh(z_3 L_2) & k_u \sinh(z_3 L_2) & -k_u \cosh(z_4 L_2) & k_u \sinh(z_4 L_2) \end{bmatrix},$$

$$V_3 = \begin{bmatrix} W & 0 & Y & 0 \\ We^{sL} \cos(z_1 L_1) & We^{sL} \sin(z_1 L_1) & Ye^{sL} \cosh(z_2 L_1) & Ye^{sL} \sinh(z_2 L_1) \\ 0 & Wz_1 & 0 & Yz_2 \\ -Wz_1 e^{sL} \sin(z_1 L_1) & Wz_1 e^{sL} \cos(z_1 L_1) & Yz_3 e^{sL} \sinh(z_2 L_1) & Yz_2 e^{sL} \cosh(z_2 L_1) \end{bmatrix},$$

$$V_4 = \begin{bmatrix} Mk_v & 0 & Nk_v & 0 \\ Mk_v \cosh(z_3 L_2) & -Mk_v \sinh(z_3 L_2) & Nk_v \cosh(z_4 L_2) & -Nk_v \sinh(z_4 L_2) \\ 0 & MD_v z_3 & 0 & ND_v z_4 \\ -MD_v z_3 \sinh(z_3 L_2) & MD_v z_3 \cosh(z_3 L_2) & -ND_v z_4 \sinh(z_4 L_2) & ND_v z_4 \cosh(z_4 L_2) \end{bmatrix},$$

with

$$W = r\left(D_{u_1}s^2 + D_{u_1}z_1^2 + \beta\right), \quad Y = r\left(D_{u_1}s^2 - D_{u_1}z_2^2 + \beta\right), \tag{3.1.29}$$

$$M = -D_{u_2}s^2 + D_{u_2}z_3^2 - \delta, \quad N = -D_{u_2}s^2 + D_{u_2}z_4^2 - \delta, \tag{3.1.30}$$

$$L = L_1 + L_2, \quad D_u = \frac{D_{u_2}}{D_{u_1}}, \quad D_v = \frac{D_{v_2}}{D_{v_1}}, \quad \text{and} \quad r = \frac{r_2}{r_1}.$$

A nontrivial solution of g_1, g_2 exists only if the determinant of V is zero. This condition gives us the dispersion relation between decay rate s and speed C of a traveling periodic wave. We calculated this determinant with Mathematica, but the expression is too large and cumbersome to be displayed here. However, we will use it to illustrate how the minimal speed of traveling periodic waves depends on parameters. We summarize our results as follows.

Proposition 3.1.1. *The dispersion relation $C = C(s)$ for a traveling periodic wave is given implicitly by setting the determinant of the coefficient matrix V equal to zero.*

In Figure 3.1, we plot the wave speed $C(s)$ as a function of wave shape parameter s. The plots shows that C is continuous and $C(s) \to \infty$ as $s \to 0^+$ and as $s \to \infty$, which ensures the existence of the minimum wave speed, C^*.

In Figure 3.2(a), we plot the spread speed $C^* = \min_{s>0} C(s)$, as a function of bad patch size, L_2, for different values of good patch size, L_1. Similarly, in Figure 3.2(b), we plot the spread speed as a function of good patch size for different values of bad patch size. As expected, the plot indicates that the speed decreases with bad patch size and increases with good patch size. Ecologically, increasing L_2 increases loss rates, and so decreases the spread speed, while increasing L_1 increases reproduction rates, which increases population speed. The points where $C^* = 0$ correspond to the critical sizes for good and bad patches with regards to population persistence from Chapter 2.

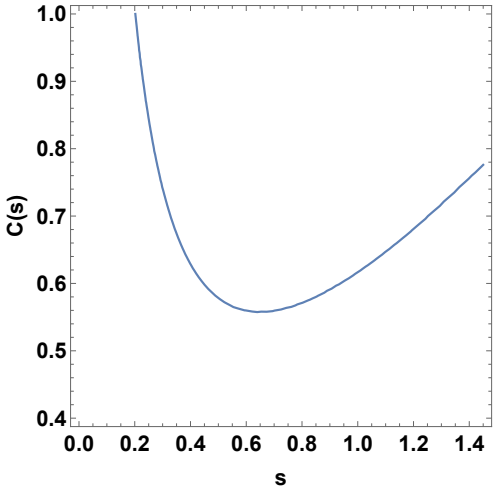

Figure 3.1.: Traveling periodic wave speed $C(s)$ for the juveniles-adults model in a patchy landscape as functions of wave shape parameter, s. Parameters are as follows $L_1 = L_2 = 1$, $r_1 = 7$, $r_2 = 0.2$, $D_{u_1} = D_{v_1} = 0.5$, $D_{u_2} = D_{v_2} = 0.5$, $\mu_{u_1} = \mu_{v_1} = 1$, $\mu_{u_2} = \mu_{v_2} = 2$, $m_1 = m_2 = 1$, and $\alpha_u = \alpha_v = 0.5$.

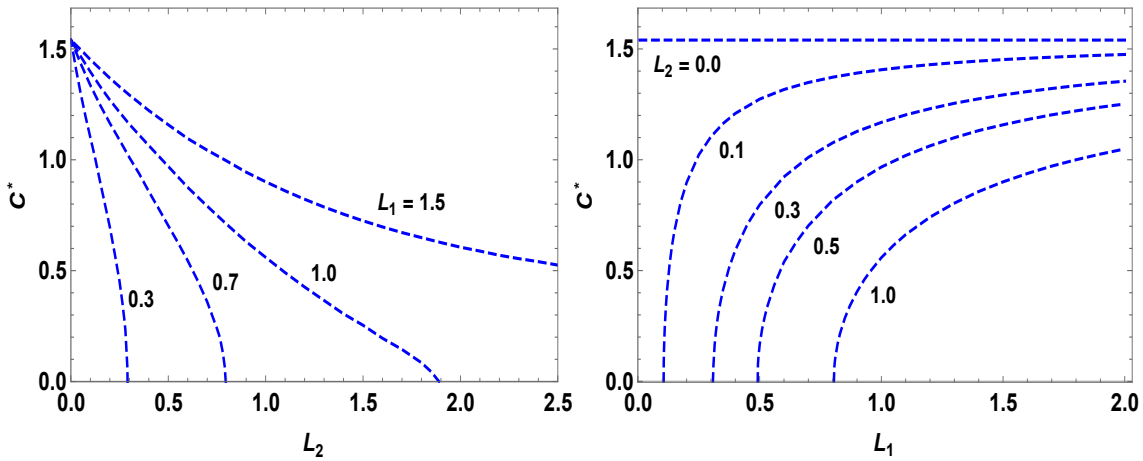

Figure 3.2.: Minimal traveling periodic wave speed C^* for the juveniles-adults model in a heterogeneous landscape: (a) as a function of bad patch size, L_2, for different values of good patch size, L_1; (b) as a function of good patch size, L_1, for different values of bad patch size, L_2. Parameters are as follows $r_1 = 7$, $r_2 = 0.2$, $D_{u_1} = D_{v_1} = 0.5$, $D_{u_2} = D_{v_2} = 0.5$, $\mu_{u_1} = \mu_{v_1} = 1$, $\mu_{u_2} = \mu_{v_2} = 2$, $m_1 = m_2 = 1$, and $\alpha_u = \alpha_v = 0.5$.

Remark 3.1.2. *For the plots in Figures 3.1 and 3.2, we used the formulas of* ***Case***

A *and* ***Case B*** *(see Appendix B). In* ***Case A****,* g_1 *consists of hyperbolic and trigonometric functions whereas in* ***Case B****, there are only hyperbolic functions. To switch between these two in the numerical computations, we use the hyperbolic-trigonometric formulas as in [73].*

3.2. Wave Speed in a Homogeneous Landscape

In this section, we find the wave speed for the special case where the environment is homogeneous, i.e. $L_2 = 0$. By following the procedure that we used in Section 3.1 and by substituting $L_2 = 0$ into equations (3.1.22)-(3.1.28), we get

$$\begin{aligned}\det V = &(W-Y)^2 (M-N)^2 \left(1 + e^{2sL_1} - 2e^{sL_1}\cos(L_1 z_1)\right) \\ &\times \left(1 + e^{2sL_1} - 2e^{sL_1}\cosh(L_1 z_2)\right), \end{aligned} \tag{3.2.1}$$

where W, Y, M, and N are as defined in (3.1.29) and (3.1.30) . Since we search for a positive solution, we set the determinant of the matrix V equal to zero and factor the expression to obtain

$$\left(z_1^2 + z_2^2\right)^2 \left(z_3^2 - z_4^2\right)^2 \left(1 + e^{2sL_1} - 2e^{sL_1}\cos(L_1 z_1)\right)\left(1 + e^{2sL_1} - 2e^{sL_1}\cosh(L_1 z_2)\right) = 0.$$

Since $(z_1)^2 + (z_2)^2 \neq 0$ and $z_3 \neq z_4$, the last condition becomes

$$\left(1 + e^{2sL_1} - 2e^{sL_1}\cos(L_1 z_1)\right)\left(1 + e^{2sL_1} - 2e^{sL_1}\cosh(L_1 z_2)\right) = 0.$$

Dividing by $2e^{sL_1}$ gives $(\cosh(sL_1) - \cos(L_1 z_1))(\cosh(sL_1) - \cosh(L_1 z_2)) = 0$. Since L_1 has to be positive, we obtain the condition $\cosh(sL_1) - \cosh(L_1 z_2) = 0$, or

equivalently, $s = z_2$. This condition generates the dispersion relation

$$s = \frac{1}{\sqrt{2D_{u_1}D_{v_1}}}\sqrt{D_{v_1}(m_1 + sC + \mu_{u_1}) + D_{u_1}(sC + \mu_{v_1}) + \Delta_1}, \tag{3.2.2}$$

where

$$\Delta_1 = \sqrt{[D_{v_1}(m_1 + sC + \mu_{u_1}) - D_{u_1}(sC + \mu_{v_1})]^2 + 4D_{u_1}D_{v_1}r_1m_1}.$$

We can write the wave speed C explicitly as a function of wave shape parameter s. We square equation (3.2.2) and multiply both sides by $2D_{u_1}D_{v_1}$ to get

$$\begin{aligned} 0 = {} & 2s^2D_{u_1}D_{v_1} - D_{v_1}\left(m_1 + sC + \mu_{u_1}\right) - D_{u_1}\left(sC + \mu_{v_1}\right) \\ & - \sqrt{\left[D_{v_1}\left(m_1 + sC + \mu_{u_1}\right) - D_{u_1}\left(sC + \mu_{v_1}\right)\right]^2 + 4D_{u_1}D_{v_1}r_1m_1}. \end{aligned} \tag{3.2.3}$$

Squaring (3.2.3) again and simplifying the expression produce the following equation

$$\begin{aligned} 0 = {} & 4s^4D_{u_1}^2D_{v_1}^2 - 4s^2D_{u_1}D_{v_1}\left(D_{v_1}\left(m_1 + sC + \mu_{u_1}\right) + D_{u_1}\left(sC + \mu_{v_1}\right)\right) \\ & + 4D_{u_1}D_{v_1}\left(m_1 + sC + \mu_{u_1}\right)\left(sC + \mu_{v_1}\right) - 4D_{u_1}D_{v_1}r_1m_1. \end{aligned} \tag{3.2.4}$$

We then rewrite (3.2.4) as the quadratic equation

$$\begin{aligned} 0 = {} & C^2 + C\left(\frac{\mu_{v_1} + \mu_{u_1} + m_1}{s} - sD_{u_1} - sD_{v_1}\right) \\ & + s^2D_{u_1}D_{v_1} - D_{v_1}m_1 - D_{v_1}\mu_{u_1} - D_{u_1}\mu_{v_1} + \frac{m_1\mu_{v_1} + \mu_{u_1}\mu_{v_1} - r_1m_1}{s^2}. \end{aligned} \tag{3.2.5}$$

Accordingly, we obtain the two roots

$$C = \frac{1}{2s}\left(-m_1 - \mu_{u_1} - \mu_{v_1} + D_{u_1}s^2 + D_{v_1}s^2 \pm \Delta\right), \tag{3.2.6}$$

where $\Delta = \sqrt{4r_1m_1 + \left(D_{u_1}s^2 - m_1 - D_{v_1}s^2 - \mu_{u_1} + \mu_{v_1}\right)^2}$.

To obtain the spread speed $C^* = \min_{s>0}[C(s)]$, we need the minimum to exist. We show that the expression in (3.2.6) with '+' has a global minimum whereas the expression with '−' does not. To prove this claim, we show that the limit of (3.2.6) with '+', goes to infinity as $s \to 0^+$ and as $s \to \infty$.

$$\begin{aligned}\lim_{s\to 0^+} \frac{1}{2s}\left(-m_1 - \mu_{u_1} - \mu_{v_1} + D_{u_1}s^2 + D_{v_1}s^2 + \Delta\right)\\ = \left(-m_1 - \mu_{u_1} - \mu_{v_1} + \sqrt{4r_1m_1 + \left(-m_1 - \mu_{u_1} + \mu_{v_1}\right)^2}\right) \lim_{s\to 0^+}\left(\frac{1}{2s}\right). \quad (3.2.7)\end{aligned}$$

From Proposition 2.1.1, we have $r_1 > \frac{1}{m_1}\left(m_1 + \mu_{u_1}\right)\left(\mu_{v_1}\right)$. Consequently,

$$\begin{aligned}&\left(-m_1 - \mu_{u_1} - \mu_{v_1} + \sqrt{4r_1m_1 + \left(-m_1 - \mu_{u_1} + \mu_{v_1}\right)^2}\right)\\ &> \left(-m_1 - \mu_{u_1} - \mu_{v_1} + \sqrt{4\mu_{v_1}\left(m_1 + \mu_{u_1}\right) + \left(-m_1 - \mu_{u_1} + \mu_{v_1}\right)^2}\right)\\ &= \left(-m_1 - \mu_{u_1} - \mu_{v_1} + \sqrt{\left(m_1 + \mu_{u_1} + \mu_{v_1}\right)^2}\right) = 0.\end{aligned}$$

This proves that the limit of (3.2.6) with '+' goes to infinity as $s \to 0^+$. Similarly,

$$\begin{aligned}&\lim_{s\to\infty} \frac{1}{2s}\left(-m_1 - \mu_{u_1} - \mu_{v_1} + D_{u_1}s^2 + D_{v_1}s^2 + \Delta\right)\\ &= \lim_{s\to\infty} \frac{s}{2}\left(\frac{-m_1 - \mu_{u_1} - \mu_{v_1}}{s^2} + D_{u_1} + D_{v_1} + \frac{\Delta}{s^2}\right)\\ &= \left(D_{u_1} + D_{v_1} + \sqrt{(D_{u_1} - D_{v_1})^2}\right) \lim_{s\to\infty}\left(\frac{s}{2}\right)\\ &= \left(D_{u_1} + D_{v_1} + \mid D_{u_1} - D_{v_1} \mid\right) \lim_{s\to\infty}\left(\frac{s}{2}\right).\end{aligned}$$

The previous expression implies that the limit of (3.2.6) with '+' goes to infinity when $s \to \infty$.

Since the expression is continuous on $(0, \infty)$ and approaches infinity at either end, it must have a global minimum.

Similar calculations show that

$$\lim_{s\to 0^+}\frac{1}{2s}\left(-m_1-\mu_{u_1}-\mu_{v_1}+D_{u_1}s^2+D_{v_1}s^2-\Delta\right)=-\infty, \tag{3.2.8}$$

and

$$\lim_{s\to \infty}\frac{1}{2s}\left(-m_1-\mu_{u_1}-\mu_{v_1}+D_{u_1}s^2+D_{v_1}s^2-\Delta\right)=\infty. \tag{3.2.9}$$

Hence, there is no global extremum for this case.

Proposition 3.2.1. *The dispersion relation for the homogeneous landscape is given explicitly by*

$$C\left(s\right)=\frac{1}{2s}\left(-m_1-\mu_{u_1}-\mu_{v_1}+D_{u_1}s^2+D_{v_1}s^2+\Delta\right), \tag{3.2.10}$$

where

$$\Delta=\sqrt{4r_1m_1+\left(D_{u_1}s^2-m_1-D_{v_1}s^2-\mu_{u_1}+\mu_{v_1}\right)^2}. \tag{3.2.11}$$

We can not obtain an explicit expression for the minimum value C^* but we compute it numerically. In Figure 3.3, we plot the wave speed $C(s)$ as a function of wave shape parameter s. The minimum wave speed $C^*=2$ occurs at $s^*=1$.

To see how population parameters affect the spreading speed in a homogeneous landscape, we illustrate the relations between the spreading speed C^* and the population parameters m_1, r_1, D_{u_1}, D_{v_1}, μ_{u_1} and μ_{v_1}. While the spread speed in a homogeneous landscape increases with r_1 (Figure 3.4), m_1, D_{u_1} and D_{v_1} (plots not shown) it decreases with μ_{u_1} (Figure 3.5) and μ_{v_1} (plot not shown).

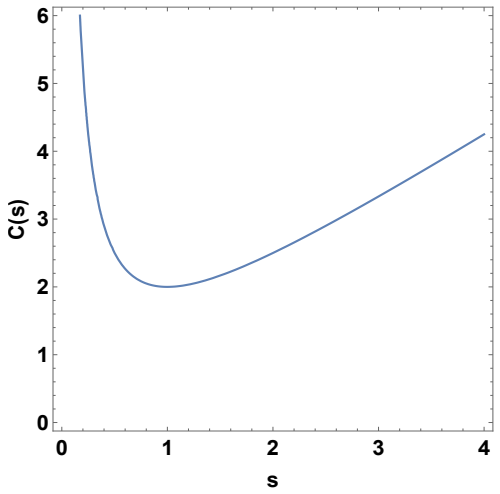

Figure 3.3.: Traveling periodic wave speed, $C(s)$, for the juveniles-adults model in a homogeneous landscape (3.2.10) as a function of wave shape parameter s. Parameters are as follows $r_1 = 6$, $D_{u_1} = D_{v_1} = 1$, $\mu_{u_1} = \mu_{v_1} = 1$, and $m_1 = 1$.

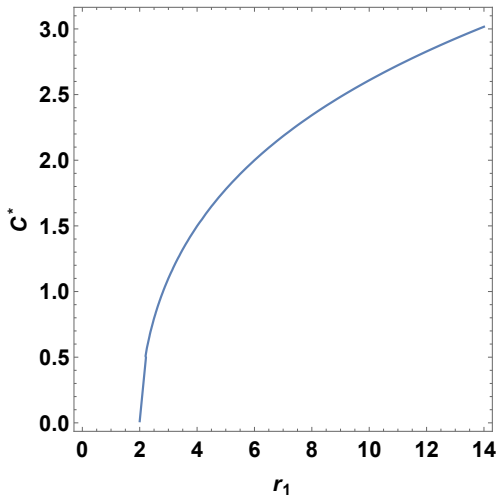

Figure 3.4.: Spreading speed in a homogeneous landscape (3.2.10) as a function of reproduction rate, r_1. Parameters are as follows $D_{u_1} = D_{v_1} = 1$, $\mu_{u_1} = \mu_{v_1} = 1$, and $m_1 = 1$.

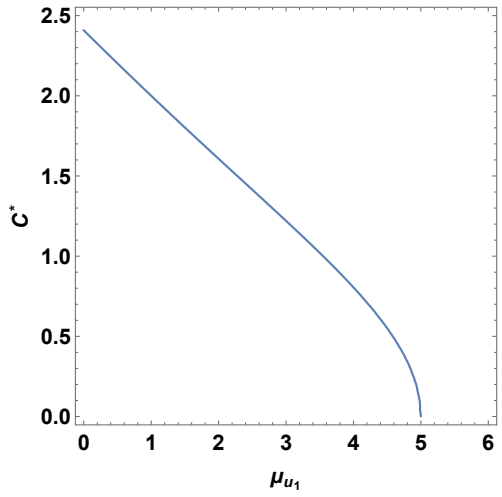

Figure 3.5.: Spreading speed in a homogeneous landscape (3.2.10) as a function of mortality coefficient for juveniles, μ_{u_1}. Parameters are as follows $D_{u_1} = D_{v_1} = 1$, $\mu_{v_1} = 1$, $m_1 = 1$, and $r_1 = 6$.

3.3. Sensitivity and Elasticity for Minimal Traveling Wave Speed in a homogeneous Landscape

We apply the sensitivity and elasticity formulas from Section 2.6 to the explicit expression of C^* in (3.2.10). If p is any of the model parameters, we can differentiate the expression

$$C^*(p) = \min_{s>0} C(s,p) = C(s^*(p), p) \tag{3.3.1}$$

according to the chain rule and obtain

$$\frac{\partial C^*}{\partial p} = \left(\frac{\partial C}{\partial s}.\frac{\partial s}{\partial p}\right) + \frac{\partial C}{\partial p} = \frac{\partial C}{\partial p}. \tag{3.3.2}$$

The last equality holds since all derivatives are evaluated at $s = s^*$, where $\frac{\partial C}{\partial s} = 0$. The sensitivities are then given as follows with $s = s^*$

$$\frac{\partial C^*}{\partial r_1} = \frac{m_1}{s\sqrt{4r_1m_1 + (D_{u_1}s^2 - m_1 - D_{v_1}s^2 - \mu_{u_1} + \mu_{v_1})^2}}, \tag{3.3.3}$$

$$\frac{\partial C^*}{\partial m_1} = \frac{-1}{2s} + \frac{4r_1 - 2(D_{u_1}s^2 - m_1 - D_{v_1}s^2 - \mu_{u_1} + \mu_{v_1})}{4s\sqrt{4r_1m_1 + (D_{u_1}s^2 - m_1 - D_{v_1}s^2 - \mu_{u_1} + \mu_{v_1})^2}}, \tag{3.3.4}$$

$$\frac{\partial C^*}{\partial D_{u_1}} = \frac{s}{2} + \frac{s(D_{u_1}s^2 - m_1 - D_{v_1}s^2 - \mu_{u_1} + \mu_{v_1})}{2\sqrt{4r_1m_1 + (D_{u_1}s^2 - m_1 - D_{v_1}s^2 - \mu_{u_1} + \mu_{v_1})^2}}, \tag{3.3.5}$$

$$\frac{\partial C^*}{\partial D_{v_1}} = \frac{s}{2} - \frac{s(D_{u_1}s^2 - m_1 - D_{v_1}s^2 - \mu_{u_1} + \mu_{v_1})}{2\sqrt{4r_1m_1 + (D_{u_1}s^2 - m_1 - D_{v_1}s^2 - \mu_{u_1} + \mu_{v_1})^2}}, \tag{3.3.6}$$

$$\frac{\partial C^*}{\partial \mu_{u_1}} = \frac{-1}{2s} - \frac{(D_{u_1}s^2 - m_1 - D_{v_1}s^2 - \mu_{u_1} + \mu_{v_1})}{2s\sqrt{4r_1m_1 + (D_{u_1}s^2 - m_1 - D_{v_1}s^2 - \mu_{u_1} + \mu_{v_1})^2}}, \tag{3.3.7}$$

and

$$\frac{\partial C^*}{\partial \mu_{v_1}} = \frac{-1}{2s} + \frac{(D_{u_1}s^2 - m_1 - D_{v_1}s^2 - \mu_{u_1} + \mu_{v_1})}{2s\sqrt{4r_1m_1 + (D_{u_1}s^2 - m_1 - D_{v_1}s^2 - \mu_{u_1} + \mu_{v_1})^2}}. \tag{3.3.8}$$

By using sensitivity and elasticity formulas and by using the partial derivatives (3.3.3)-(3.3.8), we get the numerical values of sensitivity and elasticity of C^* to our default parameters in Table 3.1. As expected from illustrations in Section 3.2, C^* decreases with mortality parameters and increases with all other parameters.

Table 3.1.: Sensitivity and Elasticity of the spread speed C^* to population parameters

Population Parameter	Sensitivity Value	Elasticity Value
reproduction rate in patch type I (r_1)	0.2	0.6
maturation rate in patch type I (m_1)	0.8	0.4
juveniles diffusion term in patch type I (D_{u_1})	0.4	0.2
adults diffusion term in patch type I (D_{v_1})	0.6	0.3
juveniles mortality term in patch type I (μ_{u_1})	-0.4	-0.2
adults mortality term in patch type I (μ_{v_1})	-0.6	-0.3

The numerical values in Table 3.1 show that the minimal traveling wave speed C^* is most sensitive to maturation rate and most elastic to reproduction rate.

3.4. Effects of Habitat Preference

Individuals usually prefer moving to good patches over moving to bad patches because of abundant resources (Levy and Stiles [48]; Prange et al. [71]) and low risks (Samelius et al. [75]; Creel et al. [16]; Mao et al. [57]). This mechanism increases the chance of the population to persist but not necessarily to spread [55]. In structured population models, we have habitat preference parameters for juveniles and adults, therefore, we have the chance to illustrate how the biased movement of one age group affects population persistence and spread.

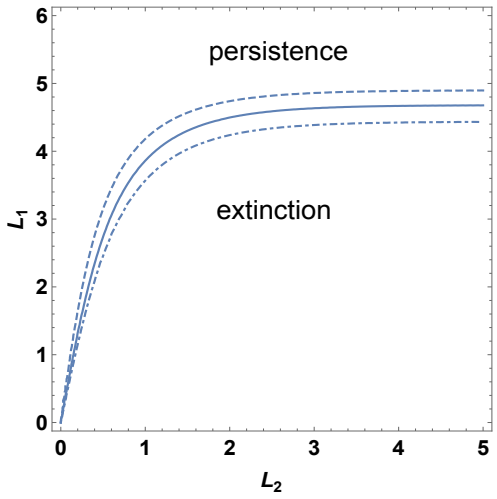

Figure 3.6.: Persistence conditions for the juveniles-adults model in heterogeneous landscapes (2.3.20) as a function of good patch size L_1 and bad patch size L_2 for juveniles habitat preference $\alpha_u = 0.5$ (solid curve), $\alpha_u = 0.25$ (dashed curve) and $\alpha_u = 0.75$ (dash-dot curve). Default parameters are as follows: $r_1 = 2$, $r_2 = 0.2$, $\mu_{u_1} = \mu_{v_1} = 1$, $\mu_{u_2} = \mu_{v_2} = 2$, $D_{u_1} = D_{v_1} = 2$, $D_{u_2} = D_{v_2} = 1$, $m_1 = 5$, and $m_2 = 1$.

In Figure 3.6, we plot the good patch size as a function of bad patch size for different juveniles habitat preference. As expected, the chance of the population to persist increases with juveniles habitat preference. Similarly, as adults habitat preference increases, we expect more adults to transfer from bad patches to good patches, which increases the chance of the population to persist.

To see how population spread can be affected by habitat preference, we plot the minimal traveling wave speed for the juveniles-adults model as a function of reproduction rate in the good patch for different juveniles habitat preference (Figure 3.7). As expected, the plot indicates that juveniles preference to the good patch increases the population spread.

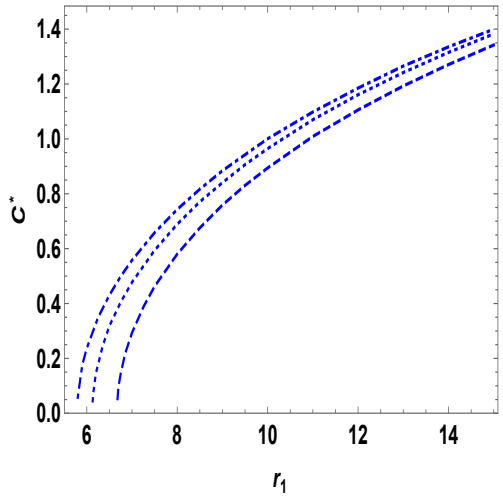

Figure 3.7.: : Minimal traveling wave speed for the juveniles-adults model in patchy landscapes as a function of reproduction rate in the good patch for different juveniles habitat preference $\alpha_u = 0.4$ (dotted), $\alpha_u = 0.25$ (dashed) or the default value $\alpha_u = 0.5$ (dash-dot). The other default parameters are $\alpha_v = 0.5$, as well as $r_1 = 7$, $r_2 = 0.2$, $L_1 = 1$, $L_2 = 1$, $D_{u_1} = D_{v_1} = 0.5$, $D_{u_2} = D_{v_2} = 0.5$, $\mu_{u_1} = \mu_{v_1} = 1$, $\mu_{u_2} = \mu_{v_2} = 2$, and $m_1 = m_2 = 1$.

The dependence of the traveling wave speed on the preference parameters $\alpha_{u,v}$ is more complicated and differs significantly from the case of unstructured populations, see Figure 3.8. When both age groups have the same preference for good patches (dotted curve), then the speed is a hump-shaped function: when preference for good patches is weak, individuals remain in bad patches and the population declines or spreads only slowly. When preference for good patches is very strong, individuals do not leave good patches so that the population spreads only slowly or not at all. This behavior is the same as in the unstructured model [55].

If, however, only one of the two age groups shows habitat preference whereas the other is neutral then the speed does not necessarily decrease to zero as preference approaches unity (dashed and dash-dot curve in Figure 3.8). In fact, the two curves indicate that the speed increases over almost the entire range of habitat preference. Details will depend on parameters chosen. There is, however, an intuitive biological explanation for the observed pattern: A population with two stages could rely on

only one stage for dispersal while reducing dispersal loss by high habitat preference in the other stage. In fact, many marine species have sessile adult populations and disperse only through the larval stage.

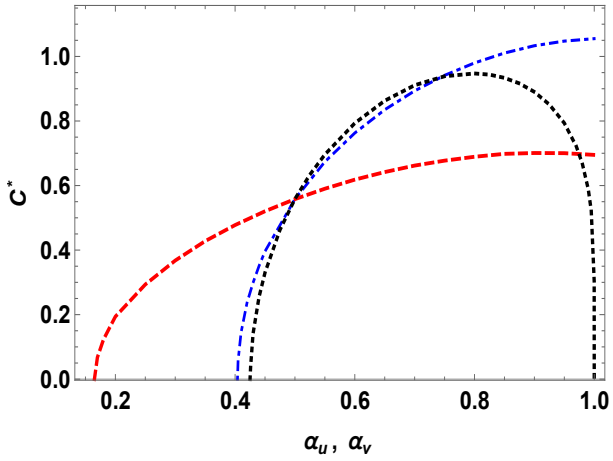

Figure 3.8.: Minimal traveling wave speed for the juveniles-adults model in patchy landscapes as a function of juveniles habitat preference, α_u, (dashed curve), habitat preference for adults, α_v, (dot-dash curve), and equal habitat preference of both, $\alpha_u = \alpha_v$, (dotted curve). Parameters are $L_1 = 1 = L_2$, $r_1 = 7$, $r_2 = 0.2$, $D_{u_1} = D_{v_1} = 0.5$, $D_{u_2} = D_{v_2} = 0.5$, $\mu_{u_1} = \mu_{v_1} = 1$, $\mu_{u_2} = \mu_{v_2} = 2$, and $m_1 = m_2 = 1$. Default habitat preference parameters are $\alpha_u = \alpha_v = 0.5$.

3.5. The Importance of Maturation Rate

We illustrate our results about persistence conditions and spread rates by focusing on the effect of the maturation rate. Specifically, we answer the question of when a simple, unstructured population model is sufficient and when the more complex, structured model that we studied here is required. Since the unstructured model assumes that individuals can reproduce immediately after being born, we expect that our model reduces to the unstructured model in the limit of high maturation rates. Recall the non-spatial model

$$\dot{u} = rv - (m + \mu_u)\, u, \quad \dot{v} = mu - \mu_v v, \tag{3.5.1}$$

and the persistence condition $r > \mu_v \left(1 + \frac{\mu_u}{m}\right)$ from Proposition 2.1.1. In the extreme case when $m \to 0$, the persistence condition will be violated. Juveniles die before they mature, and the population declines. On the other hand, when $m \to \infty$, the persistence condition reduces to $r > \mu_v$. The juveniles stage is so short that juvenile mortality becomes irrelevant.

In the limit of large m, we have $m + \mu_u \approx m$ so that we can add the equations for u and v and get $\frac{d}{dt}(u + v) \approx (r - \mu_v) v$. Dividing the equation for u by m, we find

$$\frac{\dot{u}}{m} = \frac{rv}{m} - \left(1 + \frac{\mu_u}{m}\right) u, \tag{3.5.2}$$

so that in the limit for large m, we find $u \approx 0$. Hence, in the limit of large m, we obtain the unstructured (linear) model $\dot{v} = (r - \mu_v) v$, which we will use for comparison with our structured model.

We begin with comparing the minimal domain size for the structured model (2.2.14) with the unstructured Skellam model [82]:

$$\frac{\partial v}{\partial t} = D_v \frac{\partial^2 v}{\partial x^2} + (r - \mu_v) v. \tag{3.5.3}$$

Taking the limit $m \to \infty$ in formula (2.2.14) gives

$$\lim_{m \to \infty} L^* = \lim_{m \to \infty} \frac{\pi}{z_2} = \pi \sqrt{\frac{D_v}{r - \mu_v}},$$

which is exactly the formula derived by Skellam [82].

In Figure 3.9, we plot the critical patch size for structured populations in a single-patch landscape as a function of maturation rate. The plot indicates that when the maturation rate decreases, the minimal patch size increases. As individuals spend more time in the juvenile stage, they risk mortality and loss from the domain by moving across the hostile boundary. The combined effect is a larger area requirement for persistence. The critical size of the structured population decreases to the critical

size for the unstructured population, which was derived by Skellam [82], as maturation increases.

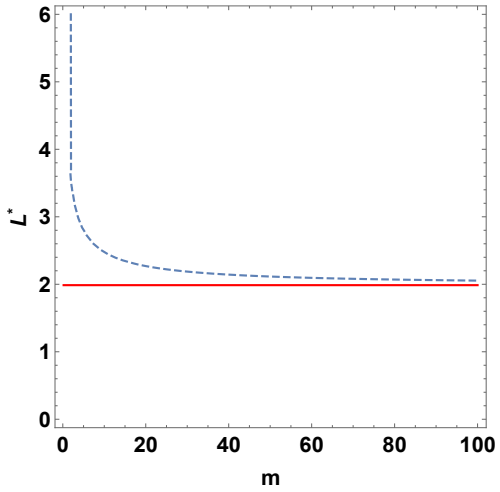

Figure 3.9.: Minimal patch size in a single-patch landscape as a function of maturation coefficients. The dashed curve corresponds to the structured population formula (2.2.14), while the solid curve indicate the value from Skellam's formula $L^* = \pi\sqrt{\frac{D}{r}}$. Parameters are as follows: $\mu_u = \mu_v = 1$, $D_u = D_v = 2$, and $r = 6$.

For a heterogeneous landscape consisting of two periodically alternating patch types, we compare our results for the structured population from Proposition 2.3.1 to the results for the unstructured population; see Equation (10) in [55]. The implicit formula from Proposition 2.3.1 cannot simply be reduced by letting $m \to \infty$. The numerical comparison in Figure 3.10 shows that the critical size for a good patch according to (2.3.20) decreases to the critical size for the unstructured population.

For a comparison of the spreading speed between the structured and unstructured population, we begin with the homogeneous landscape. We find the limit as $m \to \infty$ by rationalizing the numerator of the dispersion relation (3.2.10) to get

$$\begin{aligned} &\lim_{m\to\infty} \frac{1}{2s}\left(D_{u_1}s^2 + D_{v_1}s^2 - m_1 - \mu_{u_1} - \mu_{v_1} + \Delta\right) \\ &= \lim_{m\to\infty} \frac{1}{2s} \frac{-4\left(m_1 - D_{u_1}s^2 + \mu_{u_1}\right)\left(D_{v_1}s^2 - \mu_{v_1}\right) - 4r_1m_1}{D_{u_1}s^2 + D_{v_1}s^2 - m_1 - \mu_{u_1} - \mu_{v_1} - \Delta}, \end{aligned} \tag{3.5.4}$$

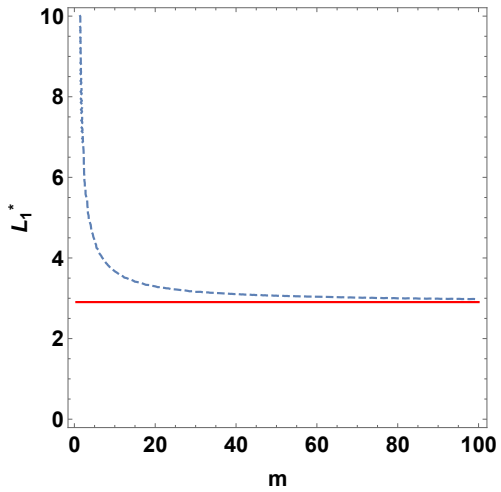

Figure 3.10.: Minimal size of good patches in a patchy periodic landscape as a function of maturation coefficient. The dashed curve corresponds to the structured populations persistence condition (2.3.20), while the solid curve indicates the value for the unstructured population (Equation (10) in [55]). Parameters are as follows: $D_{v_1} = D_{u_1} = 1$, $D_{v_2} = D_{u_2} = 2$, $\mu_{u_1} = \mu_{v_1} = 1$, $\mu_{v_2} = \mu_{u_2} = 2$, $L_2 = 2$, $\alpha_u = \alpha_v = 0.5$, $r_1 = 2$, and $r_2 = 0.2$.

where $\Delta = \sqrt{4r_1m_1 + (D_{u_1}s^2 - m_1 - D_{v_1}s^2 - \mu_{u_1} + \mu_{v_1})^2}$. Dividing numerator and denominator in (3.5.4) by m_1, we can evaluate the limit when $m_1 \to \infty$, as

$$\lim_{m_1 \to \infty} C(s) = \frac{r_1 - \mu_{v_1}}{s} + sD_{v_1}. \tag{3.5.5}$$

The minimum value of (3.5.5) occurs at $s = \sqrt{\frac{r_1 - \mu_{v_1}}{D_{v_1}}}$ and is given by

$$C^* = 2\sqrt{D_{v_1}(r_1 - \mu_{v_1})}. \tag{3.5.6}$$

The expression in (3.5.6) is exactly the spread speed for the unstructured population in (3.5.3) in a homogeneous landscape that was derived by Fisher [23].

Figure 3.11 shows that the spread speed for a structured population in a homogeneous landscape is lower than the spread speed for the corresponding unstructured population. This result could be expected because in structured populations some juveniles

die before they reproduce so that the overall population proceeds more slowly.

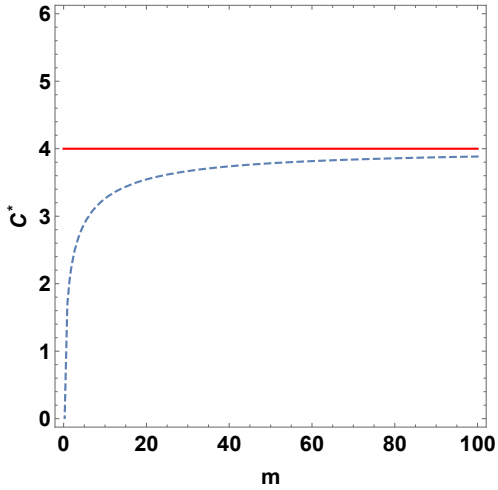

Figure 3.11.: Spread speed in a homogeneous landscape as a function of the maturation coefficient. The dashed curve corresponds to the spread speed for structured populations in homogeneous landscapes (3.2.10), while the solid curve represents Fisher's speed for the unstructured population model, $C^* = 2\sqrt{Dr}$. Parameters are as follows: $D_{v_1} = D_{u_1} = 1$, $\mu_{u_1} = \mu_{v_1} = 1$, and $r_1 = 5$.

So far, we only observed a monotone relationship between the quantity of interest and the maturation rate. For the critical patch size, a monotone relationship seems intuitive since longer maturation times imply higher loss rates either through death or through dispersal. In the context of spread rates, however, dispersal plays an ambivalent role: it increases loss when individuals move into bad patches, but it also increases spread rate since individuals move further (or faster). To obtain a high spread rate, a population needs to grow well and move far. A structured population can divide these two tasks between the different stages. For example, adults could have a high preference for good patches and thereby ensure high growth rate, while juveniles could have a high dispersal rate, thereby ensuring fast propagation. Figure 3.12 shows that such a combination of parameters can indeed lead to spread rates at intermediate maturation rates being higher than at high maturation rates. The two curves are based on the implicit relation for the structured population (dashed) in Proposition

3.1.1 and on the corresponding dispersion relation (equation A32 in [55]) for the corresponding unstructured population (solid).

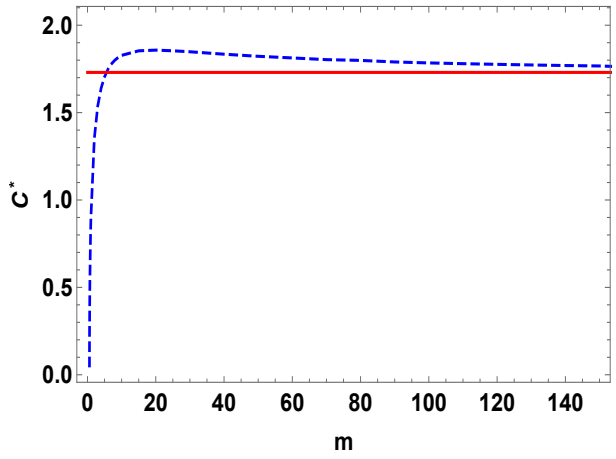

Figure 3.12.: Spread speed in a heterogeneous landscape as a function of the maturation coefficient. The dashed curve corresponds to the structured populations, while the solid curve refers to unstructured population. Parameters are as follows: $L_1 = L_2 = 1$, $r_1 = 2.8$, $r_2 = 0.2$, $D_{u_1} = D_{v_1} = 0.6$, $\mu_{u_1} = \mu_{v_1} = 0.9$, $\mu_{u_2} = \mu_{v_2} = 1$, $D_{u_2} = 16$, $D_{v_2} = 1$, $\alpha_u = 0.162$, and $\alpha_v = 0.756$.

Both analysis and illustrations show that results from the two models will not be the same unless the maturation coefficient is very large. Most actual species, however, have highly structured life cycles with reproductive rates and dispersal ability differing significantly between different stages. For example, Blanding's turtle which is a Canadian species at risk (Paterson et al. [70]) has a very long pre-reproductive stage (14-20 years) [15, 13], which has implications for the management of the species. And so, it is expected that data from structured population models about persistence and spread for this species will be more accurate than those from unstructured population models.

4. Structured Populations With a Sessile Age-Group

In Chapters 2 and 3, we assumed that individuals of all age groups are mobile. We studied in detail the persistence conditions and the traveling periodic waves for these populations in periodically varying landscapes. Many organisms, however, have a life cycle with a sessile age-group. For example, reef fish have sedentary adults (White [89]) whereas urban peregrines have immobile juveniles (Drewitt [20]). These scenarios are represented by setting the diffusion coefficients for the non-moving age group to zero. It is tempting to simply set the corresponding diffusion coefficient in the formulas in the previous chapters to zero. However, since the diffusion coefficient appears in the highest order derivative, the problem is a singular perturbation, and it is not clear that we obtain the correct result. In addition, some of the expressions are so complicated that it is not easy to see what the results would be. Instead, we illustrate how the calculations in Chapters 2 and 3 carry over, and sometimes simplify significantly in that case.

4.1. Persistence Conditions in a Single-Patch Landscape

We only present the calculations for the case of sessile adults here and supply the corresponding calculations for the sessile juveniles case in Appendix C. Hence, on a single good patch, we have the following differential equations

$$\frac{\partial}{\partial t}u(t,x) = D_u\frac{\partial^2 u(t,x)}{\partial x^2} + rv(t,x) - (m+\mu_u)\,u(t,x),\; x\in(0,L)\,, \tag{4.1.1}$$

$$\frac{\partial}{\partial t}v(t,x) = mu(t,x) - \mu_v v(t,x),\; x\in(0,L)\,, \tag{4.1.2}$$

with hostile boundary conditions

$$u\,(t,0) = u(t,L) = 0, \quad \text{and} \quad v(t,0) = v(t,L) = 0, \tag{4.1.3}$$

where L is the length of the patch.

The corresponding eigenvalue problem to determine stability of the trivial solution is

$$\lambda U(x) = D_u U_{xx}(x) - (m+\mu_u)\,U(x) + rV(x), \tag{4.1.4}$$

$$\lambda V(x) = m\,U(x) - \mu_v V(x). \tag{4.1.5}$$

We use (4.1.5) to write an explicit formula for $V\,(x)$ and substitute it into (4.1.4) to get the second order equation

$$\frac{d^2U\,(x)}{dx^2} = \frac{1}{D_u}\left(\lambda - \frac{rm}{\lambda+\mu_v} + m + \mu_u\right)U\,(x)\,,\; x\in(0,L)\,. \tag{4.1.6}$$

The solution of the differential equation (4.1.6) depends mainly on the sign of the the quantity $\left(\lambda - \frac{rm}{\lambda+\mu_v} + m + \mu_u\right)$. Since we are interested in the persistence conditions, we set $\lambda = 0$. Since we are considering a good patch, we conclude from Proposition

2.1.1 that $\left(-\frac{rm}{\mu_v}+m+\mu_u\right)<0$. Then solutions of (4.1.6) can be written in the form

$$U(x)=A\cos(q_1x)+B\sin(q_1x), \tag{4.1.7}$$

where

$$q_1=\sqrt{\frac{1}{D_u}\left(\frac{rm}{\mu_v}-m-\mu_u\right)}.$$

Applying the boundary condition $u(t,0)=0$ to equation (4.1.7), we get $A=0$. The other boundary condition $u(t,L)=0$ requires

$$\sin(q_1L)=0. \tag{4.1.8}$$

Proposition 4.1.1. *The critical patch size formula of model (4.1.1, 4.1.2) with hostile boundary is given by*

$$L^*=\pi\sqrt{\frac{D_u}{\frac{rm}{\mu_v}-m-\mu_u}}. \tag{4.1.9}$$

Remark 4.1.2. *In comparison with the corresponding result in formula* (2.2.14)*, it turns out that the critical patch size in the case of sessile adults does indeed arise from the formula where both age groups are mobile by setting D_{v_1} equal to zero.*

4.2. Persistence Conditions in Periodically Varying Landscapes

As in Section 2.3, we assume that the landscape contains infinitely many patches of two types, periodically alternating: 'good patches' and 'bad patches'. We use L_1 and L_2 to represent the good and bad patch size, respectively, and $L=L_1+L_2$ to represent the spatial period.

Since adult diffusion coefficients in both patches are equal to zero, we write the

periodic system of differential equations in good and bad patches as follows

$$\begin{cases} \frac{\partial u_1(t,x)}{\partial t} = D_{u_1}\frac{\partial^2 u_1(t,x)}{\partial x^2} + r_1 v_1(t,x) - (m_1 + \mu_{u_1})\, u_1(t,x), \\ \frac{\partial v_1(t,x)}{\partial t} = m_1 u_1(t,x) - \mu_{v_1} v_1(t,x), \\ x \in \left(\frac{-L_1}{2}, \frac{L_1}{2}\right) + L\mathbb{Z}, \quad t \geq 0, \end{cases} \tag{4.2.1}$$

and

$$\begin{cases} \frac{\partial u_2(t,x)}{\partial t} = D_{u_2}\frac{\partial^2 u_2(t,x)}{\partial x^2} + r_2 v_2(t,x) - (m_2 + \mu_{u_2})\, u_2(t,x), \\ \frac{\partial v_2(t,x)}{\partial t} = m_2 u_2(t,x) - \mu_{v_2} v_2(t,x), \\ x \in \left(\frac{L_1}{2}, L - \frac{L_1}{2}\right) + L\mathbb{Z}, \quad t \geq 0. \end{cases} \tag{4.2.2}$$

We look for exponential solutions in time which lead us to the following eigenvalue problem for (4.2.1)

$$\lambda U_1(x) = D_{u_1}\frac{d^2U(x)}{dx^2} + r_1 V_1(x) - (m_1 + \mu_{u_1})\, U_1(x), \tag{4.2.3}$$

$$\lambda V_1(x) = m_1 U_1(x) - \mu_{v_1} V_1(x). \tag{4.2.4}$$

We use (4.2.4) to write an explicit formula for $V_1(x)$ and substitute it into (4.2.3) to get the ordinary differential equation

$$\frac{d^2U_1(x)}{dx^2} = \frac{1}{D_{u_1}}\left(\lambda - \frac{r_1 m_1}{\lambda + \mu_{v_1}} + m_1 + \mu_{u_1}\right) U_1(x), \quad x \in \left(\frac{-L_1}{2}, \frac{L_1}{2}\right) + L\mathbb{Z}. \tag{4.2.5}$$

Applying the same procedure to (4.2.2), produces the periodic differential equation

$$\frac{d^2U_2(x)}{dx^2} = \frac{1}{D_{u_2}}\left(\lambda - \frac{r_2 m_2}{\lambda + \mu_{v_2}} + m_2 + \mu_{u_2}\right) U_2(x), \quad x \in \left(\frac{L_1}{2}, L - \frac{L_1}{2}\right) + L\mathbb{Z}. \tag{4.2.6}$$

Since the landscape is periodically varying and the differential equations (4.2.5), (4.2.6) are symmetric with respect to $x \mapsto -x$, it is enough to consider the interval $\left(0, \frac{L}{2}\right)$ if we are looking for symmetric solutions.

We set $\lambda = 0$ and note that, according to Proposition 2.1.1, the sign of the quantity $\left(-\frac{r_i m_i}{\mu_{v_i}} + m_i + \mu_{u_i}\right)$ is negative in the good patch and positive in the bad patch. If we assume that patch I where $x \in \left(\frac{-L_1}{2}, \frac{L_1}{2}\right)$ is the good patch, and patch II where $x \in \left(\frac{L_1}{2}, L - \frac{L_1}{2}\right)$ is the bad patch, then the solution for the differential equations (4.2.5) and (4.2.6) will be respectively as follows

$$U_1(x) = A\cos(q_1 x) + B\sin(q_2 x), \quad x \in \left(\frac{-L_1}{2}, \frac{L_1}{2}\right), \tag{4.2.7}$$

$$U_2(x) = A'\cosh\left(q_2\left(\frac{L}{2} - x\right)\right) + B'\sinh\left(q_2\left(\frac{L}{2} - x\right)\right), \quad x \in \left(\frac{L_1}{2}, L - \frac{L_1}{2}\right), \tag{4.2.8}$$

where

$$q_1 = \sqrt{\frac{1}{D_{u_1}}\left(\frac{r_1 m_1}{\mu_{v_1}} - m_1 - \mu_{u_1}\right)}, \quad q_2 = \sqrt{\frac{1}{D_{u_2}}\left(-\frac{r_2 m_2}{\mu_{v_2}} + m_2 + \mu_{u_2}\right)}. \tag{4.2.9}$$

By symmetry on the unbounded domain, we have the boundary conditions

$$\frac{\partial u_1}{\partial x}(t, 0) = 0, \quad \frac{\partial u_2}{\partial x}\left(t, \frac{L}{2}\right) = 0. \tag{4.2.10}$$

Applying these boundary conditions implies that $B = B' = 0$.

At the interface $x = \frac{L_1}{2}$ we have the matching conditions

$$u_1\left(t, \frac{L_1^+}{2}\right) = k_u u_2\left(t, \frac{L_1^-}{2}\right), \tag{4.2.11}$$

and

$$\frac{\partial u_1}{\partial x}\left(t, \frac{L_1^+}{2}\right) = D_u \frac{\partial u_2}{\partial x}\left(t, \frac{L_1^-}{2}\right), \tag{4.2.12}$$

where k_u is the parameter that measures the discontinuity in juveniles density at the interface.

Applying the interface conditions (4.2.11) and (4.2.12), gives the linear equations

$$A\cos\left(q_1\frac{L_1}{2}\right) - A'k_u\cosh\left(q_2\frac{L_2}{2}\right) = 0, \tag{4.2.13}$$

and

$$Aq_1\sin\left(q_1\frac{L_1}{2}\right) - A'q_2D_u\sinh\left(q_2\frac{L_2}{2}\right) = 0, \tag{4.2.14}$$

where $D_u = \frac{D_{u_2}}{D_{u_1}}$. We write the coefficient matrix for this linear system as follows

$$W = \begin{bmatrix} \cos\left(q_1\frac{L_1}{2}\right) & -k_u\cosh\left(q_2\frac{L_2}{2}\right) \\ \\ q_1\sin\left(q_1\frac{L_1}{2}\right) & -q_2D_u\sinh\left(q_2\frac{L_2}{2}\right) \end{bmatrix}. \tag{4.2.15}$$

A non-trivial solution for a system of linear equations exists if the determinant of the coefficient matrix of this system is equal to zero.

Proposition 4.2.1. *The persistence boundary of model (4.2.1, 4.2.2) with interface conditions (4.2.11, 4.2.12) is given implicitly by*

$$D_uq_2\tanh\left(q_2\frac{L_2}{2}\right) = k_uq_1\tan\left(q_1\frac{L_1}{2}\right), \tag{4.2.16}$$

where q_i are defined in (4.2.9).

We compare the critical patch size L_1^*, from (4.2.16) with the limiting case of very low mobility in the general formula (2.3.20). We observe that, as the diffusion rates for adults in (2.3.20) approach zero, the critical good patch size approaches that of formula (4.2.16). When adults are mobile, larger good patches are required for population persistence since mobile adults may leave good patches and enter bad patches (see Figure 4.1). As adults preference for good habitat increases, the size requirement for good patches decreases.

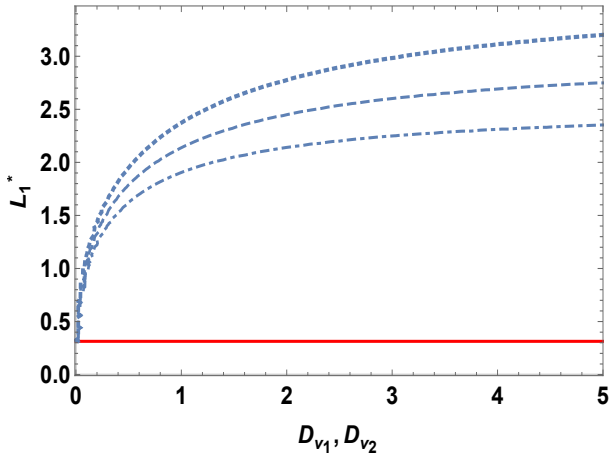

Figure 4.1.: Minimal good patch size for a structured population of juveniles and adults, L_1^*, as a function of adults diffusion rate ($D_{v_1} = D_{v_2}$) according to (2.3.20). The three curves correspond to adults habitat preference $\alpha_v = 0.45$ (dotted), $\alpha_v = 0.5$ (dashed), and $\alpha_v = 0.55$ (dash-dot). The solid line represents the critical good patch size in the case of sessile adults according to (4.2.16). Other parameters are as follows: $L_2 = 1$, $r_1 = 2$, $r_2 = 0.2$, $D_{u_1} = 1$, $D_{u_2} = 2$, $\mu_{u_1} = \mu_{v_1} = 1$, $\mu_{u_2} = \mu_{v_2} = 2$, $m_1 = 5$, $m_2 = 1$, and $\alpha_u = 0.5$.

4.3. The Critical Size of a Single Patch Surrounded by a Non-Lethal Matrix Habitat

In this section, we find the persistence condition for the juveniles-adults model with sessile adult stage on a single 'good patch' surrounded by an infinite 'bad patch'. In the previous section we reached the following differential equations in patch type I and patch type II

$$\frac{d^2U_1(x)}{dx^2} = \frac{1}{D_{u_1}}\left(\lambda - \frac{r_1 m_1}{\lambda + \mu_{v_1}} + m_1 + \mu_{u_1}\right) U_1(x), \quad x \in \left(\frac{-L}{2}, \frac{L}{2}\right), \tag{4.3.1}$$

$$\frac{d^2U_2(x)}{dx^2} = \frac{1}{D_{u_2}}\left(\lambda - \frac{r_2 m_2}{\lambda + \mu_{v_2}} + m_2 + \mu_{u_2}\right) U_2(x), \quad x > \frac{L}{2} \quad \text{or} \quad x < \frac{-L}{2}. \tag{4.3.2}$$

Consequently, the solution of the differential equations (4.3.2, 4.3.1) will be respectively as follows

$$U_1(x) = A\cos(q_1 x) + B\sin(q_1 x), \tag{4.3.3}$$

and

$$U_2(x) = A'e^{-q_2|x|} + B'e^{q_2|x|}, \tag{4.3.4}$$

where q_1 and q_2 are as defined in (4.2.9). Since we require solutions to be bounded in patch type II, we conclude that $B' = 0$.

We apply continuity of flux at the interface $x = -\frac{L}{2}$, to get

$$\begin{aligned} D_{u_1}U_1'\left(-\frac{L}{2}^+\right) &= D_{u_2}U_2'\left(-\frac{L}{2}^-\right) \\ &= q_2 D_{u_2}A'e^{-q_2\frac{L}{2}} \\ &= q_2 D_{u_2}U_2\left(-\frac{L}{2}^-\right) \\ &= \frac{q_2 D_{u_2}}{k_u}U_1\left(-\frac{L}{2}^+\right). \end{aligned} \tag{4.3.5}$$

Similarly, applying continuity of flux at the other interface, $x = \frac{L}{2}$, gives

$$D_{u_1}U_1'\left(\frac{L}{2}^-\right) = -\frac{q_2 D_{u_2}}{k_u}U_1\left(\frac{L}{2}^-\right). \tag{4.3.6}$$

Hence, applying the boundary conditions (4.3.5, 4.3.6), produces the linear equations

$$A\left[\frac{q_2 D_u}{k_u}\cos\left(q_1\frac{L}{2}\right) - q_1\sin\left(q_1\frac{L}{2}\right)\right] + B\left[q_1\cos\left(q_1\frac{L}{2}\right) + \frac{q_2 D_u}{k_u}\sin\left(q_1\frac{L}{2}\right)\right] = 0, \tag{4.3.7}$$

$$A\left[q_1\sin\left(q_1\frac{L}{2}\right) - \frac{q_2 D_u}{k_u}\cos\left(q_1\frac{L}{2}\right)\right] + B\left[q_1\cos\left(q_1\frac{L}{2}\right) + \frac{q_2 D_u}{k_u}\sin\left(q_1\frac{L}{2}\right)\right] = 0. \tag{4.3.8}$$

We write the coefficient matrix of the linear system (4.3.7, 4.3.8) as

$$W = \begin{bmatrix} \frac{q_2 D_u}{k_u}\cos\left(q_1\frac{L}{2}\right) - q_1\sin\left(q_1\frac{L}{2}\right) & q_1\cos\left(q_1\frac{L}{2}\right) + \frac{q_2 D_u}{k_u}\sin\left(q_1\frac{L}{2}\right) \\ \\ q_1\sin\left(q_1\frac{L}{2}\right) - \frac{q_2 D_u}{k_u}\cos\left(q_1\frac{L}{2}\right) & q_1\cos\left(q_1\frac{L}{2}\right) + \frac{q_2 D_u}{k_u}\sin\left(q_1\frac{L}{2}\right) \end{bmatrix}. \quad (4.3.9)$$

To obtain a nontrivial solution for the linear system (4.3.7, 4.3.8), we equate the determinant of the coefficient matrix to zero

$$\tan^2\left(q_1\frac{L}{2}\right) + \frac{q_1^2 - \left(\frac{D_u q_2}{k_u}\right)^2}{q_1 q_2 \frac{D_u}{k_u}}\tan\left(q_1\frac{L}{2}\right) - 1 = 0. \quad (4.3.10)$$

The last equation has two solutions

$$\tan\left(q_1\frac{L}{2}\right) = \frac{q_2 D_u}{q_1 k_u} \quad \text{or} \quad \tan\left(q_1\frac{L}{2}\right) = -\frac{q_1 k_u}{q_2 D_u}. \quad (4.3.11)$$

If $\tan\left(q_1\frac{L}{2}\right) = -\frac{q_1 k_u}{q_2 D_u}$, then the second boundary condition (4.3.6) produces the equation

$$\left(q_1 A + \frac{D_u q_2}{k_u}B\right)\tan\left(q_1\frac{L}{2}\right) = \frac{D_u q_2}{k_u}A - q_1 B. \quad (4.3.12)$$

We then replace $\tan\left(q_1\frac{L}{2}\right)$ by $\left(-\frac{q_1 k_u}{q_2 D_u}\right)$ in (4.3.12) to get

$$\left(q_1 A + \frac{D_u q_2}{k_u}B\right)\left(-\frac{q_1 k_u}{q_2 D_u}\right) = \frac{D_u q_2}{k_u}A - q_1 B. \quad (4.3.13)$$

Or equivalently, $\left(\frac{D_u q_2}{k_u} + \frac{q_1^2 k_u}{q_2 D_u}\right)A = 0$. Since $\left(\frac{D_u q_2}{k_u} + \frac{q_1^2 k_u}{q_2 D_u}\right)$ is different from zero, we conclude $A = 0$. As a result, the eigenfunction in the good patch becomes

$$U_1(x) = B\sin(q_1 x), \quad x \in \left(\frac{-L}{2}, \frac{L}{2}\right). \quad (4.3.14)$$

But $\sin(q_1 x)$ changes sign at $x = 0$, and this contradicts the symmetry of solutions

in the good patch. Therefore, (4.3.10) should have the solution

$$\tan\left(q_1\frac{L}{2}\right)=\frac{q_2D_u}{q_1k_u}. \tag{4.3.15}$$

Proposition 4.3.1. *The critical patch size formula of a single patch surrounded by a non-lethal matrix habitat is given by*

$$L^*=\frac{2}{q_1}\arctan\left(\frac{q_2D_u}{q_1k_u}\right), \tag{4.3.16}$$

where q_1 *and* q_2 *are defined in* (4.2.9).

4.4. Minimal Speed of Traveling Waves

In this section, we find the dispersion relation to obtain the minimal traveling periodic wave speed for the juveniles-adults model with sessile adult stage. For a TPW of speed $C>0$ to the right, we make the same ansatz as in Section 3.1 with $z=x-Ct$ and find the same form, namely

$$u_1(t,x)=e^{-sz}g_1(x), \tag{4.4.1}$$

and

$$v_1(t,x)=e^{-sz}\widetilde{g_1}(x). \tag{4.4.2}$$

Substituting the expressions in (4.4.1, 4.4.2) into equations (4.1.1, 4.1.2) on good patches, we obtain the system

$$sCg_1(x)=D_{u_1}\left(s^2g_1(x)+g_1''(x)-2sg_1'(x)\right)+r_1\widetilde{g_1}(x)-(m_1+\mu_{u_1})g_1(x). \tag{4.4.3}$$

$$sC\widetilde{g_1}(x)=m_1g_1(x)-\mu_{v_1}\widetilde{g_1}(x). \tag{4.4.4}$$

We use (4.4.4) to write an explicit formula for $\widetilde{g_1}(x)$ and substitute it into (4.4.3) to get the differential equation

$$sCg_1(x) = D_{u_1}\left(s^2 g_1(x) + g_1''(x) - 2sg_1'(x)\right) + \frac{r_1 m_1}{sC+\mu_{v_1}} g_1(x) - (m_1+\mu_{u_1})\, g_1(x).$$

We sort the last equation by derivatives of $g_1(x)$ to get

$$g_1''(x) - 2sg_1'(x) + \frac{1}{D_{u_1}}\left(D_{u_1}s^2 + \frac{r_1 m_1}{sC+\mu_{v_1}} - m_1 - \mu_{u_1} - sC\right) g_1(x) = 0. \quad (4.4.5)$$

The linear differential equation (4.4.5) has the quadratic characteristic equation

$$z^2 - 2sz + \frac{1}{D_{u_1}}\left(D_{u_1}s^2 + \frac{r_1 m_1}{sC+\mu_{v_1}} - m_1 - \mu_{u_1} - sC\right) = 0, \quad (4.4.6)$$

which has the two roots

$$z = s \pm \frac{1}{\sqrt{D_{u_1}}}\sqrt{m_1 + sC + \mu_{u_1} - \frac{r_1 m_1}{sC+\mu_{v_1}}}. \quad (4.4.7)$$

The same procedure applied on bad patches gives the the differential equation

$$g_2''(x) - 2sg_2'(x) + \frac{1}{D_{u_2}}\left(D_{u_2}s^2 + \frac{r_2 m_2}{sC+\mu_{v_2}} - m_2 - \mu_{u_2} - sC\right) g_2(x) = 0, \quad (4.4.8)$$

The form of the solution of the differential equation (4.4.5) depends on the sign of the quantity

$$m_1 + sC + \mu_{u_1} - \frac{r_1 m_1}{sC+\mu_{v_1}}. \quad (4.4.9)$$

The expression is negative if and only if

$$r_1 > \frac{(m_1 + sC + \mu_{u_1})(sC+\mu_{v_1})}{m_1}. \quad (4.4.10)$$

In bad patches, according to Proposition 2.1.1 and since s, $C > 0$, we have the inequality

$$r_2 < \frac{\mu_{v_2}\left(m_2 + \mu_{u_2}\right)}{m_2} < \frac{\left(m_2 + sC + \mu_{u_2}\right)\left(sC + \mu_{v_2}\right)}{m_2}. \tag{4.4.11}$$

Therefore, solutions of the differential equation (4.4.8) will be of the form

$$g_2\left(x\right) = e^{sx}\left[A' \cosh\left(q_2 x\right) + B' \sinh\left(q_2 x\right)\right], \tag{4.4.12}$$

where $q_2 = \frac{1}{\sqrt{D_{u_2}}}\sqrt{m_2 + sC + \mu_{u_2} - \frac{r_2 m_2}{sC+\mu_{v_2}}}$.
In good patches, we have to distinguish cases, depending on whether (4.4.10) holds or not. If it holds, we can write the solution of (4.4.5) as

$$g_1\left(x\right) = e^{sx}\left[A \cosh\left(q_1 x\right) + B \sinh\left(q_1 x\right)\right], \tag{4.4.13}$$

where $q_1 = \frac{1}{\sqrt{D_{u_1}}}\sqrt{m_1 + sC + \mu_{u_1} - \frac{r_1 m_1}{sC+\mu_{v_1}}}$. If the reverse inequality holds, we can use hyperbolic-trigonometric formulas to convert between the two; see e.g. [77].
Equations (4.4.12) and (4.4.13) have four constants. To find their values, we use the interface conditions at $x = 0$ and $x = L_1$

$$g_1\left(0^+\right) = k_u g_2\left(0^-\right), \quad g_1\left(L_1^-\right) = k_u g_2\left(-L_2^+\right), \tag{4.4.14}$$

$$g_1'\left(0^+\right) - s g_1\left(0^+\right) = D_u\left[g_2'\left(0^-\right) - s g_2\left(0^-\right)\right], \tag{4.4.15}$$

and

$$g_1'\left(L_1^-\right) - s g_1\left(L_1^-\right) = D_u\left[g_2'\left(-L_2^+\right) - s g_2\left(-L_2^+\right)\right]. \tag{4.4.16}$$

The interface conditions (4.4.14)-(4.4.16) produce the following system of linear equations

$$A = k_u A', \quad B q_1 = B' D_u q_2, \tag{4.4.17}$$

$$A e^{sL} \cosh\left(q_1 L_1\right) + B e^{sL} \sinh\left(q_1 L_1\right) = A' k_u \cosh\left(q_2 L_2\right) - B' k_u \sinh\left(q_2 L_2\right), \tag{4.4.18}$$

and

$$Aq_1e^{sL}\sinh(q_1L_1)+Bq_1e^{sL}\cosh(q_1L_1)=-A'q_2D_u\sinh(q_2L_2)+B'q_2D_u\cosh(q_2L_2)\,. \tag{4.4.19}$$

The corresponding coefficient matrix of the linear system (4.4.17)-(4.4.19) turns out to be

$$W=\begin{bmatrix} 1 & 0 & -k_u & 0 \\ e^{sL}\cosh(q_1L_1) & e^{sL}\sinh(q_1L_1) & -k_u\cosh(q_2L_2) & k_u\sinh(q_2L_2) \\ 0 & q_1 & 0 & -D_uq_2 \\ q_1e^{sL}\sinh(q_1L_1) & q_1e^{sL}\cosh(q_1L_1) & q_2D_u\sinh(q_2L_2) & -q_2D_u\cosh(q_2L_2) \end{bmatrix}.$$

The linear system of equations has a nontrivial solution if and only if the determinant of the coefficient matrix for this system is zero.

Proposition 4.4.1. *The dispersion relation for a TPW in a periodic alternating landscape and with sessile adult stage is given implicitly by*

$$\cosh(sL)=\cosh(q_1L_1)\cosh(q_2L_2)+\frac{(k_uq_1)^2+(D_uq_2)^2}{2D_uk_uq_1q_2}\sinh(q_1L_1)\sinh(q_2L_2)\,. \tag{4.4.20}$$

We compare the minimal TPW speed calculated here with the minimal speed for the structured population from Proposition 3.1.1 in the limit of vanishing adult dispersal. Figure 4.2 shows that when adult mobility decreases to zero, the spread speed will approach the one from (4.4.20). Increasing adult mobility can decrease the population spread rate. This decrease indicates that the loss of individuals due to movement into bad patches has a strong negative impact; stronger than the positive impact that

could be expected from having adults move and contribute to spread. If adults have a strong enough preference for good patches, then the population spread rate can eventually be higher with mobile than with sessile adults (dotted line in Figure 4.2). But when adult preference for good patches is low, increased adult dispersal can slow the invasion and eventually bring it to a halt. In this case, too many adults enter the bad patches and die there before they make it to the next nearest good patch.

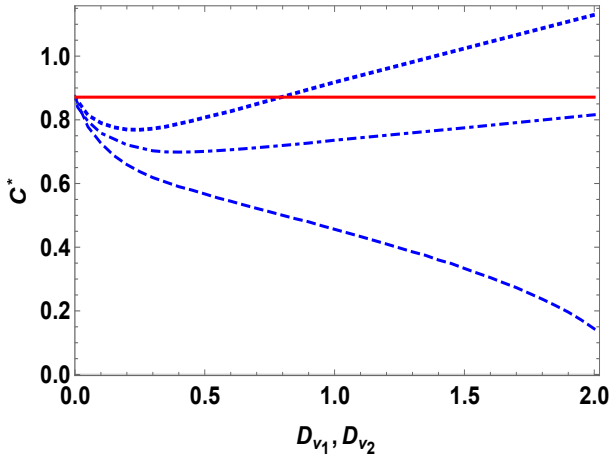

Figure 4.2.: Minimal traveling wave speed for a structured population of two age groups (see Proposition 3.1.1) as a function of adult mobility ($D_{v_1} = D_{v_2}$) with adult habitat preference at $\alpha_v = 0.55$ (dotted), $\alpha_v = 0.5$ (dash-dot), and $\alpha_v = 0.45$ (dashed). The straight line represents the minimal traveling wave speed with sessile adults according to (4.4.20). The remaining parameter values are $L_1 = L_2 = 1$, $r_1 = 7$, $r_2 = 0.2$, $D_{u_1} = 0.5$, $D_{u_2} = 1$, $\mu_{u_1} = \mu_{v_1} = 1$, $\mu_{u_2} = \mu_{v_2} = 2$, $m_1 = m_2 = 1$ and $\alpha_u = 0.5$.

4.5. Wave Speed in a homogeneous Landscape

In this section, we find the wave speed formula for the juveniles-adults model with sessile adult stage in a homogeneous landscape. By substituting $L_2 = 0$ into the dispersion relation (4.4.20), we get

$$\cosh(sL_1) = \cosh(q_1 L_1), \tag{4.5.1}$$

which is equivalent to

$$s = \frac{1}{\sqrt{D_{u_1}}}\sqrt{m_1 + sC + \mu_{u_1} - \frac{r_1 m_1}{sC + \mu_{v_1}}}. \tag{4.5.2}$$

We can find an explicit expression for the wave speed C as a function of wave shape parameter s. Firstly, we square equation (4.5.2) and multiply both sides by D_{u_1} to get

$$s^2 D_{u_1} = m_1 + sC + \mu_{u_1} - \frac{r_1 m_1}{sC + \mu_{v_1}}. \tag{4.5.3}$$

We then multiply (4.5.3) by $(sC + \mu_{v_1})$ to reach

$$r_1 m_1 = m_1 sC + s^2 C^2 + \mu_{u_1} sC - s^3 D_{u_1} C + m_1 \mu_{v_1} + s\mu_{v_1} C + \mu_{u_1}\mu_{v_1} - s^2 D_{u_1}\mu_{v_1}. \tag{4.5.4}$$

We rewrite (4.5.4) as a quadratic equation in C

$$C^2 + C\left(\frac{m_1 + \mu_{u_1} + \mu_{v_1}}{s} - sD_{u_1}\right) + \frac{m_1\mu_{v_1} + \mu_{u_1}\mu_{v_1} - r_1 m_1}{s^2} - D_{u_1}\mu_{v_1} = 0. \tag{4.5.5}$$

The two roots of equation (4.5.5) are

$$\frac{1}{2s}\left(-m_1 - \mu_{u_1} - \mu_{v_1} + D_{u_1}s^2 \pm \sqrt{4r_1 m_1 + \left(D_{u_1}s^2 - m_1 - \mu_{u_1} + \mu_{v_1}\right)^2}\right). \tag{4.5.6}$$

Since the population spread speed is the minimum value of the wave speed over all positive values for s, the wave speed formula will be the root that has a minimum value. By following the same procedure that we used in Section 3.2, we conclude that the root

$$\frac{1}{2s}\left(-m_1 - \mu_{u_1} - \mu_{v_1} + D_{u_1}s^2 + \sqrt{4r_1 m_1 + \left(D_{u_1}s^2 - m_1 - \mu_{u_1} + \mu_{v_1}\right)^2}\right), \tag{4.5.7}$$

has a minimum value over $s > 0$, while the other root does not.

Proposition 4.5.1. *The wave speed formula for the juveniles-adults model with sessile adult stage in a homogeneous landscape is given explicitly by*

$$C(s) = \frac{1}{2s}\left(-m_1 - \mu_{u_1} - \mu_{v_1} + D_{u_1}s^2 + \sqrt{4r_1m_1 + (D_{u_1}s^2 - m_1 - \mu_{u_1} + \mu_{v_1})^2}\right). \tag{4.5.8}$$

Remark 4.5.2. *The corresponding calculations for the case of sessile juveniles are written in Appendix C.*

5. Spread Speed for Structured Populations by Homogenization Techniques

Homogenization is a technique that can proficiently accommodate small-scale variation in environmental heterogeneity for large-scale movement patterns (Yurk [90]). This process is an efficient tool to predict large-scale dispersal for populations with individuals moving differently in different habitat types.

Homogenization techniques have been applied to partial differential equations with Fickian diffusion terms (Othmer [68]) and with ecological diffusion (see Garlick et al. [26, 25]) in order to determine the impact of small-scale habitat variation on large-scale movement, and to explore the asymptotic spread speed. Yurk and Cobbold [91] used homogenization techniques to find the wave speed for unstructured populations in periodically varying landscapes, with the same interface matching conditions as those considered here.

In this chapter, we extend the approach by Yurk and Cobbold [91] to the juveniles-adults model. We then compare numerically the speed of homogenized equations and the dispersion relation for the juveniles-adults model in a heterogeneous landscape. We also generalize this work to structured populations of n age groups.

5.1. Homogenizing the Environment

As in Section 2.3, we denote by L_1 and L_2, the length of good and bad patches, respectively, and by $L = L_1 + L_2$ the period of the landscape. Without loss of generality, we pick a good patch to be located at $(0, L_1)$ and all other good patches L-periodic from thereon. Accordingly, bad patches are are located at $(-L_2, 0)$ and L-periodic from thereon. Hence, in patch j we have the differential equations

$$\frac{\partial u_j(t,x)}{\partial t} = D_{u_j}\frac{\partial^2 u_j(t,x)}{\partial x^2} + f_j(u_j, v_j), \tag{5.1.1}$$

and

$$\frac{\partial v_j(t,x)}{\partial t} = D_{v_j}\frac{\partial^2 v_j(t,x)}{\partial x^2} + \widetilde{f_j}(u_j, v_j), \tag{5.1.2}$$

where $x \in (x_{j-1}, x_j), \quad j = 0, \pm 1, \pm 2, \ldots,$

$$f_j(u_j, v_j) = r_j v_j(t,x) - \left(\mu_{u_j} + m_j\right) u_j(t,x), \tag{5.1.3}$$

and

$$\widetilde{f_j}(u_j, v_j) = m_j u_j(t,x) - \mu_{v_j} v_j(t,x). \tag{5.1.4}$$

The interface conditions are

$$D_{u_{i+1}}\frac{\partial u_{i+1}}{\partial x}\left(t, x_i^+\right) = D_{u_i}\frac{\partial u_i}{\partial x}\left(t, x_i^-\right), \tag{5.1.5}$$

$$u_{i+1}\left(t, x_i^+\right) = k_{u_i} u_i\left(t, x_i^-\right), \tag{5.1.6}$$

$$D_{v_{i+1}}\frac{\partial v_{i+1}}{\partial x}\left(t, x_i^+\right) = D_{v_i}\frac{\partial v_i}{\partial x}\left(t, x_i^-\right), \tag{5.1.7}$$

and

$$v_{i+1}\left(t, x_i^+\right) = k_{v_i} v_i\left(t, x_i^-\right), \tag{5.1.8}$$

where

$$k_{u_i} = \begin{cases} \frac{1}{k_u} & \text{if } i \text{ is odd,} \\ k_u & \text{if } i \text{ is even,} \end{cases} \quad \text{and} \quad k_{v_i} = \begin{cases} \frac{1}{k_v} & \text{if } i \text{ is odd,} \\ k_v & \text{if } i \text{ is even.} \end{cases} \tag{5.1.9}$$

Here, k_u and k_v denote the parameters that measure the discontinuity in density at the interface for juveniles and adults, respectively, see (2.3.3). We choose the period $\epsilon = L = L_1 + L_2 \ll 1$ as our small scale and introduce $y = \frac{x}{\epsilon}$ as a new variable. We assume that diffusion terms and the growth functions vary according to the variable y inside all patches, and the density functions of juveniles and adults depend on both scales x and y. We write the diffusion terms $D_u(y)$ as D_{u_1}, D_{u_2} on good and bad patches, respectively, and similarly for $D_v(y)$. Accordingly, we write (5.1.1) with ecological diffusion as

$$\frac{\partial u(t,x,y)}{\partial t} = \frac{\partial^2}{\partial x^2}\left(D_u(y)\, u(t,x,y)\right) + f_i(u,v) \tag{5.1.10}$$

and similarly for (5.1.2). Consequently, the differential equations in (5.1.1) and (5.1.2) become

$$\frac{\partial u(t,x,y)}{\partial t} = \left[\frac{\partial^2}{\partial x^2} + \frac{2}{\epsilon}\frac{\partial^2}{\partial x \partial y} + \frac{1}{\epsilon^2}\frac{\partial^2}{\partial y^2}\right]\left(D_u(y)\, u(t,x,y)\right) + f_i(u,v), \tag{5.1.11}$$

and

$$\frac{\partial v(t,x,y)}{\partial t} = \left[\frac{\partial^2}{\partial x^2} + \frac{2}{\epsilon}\frac{\partial^2}{\partial x \partial y} + \frac{1}{\epsilon^2}\frac{\partial^2}{\partial y^2}\right]\left(D_v(y)\, v(t,x,y)\right) + \widetilde{f}_i(u,v). \tag{5.1.12}$$

Similarly, the interface conditions (5.1.5)-(5.1.8) will change to

$$D_{u_{i+1}}\left[\frac{\partial}{\partial x} + \frac{1}{\epsilon}\frac{\partial}{\partial y}\right] u\left(t,x,y_i^+\right) = D_{u_i}\left[\frac{\partial}{\partial x} + \frac{1}{\epsilon}\frac{\partial}{\partial y}\right] u\left(t,x,y_i^-\right), \tag{5.1.13}$$

$$u\left(t,x,y_i^+\right) = k_{u_i} u\left(t,x,y_i^-\right), \tag{5.1.14}$$

$$D_{v_{i+1}}\left[\frac{\partial}{\partial x}+\frac{1}{\epsilon}\frac{\partial}{\partial y}\right]v\left(t,x,y_i^+\right)=D_{v_i}\left[\frac{\partial}{\partial x}+\frac{1}{\epsilon}\frac{\partial}{\partial y}\right]v\left(t,x,y_i^-\right), \tag{5.1.15}$$

and

$$v\left(t,x,y_i^+\right)=k_{v_i}v\left(t,x,y_i^-\right). \tag{5.1.16}$$

We then expand the density functions in formal power series in ϵ, i.e.

$$u\left(t,x,y\right)=u_0\left(t,x,y\right)+\epsilon u_1\left(t,x,y\right)+\epsilon^2 u_2\left(t,x,y\right)+\ldots, \tag{5.1.17}$$

and

$$v\left(t,x,y\right)=v_0\left(t,x,y\right)+\epsilon v_1\left(t,x,y\right)+\epsilon^2 v_2\left(t,x,y\right)+\ldots. \tag{5.1.18}$$

We insert the ansatz from (5.1.17) into (5.1.11), to get

$$\begin{aligned}\frac{\partial}{\partial t}\left(u_0+\epsilon u_1+\epsilon^2 u_2+\ldots\right)&=\left(\frac{\partial}{\partial x}+\frac{1}{\epsilon}\frac{\partial}{\partial y}\right)\times\\&\left[\left(\frac{\partial}{\partial x}+\frac{1}{\epsilon}\frac{\partial}{\partial y}\right)\left(D_u\left(y\right)\left(u_0+\epsilon u_1+\epsilon^2 u_2+\ldots\right)\right)\right]+f_i\left(u,v\right),\end{aligned} \tag{5.1.19}$$

and similarly for v. We then multiply (5.1.19) by ϵ^2 and sort the resulting terms by the order of ϵ.

5.2. Equation of Order $\left(\epsilon^0\right)$

We refer to (5.1.19) to write the equation of order (ϵ^0) as

$$\frac{\partial^2\left(D_u\left(y\right)u_0\left(t,x,y\right)\right)}{\partial y^2}=0. \tag{5.2.1}$$

This is equivalent to the differential equation

$$D_{u_i}\frac{\partial^2 u_0\left(t,x,y\right)}{\partial y^2}=0,\ \text{for } y\in\left(y_{i-1},y_i\right),\ i=0,\pm1,\pm2,\ldots, \tag{5.2.2}$$

with interface conditions

$$D_{u_{i+1}}\frac{\partial}{\partial y}u_0\left(t,x,y_i^+\right)=D_{u_i}\frac{\partial}{\partial y}u_0\left(t,x,y_i^-\right), \tag{5.2.3}$$

and

$$u_0\left(t,x,y_i^+\right)=k_{u_i}u_0\left(t,x,y_i^-\right). \tag{5.2.4}$$

We write the integral $\int_0^y \frac{\partial^2(D_u(s)u_0(t,x,s))}{\partial y^2}ds$ as

$$\int_{y_{i-1}}^{y} D_{u_i}\frac{\partial^2 u_0\left(t,x,s\right)}{\partial y^2}ds+\sum_{j=1}^{i-1}\int_{y_{j-1}}^{y_j} D_{u_j}\frac{\partial^2 u_0\left(t,x,s\right)}{\partial y^2}ds, \tag{5.2.5}$$

where $y\in(y_{i-1},y_i)$ for some $i\in\mathbb{Z}$, and integrate (5.2.1) to get

$$\begin{aligned}0=&D_{u_i}\left(\frac{\partial u_0\left(t,x,y\right)}{\partial y}-\frac{\partial u_0\left(t,x,y_{i-1}^+\right)}{\partial y}\right)\\&+\sum_{j=1}^{i-1}D_{u_j}\left(\frac{\partial u_0\left(t,x,y_j^-\right)}{\partial y}-\frac{\partial u_0\left(t,x,y_{j-1}^+\right)}{\partial y}\right).\end{aligned} \tag{5.2.6}$$

We then use the interface condition (5.2.3) to simplify (5.2.6) and obtain

$$D_{u_i}\frac{\partial u_0\left(t,x,y\right)}{\partial y}=D_{u_1}\frac{\partial u_0\left(t,x,y_0^+\right)}{\partial y}, \tag{5.2.7}$$

or equivalently,

$$\frac{\partial u_0\left(t,x,y\right)}{\partial y}=\frac{D_{u_1}}{D_u\left(y\right)}\frac{\partial u_0\left(t,x,y_0^+\right)}{\partial y}. \tag{5.2.8}$$

Define h_i and $\widetilde{h}_i$ as follows

$$h_i=\begin{cases}1, & \text{if } i \text{ is odd},\\ k_u, & \text{if } i \text{ is even},\end{cases}\quad\text{and}\quad \widetilde{h}_i=\begin{cases}1, & \text{if } i \text{ is odd},\\ k_v, & \text{if } i \text{ is even}.\end{cases} \tag{5.2.9}$$

Let $h(y) = h_i;\ y_{i-1} < y < y_i,$ and write the integral $\int_0^y \frac{\partial}{\partial y}\left[h(s)\, u_0(t,x,s)\right] ds$ as

$$\begin{aligned}
&\int_{y_{j-1}}^{y} h_j \frac{\partial u_0(t,x,s)}{\partial y} ds + \sum_{i=1}^{j-1} \int_{y_{i-1}}^{y_i} h_i \frac{\partial u_0(t,x,s)}{\partial y} ds \\
&= h_j \left[u_0(t,x,y) - u_0\left(t,x,y_{j-1}^{+}\right)\right] + \sum_{i=1}^{j-1} h_i \left[u_0\left(t,x,y_i^{-}\right) - u_0\left(t,x,y_{i-1}^{+}\right)\right]. \quad (5.2.10)
\end{aligned}$$

Using the definition of h_i and the interface condition (5.2.4), we get

$$\int_0^y \frac{\partial}{\partial y}\left[h(s)\, u_0(t,x,s)\right] ds = h_j u_0(t,x,y) - h_1 u_0\left(t,x,y_0^{+}\right). \quad (5.2.11)$$

Multiply (5.2.8) by $h(y)$ and integrate the resulting equation to obtain

$$\int_0^y \frac{\partial}{\partial y}\left[h(s)\, u_0(t,x,s)\right] ds = D_{u_1} \frac{\partial}{\partial y} u_0\left(t,x,y_0^{+}\right) \int_0^y \frac{h(s)}{D_u(s)} ds. \quad (5.2.12)$$

We then write the integral $\int_0^y \frac{h(s)}{D_u(s)} ds$ as

$$\begin{aligned}
&\int_{y_{j-1}}^{y} \frac{h(s)}{D_u(s)} ds + \sum_{i=1}^{j-1} \int_{y_{i-1}}^{y_i} \frac{h(s)}{D_u(s)} ds \\
&= \frac{h_j}{D_{u_j}} (y - y_{j-1}) + \sum_{i=1}^{j-1} \frac{h_i}{D_{u_i}} (y_i - y_{i-1}) \\
&= \frac{h_j}{D_{u_j}} (y - y_{j-1}) + \frac{1}{D_{u_1}} (y_1 - y_0) + \frac{k_u}{D_{u_2}} (y_2 - y_1) + \frac{1}{D_{u_1}} (y_3 - y_2) \\
&\quad + \frac{k_u}{D_{u_2}} (y_4 - y_3) + \ldots + \frac{h_{j-1}}{D_{u_{j-1}}} (y_{j-1} - y_{j-2}). \quad (5.2.13)
\end{aligned}$$

We recall that $L_1,\ L_2$ represent the good and the bad patch size, respectively. Hence, $\int_0^y \frac{h(s)}{D_u(s)} ds$ in (5.2.13) can be written as

$$\frac{h_j}{D_{u_j}} (y - y_{j-1}) + \frac{L_1}{L D_{u_1}} + \frac{k_u L_2}{L D_{u_2}} + \frac{L_1}{L D_{u_1}} + \frac{k_u L_2}{L D_{u_2}} + \ldots + \frac{h_{j-1}}{D_{u_{j-1}}} (y_{j-1} - y_{j-2}). \quad (5.2.14)$$

We consider the two cases for j: odd and even. If j is odd, then (5.2.14) becomes

$$\int_0^y \frac{h(s)}{D_u(s)}ds = \frac{1}{D_{u_1}}(y - y_{j-1}) + \frac{j-1}{2}\frac{L_1}{LD_{u_1}} + \frac{j-1}{2}\frac{k_u L_2}{LD_{u_2}}. \tag{5.2.15}$$

Since j is odd and $y = \frac{x}{L}$, we get $y_{j-1} = \frac{x_{j-1}}{L} = \left(\frac{j-1}{2}\right)\frac{L_1}{L} + \left(\frac{j-1}{2}\right)\frac{L_2}{L} = \left(\frac{j-1}{2}\right)$. We replace $\left(\frac{j-1}{2}\right)$ by y_{j-1} in (5.2.15) and write $\int_0^y \frac{h(s)}{D_u(s)}ds$ as

$$\begin{aligned}
&\frac{1}{D_{u_1}}(y - y_{j-1}) + \frac{y_{j-1}}{L}\left[\frac{L_1}{D_{u_1}} + \frac{k_u L_2}{D_{u_2}}\right] \\
&= \frac{y}{D_{u_1}} + \frac{y_{j-1}}{L}\left[\frac{L_1}{D_{u_1}} + \frac{k_u L_2}{D_{u_2}} - \frac{L}{D_{u_1}}\right] \\
&= (y - y_{j-1})\frac{1}{L}\left[\frac{L}{D_{u_1}} - \frac{L_1}{D_{u_1}} - \frac{k_u L_2}{D_{u_2}}\right] + \frac{y}{D_{u_1}} - \frac{y}{L}\left[\frac{L}{D_{u_1}} - \frac{L_1}{D_{u_1}} - \frac{k_u L_2}{D_{u_2}}\right] \\
&= \frac{y}{L}\left[\frac{L_1}{D_{u_1}} + \frac{k_u L_2}{D_{u_2}}\right] + \frac{(y - y_{j-1})}{L}\left[\frac{L}{D_{u_1}} - \frac{L_1}{D_{u_1}} - \frac{k_u L_2}{D_{u_2}}\right].
\end{aligned} \tag{5.2.16}$$

Hence, if j is odd, then

$$\int_0^y \frac{h(s)}{D_u(s)}ds = \frac{y}{L}\left[\frac{L_1}{D_{u_1}} + \frac{k_u L_2}{D_{u_2}}\right] + \frac{(y - y_{j-1})}{L}\left[\frac{L}{D_{u_1}} - \frac{L_1}{D_{u_1}} - \frac{k_u L_2}{D_{u_2}}\right]. \tag{5.2.17}$$

If j is even, then (5.2.14) becomes

$$\int_0^y \frac{h(s)}{D_u(s)}ds = \frac{k_u}{D_{u_2}}(y - y_{j-1}) + \frac{j}{2}\frac{L_1}{LD_{u_1}} + \frac{j}{2}\frac{k_u L_2}{LD_{u_2}} - \frac{k_u L_2}{D_{u_2}L}, \tag{5.2.18}$$

and $y_{j-1} = \frac{j}{2}\frac{L_1}{L} + \frac{j}{2}\frac{L_2}{L} - \frac{L_2}{L}$. We then rewrite $\int_0^y \frac{h(s)}{D_u(s)}ds$ in (5.2.18) as

$$\begin{aligned}
&\frac{k_u}{D_{u_2}}(y - y_{j-1}) + \left(y_{j-1} + \frac{L_2}{L}\right)\frac{L_1}{LD_{u_1}} + \left(y_{j-1} + \frac{L_2}{L}\right)\frac{k_u L_2}{LD_{u_2}} - \frac{k_u L_2}{D_{u_2}L} \\
&= \frac{k_u}{D_{u_2}}(y - y_{j-1}) + \frac{L_1}{L}\frac{y_{j-1}}{D_{u_1}} + \frac{L_1 L_2}{L^2 D_{u_1}} + y_{j-1}\frac{k_u L_2}{LD_{u_2}} + \frac{k_u (L_2)^2}{L^2 D_{u_2}} - \frac{k_u L_2}{D_{u_2}L} \\
&= \frac{k_u}{D_{u_2}}y + \frac{y_{j-1}}{L}\left[\frac{L_1}{D_{u_1}} + \frac{k_u L_2}{D_{u_2}} - \frac{k_u L}{D_{u_2}}\right] + \frac{L_1 L_2 D_{u_2} - k_u D_{u_1} L_1 L_2}{L^2 D_{u_1} D_{u_2}}.
\end{aligned} \tag{5.2.19}$$

Since j is even, we write $y_{j-1} = y_j - \frac{L_2}{L}$ and $y - y_{j-1} = y - y_j + \frac{L_2}{L}$. Hence, replacing y_{j-1} in (5.2.19) by $y_j - \frac{L_2}{L}$ gives

$$\begin{aligned}\int_0^y \frac{h(s)}{D_u(s)}ds &= \frac{k_u}{D_{u_2}}y + \frac{y_j}{L}\left[\frac{L_1}{D_{u_1}} + \frac{k_u L_2}{D_{u_2}} - \frac{k_u L}{D_{u_2}}\right] \\ &= \frac{(y_j - y)}{L}\left[\frac{L_1}{D_{u_1}} + \frac{k_u L_2}{D_{u_2}} - \frac{k_u L}{D_{u_2}}\right] + \frac{k_u}{D_{u_2}}y + \frac{y}{L}\left[\frac{L_1}{D_{u_1}} + \frac{k_u L_2}{D_{u_2}} - \frac{k_u L}{D_{u_2}}\right] \\ &= \frac{y}{L}\left[\frac{L_1}{D_{u_1}} + \frac{k_u L_2}{D_{u_2}}\right] + \frac{(y_j - y)}{L}\left[\frac{L_1}{D_{u_1}} + \frac{k_u L_2}{D_{u_2}} - \frac{k_u L}{D_{u_2}}\right]. \qquad (5.2.20)\end{aligned}$$

We conclude that if j is even, then

$$\int_0^y \frac{h(s)}{D_u(s)}ds = \frac{y}{L}\left[\frac{L_1}{D_{u_1}} + \frac{k_u L_2}{D_{u_2}}\right] + \frac{(y_j - y)}{L}\left[\frac{L_1}{D_{u_1}} + \frac{k_u L_2}{D_{u_2}} - \frac{k_u L}{D_{u_2}}\right]. \qquad (5.2.21)$$

Define $\Delta(y)$ as follows

$$\Delta(y) = \begin{cases} \frac{(y - y_{i-1})L_2}{L}, & \text{for } i \text{ odd}, \\ \frac{(y_i - y)L_1}{L}, & \text{for } i \text{ even}. \end{cases} \qquad (5.2.22)$$

We use the definition of $\Delta(y)$ and (5.2.17, 5.2.21) to write $\int_0^y \frac{h(s)}{D_u(s)}ds$ as

$$\int_0^y \frac{h(s)}{D_u(s)}ds = \frac{y}{L}\left[\frac{L_1}{D_{u_1}} + \frac{k_u L_2}{D_{u_2}}\right] + \Delta(y)\left[\frac{1}{D_{u_1}} - \frac{k_u}{D_{u_2}}\right]. \qquad (5.2.23)$$

Recall equations (5.2.11, 5.2.12)

$$\int_0^y \frac{\partial}{\partial y}\left[h(s)\, u_0(t, x, s)\right] ds = h_j u_0(t, x, y) - h_1 u_0\left(t, x, y_0^+\right),$$

and

$$\int_0^y \frac{\partial}{\partial y}\left[h(s)\, u_0(t, x, s)\right] ds = D_{u_1}\frac{\partial}{\partial y}u_0\left(t, x, y_0^+\right)\int_0^y \frac{h(s)}{D_u(s)}ds.$$

We then substitute (5.2.23) into (5.2.12), and apply (5.2.11) to get

$$u_0(t,x,y) = \frac{h_1 u_0\left(t,x,y_0^+\right)}{h(y)} + \frac{D_{u_1}}{h(y)}\frac{\partial}{\partial y}u_0\left(t,x,y_0^+\right)\left[\frac{y}{L}\left(\frac{L_1}{D_{u_1}}+\frac{k_u L_2}{D_{u_2}}\right)+\Delta(y)\left(\frac{1}{D_{u_1}}-\frac{k_u}{D_{u_2}}\right)\right].$$

We need $u_0(t,x,y)$ to be bounded as $y\to\infty$. Hence, $\frac{\partial}{\partial y}u_0\left(t,x,y_0^+\right)=0$, so that

$$u_0(t,x,y) = \frac{g_1(t,x)}{h(y)}, \quad \text{where} \quad g_1(t,x) = h_1 u_0\left(t,x,y_0^+\right). \tag{5.2.24}$$

Remark 5.2.1. *By applying the same procedure to* (5.1.12)*, we find that the lowest-order term of* v *is given by*

$$v_0(t,x,y) = \frac{g_2(t,x)}{\widetilde{h}(y)}, \text{ where } g_2(t,x) = \widetilde{h}_1 v_0\left(t,x,y_0^+\right). \tag{5.2.25}$$

5.3. Equation of Order (ϵ^1)

We refer again to (5.1.19) and write the equation of order (ϵ^1)

$$2\frac{\partial^2}{\partial x\partial y}\left[D_u(y)\,u_0(t,x,y)\right]+\frac{\partial^2}{\partial y^2}\left[D_u(y)\,u_1(t,x,y)\right]=0, \tag{5.3.1}$$

where $y_{i-1}<y<y_i$ and $i=0,\pm1,\pm2,\ldots$. This is equivalent to the differential equation

$$D_{u_i}\left(2\frac{\partial^2}{\partial x\partial y}u_0(t,x,y)+\frac{\partial^2}{\partial y^2}u_1(t,x,y)\right)=0, \tag{5.3.2}$$

with interface conditions

$$D_{u_{i+1}}\left(\frac{\partial u_0}{\partial x}+\frac{\partial u_1}{\partial y}\right)\left(t,x,y_i^+\right)=D_{u_i}\left(\frac{\partial u_0}{\partial x}+\frac{\partial u_1}{\partial y}\right)\left(t,x,y_i^-\right), \tag{5.3.3}$$

and

$$u_1\left(t,x,y_i^+\right)=k_{u_i}u_1\left(t,x,y_i^-\right), \tag{5.3.4}$$

where $i=0,\pm1,\pm2,\ldots$.

Since $h(y)$ is constant inside each patch, we conclude from (5.2.24) that $\frac{\partial u_0}{\partial y}=0$. Hence, equation (5.3.2) becomes

$$D_{u_i}\frac{\partial^2}{\partial y^2}u_1(t,x,y)=0,\quad \text{for}\quad y_{i-1}<y<y_i\quad\text{and}\quad i=0,\pm1,\pm2,\ldots. \tag{5.3.5}$$

We then write the integral $\int_0^y \frac{\partial^2}{\partial y^2}\left[D_u(s)\,u_1(t,x,s)\right]ds$ as

$$\int_{y_{j-1}}^{y} D_{u_j}\frac{\partial^2}{\partial y^2}u_1(t,x,s)\,ds+\sum_{i=1}^{j-1}\int_{y_{j-1}}^{y} D_{u_i}\frac{\partial^2}{\partial y^2}u_1(t,x,s)\,ds, \tag{5.3.6}$$

where $y_{j-1}<y<y_j$. According to equation (5.3.5), $\int_0^y \frac{\partial^2}{\partial y^2}\left[D_u(s)\,u_1(t,x,s)\right]ds=0$. Consequently, (5.3.6) becomes

$$0=D_{u_j}\left[\frac{\partial}{\partial y}u_1(t,x,y)-\frac{\partial}{\partial y}u_1\left(t,x,y_{j-1}^+\right)\right]+\sum_{i=1}^{j-1}\left[\frac{\partial}{\partial y}u_1\left(t,x,y_i^-\right)-\frac{\partial}{\partial y}u_1\left(t,x,y_{i-1}^+\right)\right]. \tag{5.3.7}$$

Since $\frac{\partial}{\partial y}u_0(t,x,y)=0$ and $y=\frac{x}{\epsilon}$, we conclude that $\frac{\partial}{\partial x}u_0(t,x,y)=0$ for all $y\in(y_{i-1},y_i)$, $i=0,\pm1,\pm2,\ldots$. We then write (5.3.7) as

$$\begin{aligned}0=&D_{u_j}\left[\left(\frac{\partial}{\partial y}u_1+\frac{\partial}{\partial x}u_0\right)(t,x,y)-\left(\frac{\partial}{\partial y}u_1+\frac{\partial}{\partial x}u_0\right)\left(t,x,y_{j-1}^+\right)\right]\\&+\sum_{i=1}^{j-1}D_{u_i}\left[\left(\frac{\partial}{\partial y}u_1+\frac{\partial}{\partial x}u_0\right)\left(t,x,y_i^-\right)-\left(\frac{\partial}{\partial y}u_1+\frac{\partial}{\partial x}u_0\right)\left(t,x,y_{i-1}^+\right)\right].\end{aligned} \tag{5.3.8}$$

Applying the interface condition (5.3.3) to equation (5.3.8), gives

$$\frac{\partial}{\partial y}u_1(t,x,y)=\frac{D_{u_1}}{D_u(y)}\left(\frac{\partial}{\partial y}u_1+\frac{\partial}{\partial y}u_0\right)\left(t,x,y_0^+\right)-\frac{\partial}{\partial y}u_1(t,x,y). \tag{5.3.9}$$

We write the integral $\int_0^y \frac{\partial}{\partial y}\left[h\left(s\right)u_1\left(t,x,s\right)\right]ds$ as

$$\int_{y_{j-1}}^{y} h_j \frac{\partial u_1\left(t,x,s\right)}{\partial y}ds + \sum_{i=1}^{j-1}\int_{y_{i-1}}^{y_i} h_i \frac{\partial u_1\left(t,x,s\right)}{\partial y}ds$$
$$= h_j\left[u_1\left(t,x,y\right) - u_1\left(t,x,y_{j-1}^{+}\right)\right] + \sum_{i=1}^{j-1} h_i\left[u_1\left(t,x,y_i^{-}\right) - u_1\left(t,x,y_{i-1}^{+}\right)\right]. \quad (5.3.10)$$

By using the definition of h_i and the condition (5.3.4), equation (5.3.10) becomes

$$\int_0^y \frac{\partial}{\partial y}\left[h\left(s\right)u_1\left(t,x,s\right)\right]ds = h_j u_1\left(t,x,y\right) - h_1 u_1\left(t,x,y_0^{+}\right). \quad (5.3.11)$$

We multiply (5.3.9) by $h\left(y\right)$ and integrate to get

$$\int_0^y \frac{\partial}{\partial y}\left[h\left(s\right)u_1\left(t,x,s\right)\right]ds = D_{u_1}\left(\frac{\partial u_1}{\partial y} + \frac{\partial u_0}{\partial y}\right)\left(t,x,y_0^{+}\right)\int_0^y \frac{h\left(s\right)}{D_u\left(s\right)}ds$$
$$- \int_0^y h\left(s\right)\frac{\partial}{\partial x}u_0\left(t,x,s\right)ds. \quad (5.3.12)$$

Applying (5.2.23) and (5.2.24) to the last equation gives

$$\int_0^y \frac{\partial}{\partial y}\left[h\left(s\right)u_1\left(t,x,s\right)\right]ds = -y\frac{\partial}{\partial x}g_1\left(t,x\right) + D_{u_1}\left(\frac{\partial u_1}{\partial y} + \frac{\partial u_0}{\partial y}\right)\left(t,x,y_0^{+}\right)\times$$
$$\left[\frac{y}{L}\left(\frac{L_1}{D_{u_1}} + \frac{k_u L_2}{D_{u_2}}\right) + \Delta\left(y\right)\left(\frac{1}{D_{u_1}} - \frac{k_u}{D_{u_2}}\right)\right]. \quad (5.3.13)$$

Since the left hand sides in (5.3.11) and (5.3.13) are equal, we get

$$u_1\left(t,x,y\right) = \frac{D_{u_1}}{h\left(y\right)}\left(\frac{\partial u_1}{\partial y} + \frac{\partial u_0}{\partial y}\right)\left(t,x,y_0^{+}\right)\left[\frac{y}{L}\left(\frac{L_1}{D_{u_1}} + \frac{k_u L_2}{D_{u_2}}\right) + \Delta\left(y\right)\left(\frac{1}{D_{u_1}} - \frac{k_u}{D_{u_2}}\right)\right]$$
$$- \frac{y}{h\left(y\right)}\frac{\partial}{\partial x}g_1\left(t,x\right) + \frac{h_1}{h\left(y\right)}u_1\left(t,x,y_0^{+}\right). \quad (5.3.14)$$

We need $u_1(t,x,y)$ to be bounded as $y \to \infty$. Applying this to (5.3.14) gives

$$\frac{\partial}{\partial x} g_1(t,x) = \lim_{y\to\infty} \frac{D_{u_1}}{y} \left(\frac{\partial u_1}{\partial y} + \frac{\partial u_0}{\partial y} \right) \left(t, x, y_0^+ \right) \times \left[\frac{y}{L} \left(\frac{L_1}{D_{u_1}} + \frac{k_u L_2}{D_{u_2}} \right) + \Delta(y) \left(\frac{1}{D_{u_1}} - \frac{k_u}{D_{u_2}} \right) \right]. \tag{5.3.15}$$

By using the definition of $\Delta(y)$, we conclude that $\lim_{y\to\infty} \Delta(y) = 0$. Hence, (5.3.15) can be written as

$$\frac{\partial}{\partial x} g_1(t,x) = \frac{D_{u_1}}{L} \left(\frac{\partial u_1}{\partial y} + \frac{\partial u_0}{\partial y} \right) \left(t, x, y_0^+ \right) \left[\frac{L_1}{D_{u_1}} + \frac{k_u L_2}{D_{u_2}} \right]. \tag{5.3.16}$$

Lastly, we substitute (5.3.16) into (5.3.14) to get

$$u_1(t,x,y) = \frac{a_1(t,x)}{h(y)} + \Delta(y) \frac{a_2(t,x)}{h(y)}, \tag{5.3.17}$$

where

$$a_1(t,x) = h_1 u_1 \left(t, x, y_0^+ \right), \tag{5.3.18}$$

and

$$a_2(t,x) = D_{u_1} \left(\frac{1}{D_{u_1}} - \frac{k_u}{D_{u_2}} \right) \left(\frac{\partial u_1}{\partial y} + \frac{\partial u_0}{\partial y} \right) \left(t, x, y_0^+ \right). \tag{5.3.19}$$

5.4. Equation of Order (ϵ^2)

We refer to (5.1.19) and write the equation of order (ϵ^2)

$$\frac{\partial}{\partial t} u_0(t,x,y) = D_{u_i} \left[\frac{\partial^2}{\partial y^2} u_2(t,x,y) + 2 \frac{\partial^2}{\partial x \partial y} u_1(t,x,y) + \frac{\partial^2}{\partial x^2} u_0(t,x,y) \right] + f_i(u_0, v_0), \tag{5.4.1}$$

where $y_{i-1} < y < y_i$ and $i = 0, \pm 1, \pm 2, \ldots$, with interface conditions

$$D_{u_{i+1}} \left[\frac{\partial u_2}{\partial y} + \frac{\partial u_1}{\partial x} \right] \left(t, x, y_i^+ \right) = D_{u_i} \left[\frac{\partial u_2}{\partial y} + \frac{\partial u_1}{\partial x} \right] \left(t, x, y_i^- \right) \tag{5.4.2}$$

and

$$u_2\left(t,x,y_i^+\right)=k_{u_i}u_2\left(t,x,y_i^-\right). \tag{5.4.3}$$

Consider the integral

$$\begin{aligned}&\int_0^y\left[\frac{\partial^2}{\partial y^2}\left(D_u\left(s\right)u_2\left(t,x,s\right)\right)+\frac{\partial^2}{\partial x\partial y}\left(D_u\left(s\right)u_1\left(t,x,s\right)\right)\right]ds\\&=D_{u_j}\left[\left(\frac{\partial u_2}{\partial y}+\frac{\partial u_1}{\partial x}\right)\left(t,x,y\right)-\left(\frac{\partial u_2}{\partial y}+\frac{\partial u_1}{\partial x}\right)\left(t,x,y_{j-1}^+\right)\right]\\&\quad+\sum_{i=1}^{j-1}D_{u_i}\left[\left(\frac{\partial u_2}{\partial y}+\frac{\partial u_1}{\partial x}\right)\left(t,x,y_i^-\right)-\left(\frac{\partial u_2}{\partial y}+\frac{\partial u_1}{\partial x}\right)\left(t,x,y_{i-1}^+\right)\right].\end{aligned} \tag{5.4.4}$$

Applying the interface condition (5.4.2) to equation (5.4.4), we get

$$\begin{aligned}&\int_0^y\left[\frac{\partial^2}{\partial y^2}\left(D_u\left(s\right)u_2\left(t,x,s\right)\right)+\frac{\partial^2}{\partial x\partial y}\left(D_u\left(s\right)u_1\left(t,x,s\right)\right)\right]ds\\&=D_{u_j}\left(\frac{\partial u_2}{\partial y}+\frac{\partial u_1}{\partial x}\right)\left(t,x,y\right)-D_{u_1}\left(\frac{\partial u_2}{\partial y}+\frac{\partial u_1}{\partial x}\right)\left(t,x,y_0^+\right).\end{aligned} \tag{5.4.5}$$

On the other hand, equation (5.4.1) is equivalent to

$$\begin{aligned}&\frac{\partial^2}{\partial y^2}\left(D_u\left(y\right)u_2\left(t,x,y\right)\right)+\frac{\partial^2}{\partial x\partial y}\left(D_u\left(y\right)u_1\left(t,x,y\right)\right)=\frac{\partial}{\partial t}u_0\left(t,x,y\right)\\&\quad-\frac{\partial^2}{\partial x\partial y}\left(D_u\left(y\right)u_1\left(t,x,y\right)\right)-\frac{\partial^2}{\partial x^2}\left(D_u\left(y\right)u_0\left(t,x,y\right)\right)-f_i\left(u_0,v_0\right).\end{aligned} \tag{5.4.6}$$

In equation (5.4.6), we replace $u_0\left(t,x,y\right)$ and $u_1\left(t,x,y\right)$ by their values in (5.2.24, 5.3.17), and integrate the resulting equation to get

$$\begin{aligned}&\int_0^y\left[\frac{\partial^2}{\partial y^2}\left(D_u\left(s\right)u_2\left(t,x,s\right)\right)+\frac{\partial^2}{\partial x\partial y}\left(D_u\left(s\right)u_1\left(t,x,s\right)\right)\right]ds\\&=\frac{\partial}{\partial t}g_1\left(t,x\right)\int_0^y\frac{ds}{h\left(s\right)}-\frac{\partial}{\partial x}a_2\left(t,x\right)\int_0^y\frac{\partial}{\partial y}\left(\frac{D_u\left(s\right)\Delta\left(s\right)}{h\left(s\right)}\right)ds\\&\quad-\frac{\partial^2}{\partial x^2}g_1\left(t,x\right)\int_0^y\frac{D_u\left(s\right)}{h\left(s\right)}ds-\int_0^y f_i\left(\frac{g_1\left(t,x\right)}{h\left(s\right)},\frac{g_2\left(t,x\right)}{\widetilde{h}\left(s\right)}\right)ds.\end{aligned} \tag{5.4.7}$$

We write the first integral on the right hand side of (5.4.7) as follows

$$\int_0^y \frac{ds}{h\left(s\right)} = \int_{y_{j-1}}^y \frac{ds}{h\left(s\right)} + \sum_{i=1}^{j-1} \int_{y_{i-1}}^{y_i} \frac{ds}{h\left(s\right)} = \frac{1}{h_j}\left(y - y_{j-1}\right) + \sum_{i=1}^{j-1} \frac{1}{h_i}\left(y_i - y_{i-1}\right). \quad (5.4.8)$$

If j is odd, then (5.4.8) becomes

$$\begin{aligned} \int_0^y \frac{ds}{h\left(s\right)} &= \left(y - y_{j-1}\right) + \frac{L_1}{L} + \frac{1}{k_u}\frac{L_2}{L} + \ldots + \frac{1}{k_u}\frac{L_2}{L} \\ &= \left(y - y_{j-1}\right) + \frac{j-1}{2}\frac{L_1}{L} + \frac{j-1}{2}\frac{L_2}{k_u L}. \end{aligned} \quad (5.4.9)$$

Since j is odd, we write y_{j-1} as $y_{j-1} = \frac{j-1}{2}\frac{L_1}{L} + \frac{j-1}{2}\frac{L_2}{L} = \frac{j-1}{2}$. As a result, equation (5.4.9) becomes

$$\begin{aligned} \int_0^y \frac{ds}{h\left(s\right)} &= \left(y - y_{j-1}\right) + y_{j-1}\frac{L_1}{L} + y_{j-1}\frac{1}{k_u}\frac{L_2}{L} \\ &= y + y_{j-1}\frac{L_2}{L}\left[\frac{-L}{L_2} + \frac{L_1}{L_2} + \frac{1}{k_u}\right] \\ &= y + y_{j-1}\frac{L_2}{L}\left[\frac{1}{k_u} - 1\right] \\ &= \left(y - y_{j-1}\right)\frac{L_2}{L}\left[1 - \frac{1}{k_u}\right] + y - y\frac{L_2}{L}\left[1 - \frac{1}{k_u}\right] \\ &= y\left(\frac{L_1 + \frac{L_2}{k_u}}{L}\right) + \frac{L_2}{L}\left(y - y_{j-1}\right)\left[1 - \frac{1}{k_u}\right]. \end{aligned} \quad (5.4.10)$$

If j is even, then we write $\int_0^y \frac{ds}{h(s)}$ as

$$\int_{y_{j-1}}^y \frac{ds}{h\left(s\right)} + \sum_{i=1}^{j-1} \int_{y_{i-1}}^{y_i} \frac{ds}{h\left(s\right)} = \frac{\left(y - y_{j-1}\right)}{k_u} + \frac{y_1 - y_0}{1} + \frac{y_2 - y_1}{k_u} + \ldots + \frac{y_{j-1} - y_{j-2}}{1}. \quad (5.4.11)$$

Since j is even, the last integral can be written as

$$\int_0^y \frac{ds}{h\left(s\right)} = \frac{\left(y - y_{j-1}\right)}{k_u} + \frac{j}{2}\frac{L_1}{L} + \frac{j}{2}\frac{L_2}{k_u L} - \frac{L_2}{k_u L}. \quad (5.4.12)$$

We use the formulas: $y_j = \frac{j}{2}$ and $y_{j-1} = y_j - \frac{L_2}{L}$ to write (5.4.12) as

$$\begin{aligned}\int_0^y \frac{ds}{h(s)} &= \frac{y}{k_u} - \frac{y_j}{k_u} + \frac{L_2}{k_u L} + y_j \frac{L_1}{L} + y_j \frac{L_2}{k_u L} - \frac{L_2}{k_u L} \\ &= \frac{y}{k_u} + y_j \frac{L_1}{L}\left[1 + \frac{L_2}{L_1 k_u} - \frac{L}{L_1 k_u}\right] \\ &= \frac{(y_j - y) L_1}{L}\left(1 - \frac{1}{k_u}\right) + y\left(\frac{1}{k_u} + \frac{L_1}{L}\left(1 - \frac{1}{k_u}\right)\right) \\ &= \frac{y}{L}\left(L_1 + \frac{L_2}{k_u}\right) + \frac{(y_j - y) L_1}{L}\left(1 - \frac{1}{k_u}\right). \end{aligned} \tag{5.4.13}$$

By looking at the results in (5.4.10) and (5.4.13), we conclude

$$\int_0^y \frac{ds}{h(s)} = \frac{y}{L}\left(L_1 + \frac{L_2}{k_u}\right) + \Delta(y)\left(1 - \frac{1}{k_u}\right). \tag{5.4.14}$$

We then consider the second integral on the right hand side of (5.4.7)

$$\begin{aligned}&\int_0^y \frac{\partial}{\partial y}\left(\frac{D_u(s)\Delta(s)}{h(s)}\right) ds \\ &= \int_{y_{j-1}}^y \frac{\partial}{\partial y}\left(\frac{D_u(s)\Delta(s)}{h(s)}\right) ds + \sum_{i=1}^{j-1} \int_{y_{i-1}}^{y_i} \frac{\partial}{\partial y}\left(\frac{D_u(s)\Delta(s)}{h(s)}\right) ds \\ &= \frac{D_{u_j}}{h_j}\left(\Delta(y) - \Delta(y_{j-1})\right) + \sum_{i=1}^{j-1} \frac{D_{u_i}}{h_i}\left(\Delta(y_i) - \Delta(y_{i-1})\right). \end{aligned} \tag{5.4.15}$$

If j is odd, then (5.4.15) becomes

$$\begin{aligned}\int_0^y \frac{\partial}{\partial y}\left(\frac{D_u(s)\Delta(s)}{h(s)}\right) ds = (y - y_{j-1})\frac{D_{u_1} L_2}{L} + (y_1 - y_0)\frac{D_{u_1} L_2}{L} - (y_2 - y_1)\frac{D_{u_2} L_1}{k_u L} \\ + \ldots - (y_{j-1} - y_{j-2})\frac{D_{u_2} L_1}{k_u L}. \end{aligned} \tag{5.4.16}$$

Since j is odd, we use the formula $y_{j-1} = \frac{j-1}{2}$ to write (5.4.16) as follows

$$\int_0^y \frac{\partial}{\partial y}\left(\frac{D_u(s)\Delta(s)}{h(s)}\right) ds = D_{u_1}(y - y_{j-1})\frac{L_2}{L} + D_{u_1}\frac{j-1}{2}\frac{L_1 L_2}{L^2} - \frac{D_{u_2}}{k_u}\frac{j-1}{2}\frac{L_1 L_2}{L^2}$$

$$
\begin{aligned}
&= D_{u_1}\frac{L_2}{L}y - D_{u_1}\frac{L_2}{L}y_{j-1} + D_{u_1}\frac{L_1L_2}{L^2}y_{j-1} - \frac{D_{u_2}}{k_u}\frac{L_1L_2}{L^2}y_{j-1} \\
&= D_{u_1}\frac{L_2}{L}y - y_{j-1}\frac{L_2}{L}\left[D_{u_1} - \frac{D_{u_1}L_1}{L} + \frac{D_{u_2}}{k_u}\frac{L_1}{L}\right] \\
&= -\frac{yL_2}{L^2}\left(D_{u_1}L_2 + \frac{D_{u_2}L_1}{k_u}\right) + (y - y_{j-1})\frac{L_2}{L^2}\left[D_{u_1}L_2 + \frac{D_{u_2}L_1}{k_u}\right] + \frac{D_{u_1}L_2}{L}y \\
&= \frac{yL_1L_2}{L^2}\left(D_{u_1} - \frac{D_{u_2}}{k_u}\right) + \frac{(y - y_{j-1})L_2}{L}\left[\frac{D_{u_1}L_2 + \frac{L_1D_{u_2}}{k_u}}{L}\right]. \qquad (5.4.17)
\end{aligned}
$$

Similarly, if j is even, then

$$
\begin{aligned}
&\int_0^y \frac{\partial}{\partial y}\left(\frac{D_u(s)\Delta(s)}{h(s)}\right)ds \\
&= \int_{y_{j-1}}^y \frac{\partial}{\partial y}\left(\frac{D_u(s)\Delta(s)}{h(s)}\right)ds + \sum_{i=1}^{j-1}\int_{y_{i-1}}^{y_i}\frac{\partial}{\partial y}\left(\frac{D_u(s)\Delta(s)}{h(s)}\right)ds \\
&= \frac{D_{u_j}}{h_j}\left(\Delta(y) - \Delta(y_{j-1})\right) + \sum_{i=1}^{j-1}\frac{D_{u_i}}{h_i}\left(\Delta(y_i) - \Delta(y_{i-1})\right). \qquad (5.4.18)
\end{aligned}
$$

Since j is even and $y_{j-1} = y_j - \frac{L_2}{L}$, we write the R.H.S. in (5.4.18) as

$$
\begin{aligned}
&\frac{D_{u_2}}{k_u}\frac{L_1}{L}(y_{j-1} - y) + D_{u_1}\frac{L_1L_2}{L^2} - \frac{D_{u_2}}{k_u}\frac{L_1L_2}{L^2} + \ldots + D_{u_1}\frac{L_1L_2}{L^2} \\
&= \frac{D_{u_2}}{k_u}\frac{L_1}{L}(y_{j-1} - y) + \frac{j}{2}D_{u_1}\frac{L_1L_2}{L^2} - \frac{j}{2}\frac{D_{u_2}}{k_u}\frac{L_1L_2}{L^2} + \frac{D_{u_2}}{k_u}\frac{L_1L_2}{L^2} \\
&= \frac{D_{u_2}}{k_u}\frac{L_1}{L}\left(y_j - \frac{L_2}{L} - y\right) + y_jD_{u_1}\frac{L_1L_2}{L^2} - y_j\frac{D_{u_2}}{k_u}\frac{L_1L_2}{L^2} + \frac{D_{u_2}}{k_u}\frac{L_1L_2}{L^2} \\
&= y_j\frac{D_{u_2}}{k_u}\frac{L_1}{L} - y\frac{D_{u_2}}{k_u}\frac{L_1}{L} + y_jD_{u_1}\frac{L_1L_2}{L^2} - y_j\frac{D_{u_2}}{k_u}\frac{L_1L_2}{L^2} \\
&= y_j\frac{L_1}{L}\left[\frac{D_{u_2}}{k_u} + D_{u_1}\frac{L_2}{L} - \frac{D_{u_2}}{k_u}\frac{L_2}{L}\right] - y\frac{D_{u_2}}{k_u}\frac{L_1}{L} \\
&= y_j\frac{L_1}{L}\left[\frac{D_{u_2}L_1}{k_uL} + D_{u_1}\frac{L_2}{L}\right] - y\frac{D_{u_2}}{k_u}\frac{L_1}{L} \\
&= (y_j - y)\frac{L_1}{L^2}\left[\frac{D_{u_2}L_1}{k_u} + D_{u_1}L_2\right] - y\frac{D_{u_2}}{k_u}\frac{L_1}{L} + y\frac{L_1}{L}\left[\frac{D_{u_2}L_1}{k_u} + D_{u_1}L_2\right] \\
&= y\frac{L_1L_2}{L^2}\left[D_{u_1} - \frac{D_{u_2}}{k_u}\right] + (y_j - y)\frac{L_1}{L^2}\left[\frac{D_{u_2}L_1}{k_u} + D_{u_1}L_2\right]. \qquad (5.4.19)
\end{aligned}
$$

Hence, if j is even, then

$$\int_0^y \frac{\partial}{\partial y}\left(\frac{D_u(s)\,\Delta(s)}{h(s)}\right)ds = y\frac{L_1L_2}{L^2}\left[D_{u_1}-\frac{D_{u_2}}{k_u}\right]+(y_j-y)\,\frac{L_1}{L^2}\left[\frac{D_{u_2}L_1}{k_u}+D_{u_1}L_2\right]. \tag{5.4.20}$$

We conclude from (5.4.17) and (5.4.20) that the second integral in the right hand side of (5.4.7) can be written as

$$\int_0^y \frac{\partial}{\partial y}\left(\frac{D_u(s)\,\Delta(s)}{h(s)}\right)ds = y\frac{L_1L_2}{L^2}\left[D_{u_1}-\frac{D_{u_2}}{k_u}\right]+\Delta(y)\left[\frac{\frac{D_{u_2}L_1}{k_u}+D_{u_1}L_2}{L}\right]. \tag{5.4.21}$$

We then consider the third integral in the right hand side of (5.4.7). As before, we study the two cases for j: odd and even. If j is odd, then

$$\begin{aligned}
\int_0^y \frac{D_u(s)}{h(s)}ds &= \frac{D_{u_j}}{h_j}(y-y_{j-1})+\sum_{i=1}^{j-1}\frac{D_{u_i}}{h_i}(y_i-y_{i-1})\\
&= D_{u_1}(y-y_{j-1})+\frac{D_{u_1}L_1}{L}+\frac{D_{u_2}L_2}{k_uL}+\ldots+\frac{D_{u_2}L_2}{k_uL}\\
&= D_{u_1}(y-y_{j-1})+y_{j-1}\frac{D_{u_1}L_1}{L}+y_{j-1}\frac{D_{u_2}L_2}{k_uL}\\
&= D_{u_1}y-\frac{y_{j-1}L_2}{L}\left[\frac{LD_{u_1}}{L_2}-\frac{L_1D_{u_1}}{L_2}-\frac{D_{u_2}}{k_u}\right]\\
&= \frac{(y-y_{j-1})\,L_2}{L}\left[D_{u_1}-\frac{D_{u_2}}{k_u}\right]+y\left[D_{u_1}-\frac{L_2}{L}\left(D_{u_1}-\frac{D_{u_2}}{k_u}\right)\right]\\
&= \frac{y}{L}\left[D_{u_1}L_1+\frac{D_{u_2}L_2}{k_u}\right]+\frac{(y-y_{j-1})\,L_2}{L}\left[D_{u_1}-\frac{D_{u_2}}{k_u}\right].
\end{aligned} \tag{5.4.22}$$

Using the definition of $\Delta(y)$ in (5.2.22), we write (5.4.22) as

$$\int_0^y \frac{D_u(s)}{h(s)}ds = \frac{y}{L}\left[D_{u_1}L_1+\frac{D_{u_2}L_2}{k_u}\right]+\Delta(y)\left[D_{u_1}-\frac{D_{u_2}}{k_u}\right]. \tag{5.4.23}$$

For j even, we have

$$\begin{aligned}\int_0^y \frac{D_u(s)}{h(s)}ds &= \frac{D_{u_2}}{k_u}(y-y_{j-1}) + \frac{D_{u_1}L_1}{L} + \frac{D_{u_2}L_2}{k_uL} + \ldots + \frac{D_{u_1}L_1}{L} \\ &= \frac{D_{u_2}}{k_u}(y-y_{j-1}) + y_j\frac{D_{u_1}L_1}{L} + y_j\frac{D_{u_2}L_2}{k_uL} - \frac{D_{u_2}L_2}{k_uL} \\ &= \frac{D_{u_2}}{k_u}\left(y-y_j+\frac{L_2}{L}\right) + y_j\frac{D_{u_1}L_1}{L} + y_j\frac{D_{u_2}L_2}{k_uL} - \frac{D_{u_2}L_2}{k_uL} \\ &= y\frac{D_{u_2}}{k_u} - y_j\frac{D_{u_2}}{k_u} + y_j\frac{D_{u_1}L_1}{L} + y_j\frac{D_{u_2}L_2}{k_uL} \\ &= y\frac{D_{u_2}}{k_u} - y_j\left[\frac{D_{u_2}L_1}{k_uL} - \frac{D_{u_1}L_1}{L}\right] \\ &= \frac{y}{L}\left[D_{u_1}L_1 + \frac{D_{u_2}L_2}{k_u}\right] + \frac{(y_j-y)L_1}{L}\left[D_{u_1} - \frac{D_{u_2}}{k_u}\right]. \end{aligned} \tag{5.4.24}$$

Using the definition of $\Delta(y)$ in (5.2.22) with (5.4.24) and (5.4.23), we write the third integral on the right hand side of (5.4.7) as

$$\int_0^y \frac{D_u(s)}{h(s)}ds = \frac{y}{L}\left[D_{u_1}L_1 + \frac{D_{u_2}L_2}{k_u}\right] + \Delta(y)\left[D_{u_1} - \frac{D_{u_2}}{k_u}\right]. \tag{5.4.25}$$

We then consider the last integral on the right hand side of (5.4.7)

$$\begin{aligned}&\int_0^y f_j\left(\frac{g_1(t,x)}{h(s)}, \frac{g_2(t,x)}{\widetilde{h}(s)}\right)ds \\ &= \int_{y_{j-1}}^y f_j\left(\frac{g_1(t,x)}{h(s)}, \frac{g_2(t,x)}{\widetilde{h}(s)}\right)ds + \sum_{i=1}^{j-1}\int_{y_{i-1}}^{y_i} f_i\left(\frac{g_1(t,x)}{h(s)}, \frac{g_2(t,x)}{\widetilde{h}(s)}\right)ds \\ &= f_j\left(\frac{g_1(t,x)}{h_j}, \frac{g_2(t,x)}{\widetilde{h}_j}\right)(y-y_{j-1}) + \sum_{i=1}^{j-1} f_i\left(\frac{g_1(t,x)}{h_i}, \frac{g_2(t,x)}{\widetilde{h}_i}\right)(y_i-y_{i-1}), \end{aligned} \tag{5.4.26}$$

where

$$f_i(u,v) = \begin{cases} f_1(u,v), & \text{if } i \text{ is odd,} \\ f_2(u,v), & \text{if } i \text{ is even.} \end{cases} \tag{5.4.27}$$

If j is odd, then (5.4.26) becomes

$$\begin{aligned}
&= f_1(g_1,g_2)(y-y_{j-1}) + (y_{j-1}) f_1(g_1,g_2)\frac{L_1}{L} + (y_{j-1}) f_2\left(\frac{g_1}{k_u},\frac{g_2}{k_v}\right)\frac{L_2}{L} \\
&= (y) f_1(g_1,g_2) - y_{j-1}\frac{L_2}{L}\left[\frac{L}{L_2}f_1(g_1,g_2) - \frac{L_1}{L_2}f_1(g_1,g_2) - f_2\left(\frac{g_1}{k_u},\frac{g_2}{k_v}\right)\right] \\
&= f_1(g_1,g_2)\, y + (y-y_{j-1})\frac{L_2}{L}\left[f_1(g_1,g_2) - f_2\left(\frac{g_1}{k_u},\frac{g_2}{k_v}\right)\right] \\
&\quad - y\frac{L_2}{L}\left[f_1(g_1,g_2) - f_2\left(\frac{g_1}{k_u},\frac{g_2}{k_v}\right)\right] \\
&= \frac{y}{L}\left[L_1 f_1(g_1,g_2) + L_2 f_2\left(\frac{g_1}{k_u},\frac{g_2}{k_v}\right)\right] + (y-y_{j-1})\frac{L_2}{L}\left[f_1(g_1,g_2) - f_2\left(\frac{g_1}{k_u},\frac{g_2}{k_v}\right)\right].
\end{aligned} \tag{5.4.28}$$

Similarly, if j is even, then we write (5.4.26) as follows

$$\begin{aligned}
&= f_2\left(\frac{g_1}{k_u},\frac{g_2}{k_v}\right)(y-y_{j-1}) + (y_j) f_1(g_1,g_2)\frac{L_1}{L} + (y_j-1) f_2\left(\frac{g_1}{k_u},\frac{g_2}{k_v}\right)\frac{L_2}{L} \\
&= (y) f_2\left(\frac{g_1}{k_u},\frac{g_2}{k_v}\right) - (y_j) f_2\left(\frac{g_1}{k_u},\frac{g_2}{k_v}\right) + (y_j) f_1(g_1,g_2)\frac{L_1}{L} + (y_j) f_2\left(\frac{g_1}{k_u},\frac{g_2}{k_v}\right)\frac{L_2}{L} \\
&= (y) f_2\left(\frac{g_1}{k_u},\frac{g_2}{k_v}\right) - \frac{y_j}{L}\left[f_2\left(\frac{g_1}{k_u},\frac{g_2}{k_v}\right)L - f_1(g_1,g_2)L_1 - f_2\left(\frac{g_1}{k_u},\frac{g_2}{k_v}\right)L_2\right] \\
&= (y) f_2\left(\frac{g_1}{k_u},\frac{g_2}{k_v}\right) - (y_j)\frac{L_1}{L}\left[f_2\left(\frac{g_1}{k_u},\frac{g_2}{k_v}\right) - f_1(g_1,g_2)\right] \\
&= \frac{y}{L}\left[L_1 f_1(g_1,g_2) + L_2 f_2\left(\frac{g_1}{k_u},\frac{g_2}{k_v}\right)\right] + (y_j-y)\frac{L_1}{L}\left[f_1(g_1,g_2) - f_2\left(\frac{g_1}{k_u},\frac{g_2}{k_v}\right)\right].
\end{aligned} \tag{5.4.29}$$

Using (5.4.28) and (5.4.29), we write the last integral on the right hand side of (5.4.7) as follows

$$\begin{aligned}
\int_0^y f_j\left(\frac{g_1(t,x)}{h(s)},\frac{g_2(t,x)}{\widetilde{h}(s)}\right)ds = y&\left[\frac{L_1 f_1(g_1,g_2) + L_2 f_2\left(\frac{g_1}{k_u},\frac{g_2}{k_v}\right)}{L}\right] \\
&+ \Delta(y)\left[f_1(g_1,g_2) - f_2\left(\frac{g_1}{k_u},\frac{g_2}{k_v}\right)\right].
\end{aligned} \tag{5.4.30}$$

Substitute (5.4.14), (5.4.21), (5.4.25) and (5.4.30) into (5.4.7) and use (5.4.5) to get

$$\begin{aligned}
0 = & \frac{\partial}{\partial t} g_1(t,x) \left[\frac{y}{L} \left(L_1 + \frac{L_2}{k_u} \right) + \Delta(y) \left(1 - \frac{1}{k_u} \right) \right] \\
& - \frac{\partial}{\partial x} a_2(t,x) \left[y \frac{L_1 L_2}{L^2} \left(D_{u_1} - \frac{D_{u_2}}{k_u} \right) + \Delta(y) \left(\frac{D_{u_1} L_2 + \frac{L_1 D_{u_2}}{k_u}}{L} \right) \right] \\
& - \frac{\partial^2}{\partial x^2} g_1(t,x) \left[\frac{y}{L} \left(D_{u_1} L_1 + \frac{D_{u_2} L_2}{k_u} \right) + \Delta(y) \left(D_{u_1} - \frac{D_{u_2}}{k_u} \right) \right] \\
& - \left[\frac{y \left(L_1 f_1(g_1, g_2) + L_2 f_2 \left(\frac{g_1}{k_u}, \frac{g_2}{k_v} \right) \right)}{L} + \Delta(y) \left(f_1(g_1, g_2) - f_2 \left(\frac{g_1}{k_u}, \frac{g_2}{k_v} \right) \right) \right] \\
& - D_u(y) \left(\frac{\partial u_2}{\partial y} + \frac{\partial u_1}{\partial x} \right)(t,x,y) + D_{u_1} \left(\frac{\partial u_2}{\partial y} + \frac{\partial u_1}{\partial x} \right) \left(t, x, y_0^+ \right). \qquad (5.4.31)
\end{aligned}$$

Rewrite (5.4.31) as the following differential equation

$$\begin{aligned}
\frac{\partial}{\partial y} u_2(t,x,y) = & \frac{y}{D_u(y)} \left[\left(\frac{L_1 + \frac{L_2}{k_u}}{L} \right) \frac{\partial}{\partial t} g_1(t,x) - \frac{L_1 L_2}{L^2} \left(D_{u_1} - \frac{D_{u_2}}{k_u} \right) \frac{\partial}{\partial x} a_2(t,x) \right] \\
& - \frac{y}{D_u(y)} \left[\frac{1}{L} \left(D_{u_1} L_1 + \frac{D_{u_2} L_2}{k_u} \right) \frac{\partial^2}{\partial x^2} g_1(t,x) \right] \\
& - \frac{y}{D_u(y)} \left[\frac{L_1 f_1(g_1, g_2) + L_2 f_2 \left(\frac{g_1}{k_u}, \frac{g_2}{k_v} \right)}{L} \right] \\
& + \frac{\Delta(y)}{D_u(y)} \left[\left(1 - \frac{1}{k_u} \right) \frac{\partial}{\partial t} g_1(t,x) - \left(\frac{D_{u_1} L_2 + \frac{L_1 D_{u_2}}{k}}{L} \right) \frac{\partial}{\partial x} a_2(t,x) \right] \\
& - \frac{\Delta(y)}{D_u(y)} \left[\left(D_{u_1} - \frac{D_{u_2}}{k_u} \right) \frac{\partial}{\partial x} a_2(t,x) + f_1(g_1, g_2) - f_2 \left(\frac{g_1}{k_u}, \frac{g_2}{k_v} \right) \right] \\
& + \frac{D_{u_1}}{D_u(y)} \left(\frac{\partial u_2}{\partial y} + \frac{\partial u_1}{\partial x} \right) \left(t, x, y_0^+ \right) - \frac{\partial u_1}{\partial x}(t,x,y). \qquad (5.4.32)
\end{aligned}$$

We then multiply (5.4.32) by $h(y)$ and integrate both sides of the resulting equation. For the left hand side, we follow the same procedure which we used in deriving (5.2.11). The result will be

$$\int_0^y \frac{\partial}{\partial y} \left(h(s) u_2(t,x,s) \right) ds = h(y) u_2(t,x,y) - h_1 u_2 \left(t, x, y_0^+ \right). \qquad (5.4.33)$$

We need $u_2(t,x,y)$ to be bounded as $y \to \infty$. Hence, multiplying the right hand side of (5.4.32) by $h(y)$ and integrating the result, produces the condition

$$0 = \left(\frac{L_1 + \frac{L_2}{k_u}}{L}\right)\frac{\partial}{\partial t}g_1(t,x) - \frac{L_1 L_2}{L^2}\left(D_{u_1} - \frac{D_{u_2}}{k_u}\right)\frac{\partial}{\partial x}a_2(t,x)$$
$$- \frac{1}{L}\left(D_{u_1}L_1 + \frac{D_{u_2}L_2}{k_u}\right)\frac{\partial^2}{\partial x^2}g_1(t,x) - \frac{L_1 f_1(g_1,g_2) + L_2 f_2\left(\frac{g_1}{k_u},\frac{g_2}{k_v}\right)}{L}. \quad (5.4.34)$$

We then use (5.3.16) and (5.3.19) to write $a_2(t,x)$ explicitly as

$$a_2(t,x) = L\left(\frac{1}{D_{u_1}} - \frac{k_u}{D_{u_2}}\right)\left(\frac{L_1}{D_{u_1}} + \frac{k_u L_2}{D_{u_2}}\right)^{-1}\frac{\partial}{\partial x}g_1(t,x). \quad (5.4.35)$$

Substituting this expression for $a_2(t,x)$ into (5.4.34) yields

$$\left(\frac{L_1 + \frac{L_2}{k_u}}{L}\right)\frac{\partial g_1}{\partial t} = \frac{L_1 L_2}{L}\left(D_{u_1} - \frac{D_{u_2}}{k_u}\right)\left(\frac{1}{D_{u_1}} - \frac{k_u}{D_{u_2}}\right)\left(\frac{L_1}{D_{u_1}} + \frac{k_u L_2}{D_{u_2}}\right)^{-1}\frac{\partial^2 g_1}{\partial x^2}$$
$$+ \left(\frac{D_{u_1}L_1 + \frac{D_{u_2}L_2}{k_u}}{L}\right)\frac{\partial^2 g_1}{\partial x^2} + \frac{L_1 f_1(g_1,g_2) + L_2 f_2\left(\frac{g_1}{k_u},\frac{g_2}{k_v}\right)}{L}. \quad (5.4.36)$$

Equation (5.4.36) is equivalent to the differential equation

$$\frac{\partial g_1}{\partial t} = \frac{L_1 L_2}{\left(L_1 + \frac{L_2}{k_u}\right)\left(\frac{L_1}{D_{u_1}} + \frac{k_u L_2}{D_{u_2}}\right)}\left(1 - \frac{D_{u_1}k_u}{D_{u_2}} - \frac{D_{u_2}}{k_u D_{u_1}} + 1\right)\frac{\partial^2 g_1}{\partial x^2}$$
$$+ \left(\frac{D_{u_1}L_1 + \frac{D_{u_2}L_2}{k_u}}{L_1 + \frac{L_2}{k_u}}\right)\frac{\partial^2 g_1}{\partial x^2} + \left(\frac{L_1 f_1(g_1,g_2) + L_2 f_2\left(\frac{g_1}{k_u},\frac{g_2}{k_v}\right)}{L_1 + \frac{L_2}{k_u}}\right). \quad (5.4.37)$$

By simplifying (5.4.37), we reach the reaction diffusion equation

$$\frac{\partial g_1}{\partial t} = \frac{(L_1 + L_2)^2}{\left(L_1 + \frac{L_2}{k_u}\right)\left(\frac{L_1}{D_{u_1}} + \frac{k_u L_2}{D_{u_2}}\right)}\frac{\partial^2 g_1}{\partial x^2} + \left(\frac{L_1 f_1(g_1,g_2) + L_2 f_2\left(\frac{g_1}{k_u},\frac{g_2}{k_v}\right)}{L_1 + \frac{L_2}{k_u}}\right), \quad (5.4.38)$$

where

$$f_1\left(g_1, g_2\right) = r_1 g_2 - \left(\mu_{u_1} + m_1\right) g_1, \tag{5.4.39}$$

and

$$f_2\left(\frac{g_1}{k_u}, \frac{g_2}{k_v}\right) = \frac{r_2}{k_v} g_2 - \frac{\left(\mu_{u_2} + m_2\right)}{k_u} g_1. \tag{5.4.40}$$

Equation (5.4.38) can be written in the simpler form

$$\frac{\partial g_1}{\partial t} = \langle D \rangle_H \left(\widehat{L}\right)^2 \frac{\partial^2 g_1}{\partial x^2} + \langle f \rangle_A, \tag{5.4.41}$$

where

$$\langle D \rangle_H = \left(\frac{L_1 + \frac{L_2}{k_u}}{\frac{L_1}{D_{u_1}} + \frac{k_u L_2}{D_{u_2}}}\right), \qquad \widehat{L} = \left(\frac{L_1 + L_2}{L_1 + \frac{L_2}{k_u}}\right),$$

and

$$\begin{aligned}
\langle f \rangle_A &= \frac{L_1 f_1\left(g_1, g_2\right) + L_2 f_2\left(\frac{g_1}{k_u}, \frac{g_2}{k_v}\right)}{L_1 + \frac{L_2}{k_u}} \\
&= \frac{L_1 r_1 g_2 + L_2 r_2 \frac{g_2}{k_v} - L_1\left(\mu_{u_1} + m_1\right) g_1 - \frac{L_2}{k_u}\left(\mu_{u_2} + m_2\right) g_1}{L_1 + \frac{L_2}{k_u}} \\
&= \frac{\left(L_1 r_1 + \frac{L_2 r_2}{k_v}\right) g_2 - \left(L_1\left(\mu_{u_1} + m_1\right) + \frac{L_2}{k_u}\left(\mu_{u_2} + m_2\right)\right) g_1}{L_1 + \frac{L_2}{k_u}}.
\end{aligned}$$

Similarly, we write the reaction diffusion equation for $g_2\left(t, x\right)$ as

$$\frac{\partial g_2}{\partial t} = \langle \widetilde{D} \rangle_H \left(\widehat{\widetilde{L}}\right)^2 \frac{\partial^2 g_1}{\partial x^2} + \langle \widetilde{f} \rangle_A, \tag{5.4.42}$$

where

$$\langle \widetilde{D} \rangle_H = \left(\frac{L_1 + \frac{L_2}{k_v}}{\frac{L_1}{D_{v_1}} + \frac{k_v L_2}{D_{v_2}}}\right), \qquad \widehat{\widetilde{L}} = \left(\frac{L_1 + L_2}{L_1 + \frac{L_2}{k_v}}\right),$$

and

$$\langle \widetilde{f} \rangle_A = \frac{\left(L_1 m_1 + \frac{L_2 m_2}{k_u}\right) g_1 - \left(L_1 \mu_{v_1} + \frac{L_2 \mu_{v_2}}{k_v}\right) g_2}{L_1 + \frac{L_2}{k_v}}.$$

Equations (5.4.41) and (5.4.42) form a closed system of reaction diffusion equations. In the following section, we calculate the spreading speed that results from this homogenized system.

5.5. Wave Speed Formula from Homogenization

In this section, we use equations (5.4.41) and (5.4.42), which we got from homogenization, to write the wave speed and the spread speed formulas for structured populations of two age groups. Then, we compare numerically the spread speed from the homogenization technique with the spread speed from the dispersion relation for juveniles-adults model in the periodic landscape.

Firstly, we write equations (5.4.41) and (5.4.42) in the simple form

$$\frac{\partial g_i}{\partial t} = d_i \frac{\partial^2 g_i}{\partial x^2} + F_i\left(g_1, g_2\right), \qquad i = 1,\, 2, \tag{5.5.1}$$

where $d_1 = \langle D \rangle_H \left(\widehat{L}\right)^2$, $d_2 = \langle \widetilde{D} \rangle_H \left(\widehat{\widetilde{L}}\right)^2$, $F_1 = \langle f \rangle_A$, and $F_2 = \langle \widetilde{f} \rangle_A$.

We are now going to apply the formalism from Weinberger et al. [88] to the system (5.4.41, 5.4.42). According to Weinberger et al. [88], we need to form the matrix $\mathcal{C}_s$ with the auxiliary variable s as follows

$$\mathcal{C}_s = \operatorname{diag}\left(d_1 s^2, d_2 s^2\right) + \mathbf{F}'\left(\mathbf{0}\right), \tag{5.5.2}$$

where $\mathbf{F}'\left(\mathbf{0}\right)$ is the Jacobian matrix. Consequently, the coefficient matrix $\mathcal{C}_s$ for structured populations of two age groups will be

$$\mathcal{C}_s = \begin{bmatrix} s^2 \langle D \rangle_H \left(\widehat{L}\right)^2 - a & b \\ c & s^2 \langle \widetilde{D} \rangle_H \left(\widehat{\widetilde{L}}\right)^2 - d \end{bmatrix}, \tag{5.5.3}$$

where

$$a = \frac{L_1\left(\mu_{u_1} + m_1\right) + \frac{L_2}{k_u}\left(\mu_{u_2} + m_2\right)}{L_1 + \frac{L_2}{k_u}}, \qquad b = \frac{L_1 r_1 + \frac{L_2 r_2}{k_v}}{L_1 + \frac{L_2}{k_u}},$$

$$c = \frac{L_1 m_1 + \frac{L_2 m_2}{k_u}}{L_1 + \frac{L_2}{k_v}}, \quad \text{and} \quad d = \frac{L_1 \mu_{v_1} + \frac{L_2 \mu_{v_2}}{k_v}}{L_1 + \frac{L_2}{k_v}}.$$

The off-diagonal entries of $\mathcal{C}_s$ are non-negative, so we can use the wave speed formula for cooperative systems as mentioned in Weinberger et al. [88]

$$C\left(s\right) = \left[\frac{\lambda_1\left(s\right)}{s}\right], \qquad s > 0, \tag{5.5.4}$$

where $\lambda_1\left(s\right)$ is the principal eigenvalue of the diagonal blocks of the matrix $\mathcal{C}_s$.

Proposition 5.5.1. [88] *The minimal traveling wave speed for structured populations of two age groups by homogenization techniques is given by*

$$C^* = \min_{s>0}\left[\frac{\lambda_1\left(s\right)}{s}\right], \tag{5.5.5}$$

where $\lambda_1\left(s\right)$ *is the dominant eigenvalue of the coefficient matrix* $\mathcal{C}_s$ *in* (5.5.3).

Finally, we compare the wave speed from the homogenization technique (5.5.4), with the wave speed that we got from the dispersion relation of juveniles-adults model (see Section 3.1). In Figure 5.1, we plot the wave speed curves for both homogenization technique and dispersion relation. The two curves are close to each other and the difference between the minimum wave speeds for the two curves is very small. In Figure 5.2(a), we plot the spread speed as a function of diffusion coefficients in the bad patches. The difference between the spread speeds becomes very small as we increase the values of diffusion coefficients in bad patches. Also, in Figure 5.2(b), we plot the spread speed as a function of the good patch size. We see that the spread speeds from the two different techniques are very close to each other even for large values of the good patch size.

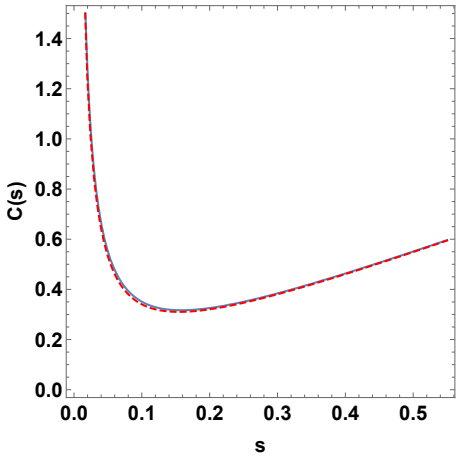

Figure 5.1.: Comparing the dispersion relation from the homogenization formula (5.5.4) (dashed curve) and the exact formula from Proposition 3.1.1 (solid). The two curves are virtually indistinguishable. Parameters are as follows: $L_1 = L_2 = 0.5$, $r_1 = 2.8$, $r_2 = 0.2$, $D_{u_1} = D_{v_1} = 0.6$, $D_{u_2} = D_{v_2} = 2$, $\mu_{u_1} = \mu_{v_1} = 0.9$, $\mu_{u_2} = \mu_{v_2} = 1$, $m_1 = m_2 = 1$, and $\alpha_u = \alpha_v = 0.35388$.

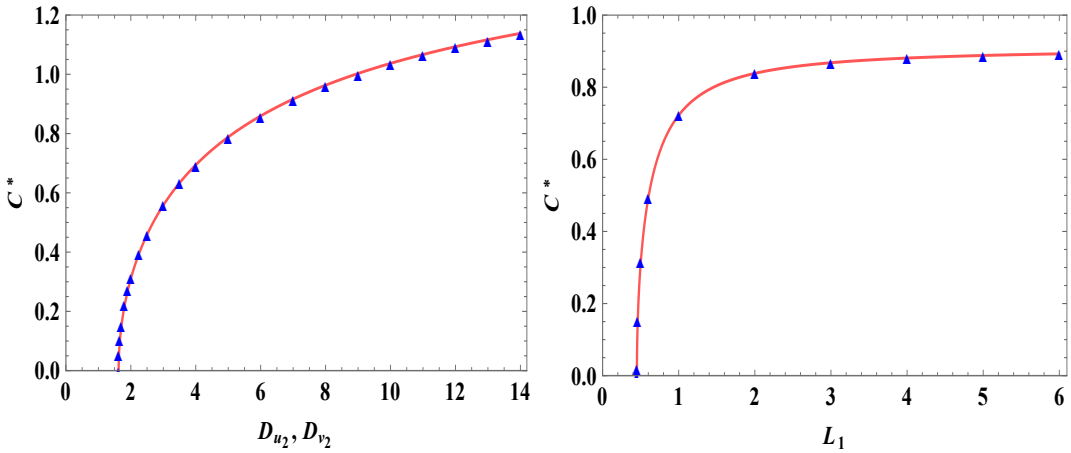

(a) **(b)**

Figure 5.2.: Spread speed for the juveniles-adults model: (a) as a function of diffusion coefficients in bad patches; (b) as a function of good patch size. The solid curves corresponds to the homogenization formula (5.5.5), while the triangles refer to the spread speeds from the exact expression in Proposition 3.1.1. Parameters are as follows: $L_1 = L_2 = 0.5$, $r_1 = 2.8$, $r_2 = 0.2$, $D_{u_1} = D_{v_1} = 0.6$, $D_{u_2} = D_{v_2} = 2$, $\mu_{u_1} = \mu_{v_1} = 0.9$, $\mu_{u_2} = \mu_{v_2} = 1$, $m_1 = m_2 = 1$, and $\alpha_u = \alpha_v = 0.35388$.

In all cases, we find an excellent agreement between the fully heterogeneous speed

(from Proposition 3.1.1) and the homogenized speed (from Formula (5.5.5)), even though the landscape period is on the same order as the diffusion coefficients and not as small as the formal derivation requires.

Remark 5.5.2. *The two expressions that we calculated for the dispersion relation in equation* (3.2.10) *correspond to the dominant and the sub-dominant eigenvalues of the coefficient matrix* $\mathcal{C}_s$ *above.*

5.6. Wave Speed Formula for Structured Populations of n Stages

In this section, we generalize the homogenization technique to structured populations of n-age groups in order to find an approximation to the wave speed and the spread speed formulas in heterogeneous landscapes.

We consider a structured population of n age groups in a periodically alternating landscape of good and bad patches of length L_1 and L_2, respectively. Hence, in patch m we have the differential equations

$$\frac{\partial}{\partial t}u_{j,i}(t,x) = D_{u_{j,i}}\frac{\partial^2}{\partial x^2}u_{j,i}(t,x) + f_{j,i}(u_{1,i}, u_{2,i}, \ldots, u_{n,i}), \tag{5.6.1}$$

where $u_{j,i}(t,x)$ is the density function at time t and location x for the jth age group in patch type i, $x \in (x_{m-1}, x_m)$, $j = 1, 2, \ldots, n$, $i = 1, 2$, and $m = 0, \pm 1, \pm 2, \ldots$. We have interface conditions

$$D_{u_{j,i+1}}\frac{\partial}{\partial x}u_{j,i+1}\left(t, x_i^+\right) = D_{u_{j,i}}\frac{\partial}{\partial x}u_{j,i}\left(t, x_i^-\right), \tag{5.6.2}$$

and

$$u_{j,i+1}\left(t, x_i^+\right) = k_{u_{j,i}}u_{j,i}\left(t, x_i^-\right), \tag{5.6.3}$$

where

$$k_{u_{j,i}} = \begin{cases} \frac{1}{k_{u_j}} & \text{for odd } i, \\ k_{u_j} & \text{for even } i, \end{cases} \tag{5.6.4}$$

and

$$D_{u_{j,i}} = \begin{cases} D_{u_{j,1}} & \text{if } i \text{ is odd}, \\ D_{u_{j,2}} & \text{if } i \text{ is even}. \end{cases} \tag{5.6.5}$$

We choose the period $\epsilon = L = L_1 + L_2 \ll 1$ as our small scale and introduce $y = \frac{x}{\epsilon}$ as a new variable. We assume that diffusion terms and the growth functions vary according to the variable y inside all patches, and the density functions for all age groups depend on both scales x and y. Then we write the density functions as functions of the large and small scale variables and expand in a formal power series in ϵ; i.e.

$$u_j(t, x, y) = u_j^{(0)} + \epsilon u_j^{(1)} + \epsilon^2 u_j^{(2)} + \dots . \tag{5.6.6}$$

By substituting this assumption into the differential equation (5.6.1) and applying the homogenization technique, we get the differential equations

$$\frac{\partial}{\partial t} g_j(t, x) = \langle D_j \rangle_H \left(\widehat{L}_j\right)^2 \frac{\partial^2}{\partial x^2} g_j(t, x) + \langle f_j \rangle_A, \qquad j = 1, 2, \dots, n, \tag{5.6.7}$$

where

$$\langle D_j \rangle_H = \left(\frac{L_1 + \frac{L_2}{k_{u_j}}}{\frac{L_1}{D_{u_{j,1}}} + \frac{k_{u_j} L_2}{D_{u_{j,2}}}} \right), \qquad \widehat{L}_j = \left(\frac{L_1 + L_2}{L_1 + \frac{L_2}{k_{u_j}}} \right),$$

and

$$\langle f_j \rangle_A = \frac{L_1 f_{j,1}(g_1, g_2, \dots, g_n) + L_2 f_{j,2}\left(\frac{g_1}{k_{u_1}}, \frac{g_2}{k_{u_2}}, \dots, \frac{g_n}{k_{un}}\right)}{L_1 + \frac{L_2}{k_{u_j}}}.$$

Equation (5.6.7) can be written in the simple form

$$\frac{\partial}{\partial t} g_j(t, x) = d_j \frac{\partial^2}{\partial x^2} g_j(t, x) + F_j(g_1, g_2, \dots, g_n), \qquad j = 1, 2, \dots, n. \tag{5.6.8}$$

The coefficient matrix $\mathcal{C}_s$ for the system (5.6.8) is

$$\mathcal{C}_s = \text{diag}\left(d_1 s^2, d_2 s^2, \ldots, d_n s^2\right) + \mathbf{F}'(\mathbf{0}), \tag{5.6.9}$$

where $\mathbf{F}'(\mathbf{0})$ is the Jacobian matrix. Consequently, the wave speed and the spread speed formulas for structured populations of n-age groups are

$$C(s) = \left[\frac{\lambda_1(s)}{s}\right], \qquad s > 0, \tag{5.6.10}$$

$$C^* = \min_{s>0}\left[\frac{\lambda_1(s)}{s}\right], \tag{5.6.11}$$

where $\lambda_1(s)$ is the principal eigenvalue of the diagonal blocks of the matrix $\mathcal{C}_s$.

6. Numerical Aspects

In Chapters 2, 3 and 4, we used analytic techniques to study persistence and spread for the juveniles-adults model. We reached explicit formulas for persistence conditions and dispersion relations in homogeneous and heterogeneous landscapes according to different scenarios of juvenile and adult movement. In Chapter 5, we used homogenization techniques to derive the asymptotic speed for the juveniles-adults model and compared it with the minimal traveling wave speed from analytic techniques.

In this chapter, we use a finite-difference method to explore numerical solutions for the juveniles-adults model. We compare the numerical solution to the analytic solution and we apply it to population dynamics with nonlinear growth functions, which we study in detail in Chapter 7.

Finite-difference schemes for reaction-diffusion equations are well developed. We will not present details for the basic schemes nor study convergence properties. The major aspect that we focus on are the interface conditions. We provide evidence that our numerical implementation of these conditions produces the correct results, so that we can apply them to study nonlinear population dynamics models in the next chapter.

6.1. Numerical Solutions in a Single-Patch Landscape

We start numerical solutions with the simplest case where the environment consists of a single good patch with the differential equations (1.4.1, 1.4.2) and hostile boundary conditions in (2.2.1). We use a finite-difference method and we consider the forward-

time central-space scheme (see Strikwerda [85]) to write the partial derivatives in reaction-diffusion equations as follows

$$\frac{\partial}{\partial t}u = \frac{u\,(n+1,k) - u\,(n,k)}{\Delta t}, \quad \text{at a grid point } (k,n)\,,$$

and

$$\frac{\partial^2}{\partial x^2}u = \frac{u\,(n,k+1) - 2u\,(n,k) + u\,(n,k-1)}{(\Delta x)^2}, \quad \text{at a grid point } (k,n)\,,$$

where $\Delta x,\ \Delta t$ represent the step sizes for space and time, respectively. This discretization gives us a time-stepping method for the vector $u\,(\cdot,k)$ that represents the density u at the spatial grid points $k = 1,\ldots,N$.

We chose Δt and Δx such that they satisfy the stability condition of the numerical scheme, see Strikwerda [85]. At the same time, in order to ensure that the numerical solution is smooth enough, we tested several values for Δx, and chose the optimal one.

We chose the eigenfunctions corresponding to the dominant eigenvalue as initial conditions for the density functions u and v. At the boundary points, the density $u\,(\cdot,1)$ and $u\,(\cdot,N)$ is set to zero in each time step. The iteration is implemented as `for`-loop in MATLAB, please see Listing D.1 in Appendix D for details.

In Figure 6.1(a), we plot the numerical solution and compare it to the analytic solution, which we got in Chapter 2. Assuming the single patch to be a 'good patch', we can expect both juveniles and adults to grow through time (Figure 6.1(b)).

Numerical techniques can also be used to find numerical solutions for more complicated models, for example, models with nonlinear growth functions. We find the numerical solution for the juveniles-adults model with nonlinear reproduction term, see Chapter 7 for a more detailed explanation of this growth function, and mixed

boundary conditions in a single-patch landscape

$$\frac{\partial}{\partial t}u\left(t,x\right)=D_u\frac{\partial^2}{\partial x^2}u\left(t,x\right)+\frac{rv\left(t,x\right)}{1+u\left(t,x\right)+v\left(t,x\right)}-\left(m+\mu_u\right)u\left(t,x\right), \tag{6.1.1}$$

$$\frac{\partial}{\partial t}v\left(t,x\right)=D_v\frac{\partial^2}{\partial x^2}v\left(t,x\right)+mu\left(t,x\right)-\mu_v v\left(t,x\right), \tag{6.1.2}$$

$$\frac{\partial}{\partial x}u\left(t,0\right)=u\left(t,L\right)=0, \quad \text{and} \quad \frac{\partial}{\partial x}v(t,0)=v\left(t,L\right)=0. \tag{6.1.3}$$

The boundary condition $\frac{\partial}{\partial x}u\left(t,0\right)=0$ is implemented by setting $u\left(\cdot,1\right)=u\left(\cdot,2\right)$ in each time step.

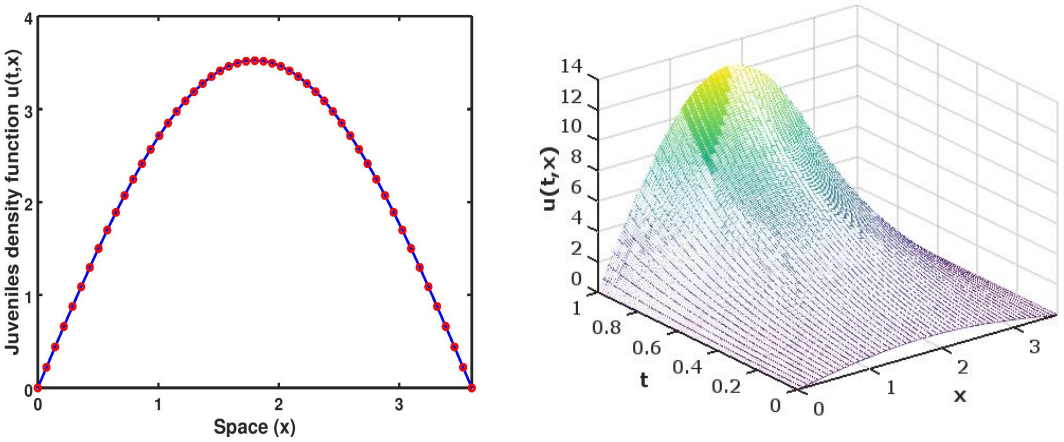

(a) (b)

Figure 6.1.: Output of the program in Listing D.1. The left panel shows the numerical solution (red circles) and the analytic solution (blue curve) for juveniles in a single-patch landscape at time $t=0.5$. The right panel shows how the juveniles density function grows through time. Parameter values are: $L=\frac{\pi}{0.872}$, $r=6$, $m=5$, $\mu_u=\mu_v=1$, $D_u=D_v=0.001$, $\Delta x=\frac{L}{50}$, $\Delta t=\frac{1}{2400}$ and number of grid points $=50$. Initial conditions are: $u\left(0,x\right)=\sin\left(0.872x\right)$ and $v\left(0,x\right)=1.420128\sin\left(0.872x\right)$.

Figure 6.2 shows that the solution grows from small initial conditions and seems to approach a steady state as $t\to\infty$. We will study the shape of steady states in Chapter 7.

The carrying capacities for juveniles and adults can be computed by equating the growth functions to zero

$$\frac{rv}{1+u+v} - (m+\mu_u)\,u = 0, \tag{6.1.4}$$

$$mu - \mu_v v = 0, \tag{6.1.5}$$

and solving the resulting equations (6.1.4, 6.1.5) for u and v to get

$$v^* = \left(\frac{rm}{\mu_v\,(m+\mu_u)} - 1\right)\left(\frac{m}{m+\mu_v}\right), \tag{6.1.6}$$

and

$$u^* = \left(\frac{rm}{\mu_v\,(m+\mu_u)} - 1\right)\left(\frac{m}{m+\mu_v}\right)\left(\frac{\mu_v}{m}\right). \tag{6.1.7}$$

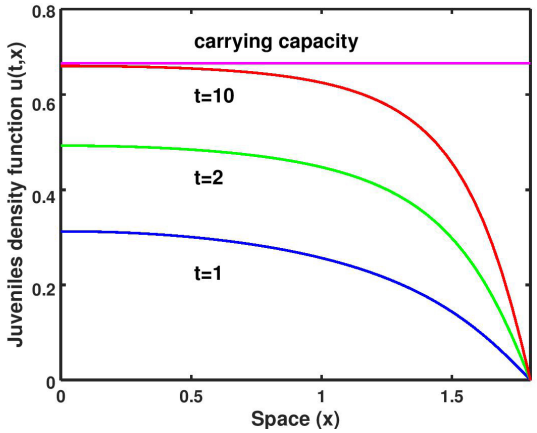

Figure 6.2.: Numerical solution for the nonlinear juveniles-adults model (6.1.1, 6.1.2) with mixed boundary conditions (6.1.3) in a single-patch landscape. Parameter values are: $L = \frac{\pi}{2(0.872)}$, $r = 6$, $m = 5$, $\mu_u = \mu_v = 1$, $D_u = D_v = 0.1$, $\Delta x = \frac{L}{50}$, $\Delta t = \frac{1}{2400}$ and number of grid points = 50. Initial conditions are: $u\,(0,x) = 0.1\cos\,(0.872x)$ and $v\,(0,x) = 0.1(1.420128)\cos\,(0.872x)$.

6.2. Heterogeneous Landscapes

To find numerical solutions for the juveniles-adults model in a heterogeneous landscape, we first derive finite-difference expressions for the interface conditions. We consider a landscape of two patches $\left[0, \frac{L_1}{2}\right]$ and $\left[\frac{L_1}{2}, \frac{L_1+L_2}{2}\right]$ with no-flux at $x = 0$ and $x = \frac{L_1+L_2}{2}$ and interface conditions at $x = \frac{L_1}{2}$ given by (2.3.12) and (2.3.15) We assume that the number of nodes in the good and bad patch are n_{p_1} and n_{p_2}, respectively. We also assume that Δx and Δt represent spatial and time step sizes. We write the interface conditions in (2.3.12) as finite differences as follows

$$0 = u\left(t + \Delta t, \frac{L_1}{2} - \frac{\Delta x}{2}\right) - k_u u\left(t + \Delta t, \frac{L_1}{2} + \frac{\Delta x}{2}\right), \tag{6.2.1}$$

$$\begin{aligned} 0 =& D_{u_1}\left(u\left(t + \Delta t, \frac{L_1}{2} - \frac{\Delta x}{2}\right) - u\left(t + \Delta t, \frac{L_1}{2} - \frac{\Delta x}{2} - \Delta x\right)\right) \\ &- D_{u_2}\left(u\left(t + \Delta t, \frac{L_1}{2} + \frac{\Delta x}{2} + \Delta x\right) - u\left(t + \Delta t, \frac{L_1}{2} + \frac{\Delta x}{2}\right)\right). \end{aligned} \tag{6.2.2}$$

We use n_{p_1} grid points on the interval $\left[0, \frac{L_1}{2}\right]$, then we have $\left(\frac{L_1}{2} - \frac{\Delta x}{2} = n_{p_1}\right)$ and $\left(\frac{L_1}{2} + \frac{\Delta x}{2} = n_{p_1} + 1\right)$. Hence, solving the linear system of (6.2.1) and (6.2.2) produces

$$u\left(t + \Delta t, n_{p_1}\right) = \frac{D_{u_1} u\left(t + \Delta t, n_{p_1} - 1\right) + D_{u_2} u\left(t + \Delta t, n_{p_1} + 2\right)}{D_{u_1} + \frac{D_{u_2}}{k_u}},$$

and

$$u\left(t + \Delta t, n_{p_1} + 1\right) = \frac{D_{u_1} u\left(t + \Delta t, n_{p_1} - 1\right) + D_{u_2} u\left(t + \Delta t, n_{p_1} + 2\right)}{k_u\left(D_{u_1} + \frac{D_{u_2}}{k_u}\right)}.$$

Similarly, the interface conditions in (2.3.15) are equivalent to the conditions

$$v\left(t + \Delta t, n_{p_1}\right) = \frac{D_{v_1} v\left(t + \Delta t, n_{p_1} - 1\right) + D_{v_2} v\left(t + \Delta t, n_{p_1} + 2\right)}{D_{v_1} + \frac{D_{v_2}}{k_v}},$$

and

$$v\left(t+\Delta t, n_{p_1}+1\right)=\frac{D_{v_1} v\left(t+\Delta t, n_{p_1}-1\right)+D_{v_2} v\left(t+\Delta t, n_{p_1}+2\right)}{k_v\left(D_{v_1}+\frac{D_{v_2}}{k_v}\right)}.$$

We use these conditions to simulate numerical solutions for the juveniles-adults model with linear reaction terms (Figure 6.3).

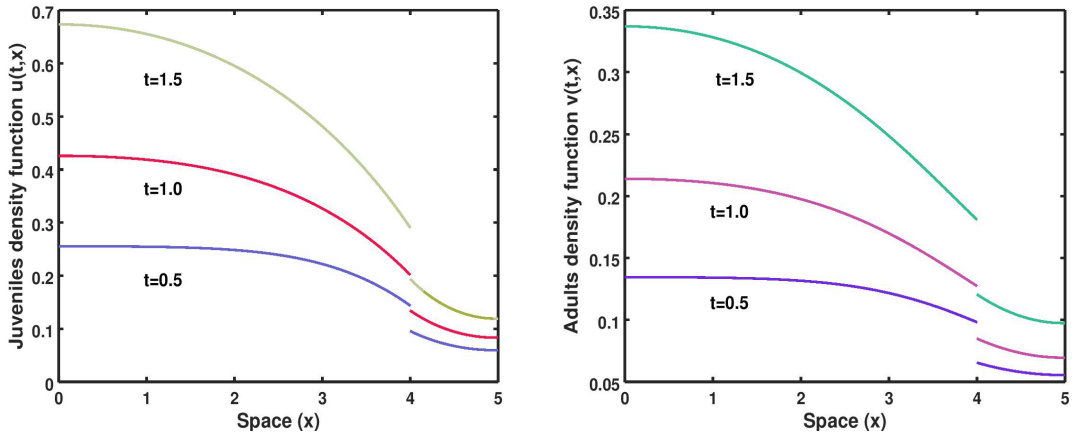

Figure 6.3.: Numerical solution for the linear juveniles-adults model (1.4.1, 1.4.2) with interface conditions (2.3.12, 2.3.15) in a heterogeneous landscape according to Listing D.2. Parameter values are: $L_1 = 4$, $L_2 = 1$, $r_1 = 6$, $r_2 = 0.2$, $m_1 = 1 = m_2$, $\mu_{u_1} = \mu_{v_1} = 1$, $\mu_{u_2} = \mu_{v_2} = 2$, $D_{u_1} = D_{v_1} = 2$, $D_{u_2} = D_{v_2} = 3$, $\alpha_u = \alpha_v = 0.5$, $\Delta x = 0.05$, $\Delta t = 3.96 \times 10^{-4}$, $n_{p_1} = 80$ and $n_{p_2} = 20$.

When we include nonlinear reproduction or nonlinear reproduction and mortality functions, we see that the numerical solution approaches a steady state, see Figure 6.4. We will study qualitative aspects of such steady-state solutions in more detail in Chapter 7.

Numerical simulations can also be used to study minimal speed of traveling periodic waves in heterogeneous landscapes. To do this, we consider a habitat of twenty patches (to allow the population to spread over the landscape through time) and we assume that adults produce juveniles non-linearly as in (6.1.1) (to keep solutions bounded).

Numerically, we find the furthest forward location where the density of adults exceeds 0.03, and we consider this location to be the front location. The movement of this front location over time is plotted in Figure 6.5, and compared with the location of theoretical speed for the juveniles-adults model in a heterogeneous landscape (see Section 3.1). The plot shows that the simulated speed is slightly slower than the theoretical speed and that the front moves faster in good patches than in bad patches.

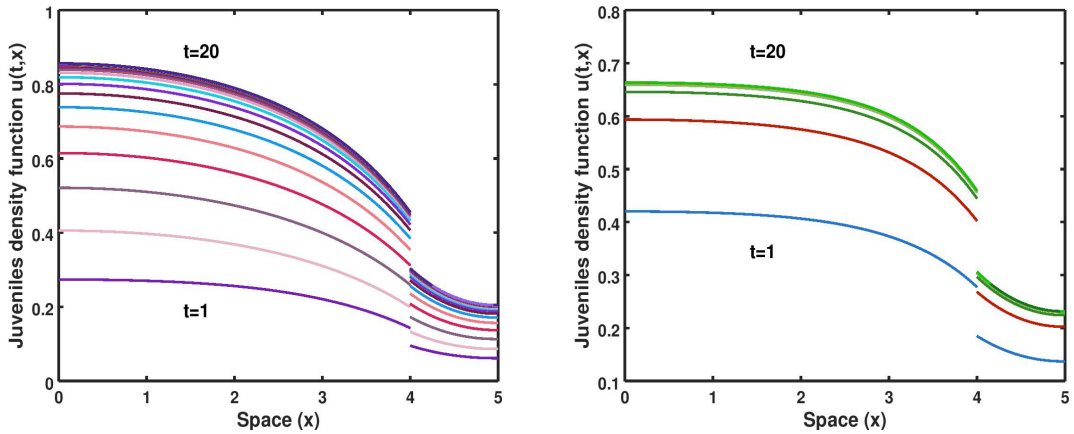

Figure 6.4.: Numerical solution for the nonlinear juveniles-adults model in a heterogeneous landscape: (a) with nonlinear reproduction function $\frac{r}{1+u+v}$; (b) with nonlinear reproduction and mortality functions $\frac{r}{1+u+v}$ and $\mu\,(u+v)$. Parameters values are: $L_1 = 4$, $L_2 = 1$, $r_1 = 6$, $r_2 = 0.2$, $m_1 = 1 = m_2$, $\mu_{u_1} = \mu_{v_1} = 1$, $\mu_{u_2} = \mu_{v_2} = 2$, $D_{u_1} = D_{v_1} = 2$, $D_{u_2} = D_{v_2} = 3$, $\alpha_u = \alpha_v = 0.5$, $\Delta x = 0.05$, $\Delta t = 3.96 \times 10^{-4}$, $n_{p_1} = 80$ and $n_{p_2} = 20$.

To explore numerical solutions for the juveniles-adults model in a homogeneous landscape, we modify the program in Listing D.2 to fit homogeneous landscapes by equating population parameters in the two different patches.

Numerical simulations show how the population grows and spreads through time (Figure 6.6(a)), and track the front location for different age groups (Figure 6.6(b)).

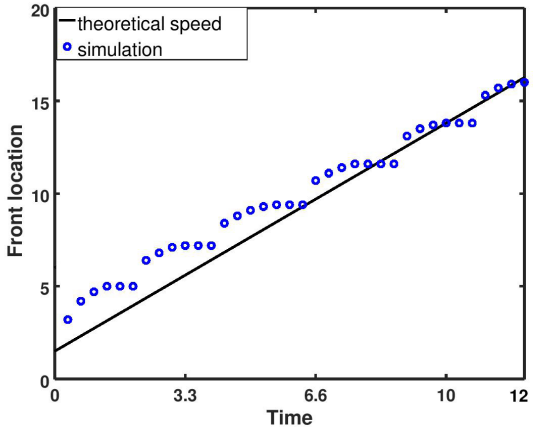

Figure 6.5.: Front location for the juveniles-adults model in a heterogeneous landscape. Parameters values are: $L_1 = 4$, $L_2 = 1$, $r_1 = 6$, $r_2 = 0.2$, $m_1 = 1 = m_2$, $\mu_{u_1} = \mu_{v_1} = 1$, $\mu_{u_2} = \mu_{v_2} = 2$, $D_{u_1} = D_{v_1} = 2$, $D_{u_2} = D_{v_2} = 3$, $\alpha_u = \alpha_v = 0.5$, $\Delta x = 0.1$, $\Delta t = 1.95 \times 10^{-3}$, $n_{p_1} = 40$ and $n_{p_2} = 10$.

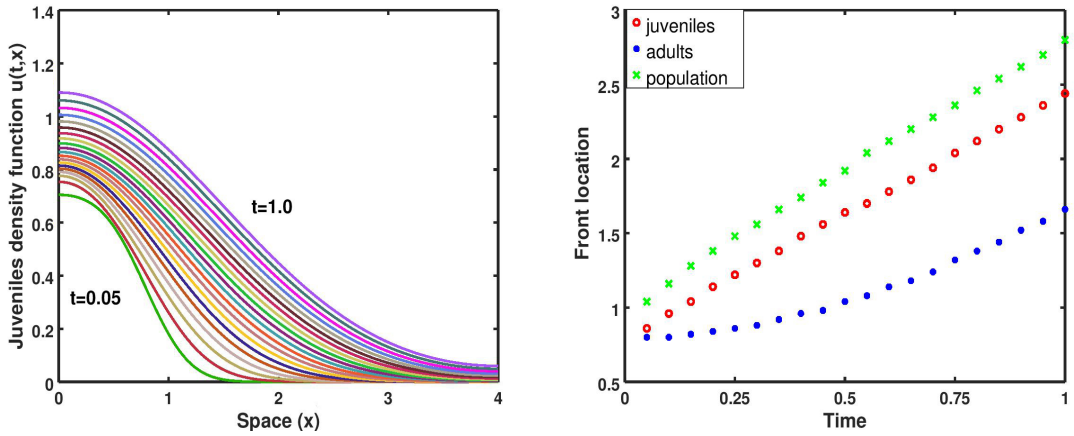

(a) (b)

Figure 6.6.: Numerical simulations for the juveniles-adults model in a homogeneous landscape. Parameters values are: $L_1 = L_2 = 2$, $r_1 = r_2 = 6$, $m_1 = m_2 = 1$, $\mu_{u_1} = \mu_{v_1} = 1$, $\mu_{u_2} = \mu_{v_2} = 1$, $D_{u_1} = D_{v_1} = 1$, $D_{u_2} = D_{v_2} = 1$, $\Delta x = 0.02$, $\Delta t = 1.9 \times 10^{-4}$ and $n_{p_1} = n_{p_2} = 100$.

7. Applications to Marine Reserves

Many studies show that overfishing has reduced marine fish stocks (Hutchings [40] and Scheffer et al. [76]) and destroyed habitats (Bohnsack [6] and Felicia and Williams [12]). Hence, there is a necessity to manage fisheries due to their ecological and economic importance. Marine reserves (or marine protected-areas (MPAs)) are an effective tool to restore habitats and to protect over-harvested stocks (Mosquera et al. [63] and Gell and Roberts [27]). MPAs have two fundamental benefits: they increase the density of harvested species (Hilborn et al. [37]), and increase yield outside MPAs when the fishery is already overexploited (Roberts et al. [74] and Gerber et al. [28]). Specifically, their benefits include increases in the diversity, biomass, body size, and reproductive capacity of many species within their boundaries (Lester et al. [47]). Furthermore, MPAs support fishing grounds through the export of eggs, larvae, and adults (Harrison et al. [33] and Almany et al. [1]).

In this chapter, we apply the model and theory presented in the previous chapters to study how the movement behavior of fish inside and outside a MPA as well as at the interface between a MPA and a fishing ground may affect sustainability and yield of the fishery.

Langebrake et al. [46] studied the dynamics of an unstructured population in MPAs and adjacent fishing grounds. Their model is described by the differential equation

$$\frac{\partial}{\partial t}n\left(t,x\right)=\frac{\partial}{\partial x}\left(D\left(x\right)\frac{\partial}{\partial x}n\left(t,x\right)\right)+R-\mu\left(x\right)n\left(t,x\right), \tag{7.0.1}$$

where $n(t,x)$ is the density of fish at time t and position x and R is a positive constant that describes recruitment. They model an infinite coastline with MPAs located at $(-l+2k, l+2k)$ and surrounded by fishing grounds situated at $(-1+2k, -l+2k)$ and $(l+2k, 1+2k)$, where $0 < l < 1$ and $k \in \mathbb{Z}$. Diffusion and mortality depend on the type of environment. For example, fish are dying of natural causes only inside MPAs while additional fish are harvested in fishing grounds. Thus, the harvesting rate, h, is defined as the difference of mortality rates inside and outside MPAs. The two processes are defined as the following piecewise constant, positive functions

$$D(x) = \begin{cases} D_1, & x \in (-l+2k, l+2k), \\ D_2, & x \in (-1+2k, -l+2k) \cup (l+2k, 1+2k), \end{cases} \tag{7.0.2}$$

and

$$\mu(x) = \begin{cases} \mu_1, & x \in (-l+2k, l+2k), \\ \mu_2 = \mu_1 + h, & x \in (-1+2k, -l+2k) \cup (l+2k, 1+2k). \end{cases} \tag{7.0.3}$$

At interfaces between MPAs and fishing grounds, the following matching conditions are applied

$$(1+\xi)\, n\left(t, (l+2k)^-\right) = (1-\xi)\, n\left(t, (l+2k)^+\right), \tag{7.0.4}$$

$$(1-\xi)\, n\left(t, (-l+2k)^-\right) = (1+\xi)\, n\left(t, (-l+2k)^+\right), \tag{7.0.5}$$

$$D_1 \frac{\partial}{\partial x} n\left(t, (l+2k)^-\right) = D_2 \frac{\partial}{\partial x} n\left(t, (l+2k)^+\right), \tag{7.0.6}$$

and

$$D_2 \frac{\partial}{\partial x} n\left(t, (-l+2k)^-\right) = D_1 \frac{\partial}{\partial x} n\left(t, (-l+2k)^+\right), \tag{7.0.7}$$

where $\frac{1+\xi}{2}$ and $\frac{1-\xi}{2}$ represent the probabilities to move from an interface to MPA or to fishing ground, respectively, and ξ takes a value in $(-1, 1)$. Comparing these

conditions to interface conditions in Section 2.3, we observe that Langebrake et al. did not include the diffusion coefficients in the density matching conditions (7.0.4) and (7.0.5). Later, we show that diffusion coefficients play a key role in determining the number of fish inside and outside MPAs.

Langebrake et al. [46] considered a periodically varying landscape and restricted their search to symmetric solutions with respect to $x = 0$. Hence, they simplified the problem to one period, $[-1, 1]$, and proved the existence and uniqueness of a positive steady-state solution for (7.0.1) with Neumann boundary conditions and interface conditions (7.0.4)-(7.0.7). They used this steady state solution, $N(x)$, to examine the effect of fish mobility and bias movement on the following quantities.

1. Fishing grounds abundance:

$$A_0[N] = \int_l^1 N(x)\,dx, \tag{7.0.8}$$

   which is the density of fish in fishing grounds at steady state.

2. Yield:

$$Y[N] = \int_l^1 hN(x)\,dx, \tag{7.0.9}$$

   the number of fish caught in fishing grounds per unit of time at steady state.

3. Total abundance:

$$A[N] = \int_0^1 N(x)\,dx, \tag{7.0.10}$$

   the total number of fish in both MPA and fishing ground at steady state.

4. The log ratio:

$$L[N] = \ln\left(\frac{\frac{1}{l}\int_0^l N(x)\,dx}{\frac{1}{1-l}\int_l^1 N(x)\,dx}\right), \tag{7.0.11}$$

   the ratio of the average abundance of fish in MPA and fishing ground evaluated at steady state.

We point here to two fundamental results from their work

- If the movement on the boundaries of MPA is unbiased ($\xi = 0$), then increasing fish mobility increases abundance in fishing ground and yield, and decreases total abundance and log ratio.
- When the movement is strongly biased towards MPA $\left(-1 < \xi < -\frac{\mu_2-\mu_1}{\mu_2+\mu_1}\right)$, the monotonicity of the four measures (as functions of fish mobility) is reversed, i.e., increasing fish mobility decreases abundance in fishing grounds and yield, and increases total abundance and log ratio.

Langebrake et al. [46] suggested that population structure might be important, but they did not include it in their model. They also assumed that recruitment is constant and independent of population size, which contradicts the fact that total reproduction in most species, including marine species declines as population density increases [2, 30].

Previous studies showed that fisheries prefer to catch large-bodied fish (Shin et al. [78], Millar [61], Tsikliras and Polymeros [86]). Size and age are usually well correlated in fish (Ramakrishna [72]). Different age groups however, have different movement rates (Gruss et al. [31]) and movement behavior at interfaces between MPAs and fishing grounds varies according to fish age (Chapman and Kramer [10]). For these reasons, we extend the work of Langebrake et al. [46] to a structured population model of juveniles and adults and test how these factors affect Langebrake's results. Specifically, our model includes

- Only adults can be harvested and only outside MPAs.
- Recruitment is density-dependent and local.
- Diffusion coefficients are included in density matching conditions at interfaces between MPAs and fishing areas.

We use numerical solutions to visualize the effect of model parameters on the steady state. Then we evaluate the relationship between the four key quantities and model parameters.

7.1. The Model

As in Chapters 2 and 3, we consider a structured population of two age groups: non-reproductive juveniles and reproductive adults. We use $u(t)$ and $v(t)$ to represent the density functions for juveniles and adults, respectively, at time t.

The non-spatial dynamics can then be described by reproduction, maturation and mortality (natural and harvesting) processes. Any one of these processes could be nonlinear. For example, reproduction typically declines as population density increases in most species, including marine species [2, 30]. Neubert and Caswell [66] studied the effect of non-linear density-dependent vital rates on population dynamics for structured populations of two stages in a discrete-time system. Our model is a continuous-time analogue to theirs. We choose the reproduction process to be density-dependent and decreasing with population levels. Hence we replace the constant birth rate r with the function $\frac{r}{1+\rho(u+v)}$, where $r > 0$ is the maximum rate at which adults produce juveniles and $\rho > 0$ represents the coefficient of intraspecific competition. By using the non-dimensionalized variables $\tilde{u} = \rho u$ and $\tilde{v} = \rho v$ and removing tilde symbols, we write the non-spatial model for reproduction, maturation and mortality as

$$\dot{u} = \frac{rv}{1+u+v} - (m + \mu_u)\, u, \tag{7.1.1}$$

and

$$\dot{v} = mu - \mu_v v, \tag{7.1.2}$$

where r is the maximum reproduction rate, m is the maturation rate, and $\mu_{u,v}$ are the mortality parameters.

To include space into our model, we use x to represent the spatial location in a one-dimensional domain and $u(t,x)$, $v(t,x)$ to represent the density functions for juveniles and adults at time t and location x. We model spatial movement by a diffusion process, which is derived from random movement in heterogeneous habitats (see Section 1.2 and [87]). We consider a periodically varying landscape of two types of patches: 'good patches', which represent MPAs, and 'bad patches', which correspond to fishing grounds. We denote by L_1 and L_2 the lengths of marine reserves and fishing grounds, respectively, and by $L = L_1 + L_2$ the period of the landscape. Without loss of generality, we choose a marine reserve to be located at $\left(\frac{-L_1}{2}, \frac{L_1}{2}\right)$ and all other marine reserves L-periodic from thereon. Accordingly, fishing areas are located at $\left(\frac{L_1}{2}, L - \frac{L_1}{2}\right)$ and L-periodic from this location.

Since the landscape contains only two types of patches, we use indices to distinguish between density and parameter functions in different patches. For example, we write $u_i(t,x)$ for the density of juveniles on patch type i (with $i = 1, 2$), and similarly for all other densities and parameters. The spatial model then consists of the following differential equations

$$\begin{aligned}\frac{\partial}{\partial t}u_1(t,x) = D_{u_1}\frac{\partial^2}{\partial x^2}u_1(t,x) + \frac{r_1 v_1(t,x)}{1+u_1(t,x)+v_1(t,x)} - (m_1 + \mu_{u_1})u_1(t,x),\\ x \in \left(\tfrac{-L_1}{2}, \tfrac{L_1}{2}\right) + L\mathbb{Z},\end{aligned} \tag{7.1.3}$$

$$\begin{aligned}\frac{\partial}{\partial t}v_1(t,x) = D_{v_1}\frac{\partial^2}{\partial x^2}v_1(t,x) + m_1 u_1(t,x) - \mu_{v_1}v_1(t,x),\\ x \in \left(\tfrac{-L_1}{2}, \tfrac{L_1}{2}\right) + L\mathbb{Z},\end{aligned} \tag{7.1.4}$$

$$\begin{aligned}\frac{\partial}{\partial t}u_2(t,x) = D_{u_2}\frac{\partial^2}{\partial x^2}u_2(t,x) + \frac{r_2 v_2(t,x)}{1+u_2(t,x)+v_2(t,x)} - (m_2 + \mu_{u_2})u_2(t,x),\\ x \in \left(\tfrac{L_1}{2}, L - \tfrac{L_1}{2}\right) + L\mathbb{Z},\end{aligned} \tag{7.1.5}$$

and

$$\frac{\partial}{\partial t}v_2(t,x) = D_{v_2}\frac{\partial^2}{\partial x^2}v_2(t,x) + m_2 u_2(t,x) - (\mu_{v_2}+h)\,v_2(t,x),$$
$$x \in \left(\tfrac{L_1}{2}, L-\tfrac{L_1}{2}\right) + L\mathbb{Z}, \tag{7.1.6}$$

where h represents the harvesting rate. At an interface between an MPA and a fishing ground, if we denote by $\alpha_u \in (0,\,1)$ the probability that a juvenile moves from this interface to the MPA, then we have the following matching conditions for juveniles at $x = x_n = \frac{L_1}{2} + nL$

$$u_1\left(t, x_n^-\right) = k_u u_2\left(t, x_n^+\right), \tag{7.1.7}$$

$$D_{u_1}\frac{\partial}{\partial x}u_1\left(t, x_n^-\right) = D_{u_2}\frac{\partial}{\partial x}u_2\left(t, x_n^+\right), \tag{7.1.8}$$

which describe continuity of flux and discontinuity in density functions. At $x = x_n = L - \frac{L_1}{2} + nL$, we apply the following matching conditions

$$u_2\left(t, x_n^-\right) = \frac{1}{k_u}u_1\left(t, x_n^+\right), \tag{7.1.9}$$

$$D_{u_2}\frac{\partial}{\partial x}u_2\left(t, x_n^-\right) = D_{u_1}\frac{\partial}{\partial x}u_1\left(t, x_n^+\right), \tag{7.1.10}$$

where $k_u = \frac{\alpha_u}{1-\alpha_u}\frac{D_{u_2}}{D_{u_1}}$. Corresponding interface conditions hold for adults with parameters α_v and k_v defined analogously.

In order to define and study the corresponding quantities (yield, fish abundance, total abundance and fish log ratio) from [46] for structured population models, we use $U(x)$ and $V(x)$ to represent a positive steady-state solution for juveniles and adults, respectively. Because the landscape is L-periodic, we expect steady-state solutions to be L-periodic as well. By the symmetry of the diffusion process, a steady-state solution should also be symmetric with respect to $x \mapsto -x$. Therefore, we can equivalently study steady-state solutions on half of a period, namely the intervals

$\left(0, \frac{L_1}{2}\right)$ and $\left(\frac{L_1}{2}, \frac{L}{2}\right)$ with the boundary conditions

$$\frac{dU_1}{dx}(0) = \frac{dV_1}{dx}(0) = \frac{dU_2}{dx}\left(\frac{L}{2}\right) = \frac{dV_2}{dx}\left(\frac{L}{2}\right) = 0. \tag{7.1.11}$$

There are no explicit expressions for the steady state solutions U and V. Instead, we solve (7.1.3)-(7.1.6) numerically to obtain the steady state. In the following section, we study how the steady-state profile depends on population parameters and harvesting rate. In Section 7.3, we define the quantities: adults yield (Y), adults abundance (A_0), total adults abundance (A), and adults log ratio (R) to explore how these quantities are affected by harvesting and adults mobility. In Section 7.3.2, we study the behavior of the quantities Y, A_0, A, and R as adults mobility increases and adults have a strong preference to marine reserves over fishing grounds. In the final section, we study the model in which diffusion coefficients for juveniles and adults in fishing grounds, and adults habitat preference are functions of harvesting rate (Section 7.3.3).

7.2. Numerical Analysis of Steady-State Solutions

Steady state solutions ($U_i(x)$ and $V_i(x)$) are functions that are independent of time, non-negative, continuous and satisfy the following differential equations

$$0 = D_{u_1}\frac{d^2}{dx^2}U_1(x) + \frac{r_1 V_1(x)}{1 + U_1(x) + V_1(x)} - (m_1 + \mu_{u_1})U_1(x), \quad x \in \left(0, \frac{L_1}{2}\right)$$

$$0 = D_{v_1}\frac{d^2}{dx^2}V_1(x) + m_1 U_1(x) - \mu_{v_1}V_1(x), \quad x \in \left(0, \frac{L_1}{2}\right)$$

$$0 = D_{u_2}\frac{d^2}{dx^2}U_2(x) + \frac{r_2 V_2(x)}{1 + U_2(x) + V_2(x)} - (m_2 + \mu_{u_2})U_2(x), \quad x \in \left(\frac{L_1}{2}, \frac{L}{2}\right)$$

and

$$0 = D_{v_2}\frac{d^2}{dx^2}V_2(x) + m_2 U_2(x) - (\mu_{v_2} + h)V_2(x), \quad x \in \left(\frac{L_1}{2}, \frac{L}{2}\right),$$

with interface conditions

$$U_1\left(\frac{L_1^-}{2}\right) = k_u U_2\left(\frac{L_1^+}{2}\right), \quad V_1\left(\frac{L_1^-}{2}\right) = k_v V_2\left(\frac{L_1^+}{2}\right),$$

$$D_{u_1}\frac{dU_1}{dx}\left(\frac{L_1^-}{2}\right) = D_{u_2}\frac{dU_2}{dx}\left(\frac{L_1^+}{2}\right),$$

$$D_{v_1}\frac{dV_1}{dx}\left(\frac{L_1^-}{2}\right) = D_{v_2}\frac{dV_2}{dx}\left(\frac{L_1^+}{2}\right),$$

and boundary conditions

$$\frac{dU_1}{dx}(0) = \frac{dV_1}{dx}(0) = \frac{dU_2}{dx}\left(\frac{L}{2}\right) = \frac{dV_2}{dx}\left(\frac{L}{2}\right) = 0.$$

The system in (7.1.3)-(7.1.6) constitutes a monotone system. Therefore, if the zero state is unstable, solutions converge to a positive steady state (Smith [83]). We used this fact to find the steady-state numerically. We solved the time-dependent problem (7.1.3)-(7.1.6) until the difference between two subsequent time steps was less than some threshold (see Listing D.3). In Section 2.3, we studied in detail the stability conditions of the zero state. The linear stability condition according to (2.2.13), gives a minimal patch-size formula, L^*, for a single-patch landscape with hostile boundary conditions. We choose $L_1 > L^*$, where L_1 is the MPA width, and solve for steady state for increasing values of h in fishing grounds (Figure 7.1). The plot shows jumps in juveniles and adults densities at the interface ($x = 2$). These jumps are defined and measured by discontinuity parameters k_u and k_v. The monotonicity of densities at the steady-state differs according to their values at the endpoints of the spatial period. When the ratio of density at the left endpoint to the right endpoint is larger than the discontinuity parameter, the density is piecewise decreasing, and vice versa. The plots also indicate that overfishing collapses stocks of juveniles and adults in fishing grounds and reduces densities in marine reserves.

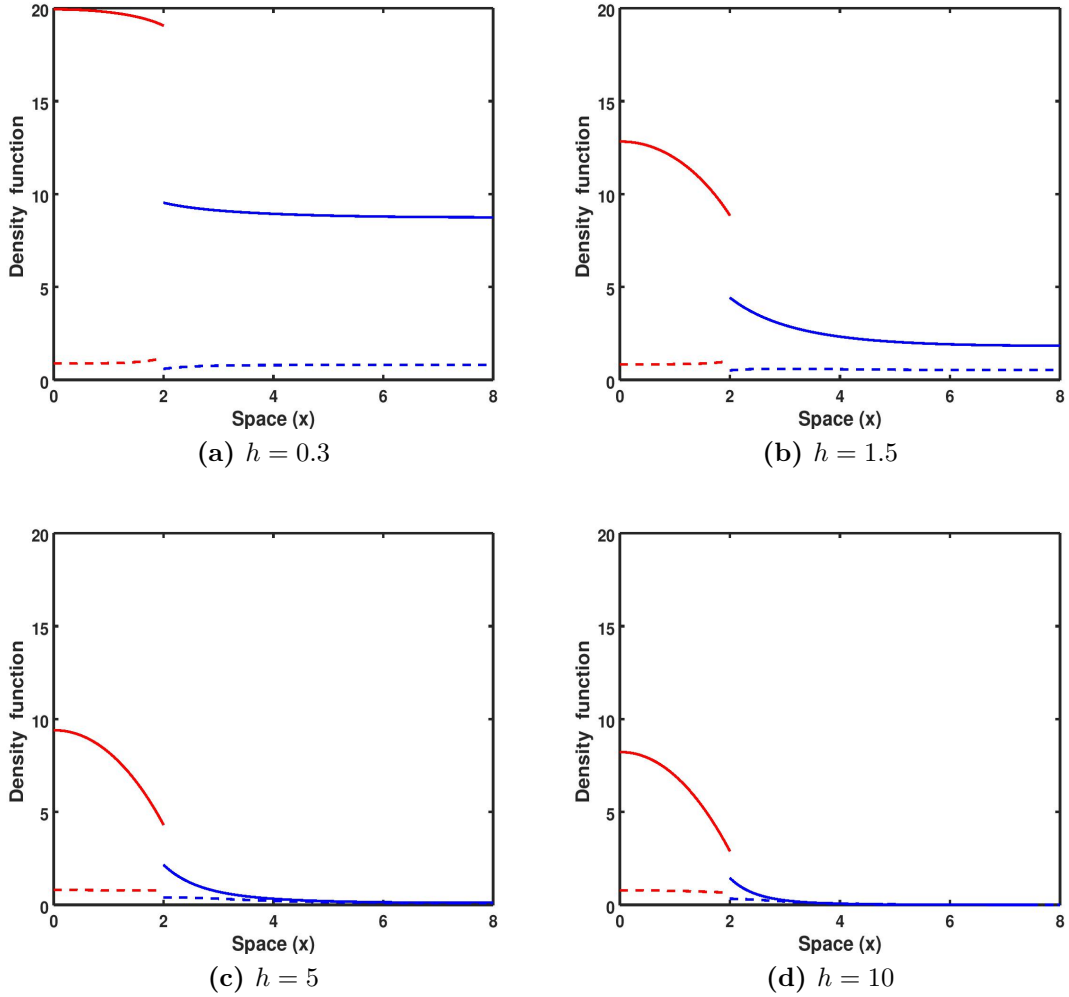

(a) $h = 0.3$ **(b)** $h = 1.5$

(c) $h = 5$ **(d)** $h = 10$

Figure 7.1.: Steady-state solutions for juveniles (dashed) and adults (solid) in MPAs $(0 < x < 2)$ and fishing grounds $(2 < x < 8)$ for different values of fishing rates (h). Parameter values are: $r_1 = r_2 = 6$, $m_1 = m_2 = 6$, $\mu_{u_1} = \mu_{v_1} = \mu_{u_2} = \mu_{v_2} = 0.25$, $D_{u_1} = D_{v_1} = 1$, $D_{u_2} = D_{v_2} = 2$, $k_u = \frac{\alpha_u}{1-\alpha_u}\frac{D_{u_2}}{D_{u_1}}$, $k_v = \frac{\alpha_v}{1-\alpha_v}\frac{D_{v_2}}{D_{v_1}}$, and $\alpha_v = \alpha_u = 0.5$.

7.3. Qualitative Analysis of the Steady-State Solution

We now study how the quantities of interest to fisheries management depend on model parameters. We begin by defining the four indicators from Langebrake et al. [46] in our context. In our age-structured model, these quantities will be in terms of adults

density only.

1. Adults yield is given by
$$Y = \int_{\frac{L_1}{2}}^{\frac{L}{2}} hV(x)\,dx, \tag{7.3.1}$$
where h represents the fishing rate and $V(x)$ is the steady state solution for adults. Adults yield is the number of mature fish caught in the fishing areas per unit of time, at steady state.

2. Adults abundance
$$A_0 = \int_{\frac{L_1}{2}}^{\frac{L}{2}} V(x)\,dx, \tag{7.3.2}$$
represents the total amount of adults in the fishing grounds at steady state.

3. Total adults abundance
$$A = \int_{0}^{\frac{L}{2}} V(x)\,dx, \tag{7.3.3}$$
is the total number of adults in MPAs and fishing grounds combined at steady state.

4. Adults log ratio
$$R = \ln\left(\frac{\frac{1}{L_1}\int_0^{\frac{L_1}{2}} V(x)\,dx}{\frac{1}{L_2}\int_{\frac{L_1}{2}}^{\frac{L}{2}} V(x)\,dx}\right), \tag{7.3.4}$$
represents the natural logarithm of the ratio of average adults abundance in MPAs and fishing grounds, at steady state.

7.3.1. Effects of Harvesting

In Figure 7.2, we explore how the quantities Y, A_0, A, and R are affected by harvesting. Adults yield shows a unique maximum at some intermediate harvesting rate (Figure 7.2(a)), as is common in many such situations. A low harvesting rate gives a low yield, whereas a high harvesting rate leads to a low steady-state density (see

Figure 7.1), which in turn gives a low yield. As expected, abundance in fishing areas and total abundance are both decreasing with harvesting (Figure 7.2(b) and (c)).

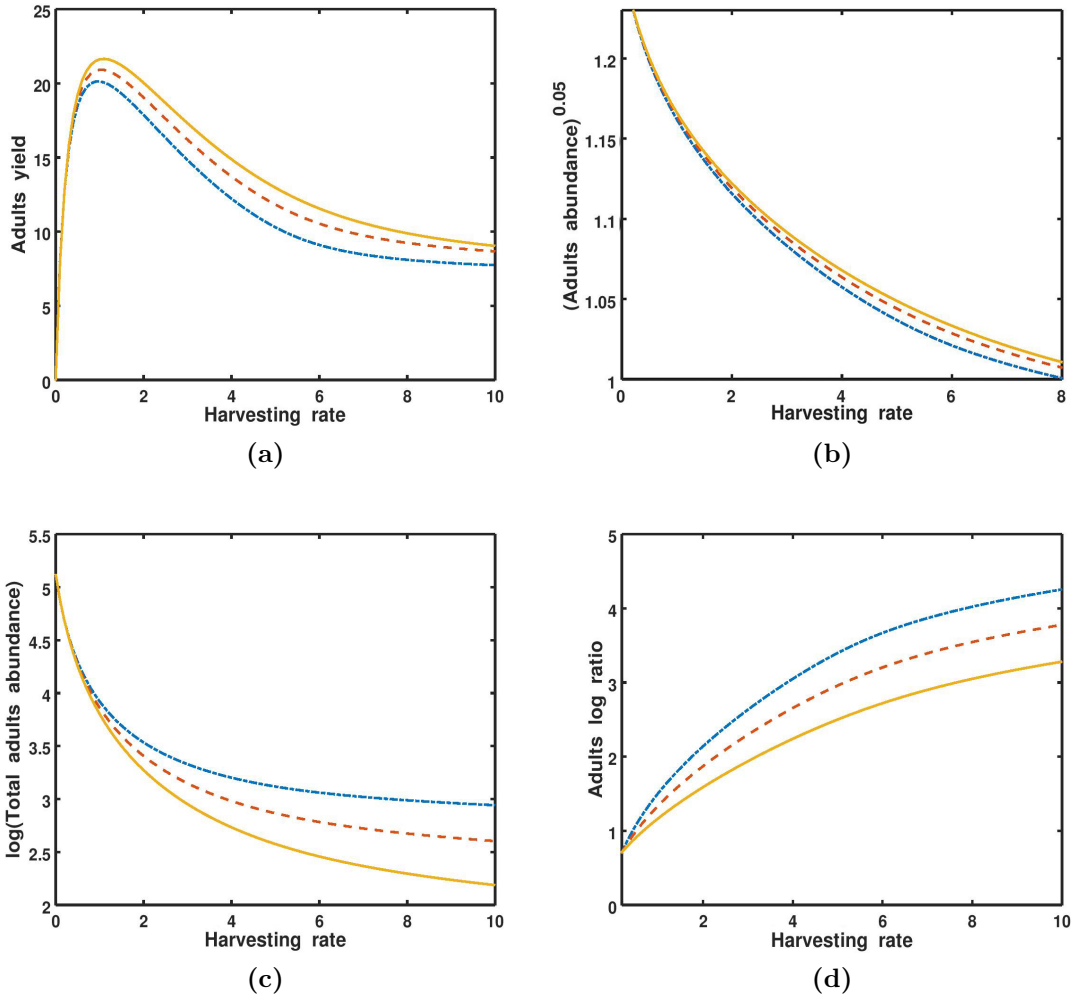

Figure 7.2.: Effect of harvesting on adults yield (Y), adults abundance (A_0), total adults abundance (A) and adults log ratio (R). The three curves correspond to three different movement scenarios: $D_{v_i} = 0.5D_{u_i}$ (dash-dot), $D_{v_i} = D_{u_i}$ (dashed) and $D_{v_i} = 2D_{u_i}$ (solid). Other parameter values are: $L_1 = 4$, $L_2 = 12$, $r_1 = r_2 = 6$, $m_1 = m_2 = 5$, $\mu_{u_1} = \mu_{v_1} = \mu_{u_2} = \mu_{v_2} = 0.25$, $D_{u_1} = 1$, $D_{u_2} = 2$ and $\alpha_u = \alpha_v = 0.5$.

It turns out that when adults have a higher movement rate than juveniles, adults abundance in fishing areas is higher (Figure 7.2(b)) but adults total density is lower

(Figure 7.2(c)). The higher movement rate pushes adults from the MPA into the fishing grounds where they will be harvested and yield increases (Figure 7.2(a)). As adult abundance inside and outside the MPA decreases with harvesting, the log ratio increases (Figure 7.2(d)). Hence, the relative decrease in abundance inside the MPA is smaller than outside.

In Figure 7.2, we kept the movement rate for each age-group piecewise constant across the habitat. In reality, we expect fish to adjust their movement behavior to local habitat conditions. For example, fishing can lead to habitat degradation (e.g. bottom trawling) or increased stress levels (e.g. noise). Hence, we explore how our four indicator quantities change as the ratio of adults movement rates inside and outside the MPA changes. We choose $D_{v_1} = D$ and fix the ratio $\beta = \frac{D_{v_1}}{D_{v_2}}$. The results are displayed in Figure 7.3. Adults yield and abundance in fishing grounds increase with adults movement (Figure 7.3(a) and (b)), whereas total abundance and log ratio decrease (Figure 7.3(c) and (d)).

Since we assumed that adults have no habitat preference toward MPA ($\alpha_v = 0.5$), the effect of the parameter β on the four quantities will be interpreted in terms of adults diffusion coefficients, D_{v_1} and D_{v_2}. If $\beta > 1$, then adults move faster in MPAs than in fishing grounds, which allows more adults to be in fishing areas and explains the order of the curves in Figure 7.3. When $D_{v_1} < D_{v_2}$ $(\beta < 1)$, we expect more adults in MPAs than in fishing grounds and this explains why the dash-dot curves are below the dashed curves in Figure 7.3(a) and (b).

Langebrake et al. [46] considered the previous scenario with their unstructured population model. In this scenario, they assumed that the population density is continuous at the interface. They obtained similar plots to those in Figure 7.3, but the order of the three curves in each plot is reversed, i.e. while higher β increases yield in our model it decreased yield in [46]. To explain this difference, we consider the discontinuity parameter at the interface $k_v = \frac{\alpha_v}{1-\alpha_v}\frac{D_{v_2}}{D_{v_1}}$. If $k_v = 1$ (as Langebrake et al. [46]

assumed in their first case) and $\beta = \frac{D_{v_1}}{D_{v_2}} > 1$, then adults habitat preference to MPA (α_v) must be larger than 0.5. This pushes more fish to cross the interface towards the MPA, which explains the curves order in the work of Langebrake et al. [46]. A similar argument can be used to explain the other case where $\beta < 1$.

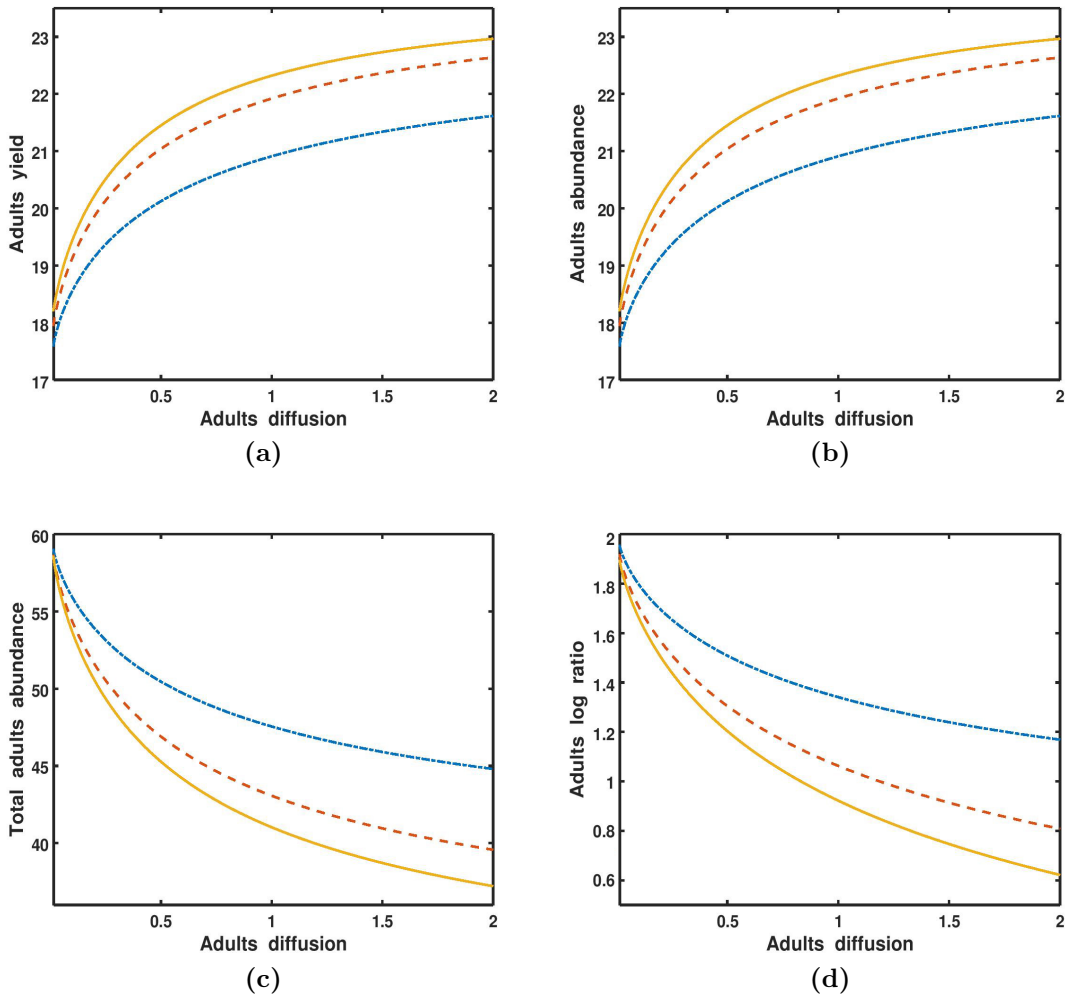

Figure 7.3.: Effect of adults movement on yield, adults abundance, total adults abundance and adults log ratio. The three curves correspond to different values of the ratio $\beta = \frac{D_{v_1}}{D_{v_2}}$. $\beta = 1$ (dashed), $\beta = 0.5$ (dash-dot) and $\beta = 1.5$ (solid). Other parameter values are: $L_1 = 4$, $L_2 = 12$, $r_1 = r_2 = 6$, $m_1 = m_2 = 5$, $\mu_{u_1} = \mu_{v_1} = \mu_{u_2} = \mu_{v_2} = 0.25$, $D_{u_1} = 1$, $D_{u_2} = 2$, $\alpha_u = \alpha_v = 0.5$ and $h = 1$.

7.3.2. Biased Movement

So far, we considered unbiased movement for both juveniles and adults. In Figure 7.3(d) we found that the relative densities of adults inside versus outside MPAs decreases as adult mobility increased. This result contradicts findings from empirical studies. For example, Claudet et al. [11] compared the relative densities inside versus outside Mediterranean MPAs for species with different adult mobility. They found that as adult mobility increased, the relative densities inside MPAs increased or stayed constant. Claudet et al. [11] suggested that a bias in movement toward MPAs is the main reason for this unexpected result. We can explore this hypothesis in our model. We study the behavior of the quantities Y, A, A_0 and R as adult mobility increases and adults exhibit preference toward MPAs, i.e. $\alpha_v > 0.5$. We assume that juveniles have no habitat preference ($\alpha_u = 0.5$).

To explain the relation between bias value and monotonicity of the four indicators, we point here to the work of Langebrake et al. [46] in which they classified the bias according to the critical value $\xi^* = -\frac{\mu_2-\mu_1}{\mu_2+\mu_1}$.

1. If $\xi^* < \xi < 0$, then the bias toward MPA is weak and their steady state solution $N(x)$ is decreasing.

2. If $0 < \xi < \xi^*$, the bias movement towards MPA is strong and their steady state solution $N(x)$ is increasing.

They obtained the critical value ξ^* by looking for piecewise constant solutions $N(x)$. It is worth mentioning that Langebrake et al. [46] considered only one scenario for density matching conditions from the work of Ovaskanian and Cornell [69], in which diffusion coefficients are equal everywhere. However, fish mobility is not necessarily similar inside and outside MPAs, and diffusion coefficients appear with habitat preference parameters in density matching conditions, see (7.1.7)-(7.1.10). By including differential movement into the model and interface conditions, we expect to find

a similar critical value for the existence of a piecewise constant function but with respect to the diffusion rates.

When the solution at the steady state is piecewise constant, we have the following equations inside MPAs

$$\frac{r_1 V_1}{1+U_1+V_1} - (m_1+\mu_{u_1})\,U_1 = 0, \tag{7.3.5}$$

$$m_1 U_1 - \mu_{v_1} V_1 = 0. \tag{7.3.6}$$

We then solve (7.3.5) and (7.3.6) to get

$$V_1 = \left(\frac{r_1 m_1}{\mu_{v_1}(m_1+\mu_{u_1})} - 1\right)\left(\frac{m_1}{m_1+\mu_{v_1}}\right) \quad \text{and} \quad U_1 = \frac{\mu_{v_1}}{m_1} V_1. \tag{7.3.7}$$

Similarly, in fishing grounds we have the following solutions

$$V_2 = \left(\frac{r_2 m_2}{(h+\mu_{v_2})(m_2+\mu_{u_2})} - 1\right)\left(\frac{m_2}{m_2+h+\mu_{v_2}}\right), \tag{7.3.8}$$

$$U_2 = \left(\frac{\mu_{v_2}+h}{m_2}\right) V_2. \tag{7.3.9}$$

At an interface, we have the matching condition

$$U_1 = k_u U_2 = k_u \left(\frac{\mu_{v_2}+h}{m_2}\right) V_2. \tag{7.3.10}$$

From (7.3.7), we get

$$U_1 = \frac{\mu_{v_1}}{m_1} V_1 = k_v \left(\frac{\mu_{v_1}}{m_1}\right) V_2. \tag{7.3.11}$$

And so, steady state solutions are piecewise constant if and only if

$$\frac{\alpha_u}{1-\alpha_u}\frac{D_{u_2}}{D_{u_1}}\left(\frac{\mu_{v_2}+h}{m_2}\right) = \frac{\alpha_v}{1-\alpha_v}\frac{D_{v_2}}{D_{v_1}}\left(\frac{\mu_{v_1}}{m_1}\right). \tag{7.3.12}$$

We use (7.3.12) to calculate the critical value of adults habitat preference, α_v^*, at which the steady state solution is a piecewise constant function. According to the default parameters in Figure 7.4, $\alpha_v^* = \frac{5}{6}$. We use this critical value to explore how the four indicators are affected by adults mobility as the bias towards MPA changes.

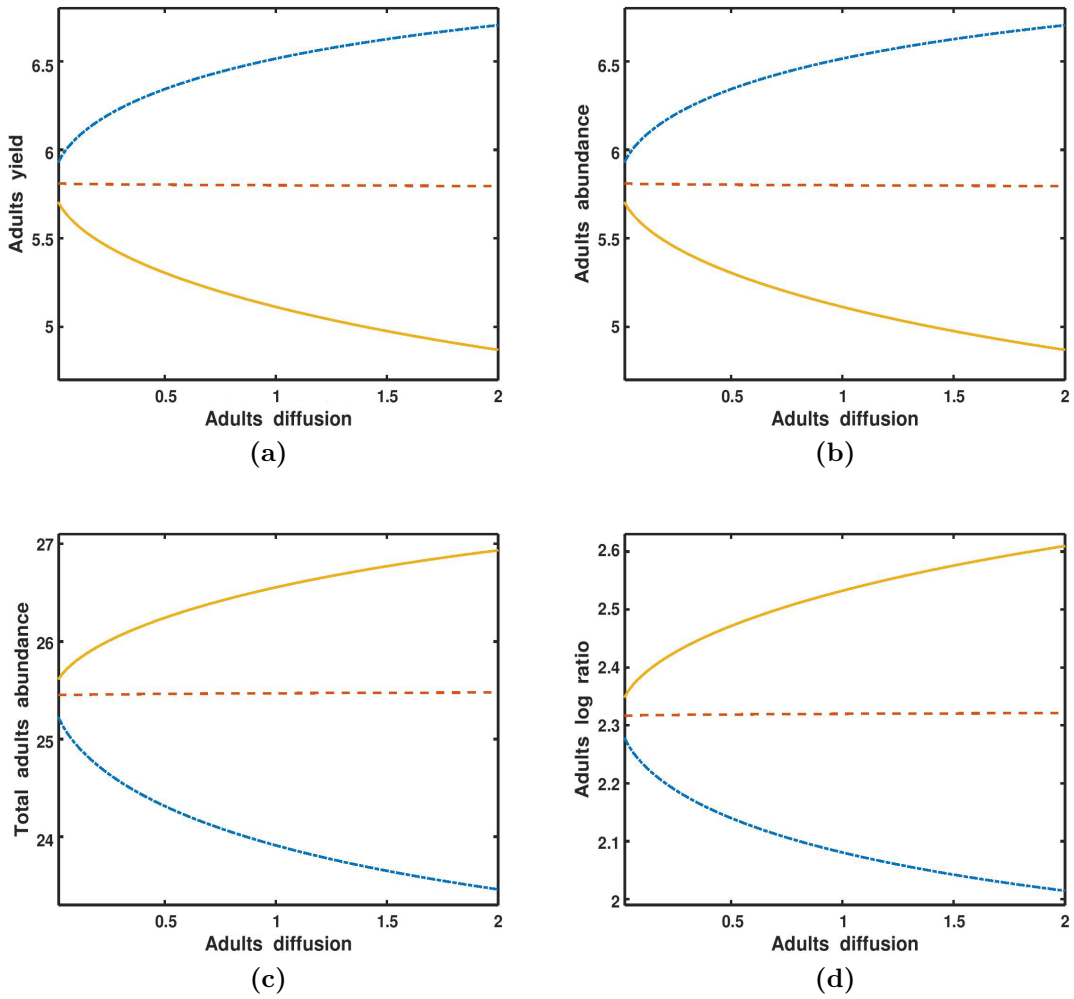

Figure 7.4.: Effect of adults movement on adults yield, adults abundance, total adults abundance and adults log ratio. The three curves correspond to different values of adults habitat preference rate, α_v. $\alpha_v = 0.9$ (solid), $\alpha_v^* = \frac{5}{6} \approx 0.83$ (dashed) and $\alpha_v = 0.75$ (dash-dot). Other parameter values are: $L_1 = 4$, $L_2 = 12$, $r_1 = r_2 = 2.9$, $m_1 = m_2 = 5$, $\mu_{u_1} = \mu_{v_1} = \mu_{u_2} = \mu_{v_2} = 0.25$, $D_{u_1} = 1$, $D_{u_2} = 2$, $\alpha_u = 0.5$, $\beta = \frac{D_{v_1}}{D_{v_2}} = 0.5$ and $h = 1$.

Figure 7.4 indicates that when adults move to MPAs with low bias, the monotonicity properties of yield, adults abundance, total adults abundance and adults log ratio are similar to the features in Figure 7.3 but when the bias is strong, the monotonicity of the four indicators is reversed. Hence, with respect to movement bias, we obtain the same qualitative results as Langebrake et al. [46].

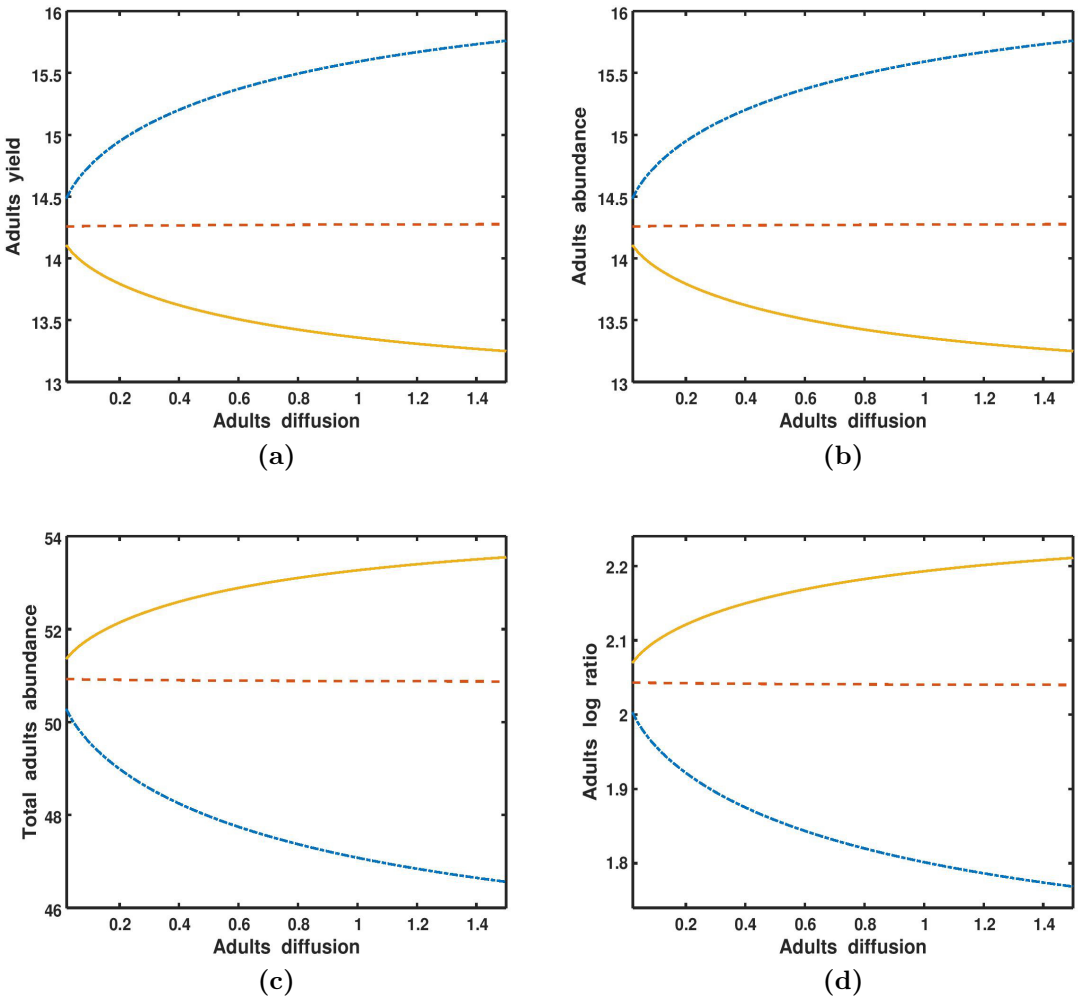

Figure 7.5.: Effect of adults movement on adults yield, adults abundance, total adults abundance and adults log ratio. The three curves correspond to different values of the constant $\beta = \frac{D_{v_1}}{D_{v_2}}$. $\beta = \frac{1}{9.5}$ (solid), $\beta = \frac{1}{7.5}$ (dashed) and $\beta = \frac{1}{5}$ (dash-dot). Other parameter values are: $L_1 = 4$, $L_2 = 12$, $r_1 = r_2 = 5.2$, $m_1 = m_2 = 5$, $\mu_{u_1} = \mu_{v_1} = \mu_{u_2} = \mu_{v_2} = 0.25$, $D_{u_1} = 5$, $D_{u_2} = 7.5$, $\alpha_u = 0.5$, $\alpha_v = 0.5$ and $h = 1$.

The latter case agrees with the empirical results of Claudet et al. [11] that the relative density of adults inside versus outside MPAs (when the bias is strong) increases as adults mobility increases (Figure 7.4(d)).

We point out here that Langebrake et al. [46] did not include diffusion coefficients in the interface conditions when they derived the critical bias value $\xi^* = -\frac{\mu_2-\mu_1}{\mu_2+\mu_1}$. Hence, they explained the 'paradox' by the strong movement bias only. In our model, the condition (7.3.12) not only explains the 'paradox' by choosing the habitat preference parameter large enough (as Langebrake et al. did) but also finds another resolution for the 'paradox' via a difference in diffusion coefficients. We use the condition (7.3.12) to explore the effect of adult mobility on monotonicity properties of the four indicators. More specifically, if we fix all other parameters, then (7.3.12) gives a critical value β^* for the existence of piecewise constant functions. In Figure 7.5, we plot each indicator as a function of adult mobility for different values of the constant $\beta = \frac{D_{v_1}}{D_{v_2}}$. The plot shows that when the ratio of adult movement $\left(\frac{D_{v_2}}{D_{v_1}}\right)$ is smaller than the critical value calculated from (7.3.12), the monotonicity properties of yield, adults abundance, total adults abundance and adults log ratio are similar to the features in Figure 7.3 but when the ratio exceeds the critical value, the monotonicity of the four indicators is reversed. This observation provides another explanation for the empirical results in [11] (the relative densities inside MPAs increases as adult mobility increases).

7.3.3. Fishing-Dependent Model

Habitat characteristics such as degradation or noise levels arguably depend on the intensity of harvesting. Consequently, the behavioral response of fish to harvesting could depend on harvesting levels. We use our model to explore how harvesting-dependent movement affects yield and abundance. Hence, to make matters more realistic, we assume that diffusion coefficients for juveniles and adults in fishing grounds, and adults habitat preference parameter depend on fishing intensity. More specifi-

cally, we assume that movement rates outside MPAs and preference for MPA increase as harvesting increases.

For simplicity, we consider the following relations for adults habitat preference and diffusion coefficients in fishing areas

$$\alpha_v(h) = 1 - \frac{e^{-sh}}{2}, \quad h \geq 0, \tag{7.3.13}$$

and

$$D_{v_2}(h) = D_{max} - (D_{max} - D_{v_1})\, e^{-\tilde{s}h}, \quad h \geq 0, \tag{7.3.14}$$

for some parameters $s, \tilde{s} > 0$ and $D_{max} > D_{v_1}$. Without fishing ($h = 0$), fish move at the same rate inside and outside MPAs, and adults have no habitat preference. As fishing activities increase, fish mobility in fishing grounds and adults preference to MPAs increase as well.

In Figure 7.6, we explore how our four indicators are affected by harvesting-dependent movement. We consider three scenarios: (i) only habitat preference depends on harvesting intensity ($s > 0$, $\tilde{s} = 0$); (ii) only movement rates depend on harvesting intensity ($s = 0$, $\tilde{s} > 0$); and (iii) both processes depend on harvesting intensity (s, $\tilde{s} > 0$). We did not include the curves of the null model ($s = 0$, $\tilde{s} = 0$) because they cannot be distinguished from the curves in scenario (ii) (dashed curves in Figure 7.6). It turns out that for low harvesting rates, the four indicators are more sensitive to adults movement than to adults habitat preference. When adults prefer moving towards MPAs (scenario (i)), we expect more fish will be available in MPAs. This decreases yield and abundance in fishing areas (Figure 7.6(a) and (b)), and increases the log ratio and total abundance (Figure 7.6(c) and (d)). If adults mobility in fishing areas is high and biased towards MPAs (scenario (iii)), more adults reach the interfaces between MPAs and fishing areas and most of them will move towards MPAs. As a result, the solid curves are pushed down to the bottom in Figure 7.6(a)

and (b), and pushed up to the top in Figure 7.6(c) and (d).

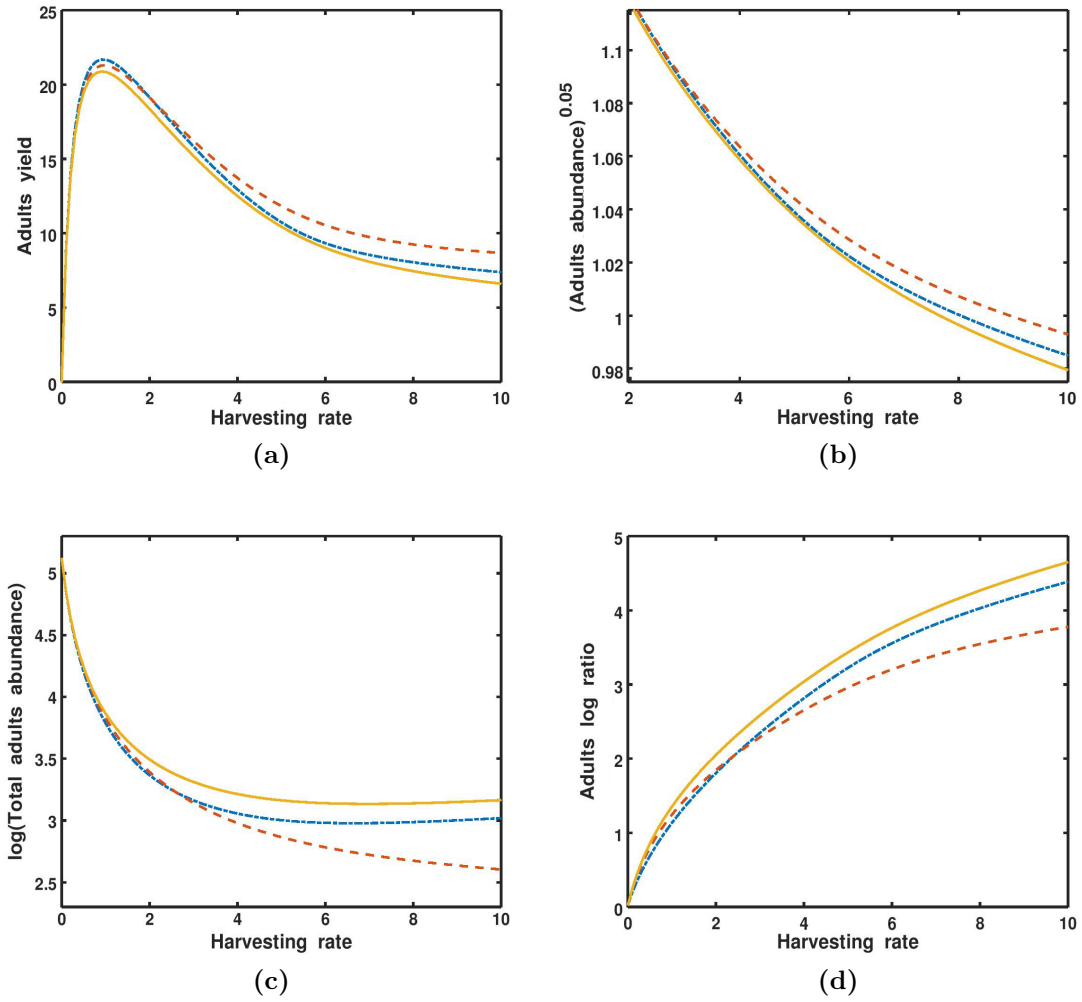

Figure 7.6.: Effect of harvesting on adults yield, adults abundance, total adults abundance and adults log ratio. The three curves correspond to three different scenarios: (i) only habitat preference depends on harvesting intensity. We set $\alpha_v(h) = 1 - \frac{e^{-0.1h}}{2}$ and $D_{v_2}(h) = 2$ (dash-dot); (ii) only movement rates depend on harvesting intensity. We set $\alpha_v(h) = 0.5$ and $D_{v_2}(h) = 2 - e^{-h}$ (dashed); and (iii) both processes depend on harvesting intensity. We set $\alpha_v(h) = 1 - \frac{e^{-0.1h}}{2}$ and $D_{v_2}(h) = 2 - e^{-h}$ (solid). Default parameter values are: $L_1 = 4$, $L_2 = 12$, $r_1 = r_2 = 6$, $m_1 = m_2 = 5$, $\mu_{u_1} = \mu_{v_1} = \mu_{u_2} = \mu_{v_2} = 0.25$, $D_{u_1} = D_{v_1} = 1$, $D_{u_2} = D_{v_2}$ and $\alpha_u = 0.5$.

In this chapter, we extended the work of Langebrake et al. [46] to a structured popu-

lation model of juveniles and adults. In our model, recruitment is density dependent and local inside MPAs and fishing grounds, and diffusion coefficients are included in the density matching conditions at interfaces between MPAs and fishing areas. We used numerical solutions at the steady state to explore the relationship between the four key indicators and model parameters. When fish movement is unbiased, our results are similar to Langebrake's and inconsistent with findings from empirical studies. To solve this 'paradox', we derived a condition for piecewise constant steady-state solutions. This condition not only explained the 'paradox' by choosing the habitat preference large enough (as Langebrake et al. did) but also found another resolution for the 'paradox' via a difference in diffusion coefficients. Finally, we suggested a more realistic model (fishing-dependent model). We used this model to explore how our four indicators are affected by harvesting-dependent movement. It turns out that when harvesting rates are low, the four indicators are more sensitive to adults movement than to adults habitat preference. As fishing activities become intense, the biased movement towards MPAs becomes more influential, and the monotonicity properties for some indicators are changed.

Clearly, movements rates and fish behavior at interfaces between MPAs and fishing grounds are of the most influential processes on the four indicators. Hence, one of the future challenges is to study the effect of juveniles biased movement on yield and abundance. Another interesting challenge is to study empirically fish movement behavior at interfaces as was done in terrestrial system [24] and estimate movement bias towards MPAs. The other is to consider several other density-dependent processes (maturation or death) and to study the effect of these nonlinear processes on the four indicators. The most challenging mathematical task is to prove the existence of the steady-state solution for our model in a patchy landscape with discontinuous densities at interfaces.

8. Summary and Discussion

In this dissertation, we considered a structured population model of two age groups: juveniles and adults. We derived persistence conditions and dispersion relations in homogeneous and heterogeneous landscapes. We also applied the model and numerical simulations to a problem in fisheries.

The problems of population persistence and spatial spread rates are fundamental to spatial ecology. Their study through the framework of reaction-diffusion equations has not only generated a number of important ecological insights but also some deep mathematical results. The work on spatial spread phenomena started with Fisher [23] and Kolmogorov et al. [44], who calculated the minimal traveling wave speed, proved the existence of traveling waves and convergence from certain initial conditions to a traveling wave. Aronson and Weinberger [3] introduced the notion of 'asymptotic spreading speed' and thereby inspired a large body of literature on the topic.

The 'minimal patch-size problem' was formulated and studied by Skellam [82] and Kierstead and Slobodkin [42] and has since been extended to more complicated models and applied to reserve design [7]. The two cases, an unbounded homogeneous landscape and a single bounded patch, are extremes. Shigesada et al. [77] studied a combination of the two scenarios, where a landscape consists of infinitely many patches of different quality, that alternate periodically. In this case, both questions arise: how much 'good' landscape is required for persistence and how fast would a population spread in a 'traveling periodic wave'? The model by Shigesada et al. [77] was refined by Maciel and Lutscher to include individual movement behavior and

patch preference at habitat edges [55].

All of these studies and many follow-up works modeled a spatially structured but physiologically unstructured population. Most actual species, however, have highly structured life cycles where individuals at different life stages have different vital rates [34, 18, 81] and different movement behavior [4, 84]. For example, Blanding's turtle, which is a Canadian species at risk [70], has a very long pre-reproductive stage ($14-20$ years) [15, 14], which has implications for the management of the species [13]. Similarly, dispersal ability and behavior can change significantly between different life stages. For example, many marine invertebrates have sessile adult stages where individuals are immobile, and also many reef fish have sedentary adults [89]. In some species, different life stages have different habitat preferences. For example, juveniles of western rock lobster (*Panulirus Cygnus*), choose limestone reef habitat ($<$ 10m from the shore), while adults prefer offshore water habitat ($30-150$m) [29].

Non-spatial structured population models have a long history in theory and application, as matrix models with discrete stages in discrete time [8] and as integral equations with continuous stage distribution in continuous time [60]. Somewhat in between are models of discrete stages in continuous time. These models gain mathematical tractability in exchange for the simplifying assumption that stage duration is exponentially distributed. Spatially structured versions of matrix models were formulated and studied quite intensively as integrodifference equations on homogeneous landscapes [65, 52, 54]. Similarly, spatial models for physiologically structured populations were studied in a reaction-diffusion setting [32, 35, 36]. A few recent works establish some more abstract mathematical properties of these kinds of models in heterogeneous landscapes [49], but more concrete and detailed studies on how the dynamics of structured populations in heterogeneous landscapes differ from those of unstructured populations have not been conducted.

With this work, we provided a framework for a structured population of two stages: a pre-reproductive juvenile stage and a reproductive adult stage. We studied in

detail persistence conditions and traveling periodic waves in homogeneous and heterogeneous environments, and we took into account various movement behaviors of juveniles and adults. In Chapter 2, we presented the model of a structured population with two age groups: juveniles and adults. We assumed all the parameters to be piecewise constant functions. We used the Routh-Hurwitz criterion for stability to write the persistence condition for the non-spatial model. Then we considered a single-patch landscape with hostile boundary conditions, we used the corresponding eigenvalue problem to derive the persistence condition. For heterogeneous landscapes, we followed the approaches by Shigesada et al. [77] and Maciel and Lutscher [55]. We wrote the eigenvalue problem, then we used boundary conditions and interface conditions to derive the population persistence condition. We then considered the case where we have a single good patch surrounded by an infinite bad patch. We used analytic techniques to find the critical size of the good patch. We used the explicit expression for the critical size of a single patch to obtain formulas for the sensitivity and elasticity of L^* with respect to population parameters. We found that the critical size of a single-patch landscape, L^*, is mostly sensitive and elastic to adult diffusion term D_v (see Table 2.1).

In Chapter 3, we investigated traveling periodic waves for structured populations. First, we followed the approaches by Shigesada et al. [77] and Maciel and Lutscher [55] to find the dispersion relation for the juveniles-adults model in patchy landscapes. We then generalized the work of Fisher [23] to the spread speed of structured populations in homogeneous landscapes. We also applied sensitivity and elasticity formulas to the spread speed of the juveniles-adults model in homogeneous landscapes. We found that C^* is most sensitive to the maturation rate and most elastic to the reproduction rate (see Table 3.1). We illustrated how the biased movement of one age group affects population persistence and spread. Illustrations showed that when both age groups have very high preference for good patches, the population spreads only slowly or not at all but if only one of the two age groups shows habitat preference whereas the

other is neutral, then the speed does not decrease to zero as preference approaches unity (see Figure 3.8). Finally, we used the maturation rate to answer the question of when a simple, unstructured population model is sufficient and when the more complex structured model that we studied is required.

In Chapter 4, we considered structured populations with a sessile age-group. This model applies to many marine invertebrates (White [89]) and some bird species (Drewit [20]). We represented this scenario by setting the diffusion coefficients for the non-moving age group to zero. We derived explicit formulas for the minimal patch-size surrounded by a hostile landscape, and for the traveling wave speed in a homogeneous habitat. In heterogeneous landscapes, we derived implicit formulas for persistence conditions and the dispersion relation of a traveling periodic wave. It turned out that persistence conditions and spread rates for the case of sessile adults do indeed arise from the corresponding formulas where both age groups are mobile by setting adult diffusion coefficients equal to zero.

In Chapter 5, we used asymptotic techniques to find the wave speed and the spread speed for structured populations in heterogeneous landscapes. We illustrated the power of the homogenization method by comparing the dispersion relation and the resulting minimal wave speeds for the approximation and the exact expression. We found an excellent agreement between the fully heterogeneous speed and the homogenized speed, even though the landscape period was on the same order as the diffusion coefficients and not as small as the formal derivation requires. We also generalized this work to the case of structured populations of n age groups.

In Chapter 6, we explored numerical solutions for the juveniles-adults model in homogeneous and heterogeneous habitats. We used the finite difference method with a forward-time central-space scheme to implement the partial derivatives. In a single-patch landscape, we compared the numerical solution to the analytic solution for the linear model and we explored how the numerical solution behaves in non-linear models. In heterogeneous landscapes, we derived the interface conditions following the

same finite difference approach and used them in numerical solutions for both linear and nonlinear models. We used numerical techniques to track the front location for different age groups and compared it with the location obtained by the theoretical speed for the juveniles-adults model in heterogeneous landscapes. We observed that the front moves faster in good patches and slower in bad patches. Numerical simulations also showed that the scheme does not capture the actual speed but is slightly slower.

In Chapter 7, we studied an application of our model to harvesting in the context of marine reserves. We developed the model of Langebrake et al. [46] by including diffusion coefficients in density matching conditions at interfaces between MPAs and fishing grounds. We examined the effect of fish mobility and bias movement on yield and fish abundance. We found that when the bias towards MPAs is strong or the difference in diffusion coefficients is large enough, the relative density of adults inside versus outside MPAs increases with adult mobility. This agrees with findings from empirical studies.

In Chapters 2, 3 and 4, we considered only the linear model for population growth, death, and maturation. This model is only valid when densities are reasonably low; at high density, we expect nonlinear effects to arise. However, the linear model still provides us with most of the important information regarding persistence and spread rates, as long as the population does not experience an Allee effect. A population experiences a (strong) Alee effect if it cannot grow below a certain density. In that case, the zero state is stable and the linearization at zero dos not give any information about population persistence, see [45] and references therein.

The stage structure ensures that the system is cooperative so that the spreading speed of a nonlinear model (without Allee effect) in a homogeneous landscape is defined by the linearization at zero [52, 92]. Hence, the speed formulas in those cases give the asymptotic spreading speed. Extending the spreading speed theory to our model in a patchy landscape with discontinuous densities at interfaces remains one of the

analytical challenges. The other is to prove the existence of a positive steady-state solution for our model in a patchy landscape with discontinuous densities at interfaces. Kinezaki et al. [43] extended the model of Shigesada et al. [77] to a two-dimensional situation. They used $n(t,x,y)$ to represent the density function at time t and spatial coordinate (x,y), and φ to indicate the direction of the two-dimensional traveling periodic wave $\left(0 \leq \varphi \leq \frac{\pi}{2}\right)$. By using the ansatz $n(t,x,y) = e^{-sz} g(x)$, where g is a periodic function and $z = x\cos\varphi + y\sin\varphi - ct$, they studied the TPW and derived the dispersion relation for unstructured population models in a periodically alternating environment. Their work can be extended to the juveniles-adults model in a two-dimensional space even when densities at interfaces are discontinuous.

On the applied level, Chapter 7 showed that movements rates and fish behavior at interfaces between MPAs and fishing grounds are the most influential processes with respect to the four indicators. Hence, one of the future challenges is to study empirically fish movement behavior at interfaces as was done in terrestrial system [24] and estimate movement bias towards MPAs. The other is to consider more density-dependent processes (maturation or death) and to study the effect of these nonlinear processes on the four indicators.

Another interesting, but possibly more challenging task, is to explore population dynamics for gender-structured population models. Iannelli et al. [41], presented different forms of marriage functions (functions to predict the number of marriages that will occur during a unit of time between males in particular age categories and females in particular age categories [58]). In a homogeneous environment, a model for the spread of a sex-structured population in discrete time was studied by Miller et al. [62]. Most of marriage functions are nonlinear, hence, numerical simulations will be a first step to study population dynamics for these models.

A. List of Variables, Parameters and Quantities

Variables

Δx	Spatial step size
Δt	Time step
T	Nondimensionalized time variable
X	Nondimensionalized spatial variable
$u(t,x)$	Juveniles density function at time t and location x
$v(t,x)$	Adults density function at time t and location x
$U(x)$	The steady-state solution (or the eigenfunction symbol) for juveniles
$V(x)$	The steady-state solution (or the eigenfunction symbol) for adults
t	Time variable
x	Spatial variable
y	Large scale variable

Parameters

α	Probability of moving from interface to patch type I
$\frac{p_i}{2}$	Probability of moving one step size to the right or to the left in patch type i
S_1	Nondimensionalized favorable patch size
S_2	Nondimensionalized unfavorable patch size
S	Nondimensionalized spatial period
s	Traveling wave shape parameter
L_1	Good patch size
L_2	Bad patch size
L	Spatial period
D_u	Juveniles diffusion coefficient
D_v	Adults diffusion coefficient
r	Reproduction rate
m	Maturation coefficient for juveniles
μ_u	Mortality parameter for juveniles
μ_v	Adults mortality parameter
k_u	Discontinuity parameter for juveniles density function at the interface
k_v	Discontinuity parameter for adults density function at the interface
h	Adults harvesting rate in fishing grounds

Quantities

t^*	The time required for traveling one spatial period
C^*	Asymptotic spread speed
L^*	Critical patch size for a single patch landscape
$C(s)$	Traveling wave speed
$\langle D \rangle_H$	Harmonic mean for diffusion coefficients
$\langle f \rangle_A$	Arithmetic mean for growth functions
Y	Adults yield
A_0	Adults abundance
A	Total adults abundance
R	Adults log ratio
$f(u)$	Population growth function
$\mathcal{C}_s$	Coefficient matrix for a system of reaction diffusion equations for cooperative species
$\lambda_1(s)$	Principal eigenvalue of diagonal blocks of of the matrix $\mathcal{C}_s$
MPA	Marine protected area

B. Dispersion Relation for the Juveniles-Adults Model (Case B)

In this appendix, we give the details of the calculation of **Case B** from Section 3.1. If

$$r_1 < \frac{(m_1 + sC + \mu_{u_1})(sC + \mu_{v_1})}{m_1}, \tag{B.0.1}$$

then we rite the solution of the differential equation

$$\begin{aligned} 0 =& g_1^{(4)}(x) - 4s g_1^{(3)}(x) - \left(\frac{\alpha}{D_{v_1}} + \frac{\beta}{D_{u_1}} - 4s^2\right) g_1''(x) \\ &+ \left(\frac{2s\alpha}{D_{v_1}} + \frac{2s\beta}{D_{u_1}}\right) g_1'(x) - \frac{(r_1 m_1 - \alpha\beta)}{D_{v_1} D_{u_1}} g_1(x). \end{aligned} \tag{B.0.2}$$

as

$$g_1(x) = e^{sx}\left[A\cosh(z_1 x) + B\sinh(z_1 x) + G\cosh(z_2 x) + H\sinh(z_2 x)\right],$$

where

$$z_1 = \frac{1}{\sqrt{2D_{u_1}D_{v_1}}}\sqrt{D_{v_1}(m_1 + sC + \mu_{u_1}) + D_{u_1}(sC + \mu_{v_1}) - \Delta_1},$$

$$z_2 = \frac{1}{\sqrt{2D_{u_1}D_{v_1}}}\sqrt{D_{v_1}(m_1 + sC + \mu_{u_1}) + D_{u_1}(sC + \mu_{v_1}) + \Delta_1},$$

and

$$\Delta_1 = \sqrt{[D_{v_1}(m_1 + sC + \mu_{u_1}) - D_{u_1}(sC + \mu_{v_1})]^2 + 4D_{u_1}D_{v_1}r_1 m_1}.$$

The solution of (3.1.14) in the bad patches remains as we have seen before

$$g_2(x) = e^{sx}\left[A'\cosh(z_3x) + B'\sinh(z_3x) + G'\cosh(z_4x) + H'\sinh(z_4x)\right],$$

where

$$z_3 = \frac{1}{\sqrt{2D_{u_2}D_{v_2}}}\sqrt{D_{v_2}(m_2 + sC + \mu_{u_2}) + D_{u_2}(sC + \mu_{v_2}) - \Delta_2},$$

$$z_4 = \frac{1}{\sqrt{2D_{u_2}D_{v_2}}}\sqrt{D_{v_2}(m_2 + sC + \mu_{u_2}) + D_{u_2}(sC + \mu_{v_2}) + \Delta_2},$$

and

$$\Delta_2 = \sqrt{[D_{v_2}(m_2 + sC + \mu_{u_2}) - D_{u_2}(sC + \mu_{v_2})]^2 + 4D_{u_2}D_{v_2}r_2m_2}.$$

To find a nontrivial solution for the function g_1 and g_2, we need to obtain relations to determine the coefficients A, B, G, H, A', B', G', and H'. We apply the following interface conditions at $x = 0$ and $x = L_1$

$$g_1\left(0^+\right) = k_u g_2\left(0^-\right), \quad g_1\left(L_1^-\right) = k_u g_2\left(-L_2^+\right), \tag{B.0.3}$$

$$g_1'\left(0^+\right) - sg_1\left(0^+\right) = D_u\left[g_2'\left(0^-\right) - sg_2\left(0^-\right)\right], \tag{B.0.4}$$

$$g_1'\left(L_1^-\right) - sg_1\left(L_1^-\right) = D_u\left[g_2'\left(-L_2^+\right) - sg_2\left(-L_2^+\right)\right], \tag{B.0.5}$$

$$\widetilde{g_1}\left(0^+\right) = k_v\widetilde{g_2}\left(0^-\right), \quad \widetilde{g_1}\left(L_1^-\right) = k_v\widetilde{g_2}\left(-L_2^+\right), \tag{B.0.6}$$

$$\widetilde{g_1}'\left(0^+\right) - s\widetilde{g_1}\left(0^+\right) = D_v\left[\widetilde{g_2}'\left(0^-\right) - s\widetilde{g_2}\left(0^-\right)\right], \tag{B.0.7}$$

and

$$\widetilde{g_1}'\left(L_1^-\right) - s\widetilde{g_1}\left(L_1^-\right) = D_v\left[\widetilde{g_2}'\left(-L_2^+\right) - s\widetilde{g_2}\left(-L_2^+\right)\right]. \tag{B.0.8}$$

The interface conditions (B.0.3)-(B.0.8) produce the following system of linear equa-

tions for our coefficients:

$$A + G = k_u \left(A' + G'\right), \quad z_1 B + z_2 H = D_u \left(z_3 B' + z_4 H'\right), \tag{B.0.9}$$

$$\begin{aligned} &e^{s(L_1+L_2)} \left[A \cosh\left(z_1 L_1\right) + B \sinh\left(z_1 L_1\right) + G \cosh\left(z_2 L_1\right) + H \sinh\left(z_2 L_1\right)\right] = \\ &k_u \left[A' \cosh\left(z_3 L_2\right) - B' \sinh\left(z_3 L_2\right) + G' \cosh\left(z_4 L_2\right) - H' \sinh\left(z_4 L_2\right)\right], \end{aligned} \tag{B.0.10}$$

$$\begin{aligned} &e^{s(L_1+L_2)} \left[z_1 A \sinh\left(z_1 L_1\right) + z_1 B \cosh\left(z_1 L_1\right) + z_2 G \sinh\left(z_2 L_1\right) + z_2 H \cosh\left(z_2 L_1\right)\right] = \\ &D_u \left[-z_3 A' \sinh\left(z_3 L_2\right) + z_3 B' \cosh\left(z_3 L_2\right) - z_4 G' \sinh\left(z_4 L_2\right) + z_4 H' \cosh\left(z_4 L_2\right)\right]. \end{aligned} \tag{B.0.11}$$

$$\begin{aligned} 0 =& A \left[D_{u_1} s^2 + D_{u_1} z_1^2 + \beta\right] r + G \left[D_{u_1} s^2 - D_{u_1} z_2^2 + \beta\right] r \\ &+ A' \left[-D_{u_2} s^2 + D_{u_2} z_3^2 - \delta\right] k_v + G' \left[-D_{u_2} s^2 + D_{u_2} z_4^2 - \delta\right] k_v, \end{aligned} \tag{B.0.12}$$

$$\begin{aligned} 0 =& A \left[D_{u_1} z_1^2 \cosh\left(z_1 L_1\right) + D_{u_1} s^2 \cosh\left(z_1 L_1\right) + \beta \cosh\left(z_1 L_1\right)\right] r e^{s(L_1+L_2)} \\ &+ B \left[D_{u_1} z_1^2 \sinh\left(z_1 L_1\right) + D_{u_1} s^2 \sinh\left(z_1 L_1\right) + \beta \sinh\left(z_1 L_1\right)\right] r e^{s(L_1+L_2)} \\ &+ G \left[-D_{u_1} z_2^2 \cosh\left(z_2 L_1\right) + D_{u_1} s^2 \cosh\left(z_2 L_1\right) + \beta \cosh\left(z_2 L_1\right)\right] r e^{s(L_1+L_2)} \\ &+ H \left[-D_{u_1} z_2^2 \sinh\left(z_2 L_1\right) + D_{u_1} s^2 \sinh\left(z_2 L_1\right) + \beta \sinh\left(z_2 L_1\right)\right] r e^{s(L_1+L_2)} \\ &+ A' \left[D_{u_2} z_3^2 \cosh\left(z_3 L_2\right) - D_{u_2} s^2 \cosh\left(z_3 L_2\right) - \delta \cosh\left(z_3 L_2\right)\right] k_v \\ &+ B' \left[-D_{u_2} z_3^2 \sinh\left(z_3 L_2\right) + D_{u_2} s^2 \sinh\left(z_3 L_2\right) + \delta \sinh\left(z_3 L_2\right)\right] k_v \\ &+ G' \left[D_{u_2} z_4^2 \cosh\left(z_4 L_2\right) - D_{u_2} s^2 \cosh\left(z_4 L_2\right) - \delta \cosh\left(z_4 L_2\right)\right] k_v \\ &+ H' \left[-D_{u_2} z_4^2 \sinh\left(z_4 L_2\right) + D_{u_2} s^2 \sinh\left(z_4 L_2\right) + \delta \sinh\left(z_4 L_2\right)\right], \end{aligned} \tag{B.0.13}$$

$$\begin{aligned}0 =& B\left[D_{u_1}z_1^3 + D_{u_1}s^2z_1 + \beta z_1\right]r + H\left[-D_{u_1}z_2^3 + D_{u_1}s^2z_2 + \beta z_2\right]r \\ &+ B'\left[D_{u_2}z_3^3 - D_{u_2}s^2z_3 - \delta z_3\right]D_v + H'\left[D_{u_2}z_4^3 - D_{u_2}s^2z_4 - \delta z_4\right]D_v, \quad \text{(B.0.14)}\end{aligned}$$

and

$$\begin{aligned}0 =& A\left[D_{u_1}s^2z_1\sinh(z_1L_1) + D_{u_1}z_1^3\sinh(z_1L_1) + \beta z_1\sinh(z_1L_1)\right]re^{s(L_1+L_2)} \\ &+ B\left[D_{u_1}s^2z_1\cosh(z_1L_1) + D_{u_1}z_1^3\cosh(z_1L_1) + \beta z_1\cosh(z_1L_1)\right]re^{s(L_1+L_2)} \\ &+ G\left[D_{u_1}s^2z_2\sinh(z_2L_1) - D_{u_1}z_2^3\sinh(z_2L_1) + \beta z_2\sinh(z_2L_1)\right]re^{s(L_1+L_2)} \\ &+ H\left[D_{u_1}s^2z_2\cosh(z_2L_1) - D_{u_1}z_2^3\cosh(z_2L_1) + \beta z_2\cosh(z_2L_1)\right]re^{s(L_1+L_2)} \\ &+ A'\left[D_{u_2}s^2z_3\sinh(z_3L_2) - D_{u_2}z_3^3\sinh(z_3L_2) + \delta z_3\sinh(z_3L_2)\right]D_v \\ &+ B'\left[-D_{u_2}s^2z_3\cosh(z_3L_2) + D_{u_2}z_3^3\cosh(z_3L_2) - \delta z_3\cosh(z_3L_2)\right]D_v \\ &+ G'\left[D_{u_2}s^2z_4\sinh(z_4L_2) - D_{u_2}z_4^3\sinh(z_4L_2) + \delta z_4\sinh(z_4L_2)\right]D_v \\ &+ H'\left[-D_{u_2}s^2z_4\cosh(z_4L_2) + D_{u_2}z_4^3\cosh(z_4L_2) - \delta z_4\cosh(z_4L_2)\right]D_v. \quad \text{(B.0.15)}\end{aligned}$$

We write the coefficient matrix of the linear system (B.0.9)-(B.0.15) as

$$V = \begin{bmatrix} V_1 & V_2 \\ V_3 & V_4 \end{bmatrix},$$

where

$$V_1 = \begin{bmatrix} 1 & 0 & 1 & 0 \\ 0 & z_1 & 0 & z_2 \\ z_1e^{sL}\sinh(z_1L_1) & z_1e^{sL}\cosh(z_1L_1) & z_2e^{sL}\sinh(z_2L_1) & z_2e^{sL}\cosh(z_2L_1) \\ e^{sL}\cosh(z_1L_1) & e^{sL}\sinh(z_1L_1) & e^{sL}\cosh(z_2L_1) & e^{sL}\sinh(z_2L_1) \end{bmatrix},$$

$$V_2 = \begin{bmatrix} -k_u & 0 & -k_u & 0 \\ 0 & -D_u z_3 & 0 & -D_u z_4 \\ D_u z_3 \sinh(z_3 L_2) & -D_u z_3 \cosh(z_3 L_2) & D_u z_4 \sinh(z_4 L_2) & -D_u z_4 \cosh(z_4 L_2) \\ -k_u \cosh(z_3 L_2) & k_u \sinh(z_3 L_2) & -k_u \cosh(z_4 L_2) & k_u \sinh(z_4 L_2) \end{bmatrix},$$

$$V_3 = \begin{bmatrix} W & 0 & Y & 0 \\ We^{sL} \cosh(z_1 L_1) & We^{sL} \sinh(z_1 L_1) & Ye^{sL} \cosh(z_2 L_1) & Ye^{sL} \sinh(z_2 L_1) \\ 0 & Wz_1 & 0 & Yz_2 \\ Wz_1 e^{sL} \sinh(z_1 L_1) & Wz_1 e^{sL} \cosh(z_1 L_1) & Yz_3 e^{sL} \sinh(z_2 L_1) & Yz_2 e^{sL} \cosh(z_2 L_1) \end{bmatrix},$$

$$V_4 = \begin{bmatrix} Mk_v & 0 & Nk_v & 0 \\ Mk_v \cosh(z_3 L_2) & -Mk_v \sinh(z_3 L_2) & Nk_v \cosh(z_4 L_2) & -Nk_v \sinh(z_4 L_2) \\ 0 & MD_v z_3 & 0 & ND_v z_4 \\ -MD_v z_3 \sinh(z_3 L_2) & MD_v z_3 \cosh(z_3 L_2) & -ND_v z_4 \sinh(z_4 L_2) & ND_v z_4 \cosh(z_4 L_2) \end{bmatrix},$$

with

$$W = r\left(D_{u_1}s^2 - D_{u_1}z_1^2 + \beta\right), \quad Y = r\left(D_{u_1}s^2 - D_{u_1}z_2^2 + \beta\right), \tag{B.0.16}$$

$$M = -D_{u_2}s^2 + D_{u_2}z_3^2 - \delta, \quad N = -D_{u_2}s^2 + D_{u_2}z_4^2 - \delta, \tag{B.0.17}$$

$$L = L_1 + L_2, \quad D_u = \frac{D_{u_2}}{D_{u_1}}, \quad D_v = \frac{D_{v_2}}{D_{v_1}}, \quad \text{and} \quad r = \frac{r_2}{r_1}.$$

A nontrivial solution of $g_1,\ g_2,$ exists only if the determinant of V is zero. This condition gives us the dispersion relation between decay rate s and speed C of a traveling periodic wave.

C. Structured Populations With Sessile Juveniles

C.1. Persistence Conditions in a Single-Patch Landscape

On a single good patch, we have the following differential equations

$$\frac{\partial}{\partial t}u(t,x) = rv(t,x) - (m+\mu_u)\,u(t,x),\; x\in(0,L)\,, \tag{C.1.1}$$

$$\frac{\partial}{\partial t}v(t,x) = D_v\frac{\partial^2 v(t,x)}{\partial x^2} + mu(t,x) - \mu_v v(t,x),\; x\in(0,L)\,, \tag{C.1.2}$$

with hostile boundary conditions

$$u\,(t,0) = u(t,L) = 0, \quad \text{and} \quad v(t,0) = v(t,L) = 0. \tag{C.1.3}$$

The corresponding eigenvalue problem to determine the stability of the trivial solution is

$$\lambda U(x) = rV(x) - (m+\mu_u)U(x), \tag{C.1.4}$$

$$\lambda V(x) = D_v V_{xx}(x) + m\,U(x) - \mu_v V(x). \tag{C.1.5}$$

We use (C.1.4) to write an explicit formula for $U(x)$ and substitute it into equation (C.1.5) to get the second-order equation

$$\frac{d^2V(x)}{dx^2} = \frac{1}{D_v}\left(\lambda - \frac{rm}{\lambda + m + \mu_u} + \mu_v\right) V(x), \; x \in (0, L). \tag{C.1.6}$$

The solution of the differential equation (C.1.6) depends mainly on the sign of the quantity $\left(\lambda - \frac{rm}{\lambda+m+\mu_u} + \mu_v\right)$. Since we are interested in the persistence conditions, we set $\lambda = 0$. Since we are considering a good patch, we conclude from Proposition 2.1.1 that $\left(-\frac{rm}{m+\mu_u} + \mu_v\right) < 0$. Then solutions of (C.1.6) can be written in the form

$$V(x) = A\cos(q_1 x) + B\sin(q_1 x), \tag{C.1.7}$$

where $q_1 = \sqrt{\frac{1}{D_v}\left(\frac{rm}{m+\mu_u} - \mu_v\right)}$.
Applying the boundary condition $v(t,0) = 0$ to equation (C.1.7), we get $A = 0$. The other boundary condition $v(t, L) = 0$ requires

$$\sin(q_1 L) = 0. \tag{C.1.8}$$

Proposition C.1.1. *The critical patch size formula of model (C.1.1, C.1.2) with hostile boundary is given by*

$$L^* = \pi\sqrt{\frac{D_v}{\frac{rm}{m+\mu_u} - \mu_v}}. \tag{C.1.9}$$

C.2. Persistence Conditions in Periodically Varying Landscapes

We assume that the landscape contains infinitely many patches of two types, periodically alternating: good and bad patches. We use L_1 and L_2 to represent the good

and bad patch size, respectively, and $L = L_1 + L_2$ represents the spatial period. Since juvenile diffusion coefficients in both batches are equal to zero, we write the periodic system of differential equations in good and bad patches as follows

$$\begin{cases} \frac{\partial u_1(t,x)}{\partial t} = r_1 v_1(t,x) - (m_1 + \mu_{u_1}) u_1(t,x), \\ \frac{\partial v_1(t,x)}{\partial t} = D_{v_1} \frac{\partial^2 v_1(t,x)}{\partial x^2} + m_1 u_1(t,x) - \mu_{v_1} v_1(t,x), \\ x \in \left(\frac{-L_1}{2}, \frac{L_1}{2}\right) + L\mathbb{Z}, \quad t \geq 0. \end{cases} \tag{C.2.1}$$

and

$$\begin{cases} \frac{\partial u_2(t,x)}{\partial t} = r_2 v_2(t,x) - (m_2 + \mu_{u_2}) u_2(t,x), \\ \frac{\partial v_2(t,x)}{\partial t} = D_{v_2} \frac{\partial^2 v_2(t,x)}{\partial x^2} + m_2 u_2(t,x) - \mu_{v_2} v_2(t,x), \\ x \in \left(\frac{L_1}{2}, L - \frac{L_1}{2}\right) + L\mathbb{Z}, \quad t \geq 0. \end{cases} \tag{C.2.2}$$

We look for exponential solutions in time which lead us to the following eigenvalue problem for (C.2.1)

$$\lambda U_1(x) = r_1 V_1(x) - (m_1 + \mu_{u_1}) U_1(x), \tag{C.2.3}$$

$$\lambda V_1(x) = D_{v_1} \frac{d^2 V(x)}{dx^2} + m_1 U_1(x) - \mu_{v_1} V_1(x). \tag{C.2.4}$$

We use (C.2.3) to write an explicit formula for $U_1(x)$ and substitute it into (C.2.4) to get the ordinary differential equation

$$\frac{d^2 V_1(x)}{dx^2} = \frac{1}{D_{v_1}} \left(\lambda - \frac{r_1 m_1}{\lambda + m_1 + \mu_{u_1}} + \mu_{v_1}\right) V_1(x), \quad x \in \left(\frac{-L_1}{2}, \frac{L_1}{2}\right) + L\mathbb{Z}. \tag{C.2.5}$$

Applying the same procedure to (C.2.2), gives the following differential equation

$$\frac{d^2 V_2(x)}{dx^2} = \frac{1}{D_{v_2}} \left(\lambda - \frac{r_2 m_2}{\lambda + m_2 + \mu_{u_2}} + \mu_{v_2}\right) V_2(x), \quad x \in \left(\frac{L_1}{2}, L - \frac{L_1}{2}\right) + L\mathbb{Z}. \tag{C.2.6}$$

Since the landscape is periodically varying and the differential equations (C.2.5),

(C.2.6) are symmetric with respect to $x \mapsto -x$, it is enough to consider the interval $\left(0, \frac{L}{2}\right)$ if we are looking for symmetric solutions.

We set $\lambda = 0$ and note that, according to Proposition 2.1.1, the sign of the quantity $\left(-\frac{r_i m_i}{m_i+\mu_{u_i}} + \mu_{v_i}\right)$ is negative in the good patch and positive in the bad patch. If we assume that patch I where $x \in \left(\frac{-L_1}{2}, \frac{L_1}{2}\right)$ is the good patch, and patch II where $x \in \left(\frac{L_1}{2}, L - \frac{L_1}{2}\right)$ is the bad patch, then the solution for the differential equations (C.2.5) and (C.2.6) will be respectively as follows

$$V_1(x) = A\cos(q_1 x) + B\sin(q_2 x), \quad x \in \left(\frac{-L_1}{2}, \frac{L_1}{2}\right), \tag{C.2.7}$$

$$V_2(x) = A'\cosh\left(q_2\left(\frac{L}{2} - x\right)\right) + B'\sinh\left(q_2\left(\frac{L}{2} - x\right)\right), \quad x \in \left(\frac{L_1}{2}, L - \frac{L_1}{2}\right), \tag{C.2.8}$$

where

$$q_1 = \sqrt{\frac{1}{D_{v_1}}\left(\frac{r_1 m_1}{m_1+\mu_{u_1}} - \mu_{v_1}\right)}, \quad q_2 = \sqrt{\frac{1}{D_{v_2}}\left(-\frac{r_2 m_2}{m_2+\mu_{u_2}} + \mu_{v_2}\right)}. \tag{C.2.9}$$

By symmetry on the unbounded domain, we have the boundary conditions

$$\frac{\partial v_1}{\partial x}(t,0) = 0, \quad \frac{\partial v_2}{\partial x}(t,0) = 0. \tag{C.2.10}$$

Applying these boundary conditions implies that $B = B' = 0$.

At the interface $x = \frac{L_1}{2}$ we have the matching conditions

$$v_1\left(t, \frac{L_1^+}{2}\right) = k_v v_2\left(t, \frac{L_1^-}{2}\right), \tag{C.2.11}$$

and

$$\frac{\partial v_1}{\partial x}\left(t, \frac{L_1^+}{2}\right) = D_v \frac{\partial v_2}{\partial x}\left(t, \frac{L_1^-}{2}\right), \tag{C.2.12}$$

where k_v is the parameter that measures the discontinuity in adults density at the

interface.

Applying the interface conditions (C.2.11) and (C.2.12), gives the linear equations

$$A\cos\left(q_1\frac{L_1}{2}\right) - A'k_v\cosh\left(q_2\frac{L_2}{2}\right) = 0, \tag{C.2.13}$$

and

$$Aq_1\sin\left(q_1\frac{L_1}{2}\right) - A'q_2D_v\sinh\left(q_2\frac{L_2}{2}\right) = 0, \tag{C.2.14}$$

where $D_v = \frac{D_{v_2}}{D_{v_1}}$. We write the coefficient matrix for the previous linear system as follows

$$W = \begin{bmatrix} \cos\left(q_1\frac{L_1}{2}\right) & -k_v\cosh\left(q_2\frac{L_2}{2}\right) \\ \\ q_1\sin\left(q_1\frac{L_1}{2}\right) & -q_2D_v\sinh\left(q_2\frac{L_2}{2}\right) \end{bmatrix}. \tag{C.2.15}$$

A non-trivial solution for a system of linear equations is exist if the determinant of the coefficient matrix of this system is equal to zero.

Proposition C.2.1. *The persistence boundary of model (C.2.1, C.2.2) with interface conditions (C.2.11, C.2.12) is given implicitly by*

$$D_vq_2\tanh\left(q_2\frac{L_2}{2}\right) = k_vq_1\tan\left(q_1\frac{L_1}{2}\right), \tag{C.2.16}$$

where q_i are defined in (C.2.9).

C.3. The Critical Size of a Single Patch Surrounded by a Non-Lethal Matrix Habitat

In this section, we find the persistence condition for the juveniles-adults model with sessile juvenile stage in a single 'good patch' surrounded by an infinite 'bad patch'. In the previous section we reached the following differential equations in patch type

I and patch type II

$$\frac{d^2V_1(x)}{dx^2} = \frac{1}{D_{v_1}}\left(\lambda - \frac{r_1 m_1}{\lambda + m_1 + \mu_{u_1}} + \mu_{v_1}\right) V_1(x), \quad x \in \left(\frac{-L}{2}, \frac{L}{2}\right), \tag{C.3.1}$$

$$\frac{d^2V_2(x)}{dx^2} = \frac{1}{D_{v_2}}\left(\lambda - \frac{r_2 m_2}{\lambda + m_2 + \mu_{u_2}} + \mu_{v_2}\right) V_2(x), \quad x > \frac{L}{2} \quad \text{or} \quad x < \frac{-L}{2}. \tag{C.3.2}$$

Consequently, the solution of the differential equations (C.3.1, C.3.2) will be respectively as follows

$$V_1(x) = A\cos(q_1 x) + B\sin(q_1 x), \quad x \in \left(\frac{-L}{2}, \frac{L}{2}\right), \tag{C.3.3}$$

and

$$V_2(x) = A' e^{-q_2|x|} + B' e^{q_2|x|}, \quad x > \frac{L}{2} \quad \text{or} \quad x < \frac{-L}{2}, \tag{C.3.4}$$

where q_1 and q_2 are as defined in (C.2.9). Since we require solutions to be bounded in patch type II, we conclude that $B' = 0$.

We apply continuity of flux at the interface $x = -\frac{L}{2}$, to get

$$\begin{aligned} D_{v_1} V_1'\left(-\frac{L}{2}^+\right) =& D_{v_2} V_2'\left(-\frac{L}{2}^-\right) \\ =& q_2 D_{v_2} A' e^{-q_2 \frac{L}{2}} \\ =& q_2 D_{v_2} V_2\left(-\frac{L}{2}^-\right) \\ =& \frac{q_2 D_{v_2}}{k_v} V_1\left(-\frac{L}{2}^+\right). \end{aligned} \tag{C.3.5}$$

Similarly, applying continuity of flux at the other interface $x = \frac{L}{2}$, gives

$$D_{v_1} V_1'\left(\frac{L}{2}^-\right) = -\frac{q_2 D_{v_2}}{k_v} V_1\left(\frac{L}{2}^-\right). \tag{C.3.6}$$

Applying the boundary conditions (C.3.5) and (C.3.6) produces the linear equations

$$A\left[\frac{q_2 D_v}{k_v}\cos\left(q_1\frac{L}{2}\right) - q_1\sin\left(q_1\frac{L}{2}\right)\right] + B\left[q_1\cos\left(q_1\frac{L}{2}\right) + \frac{q_2 D_v}{k_v}\sin\left(q_1\frac{L}{2}\right)\right] = 0, \tag{C.3.7}$$

$$A\left[q_1\sin\left(q_1\frac{L}{2}\right) - \frac{q_2 D_v}{k_v}\cos\left(q_1\frac{L}{2}\right)\right] + B\left[q_1\cos\left(q_1\frac{L}{2}\right) + \frac{q_2 D_v}{k_v}\sin\left(q_1\frac{L}{2}\right)\right] = 0. \tag{C.3.8}$$

We write the coefficient matrix for the linear system of (C.3.7, C.3.8) as

$$W = \begin{bmatrix} \frac{q_2 D_v}{k_v}\cos\left(q_1\frac{L}{2}\right) - q_1\sin\left(q_1\frac{L}{2}\right) & q_1\cos\left(q_1\frac{L}{2}\right) + \frac{q_2 D_v}{k_v}\sin\left(q_1\frac{L}{2}\right) \\ \\ q_1\sin\left(q_1\frac{L}{2}\right) - \frac{q_2 D_v}{k_v}\cos\left(q_1\frac{L}{2}\right) & q_1\cos\left(q_1\frac{L}{2}\right) + \frac{q_2 D_v}{k_v}\sin\left(q_1\frac{L}{2}\right) \end{bmatrix}. \tag{C.3.9}$$

To obtain a nontrivial solution for the linear system (C.3.7, C.3.8), we equate the determinant of the coefficient matrix to zero

$$\tan^2\left(q_1\frac{L}{2}\right) + \frac{q_1^2 - \left(\frac{D_v q_2}{k_v}\right)^2}{q_1 q_2 \frac{D_v}{k_v}}\tan\left(q_1\frac{L}{2}\right) - 1 = 0. \tag{C.3.10}$$

The last equation has two solutions

$$\tan\left(q_1\frac{L}{2}\right) = \frac{q_2 D_v}{q_1 k_v} \quad \text{or} \quad \tan\left(q_1\frac{L}{2}\right) = -\frac{q_1 k_v}{q_2 D_v}. \tag{C.3.11}$$

If $\tan\left(q_1\frac{L}{2}\right) = -\frac{q_1 k_v}{q_2 D_v}$, then the second boundary condition (C.3.6) gives the equation

$$\left(q_1 A + \frac{D_v q_2}{k_v}B\right)\tan\left(q_1\frac{L}{2}\right) = \frac{D_v q_2}{k_v}A - q_1 B. \tag{C.3.12}$$

We then replace $\tan\left(q_1\frac{L}{2}\right)$ by $\left(-\frac{q_1 k_v}{q_2 D_v}\right)$ in equation (C.3.12) to get

$$\left(q_1 A + \frac{D_v q_2}{k_v}B\right)\left(-\frac{q_1 k_v}{q_2 D_v}\right) = \frac{D_v q_2}{k_v}A - q_1 B. \tag{C.3.13}$$

Or equivalently, $\left(\frac{D_v q_2}{k_v} + \frac{q_1^2 k_v}{q_2 D_v}\right) A = 0$. Since $\left(\frac{D_v q_2}{k_v} + \frac{q_1^2 k_v}{q_2 D_v}\right)$ is different from zero, we conclude $A = 0$. As a result, the eigenfunction in the good patch becomes

$$V_1(x) = B \sin(q_1 x), \quad x \in \left(\frac{-L}{2}, \frac{L}{2}\right). \tag{C.3.14}$$

But $\sin(q_1 x)$ changes sign at $x = 0$, and this contradicts the symmetry of solutions in the good patch. Therefore, (C.3.10) should have the solution

$$\tan\left(q_1 \frac{L}{2}\right) = \frac{q_2 D_v}{q_1 k_v}. \tag{C.3.15}$$

Proposition C.3.1. *The critical patch size formula of a single patch surrounded by a non-lethal matrix habitat is given by*

$$L^* = \frac{2}{q_1} \arctan\left(\frac{q_2 D_v}{q_1 k_v}\right), \tag{C.3.16}$$

where q_i are defined in (C.2.9).

C.4. Minimal Speed of Traveling Waves

As in Section 4.4, we write the density functions $u_1(t,x)$ and $v_1(t,x)$ as follows

$$u_1(t,x) = e^{-sz} g_1(x), \tag{C.4.1}$$

and

$$v_1(t,x) = e^{-sz} \widetilde{g}_1(x). \tag{C.4.2}$$

Substituting the expressions in (C.4.1, C.4.2) into equations (C.1.1, C.1.2) on good patches, we obtain the system

$$sC\widetilde{g}_1(x) = D_{v_1}\left(s^2 \widetilde{g}_1(x) + \widetilde{g}_1''(x) - 2s\widetilde{g}_1'(x)\right) + m_1 g_1(x) - \mu_{v_1} \widetilde{g}_1(x). \tag{C.4.3}$$

$$g_1(x) = \frac{r_1}{sC + m_1 + \mu_{u_1}} \widetilde{g}_1(x). \tag{C.4.4}$$

We then substitute $g_1(x)$ into equation (C.4.3) to get

$$sC\widetilde{g}_1(x) = D_{v_1}\left(s^2\widetilde{g}_1(x) + \widetilde{g}_1''(x) - 2s\widetilde{g}_1'(x)\right) + \frac{r_1 m_1}{sC + m_1 + \mu_{u_1}}\widetilde{g}_1(x) - \mu_{v_1}\widetilde{g}_1(x).$$

We sort the last equation by derivatives of $\widetilde{g}_1(x)$ to get

$$\widetilde{g}_1''(x) - 2s\widetilde{g}_1'(x) + \frac{1}{D_{v_1}}\left(D_{v_1}s^2 + \frac{r_1 m_1}{sC + m_1 + \mu_{u_1}} - \mu_{v_1} - sC\right)\widetilde{g}_1(x) = 0. \tag{C.4.5}$$

The linear differential equation (C.4.5) has the quadratic characteristic equation

$$z^2 - 2sz + \frac{1}{D_{v_1}}\left(D_{v_1}s^2 + \frac{r_1 m_1}{sC + m_1 + \mu_{u_1}} - \mu_{v_1} - sC\right) = 0, \tag{C.4.6}$$

which has the two roots

$$z = s \pm \frac{1}{\sqrt{D_{v_1}}}\sqrt{sC + \mu_{v_1} - \frac{r_1 m_1}{sC + m_1 + \mu_{u_1}}}. \tag{C.4.7}$$

The same procedure applied on bad patches gives the differential equation

$$\widetilde{g}_2''(x) - 2s\widetilde{g}_2'(x) + \frac{1}{D_{v_2}}\left(D_{v_2}s^2 + \frac{r_2 m_2}{sC + m_2 + \mu_{u_2}} - \mu_{v_2} - sC\right)\widetilde{g}_2(x) = 0, \tag{C.4.8}$$

The form of the solution of the differential equation (C.4.5) depends on the sign of the quantity

$$sC + \mu_{v_1} - \frac{r_1 m_1}{sC + m_1 + \mu_{u_1}}. \tag{C.4.9}$$

The expression is negative if and only if

$$r_1 > \frac{(m_1 + sC + \mu_{u_1})(sC + \mu_{v_1})}{m_1}. \tag{C.4.10}$$

In bad patches, according to Proposition 2.1.1 and since $s, C > 0$, we have the inequality

$$r_2 < \frac{\mu_{v_2}\left(m_2+\mu_{u_2}\right)}{m_2} < \frac{\left(m_2+sC+\mu_{u_2}\right)\left(sC+\mu_{v_2}\right)}{m_2}. \tag{C.4.11}$$

Therefore, solutions of the differential equation (C.4.8) will be of the form

$$\widetilde{g}_2(x) = e^{sx}\left[A'\cosh\left(q_2x\right)+B'\sinh\left(q_2x\right)\right], \tag{C.4.12}$$

where $q_2 = \frac{1}{\sqrt{D_{v_2}}}\sqrt{sC+\mu_{v_2}-\frac{r_2m_2}{sC+m_2+\mu_{u_2}}}$.
In good patches, we have to distinguish cases, depending on whether (C.4.10) holds or not. If it holds, we can write the solution of (C.4.5) as

$$\widetilde{g}_1(x) = e^{sx}\left[A\cosh\left(q_1x\right)+B\sinh\left(q_1x\right)\right], \tag{C.4.13}$$

where $q_1 = \frac{1}{\sqrt{D_{v_1}}}\sqrt{sC+\mu_{v_1}-\frac{r_1m_1}{sC+m_1+\mu_{u_1}}}$. If the reverse inequality holds, we can use hyperbolic-trigonometric formulas to convert between the two.
Equations (C.4.12) and (C.4.13) have four constants. To find their values, we use the interface conditions at $x = 0$ and $x = L_1$

$$\widetilde{g}_1\left(0^+\right) = k_v\widetilde{g}_2\left(0^-\right), \quad \widetilde{g}_1\left(L_1^-\right) = k_v\widetilde{g}_2\left(-L_2^+\right), \tag{C.4.14}$$

$$\widetilde{g}_1'\left(0^+\right) - s\widetilde{g}_1\left(0^+\right) = D_u\left[\widetilde{g}_2'\left(0^-\right) - s\widetilde{g}_2\left(0^-\right)\right], \tag{C.4.15}$$

and

$$\widetilde{g}_1'\left(L_1^-\right) - s\widetilde{g}_1\left(L_1^-\right) = D_u\left[\widetilde{g}_2'\left(-L_2^+\right) - s\widetilde{g}_2\left(-L_2^+\right)\right]. \tag{C.4.16}$$

The interface conditions (C.4.14)-(C.4.16) produce the following linear equations

$$A = k_vA', \quad Bq_1 = B'D_vq_2, \tag{C.4.17}$$

$$Ae^{sL}\cosh\left(q_1L_1\right)+Be^{sL}\sinh\left(q_1L_1\right) = A'k_v\cosh\left(q_2L_2\right)-B'k_v\sinh\left(q_2L_2\right), \tag{C.4.18}$$

and

$$Aq_1e^{sL}\sinh(q_1L_1)+Bq_1e^{sL}\cosh(q_1L_1)=-A'q_2D_v\sinh(q_2L_2)+B'q_2D_v\cosh(q_2L_2)\,. \tag{C.4.19}$$

We write the coefficient matrix of the linear system (C.4.17)-(C.4.19) as

$$V=\begin{bmatrix} 1 & 0 & -k_v & 0 \\ e^{sL}\cosh(q_1L_1) & e^{sL}\sinh(q_1L_1) & -k_v\cosh(q_2L_2) & k_v\sinh(q_2L_2) \\ 0 & q_1 & 0 & -D_vq_2 \\ q_1e^{sL}\sinh(q_1L_1) & q_1e^{sL}\cosh(q_1L_1) & q_2D_v\sinh(q_2L_2) & -q_2D_v\cosh(q_2L_2) \end{bmatrix}.$$

The linear system of equations has a nontrivial solution if and only if the determinant of the coefficient matrix for this system is zero.

Proposition C.4.1. *The dispersion relation for a TPW in a periodic alternating landscape and with sessile juvenile stage is given implicitly by*

$$\cosh(sL)=\cosh(q_1L_1)\cosh(q_2L_2)+\frac{(k_vq_1)^2+(D_vq_2)^2}{2D_vk_vq_1q_2}\sinh(q_1L_1)\sinh(q_2L_2)\,. \tag{C.4.20}$$

C.5. Wave Speed in a Homogeneous Landscape

By substituting $L_2=0$ into the dispersion relation (C.4.20), we get

$$\cosh(sL_1)=\cosh(q_1L_1)\,. \tag{C.5.1}$$

Which is equivalent to

$$s = \frac{1}{\sqrt{D_{v_1}}}\sqrt{sC + \mu_{v_1} - \frac{r_1 m_1}{sC + m_1 + \mu_{u_1}}}. \tag{C.5.2}$$

We can find an explicit expression for the wave speed C as a function of wave shape parameter s. Firstly, we square equation (C.5.2) and multiply both sides by D_{v_1} to get

$$s^2 D_{v_1} = sC + \mu_{v_1} - \frac{r_1 m_1}{sC + m_1 + \mu_{u_1}}. \tag{C.5.3}$$

We then multiply (C.5.3) by $(sC + m_1 + \mu_{u_1})$ to reach

$$r_1 m_1 = m_1 sC + s^2 C^2 + \mu_{v_1} sC - s^3 D_{v_1} C + m_1 \mu_{v_1} + s\mu_{u_1} C + \mu_{u_1}\mu_{v_1} - s^2 D_{v_1}\mu_{u_1} - s^2 D_{v_1} m_1. \tag{C.5.4}$$

We rewrite (C.5.4) as a quadratic equation in C

$$C^2 + C\left(\frac{m_1 + \mu_{u_1} + \mu_{v_1}}{s} - sD_{v_1}\right) + \frac{m_1\mu_{v_1} + \mu_{u_1}\mu_{v_1} - r_1 m_1}{s^2} - D_{v_1}\mu_{u_1} - D_{v_1} m_1 = 0. \tag{C.5.5}$$

The two roots of equation (C.5.5) are

$$\frac{1}{2s}\left(-m_1 - \mu_{u_1} - \mu_{v_1} + D_{v_1}s^2 \pm \sqrt{4r_1 m_1 + \left(\mu_{v_1} - D_{v_1}s^2 - m_1 - \mu_{u_1}\right)^2}\right). \tag{C.5.6}$$

By following the same procedure which we used in sec. 3.2, we conclude that the root

$$\frac{1}{2s}\left(-m_1 - \mu_{u_1} - \mu_{v_1} + D_{v_1}s^2 + \sqrt{4r_1 m_1 + \left(\mu_{v_1} - D_{v_1}s^2 - m_1 - \mu_{u_1}\right)^2}\right), \tag{C.5.7}$$

has a minimum value over $s > 0$, while the other root does not.

Proposition C.5.1. *The wave speed formula for the juveniles-adults model with ses-*

sile juvenile stage in a homogeneous landscape is given explicitly by

$$C(s) = \frac{1}{2s}\left(-m_1 - \mu_{u_1} - \mu_{v_1} + D_{v_1}s^2 + \sqrt{4r_1m_1 + (\mu_{v_1} - D_{v_1}s^2 - m_1 - \mu_{u_1})^2}\right). \tag{C.5.8}$$

D. Matlab Codes

Listing D.1: MATLAB program to generate Figure 6.1.

```
% Parameters needed to solve the equations within the explicit
  method
L =( pi/0.872); % Length of a single-patch
T =1; % Final time
r = 6;  % reproduction rate
m = 5;  % maturation coefficient
meu_u = 1;  % mortality parameters for juveniles
meu_v = 1;  % mortality parameter fot adults
maxk = 2400; % Number of time steps
dt = T/maxk;  % Time step size
n = 50; % Number of space steps
dx = L/n;  % Spatial step size
diffus = 0.001; % Diffusion terms for juveniles and adults
b = 2*diffus*dt/(dx*dx); % Stability parameter (b=<1)
    % Initial conditions
for i = 1:n+1
    x(i)=(i-1)*dx;
    u(i,1)=sin(0.872*x(i));
    v(i,1)=1.420128*sin(0.872*x(i));
end
    % Boundary conditions at x=0 and x=L
for k=1:maxk+1
    u(1,k) = 0; % u(t,0)=0
```

```
    u(n+1,k) = 0; % u(t,L)=0
    v(1,k) = 0; % v(t,0)=0
    v(n+1,k)=0; % v(t,L)=0
    time(k) = (k-1)*dt;
end
    % Implementation of the explicit method
for k=1:maxk % Time Loop
for i=2:n; % Space Loop for juveniles and adults
u(i,k+1) = u(i,k)*(-6*dt-b+1)+u(i+1,k)*(0.5*b)+u(i-1,k)*(0.5*b)+6*
  dt*v(i,k);
v(i,k+1) = v(i,k)*(-dt-b+1)+v(i+1,k)*(0.5*b)+v(i-1,k)*(0.5*b)+5*dt*
  u(i,k);
end
end
exact= exp(2.52*(1200/2400))*sin(0.872*x);
figure(1)
plot(x,exact,'b-','LineWidth',1.5)
   hold on;
plot(x,u(:,1201),'ro')
xlabel('Space (x)','fontsize',14,'fontweight','bold')
ylabel('Juveniles density function u(t,x)','fontsize',14,'
  fontweight','bold')
xlim([0 L]); ylim([0 4])
   % 3-D graph for juveniles density function
figure(2)
mesh(x,time,u')
xlabel('x','fontsize',14,'fontweight','bold')
ylabel('t','fontsize',14,'fontweight','bold')
zlabel('u(t,x)','fontsize',14,'fontweight','bold')
```

Listing D.2: MATLAB program to generate Figure 6.3.

```
   % Population parameters
```

```
L1 =4; L2=5;  T =1.5; r1 = 6; r2=0.2; m1 = 1; m2=1; meu_u1 = 1;
  meu_v1 = 1; meu_u2 = 2; meu_v2 = 2; Du1=2; Dv1=2; Du2=3; Dv2=3;
  alpha_u=0.5; alpha_v=0.5; ku=(alpha_u/(1-alpha_u))*Du2/Du1; kv=(
  alpha_v/(1-alpha_v))*Dv2/Dv1;
    % discretization
dx=0.05; x1=0:dx:L1; np1=length(x1); x2=L1:dx:L2; np2=length(x2);
  dt=min(dx*dx/(2.1*Du1),dx*dx/(2.1*Du2));
    % diffusion matrix for simple forward explicit three-point
      scheme
A1=-2*eye(np1); A2=-2*eye(np2);
for k=1:np1-1
    A1(k,k+1)=1; A1(k+1,k)=1;
end
for k=1:np2-1
    A2(k,k+1)=1; A2(k+1,k)=1;
end
    % Initial conditions
uinit=zeros(1,np1+np2); vinit=zeros(1,np1+np2);
k1=1:1:np1; k2=np1+1:1:np1+np2;
uinit(k1)=0.1 ; vinit(k1)=0.1 ; uinit(k2)=(1/ku)*0.1; vinit(k2)=(1/
  kv)*0.1;
U=uinit'; % transpose from row to column vectors
V=vinit'; % transpose from row to column vectors
for n=1:3
for t=1:T/(3*dt) % time loop
    % reaction-diffusion equations
U(1:np1) =U(1:np1)+ Du1*dt/(dx*dx)*A1*U(1:np1) -(m1+meu_u1)*dt*U(1:
  np1)+r1*dt*V(1:np1);
V(1:np1) = V(1:np1)+Dv1*dt/(dx*dx)*A1*V(1:np1)+m1*dt*U(1:np1)-
  meu_v1*dt*V(1:np1);
U(np1+1:np1+np2) = U(np1+1:np1+np2)+Du2*dt/(dx*dx)*A2*U(np1+1:np1+
  np2) -(m2+meu_u2)*dt*U(np1+1:np1+np2)+r2*dt*V(np1+1:np1+np2);
```

```
V(np1+1:np1+np2) = V(np1+1:np1+np2)+Dv2*dt/(dx*dx)*A2*V(np1+1:np1+
  np2)+m2*dt*U(np1+1:np1+np2)-meu_v2*dt*V(np1+1:np1+np2);
            % boundary conditions
U(1)=U(2); U(end)=U(end-1); V(1)=V(2); V(end)=V(end-1);
    % interface conditions
U(np1)=(1/(Du1+Du2/ku))*(Du1*U(np1-1)+Du2*U(np1+2));
U(np1+1)=(1/ku)*(1/(Du1+Du2/ku))*(Du1*U(np1-1)+Du2*U(np1+2));
V(np1)=(1/(Dv1+Dv2/kv))*(Dv1*V(np1-1)+Dv2*V(np1+2));
V(np1+1)=(1/kv)*(1/(Dv1+Dv2/kv))*(Dv1*V(np1-1)+Dv2*V(np1+2));
end
figure(1)
plot(x1, U(1:np1),'LineWidth',1.3, x2,U(np1+1:np1+np2), 'LineWidth'
  ,1.3)
xlabel('Space (x)','fontsize',14,'fontweight','bold')
ylabel('Juveniles density function u(t,x)','fontsize',14,'
  fontweight','bold')
    hold all
figure(2)
plot(x1, V(1:np1),'LineWidth',1.3, x2,V(np1+1:np1+np2), 'LineWidth'
  ,1.3)
xlabel('Space (x)','fontsize',14,'fontweight','bold')
ylabel('Adults density function v(t,x)','fontsize',14,'fontweight',
  'bold')
    hold all
end
```

Listing D.3: MATLAB program to generate Figure 7.1.

```
    % Population parameters
L1 =2; L2=8; T =1; r1 = 6; r2=6; m1 = 5; m2=5; meu_u1 = 0.25;
  meu_v1 = 0.25; meu_u2 = 0.25; meu_v2 = 0.25; Du1=1; Dv1=1; Du2=2;
   Dv2=2; alpha_u=0.5; alpha_v=0.5; ku=(alpha_u/(1-alpha_u))*Du2/
  Du1; kv=(alpha_v/(1-alpha_v))*Dv2/Dv1; h=0.1; % harvesting rate
    % discretization
```

```
dx=0.05; x1=0:dx:L1; np1=length(x1); x2=L1:dx:L2; np2=length(x2);
  dt=min(dx*dx/(2.1*Du1),dx*dx/(2.1*Du2)); time=0:dt:T;
% diffusion matrix for simple forward explicit three-point scheme
A1=-2*eye(np1); A2=-2*eye(np2);
for k=1:np1-1
    A1(k,k+1)=1; A1(k+1,k)=1;
end
for k=1:np2-1
    A2(k,k+1)=1; A2(k+1,k)=1;
end
    % Initial conditions
uinit=zeros(1,np1+np2); vinit=zeros(1,np1+np2);
k1=1:1:np1; k2=np1+1:1:np1+np2;
uinit(k1)=0.1 ; vinit(k1)=0.1 ;
uinit(k2)=(1/ku)*0.1; vinit(k2)=(1/kv)*0.1;
U=uinit'; % transpose from row to column vectors
V=vinit'; % transpose from row to column vectors
W=zeros(size(V(np1+1:np1+np2)));
    % test of steady state
while max(abs(W-V(np1+1:np1+np2)))>0.000001
    W=V(np1+1:np1+np2);
for t=1:T/dt % time loop
    % reaction-diffusion equations
U(1:np1) = U(1:np1)+ Du1*dt/(dx*dx)*A1*U(1:np1) -(m1+meu_u1)*dt*U
  (1:np1)+r1*dt*(V./(1+(U+V)))(1:np1);
V(1:np1) = V(1:np1)+Dv1*dt/(dx*dx)*A1*V(1:np1)+m1*dt*U(1:np1)-
  meu_v1*dt*V(1:np1);
U(np1+1:np1+np2) = U(np1+1:np1+np2)+Du2*dt/(dx*dx)*A2*U(np1+1:np1+
  np2) -m2*dt*U(np1+1:np1+np2)-(meu_u2)*dt*U(np1+1:np1+np2)+r2*dt*(
  V./(1+(U+V)))(np1+1:np1+np2);
V(np1+1:np1+np2) = V(np1+1:np1+np2)+Dv2*dt/(dx*dx)*A2*V(np1+1:np1+
  np2)+m2*dt*U(np1+1:np1+np2)-(h+meu_v2)*dt*V(np1+1:np1+np2);
        % boundary conditions
```

```
U(1)=U(2); U(end)=U(end-1); V(1)=V(2); V(end)=V(end-1);
    % interface conditions
U(np1)=(1/(Du1+Du2/ku))*(Du1*U(np1-1)+Du2*U(np1+2));
U(np1+1)=(1/ku)*(1/(Du1+Du2/ku))*(Du1*U(np1-1)+Du2*U(np1+2));
V(np1)=(1/(Dv1+Dv2/kv))*(Dv1*V(np1-1)+Dv2*V(np1+2));
V(np1+1)=(1/kv)*(1/(Dv1+Dv2/kv))*(Dv1*V(np1-1)+Dv2*V(np1+2));
end
end
figure(1)
plot(x1, V(1:np1),'r','LineWidth',1.3, x2,V(np1+1:np1+np2), 'b','
  LineWidth',1.3)
hold on
plot(x1, U(1:np1),'--r','LineWidth',1.3, x2,U(np1+1:np1+np2), '--b'
  ,'LineWidth',1.3)
xlabel('Space (x)','fontsize',14,'fontweight','bold')
ylabel(' Density function','fontsize',14,'fontweight','bold')
```

Listing D.4: MATLAB program to generate Figure 7.2.

```
    % Population parameters
L1 =2; L2=8; T =1; r1 = 6; r2=6; m1 = 5; m2=5; meu_u1 = 0.25;
  meu_v1 = 0.25; meu_u2 = 0.25; meu_v2 = 0.25; Du1=1; Du2=2;
  alpha_u=0.5; alpha_v=0.5; ku=(alpha_u/(1-alpha_u))*Du2/Du1; D
  =[0.5 ;1;2];
    % discretization
dx=0.05*sqrt(2); x1=0:dx:L1; np1=length(x1); x2=L1:dx:L2; np2=
  length(x2);
for m=1:3
    Dv1=D(m)*Du1;  Dv2=D(m)*Du2;
    kv=(alpha_v/(1-alpha_v))*Dv2/Dv1;
dt=min(dx*dx/(4.2*Du1),dx*dx/(4.2*Du2));
% diffusion matrix for simple forward explicit three-point scheme
A1=-2*eye(np1); A2=-2*eye(np2);
for k=1:np1-1
```

```
    A1(k,k+1)=1; A1(k+1,k)=1;
end
for k=1:np2-1
    A2(k,k+1)=1; A2(k+1,k)=1;
end
linS={'-.','--','-'};
for n=1:101
    % Initial conditions
uinit=zeros(1,np1+np2); vinit=zeros(1,np1+np2);
k1=1:1:np1; k2=np1+1:1:np1+np2;
uinit(k1)=0.1 ; vinit(k1)=0.1 ; uinit(k2)=(1/ku)*0.1; vinit(k2)=(1/
  kv)*0.1;
U=uinit'; V=vinit'; % transpose from row to column vectors
W=zeros(size(V(np1+1:np1+np2)));
h(n)=(n-1)/10; % fishing rate
    % test of steady state
while max(abs(W-V(np1+1:np1+np2)))>0.000001
    W=V(np1+1:np1+np2);
for t=1:T/(dt) % time loop
    % reaction-diffusion equations
U(1:np1) =U(1:np1)+ Du1*dt/(dx*dx)*A1*U(1:np1) -(m1+meu_u1)*dt*U(1:
  np1)+r1*dt*(V./(1+(U+V)))(1:np1);
V(1:np1) = V(1:np1)+Dv1*dt/(dx*dx)*A1*V(1:np1)+m1*dt*U(1:np1)-
  meu_v1*dt*V(1:np1);
U(np1+1:np1+np2) = U(np1+1:np1+np2)+Du2*dt/(dx*dx)*A2*U(np1+1:np1+
  np2) -m2*dt*U(np1+1:np1+np2)-(meu_u2)*dt*U(np1+1:np1+np2)+r2*dt*(
  V./(1+(U+V)))(np1+1:np1+np2);
V(np1+1:np1+np2) = V(np1+1:np1+np2)+Dv2*dt/(dx*dx)*A2*V(np1+1:np1+
  np2)+m2*dt*U(np1+1:np1+np2)-(h(n)+meu_v2)*dt*V(np1+1:np1+np2);
    % boundary conditions
U(1)=U(2); U(end)=U(end-1); V(1)=V(2); V(end)=V(end-1);
    % interface conditions
U(np1)=(1/(Du1+Du2/ku))*(Du1*U(np1-1)+Du2*U(np1+2));
```

```
U(np1+1)=(1/ku)*(1/(Du1+Du2/ku))*(Du1*U(np1-1)+Du2*U(np1+2));
V(np1)=(1/(Dv1+Dv2/kv))*(Dv1*V(np1-1)+Dv2*V(np1+2));
V(np1+1)=(1/kv)*(1/(Dv1+Dv2/kv))*(Dv1*V(np1-1)+Dv2*V(np1+2));
end
end
yield(n)=dx*sum(h(n)*V(np1+1:np1+np2));
abundance(n)=dx*sum(V(np1+1:np1+np2));
tabundance(n)=dx*sum(V(1:np1+np2));
logratio(n)=log(((L2-L1)/L1)*sum(V(1:np1))/sum(V(np1+1:np1+np2)));
end
figure(1)
plot(h,yield,'LineWidth',1.2,'linestyle',linS{m})
xlabel('Harvesting rate','fontsize',14,'fontweight','bold')
ylabel('Adults  yield','fontsize',14,'fontweight','bold')
hold all
figure(2)
plot(h,nthroot(abundance,20),'LineWidth',1.2,'linestyle',linS{m})
xlabel('Harvesting rate','fontsize',14,'fontweight','bold')
ylabel('(Adults abundance)^{0.05}','fontsize',14,'fontweight','bold
  ')
hold all
figure(3)
plot(h,log(tabundance),'LineWidth',1.2,'linestyle',linS{m})
xlabel('Harvesting  rate','fontsize',14,'fontweight','bold')
ylabel('log(Total adults abundance)','fontsize',14,'fontweight','
  bold')
hold all
figure(4)
plot(h,logratio,'LineWidth',1.2,'linestyle',linS{m})
xlabel('Harvesting rate','fontsize',14,'fontweight','bold')
ylabel('Adults log ratio','fontsize',14,'fontweight','bold')
hold all
end
```

Bibliography

[1] G. R. Almany, R. J. Hamilton, M. Bode, M. Matawai, T. Potuku, P. Saenz-Agudelo, S. Planes, M. L. Berumen, K. L. Rhodes, S. R. Thorrold, G. R. Russ, and G. P. Jones. Dispersal of grouper larvae drives local resource sharing in a coral reef fishery. *Current Biology*, 23:626–630, 2013.

[2] P. Arcese and J. Smith. Effects of population density and supplemental food on reproduction in song sparrows. *Journal of Animal Ecology*, 57:119–136, 1988.

[3] D.G. Aronson and H.F. Weinberger. *Nonlinear diffusion in population genetics, combustion and nerve propagation. In "Proceedings of the Tulane Program in Partial Differential Equations and Related Topics"*. Lecture Notes in Mathematics, vol 466. Springer, 1975.

[4] J. Berger. *Wild Horses of The Great Basin: Social Competition and Population Size*. University of Chicago Press, 1986.

[5] G. Bocharov and K. P. Hadeler. Structured population models, conservation laws, and delay equations. *Journal of Differential Equations*, 168:212–237, 2000.

[6] J. A. Bohnsack. Marine reserves: they enhance fisheries, reduce conflicts, and protect resources. *Oceanus*, 36(1):63, 1993.

[7] R. S. Cantrell and C. Cosner. *Spatial Ecology via Reaction-Diffusion Equations*. John Wiley, 2003.

[8] H. Caswell. *Matrix Population Models*. Sinauer Associates, Inc., 2001.

[9] H. Caswell and P. A. Werner. Transient behavior and life history analysis of teasel (*Dispacus sylvestris* Huds.). *Ecology*, 59:53–66, 1978.

[10] M. R. Chapman and D. L. Kramer. Gradients in coral reef fish density and size across the Barbados Marine Reserve boundary: effects of reserve protection and habitat characteristics. *Marine Ecology Progress Series*, 181:81–96, 1999.

[11] J. Claudet, C. W. Osenberg, P. Domenici, F. Badalamenti, M. Milazzo, J. M. Falcon, I. Bertocci, L. Benedetti Cecchi, J A. Garcia Charton, R. Goni, J. A. Borg, A. Forcada, G. A. De Lucia, A. Perez-Ruzafa, P. Afonso, A. Brito, I. Guala, L. Direach, P. Sanchez Jerez, P. J. Somerfield, and S. Planes. Marine reserves: fish life history and ecological traits matter. *Ecological Applications*, 20(3):830–839, 2010.

[12] F. C. Coleman and S. L. Williams. Overexploiting marine ecosystem engineers: potential consequences for biodiversity. *Trends in Ecology and Evolution*, 17(1):40–44, 2002.

[13] J. D. Congdon, A. E. Dunham, and R. C. Van Loben Sels. Delayed sexual maturity and demographics of blanding's turtles (*Emydoidea Blandingii*): implications for conservation and management of long-lived organisims. *Conservation Biology*, 7:826–833, 1993.

[14] J. D. Congdon and R. C. Van Loben Sels. Growth and body sisi variation in blanding's tuturt (*Emydoidea Blandingii*): Relationships to reproduction. *Canadian Journal of Zoology*, 69:239–245, 1991.

[15] J. D. Congdon and R. C. Van Loben Sels. Relationships of reproductive traits and body size with attainment of sexual maturity and age in blanding's turtles

(*Emydoidea blandingii*). *Journal of Evolutionary Biology*, 6:317–327, 1993.

[16] S. Creel, J. Winnie, B. Maxwell, K. Hamlin, and M. Creel. Elk alter habitat selection as an antipredator response to wolves. *Ecology*, 86:3387–3397, 2005.

[17] G. Cruywagen, P. Kareiva, M. Lewis, and J. Murray. Competition in a spatially heterogeneous environment: modeling the risk of spread of a genetically engineered population. *Theoretical Population Biology*, 49:1–38, 1996.

[18] J. M. Cushing. *An Introduction to Structured Population Dynamics*. SIAM, 1998.

[19] H. de Kroon, A. Plaisier, J. van Groendendael, and H. Caswell. Elasticity: the relative contribution of demographic parameters to population growth. *Ecology*, 67:1427–1431, 1986.

[20] E. Drewitt. *Urban Peregrines*. Pelagic Publishing, 2014.

[21] F. Van Dyke. *Conservation Biology: Foundations, Concepts, Applications.* Springer, 2008.

[22] J. Fang, K. Lan, G. Seo, and J. Wu. Spatial dynamics of an age-structured populations of Asian clams. *SIAM Journal on Applied Mathematics*, 74(4):959–979, 2014.

[23] R. Fisher. The advance of advantageous genes. *Annals of Eugenics*, 7:355–369, 1937.

[24] J. Fryxell. Predictive modeling of patch use by terrestrial herbivores. In H. Prins and F. van Langevelde, editors, *Resource ecology: spatial and temporal dynamics of foraging*, pages 105–123. Springer, Dordrecht, 2008.

[25] M. J. Garlick, J. A. Powel, M. B. Hooten, and L. R. MacFarlane. Homogeniza-

tion, sex, and differential motility predict spread of chronic wasting disease in mule deer in southern Utah. *Journal of Mathematical Biology*, 2013.

[26] M. J. Garlick, J. A. Powell., M. B. Hooten, and L. R. McFarlane. Homogenization of large-scale movement models in ecology. *Bulletin of Mathematical Biology*, 73:2088–2108, 2011.

[27] F. R. Gell and C. M. Roberts. Benefits beyond boundaries: the fishery effects of marine reserves. *Trends in Ecology and Evolution*, 18(9):448–455, 2003.

[28] L. Gerber, L. Botsford, A. Hastings, H. Possingham, S. Gaines, S. Palumbi, and S. Andelman. Population models for marine reserve design: A retrospective and prospective synthesis. *Ecological Applications*, 13:47–64, 2003.

[29] B. M. Gillanders, K. W. Able, J. A. Brown, D.B. Eggleston, and P. F. Sheridan. Evidence of connectivity between juvenile and adult habitats for mobile marine fauna: an important component of nurseries. *Marine Ecology Progress Series*, 247:281–295, 2003.

[30] R. Goni, O. Renones, J. A. Garcia-Charton, R. Galzin, J. T. Bayle, P. Sanchez Jerez, A. Perez-Ruzafa, and A. A. Ramos. Density dependence in marine protected populations: a review. *Environmental Conservation*, 27(2):144–158, 2000.

[31] A. Grüss, D. M. Kaplan, S. Guénette, C. M. Roberts, and L. W. Botsford. Consequences of adult and juvenile movement for marine protected areas. *Journal of Biological Conservation*, 144:692–702, 2011.

[32] M. E. Gurtin and R. C. MacCamy. Diffusion models for age-structured populations. *Mathematical Biosciences*, 54:49–59, 1981.

[33] H. Harrison, D. Williamson, R. Evans, G. Almany, S. Thorrold, G. Russ, K. Feldheim, L. van Herwerden, S. Planes, M. Srinivasan, M. Berumen, and G. Jones.

Larval export from marine reserves and the recruitment benefit for fish and fisheries. *Current Biology*, 22(11):1023–1028, 2012.

[34] A. Hastings and L. J. Gross. *Encyclopedia of Theoretical Ecology*. University of California Press, 2012.

[35] G. E. Hernandes. Dynamics of populations with age-difference and diffusion: localization. *Applicable Analysis*, 29:143–163, 1988.

[36] G. E. Hernandez. Age-density dependent population dispersal in $\mathbb{R}^n$. *Mathematical Biosciences*, 149:37–56, 1998.

[37] R. Hilborn, K. Stokes, J. Maguire, T. Smith, L. Botsford, M. Mangel, J. Orensanz, A. Parma, J. Rice, J. Bell, K. Cochrane, S. Garcia, S. Hall, G. Kirkwood, K. Sainsbury, G. Stefansson, and C. Walters. When can marine reserves improve fisheries management? *Ocean and Coastal Management*, 47:197–205, 2004.

[38] D. Hillis, D. Sadava, H. Heller, and M. Price. *Principles of Life*. Sinauer Associates, Inc., 2012.

[39] R. A. Horn and C. R. Johnson. *Matrix Analysis*. Cambridge University Press, 2009.

[40] J. A. Hutchings. Collapse and recovery of marine fishes. *Nature*, 406(16798):882, 2000.

[41] M. Iannelli, M. Martcheva, and F. A. Milner. *Gender-Structured Population Modeling: Mathematical Methods, Numerics, and Simulations*. SIAM, 2005.

[42] H. Kierstead and L. B. Slobodkin. The size of water masses containing plankton blooms. *Journal of Marine Research*, 12:141–147, 1953.

[43] N. Kinezaki, K. Kawasaki, F. Takasu, and N. Shigesada. Modeling biological

invasions into periodically fragmented environments. *Theoretical Population Biology*, 64:291–302, 2003.

[44] A. N. Kolmogorov, I. G. Petroviskii, and N. S. Piskunov. A study of the equation of diffusion with increase in the quantity of matter, and its application to biological problem. *Bjul. Moskovskovo Gos. Univ.*, 17:1–72, 1937.

[45] M. Kot. *Elements of Mathematical Ecology*. Cambridge University Press, 2001.

[46] J. Langebrake, L. Lambert, C. Osenberg, and P. De Leenheer. Differential movement and movement bias models for marine protected areas. *Journal of Mathematical Biology*, 64(4):667–696, 2012.

[47] S. Lester, B. Halpern, K. Grorud-Colvert, J. Lubchenco, B. Ruttenberg, S. Gaines, S. Airame, and R. Warner. Biological effects within no-take marine reserves: A global synthesis. *Marine Ecology Progress Series*, 384:33–46, 2009.

[48] D. J. Levey and F. G. Stiles. Evolution precursors of long-distance migration: Resource availability and movement patterns in neotropical landbirds. *The American Naturalist*, 140(3):447–476, 1992.

[49] X. Liang and X-Q. Zhao. Spreading speed and traveling waves for abstract monostable evolution systems. *Journal of Functional Analysis*, 259(4):857–903, 2010.

[50] D. R. Lockwood, A. Hastings, and L. W. Botsford. The effects of dispersal patterns on marine reserves: Does the tail wag the dog? *Theoretical Population Biology*, 61:297–309, 2002.

[51] J. David Logan. *A First Course in Differential Equations*. Springer, 2015.

[52] R. Lui. Biological growth and spread modeled by systems of recursions. I. Mathematical theory. *Mathematical Biosciences*, 93:269–295, 1989.

[53] R. Lui. Biological growth and spread modeled by systems of recursions. II. Biological theory. *Mathematical Biosciences*, 93:297–312, 1989.

[54] F. Lutscher and M. A. Lewis. Spatially-explicit matrix models. *Journal of Mathematical Biology*, 48:293–324, 2004.

[55] G. Maciel and F. Lutscher. How individual movement response to hapitat edge effects population persistence and spatial spread. *The American Naturalist*, 182:42–52, 2013.

[56] G. Maciel and F. Lutscher. Allee effects and population spread in patchy landscapes. *Journal of Biological Dynamics*, 9(1):109–123, 2015.

[57] J. S. Mao, M. S. Boyce, D. W. Smith, F. J. Singer, D. J. Vales, J. Vore, and E. Merrill. Habitat selection by elk before and after wolf reintroduction in Yellowstone National Park. *Journal of Wildlife Management*, 69:1691–1707, 2005.

[58] D. McFarland. *Comparison of Alternative Marriage Models in Population Dynamics*. Academic Press, New York, London, 1972, pp. 89-106.

[59] G. Medina-Vogel, L. O. Merino, R. Monsalve Alarcon, and J. de A. Vianna. Coastal-marine discontinuities, critical patch size and isolation: implications for marine otter conservation. *Animal Conservation*, 11(1):57–64, 2008.

[60] J. A. Metz and O. Diekmann. *The dynamics of physiologically structured populations*. Lecture Notes in Biomathematics 68. Springer, 1986.

[61] R. B. Millar. Estimating the size-selectivity of fishing gear by conditioning on

the total catch. *Journal of the American Statistical Association*, 87(420):962–968, 1992.

[62] T. Miller, A. Shaw, B. Inouye, and M. Neubert. Sex-biased dispersal and the speed of two-sex invasions. *The American Naturalist*, 177(5):549–561, 2011.

[63] I. Mosquera, I. M. Côté, S. Jennings, and J. D. Reynolds. Conservation benefits of marine reserves for fish populations. *Animal Conservation*, 4:321–332, 2000.

[64] J. Musgrave. *Integrodifference Equations in Patchy Landscapes.* PhD thesis, University of Ottawa, 2013.

[65] M. G. Neubert and H. Caswell. Demography and dispersal: Calculation and sensitivity analysis of invasion speed for structured populations. *Ecology*, 81(6):1613–1628, 2000.

[66] M. G. Neubert and H. Caswell. Density-dependent vital rates and their population dynamic consequences. *Journal of Mathematical Biology*, 41:103–121, 2000.

[67] A. Novick-Cohen and L. A. Segel. A gradually slowing travelling band of chemotactic bacteria. *Journal of Mathematical Biology*, 19:125–132, 1984.

[68] H. G. Othmer. A continuum model of coupled cells. *Journal of Mathematical Biology*, 17(3):351–369, 1983.

[69] O. Ovaskainen and S. J. Cornell. Biased movement at a boundary and conditional occupancy times for diffusion processes. *Journal of Applied Probability*, 40:557–580, 2003.

[70] J. E. Paterson, B. D. Steinburg, and J. D. Litzgus. Revealing a cryptic life-history: differences in habitat selection and survivorship between hatchlings

of two turtle species at risk (*Glyptemys insculpta* and *Emydoidea blandingii*). *Wildlife Research*, 39(5):408–418, 2012.

[71] S. Prange, S. D. Gehrt, and E. P. Wiggers. Influences of anthropogenic resource on raccoon (*Procyon lotor*) movement and spatial distribution. *Journal of Mammalogy*, 85(3):483–490, 2004.

[72] G. Ramakrishna. Notes on the Indian species of the genus Argulus Muller (*Crustacea; Copepoda*) parasitic on fishes. *Records of the Indian Museum*, 69:57–63, 1951.

[73] K. F. Riley, M. P. Hobson, and S. J. Bence. *Mathematical Methods for Physics and Engineering: A Comprehensive Guide*. Cambridge University Press, 2006.

[74] C. Roberts, J. Bohnsack, F. Gell, J. Hawkins, and R. Goodridge. Effects of marine reserves on adjacent fisheries. *Science*, 294(5548):1920–1923, 2001.

[75] G. Samelius, H. Andrén, P. Kjellander, and O. Liberg. Habitat selection and risk of predation: Re-colonization by lynx had limited impact on habitat selection by roe deer. *PLoS ONE*, 8(9), 2013.

[76] M. Scheffer, S. Carpenter, and B. de Young. Cascading effects of overfishing marine systems. *Trends in Ecology and Evolution*, 20(11):579–581, 2005.

[77] N. Shigesada, K. Kawasaki, and E. Teramoto. Traveling periodic waves in heterogeneous environments. *Theoretical Population Biology*, 182:143–160, 1986.

[78] Y-J. Shin, M-J. Rochet, S. Jennings, J. Field, and H. Gislason. Using size-based indicators to evaluate the ecosystem effects of fishing. *ICES Journal of Marine Science*, 62(3):384–396, 2005.

[79] R. Shope. Global climate change and infectious diseases. *Environmental Health*

Perspectives, 96:171–174, 1991.

[80] N. W. Siegert, D. G. McCullough, A. M. Liebhold, and F. W. Telewski. Dendrochronological reconstruction of the epicentre and early spread of emerald ash borer in North America. *Journal of Conservation Biology*, 20:847–858, 2014.

[81] R. S. Singh and C. B. Krimbas, editors. *Evolution Genetics: From Molecules to Morphology*. Cambridge University Press, 2000.

[82] J. G. Skellam. Random dispersal in theoretical populations. *Biometrika*, 38:196–218, 1951.

[83] H. Smith. *Monotone dynamical systems: An introduction to the theory of competitive and cooperative systems*. American Mathematical Society, 1995.

[84] N. C. Stenseth and W. Z. Lidicker, editors. *Animal Dispersal: Small Mammals as a Model*. Springer, 1992.

[85] J. C. Strikwerda. *Finite Difference Scheme and Partial Differential Equations*. SIAM, 2004.

[86] A. C. Tsikliras and K. Polymeros. Fish market prices drive overfishing of the big ones. *PeerJ*, 2:e638, 2014.

[87] P. Turchin. *Quantative Analysis of Movement: Measuring and Modeling Population Redistribution in Animals and Plants.* Sinauer, Sunderland, MA., 1998.

[88] H. F. Weinberger, M. A. Lewis, and B. Li. Analysis of linear determinacy for spread in cooperative models. *Journal of Mathematical Biology*, 45:183–218, 2002.

[89] J. W. White. Marine reserve design theory for species with ontogenetic migration. *The Royal Society*, 11(1):20140511–20140511, 2015.

[90] B. Yurk. Homogenization of a directed dispersal model for animal movement in a heterogeneous environment. *Bulletin of Mathematical Biology*, 87(10):2034–2056, 2016.

[91] B. Yurk and C. Cobbold. Homogenization techniques for population dynamics in strongly heterogeneous landscapes. *In preparation.*

[92] X.-Q. Zhao. *Spatial dynamics of some evolution systems in biology.* World Scientific, 2009.